

NRP1 regulation of endothelial cell signalling

Anastasia Syrmalenia Lampropoulou

Thesis submitted in fulfilment for the degree of Doctor of Philosophy

University College London (UCL)

Institute of Ophthalmology

Supervisor: Prof Christiana Ruhrberg

Secondary Supervisor: Prof John Greenwood

DECLARATION

I, Anastasia Lampropoulou, confirm that the work presented in this thesis is my own. Where information has been derived from other sources, I confirm that this has been indicated in the thesis.

ACKNOWLEDGEMENTS

I greatly enjoyed my time as a PhD student thanks to the beautiful people that I have had the pleasure of working with. Firstly, I would like to thank my supervisor Christiana Ruhrberg who has been very supportive and enthusiastic over the last few years. I would also like to thank everyone in the Ruhrberg group, previous and current lab members for creating a great working environment. In particular, I would like to thank Claudio Raimondi and Alex Fantin for sharing with me the mystery of science! It was a pleasure to work with them and learn from the best in the field about new techniques and methods of research. I am also very happy that I had the chance to work with James Brash and Kirsty Naylor in their very first days in the lab. I am very grateful to both Laura Denti and Valentina Senatore for their help with the animal work and Mat Tata for his helpful comments along the way. Additionally, I would like to give special thanks to Vaso Chantzara for being so supportive and cheering me up when needed, especially during the last months of my PhD.

I am also thankful to the other staff at the UCL Institute of Ophthalmology, including members of the Biological Resources Unit, Peter Munro from the Imaging Facility and Robert Sampson, who is the FACS facility manager at the Institute.

Finally, I would like to give the very biggest thanks to my family Andreas, Chrysoula and Lilian, who have always been there for me by supporting and encouraging me to fill my soul with beautiful and inspiring things.

ABSTRACT

Neuropilin 1 (NRP1) is a transmembrane protein that is essential for blood vessel growth and the regulation of vascular barrier properties. Yet, at the time of starting my PhD research, it was poorly understood how NRP1 affects endothelial cell behaviour to enhance either blood vessel growth or modulate vascular permeability. In particular, it was controversial whether NRP1 mainly acts to promote VEGF signalling through the VEGF receptor tyrosine kinase VEGFR2, or if it has other roles that synergise with VEGFR2 pathways to promote effective tissue vascularisation or vascular permeability. The aims of this study were therefore to (a) investigate whether NRP1 modulates angiogenesis and vascular hyperpermeability together with or independently of VEGFR2, (b) determine whether NRP1 regulates gene transcription to modulate endothelial behaviour; (c) define the molecular mechanism by which NRP1 regulates angiogenesis and VEGF-induced vascular hyperpermeability. My experiments have revealed that NRP1 promotes blood vessel growth both independently of, and synergistically with, VEGFR2-driven pathways. In particular, I found that VEGFR2-independent signalling involves the intracellular signal transducers CDC42 and ABL1 kinase, which promote actin remodelling during cell migration. Instead, my experiments have revealed that NRP1 promotes VEGF-induced vascular permeability in a complex with VEGFR2. Specifically, I found that both NRP1 and VEGFR2 are required for the VEGF induced activation of SRC family kinases (SFKs), which are known to be essential for VEGF-induced vascular permeability signalling. Moreover, I found that NRP1 is important, because it is required for ABL1 activation, which in turn is essential for SFK activation in this pathway. Finally, I observed that NRP1 regulates several transcription factors and the expression of their target genes in endothelial cells, particularly genes involved in actin remodelling and cell proliferation. Together, this knowledge increases our understanding of the mechanisms of blood vessel formation and function. By identifying molecular pathways in blood vessel growth and permeability, these findings may, in the long run, benefit translational research aimed at developing novel therapies for diseases with vascular dysfunction.

CONTENTS

DECLARATION.....	2
ACKNOWLEDGEMENTS	3
ABSTRACT	4
LIST OF TABLES	9
TABLE OF FIGURES	10
ABBREVIATIONS	12
CHAPTER 1 INTRODUCTION	17
1.1 VEGF: ISOFORMS AND RECEPTORS	18
1.2 DOMAIN STRUCTURE OF NRP1 AND NRP2	19
1.3 ESSENTIAL ROLE FOR NRP1 IN DEVELOPMENTAL ANGIOGENESIS	21
1.4 NRP1 LIGANDS IN ANGIOGENESIS: SEMA3A	24
1.5 NRP1 LIGANDS IN ANGIOGENESIS: VEGF165	25
1.6 NRP1 LIGANDS IN ANGIOGENESIS: UNIDENTIFIED ADHESION MOLECULES.....	27
1.7 NRP1 SIGNALLING IN ENDOTHELIAL CELLS: ASSOCIATION WITH CO-RECEPTORS	27
1.8 NRP1 AS A REGULATOR OF TGF β SIGNALLING	29
1.9 NRP1 ASSOCIATES WITH THE CYTOPLASMIC ADAPTOR SYNECTIN TO REGULATE VEGFR2 TRAFFICKING FOR VEGF-INDUCED ARTERIOGENESIS	30
1.10 VEGFR2-INDEPENDENT NRP1 SIGNALLING IN ENDOTHELIAL CELLS.....	31
1.11 INTEGRIN ACTIVATION AND SIGNALLING MECHANISMS.....	31
1.12 INTEGRINS AND ANGIOGENESIS AND THEIR INTERACTION WITH NRP1	36
1.12.1 Possible links between NRP1 and RHO -GTPases via integrin-mediated ABL1 activation	37
1.12.2 The role of CDC42 in filopodia formation and sprouting angiogenesis .	38
1.13 THE SERUM RESPONSE FACTOR (SRF) AND ITS CO-FACTORS	39
1.13.1 The SRF co-factors MRTFs and TCFs.....	40
1.14 THE ROLE OF SRF IN POSTNATAL AND PATHOLOGICAL ANGIOGENESIS.....	44
1.15 THE ROLE OF SRF AND MRTFA IN VASCULAR HOMEOSTASIS	46
1.16 VASCULAR PERMEABILITY	48
1.16.1 Basal vascular permeability	49

1.16.2	<i>Acute and chronic vascular hyperpermeability</i>	49
1.17	THE MECHANISMS OF VASCULAR PERMEABILITY	50
1.17.1	<i>The transcellular mechanism</i>	50
1.17.2	<i>The paracellular mechanism</i>	51
1.18	THE MOLECULAR MECHANISMS OF VEGF-INDUCED VASCULAR PERMEABILITY: VEGFR2 AND ITS INTERACTORS.....	52
1.18.1	<i>VEGFR2 activation and its interaction with transmembrane proteins</i> ..	52
1.18.2	<i>Cytoplasmic mediators of vascular permeability</i>	53
1.19	ROLE OF NRP1 IN VEGF-INDUCED VASCULAR PERMEABILITY.....	55
	AIMS OF THE STUDY	56
	CHAPTER 2 MATERIALS AND METHODS	57
2.1	MATERIALS	57
2.1.1	<i>General Laboratory Materials</i>	57
2.1.2	<i>General Laboratory Solutions</i>	57
2.2	CELL CULTURE METHODS.....	57
2.2.1	<i>Cell lines and culture</i>	57
2.2.2	<i>Immunofluorescence</i>	59
2.2.3	<i>Cell migration assay</i>	60
2.2.4	<i>CDC42 pull down assay, immunoprecipitation and immunoblotting</i>	60
2.2.5	<i>Gene expression analyses (qRT-PCR)</i>	62
2.3	MOUSE METHODS	67
2.3.1	<i>Animal Maintenance and Husbandry</i>	67
2.3.2	<i>Genetic mouse strains</i>	67
2.3.3	<i>Genotyping of mouse strains</i>	69
2.3.4	<i>Whole mount immunolabelling and imaging of mouse retinas and aortas</i>	71
2.3.5	<i>Fluorescence-activated cell sorting (FACS)</i>	75
2.3.6	<i>RNA extraction from ECs collected by FACS sorting</i>	75
2.3.7	<i>RT² Profiler PCR Array</i>	76
2.4	STATISTICAL ANALYSIS.....	79
	CHAPTER 3 NRP1 PROMOTES ACTIN REMODELLING VIA ABL1 AND CDC42	80

3.1	INTRODUCTION	80
3.2	RESULTS	82
3.2.1	<i>NRP1-dependence of ECM-induced angiogenesis.....</i>	82
3.2.2	<i>NRP1 cytoplasmic domain is not required for ECM-induced PXN phosphorylation</i>	87
3.2.3	<i>NRP1 regulates CDC42 activity to promote filopodia formation in ECs.</i>	89
3.2.4	<i>CDC42 is dispensable for FN-induced PXN phosphorylation</i>	97
3.3	DISCUSSION	99
CHAPTER 4 NRP1 REGULATES GENE TRANSCRIPTION		107
4.1	INTRODUCTION	107
4.2	RESULTS	108
4.2.1	<i>Differential gene expression in postnatal brains of mice lacking endothelial NRP1.....</i>	108
4.2.2	<i>NRP1-dependent signalling regulates ERK1/2 activation</i>	116
4.2.3	<i>NRP1 regulates the expression of the SRF and MRTFA transcription factors and targeted genes</i>	121
4.3	DISCUSSION	130
CHAPTER 5 NRP1 REGULATES VEGF-165 INDUCED VASCULAR PERMEABILITY		138
5.1	INTRODUCTION	138
5.2	RESULTS	139
5.2.1	<i>NRP1 and SFK are localised in cell-cell contact areas of HUVEC after VEGF165 stimulation.....</i>	139
5.2.2	<i>NRP1 localises on the cell-cell contact areas of HDMEC.....</i>	141
5.2.3	<i>NRP1 promotes VEGF165-induced SFK activation in HDMEC.....</i>	143
5.2.4	<i>ABL1 mediates NRP1-dependent SFK activation.....</i>	151
5.2.5	<i>ABL kinases are required for both VEGF165-induced CRKL and SFK activation.....</i>	153
5.2.6	<i>NRP1 is required for VEGF-induced FAK activation.....</i>	157
5.2.7	<i>VEGF164-induced SFKs activation via ABL kinase relies on the NCD... </i>	159
5.2.8	<i>CDH5 localisation in MLEC from wild type and Nrp1^{cyto/cyto} mice.....</i>	161
5.3	DISCUSSION	163

CHAPTER 6	FINAL CONCLUSIONS AND FUTURE WORK	172
6.1	SUMMARY OF CONCLUSIONS AND FINAL REMARKS	172
6.2	FUTURE WORK	175
6.2.1	<i>Identify the specific integrins that interact with NRP1 in ECs and define their function in angiogenesis.</i>	<i>175</i>
6.2.2	<i>Determine if NRP1 regulates RAC and RHOA RHO-GTPase activation and function in angiogenic ECs.</i>	<i>175</i>
6.2.3	<i>Examine whether NRP1 regulates different set of genes in angiogenesis and in vascular homeostasis</i>	<i>176</i>
6.2.4	<i>NRP1 signalling downstream of SFK activation in response to VEGF ..</i>	<i>177</i>
6.2.5	<i>Investigate the role of ABL2 in VEGF-induced vascular permeability ..</i>	<i>177</i>
BIBLIOGRAPHY		179
APPENDIX.....		205

LIST OF TABLES

TABLE 1: PRIMERS DESIGNED FOR RT-PCR OF HUMAN ECS.....	64
TABLE 2: PCR CYCLING PARAMETERS USED IN GENOTYPING	70
TABLE 3: LIST OF ANTIBODIES USED FOR IMMUNOBLOTTING AND IMMUNOFLUORESCENCE.....	72
TABLE 4: LIST OF THE SECONDARY ANTIBODIES USED FOR IMMUNOFLUORESCENCE	74
TABLE 5: CELL MOTILITY RELATED GENES IN RT ² PROFILER PCR ARRAY.	77
TABLE 6: DIFFERENTIALLY EXPRESSED GENES IN QRT-PCR ARRAY. THE DATA WERE DISPLAYED AS FOLD CHANGE OF GENE EXPRESSION IN MUTANTS COMPARED TO CONTROLS, USING AS A THRESHOLD VALUES THAT WERE $\geq 1.5X$ OR $\leq 0.67X$	115
TABLE 7: PHOSPHORYLATION OF ERK1/2 IN SINRP1 SAMPLES. MASS SPECTROMETRY ANALYSIS USING HDMEC TRANSFECTED WITH SIRNA FOR NRP1 OR CONTROL, REVEALED THE LEVELS OF PERK1/2 PHOSPHORYLATION 72H AFTER TRANSFECTION. THE VALUES IN SINRP1 SAMPLES WERE PRESENTED AS FOLD CHANGE RELATIVE TO CONTROL.....	137

TABLE OF FIGURES

FIGURE 1: NRP1 DOMAINS AND ITS INTERACTION WITH VEGFR2.	20
FIGURE 2: ROLE OF NRP1 IN ANGIOGENESIS.	23
FIGURE 3: BALANCE BETWEEN PROLIFERATIVE AND CONTRACTILE-RELATED EVENTS VIA THE SRF AND COFACTORS.	43
FIGURE 4: NRP1 PROMOTES FN-INDUCED ACTIN REMODELLING AND FILOPODIA EXTENSION IN PRIMARY ECS.	83
FIGURE 5: NRP1 PROMOTES FN-INDUCED PXN PHOSPHORYLATION VIA ABL1 KINASE IN PRIMARY ECS.	86
FIGURE 6: THE NRP1 CYTOPLASMIC DOMAIN IS NOT REQUIRED FOR ECM-INDUCED PXN PHOSPHORYLATION.	88
FIGURE 7: NRP1 AND CDC42 ARE REQUIRED FOR ECM-INDUCED ACTIN REMODELLING IN ECS.	90
FIGURE 8: NRP1 ENABLES ECM-INDUCED CDC42 ACTIVATION.	92
FIGURE 9: NRP1 IS REQUIRED FOR ECM-INDUCED ACTIN REMODELLING AND CDC42 ACTIVATION IN ECS INDEPENDENTLY OF VEGFA.	94
FIGURE 10: ABL1 ENABLES CDC42 ACTIVATION IN ECM-STIMULATED ECS.	96
FIGURE 11: CDC42 IS DISPENSABLE FOR FN-INDUCED PXN PHOSPHORYLATION.	98
FIGURE 12: SCHEMATIC REPRESENTATION OF NRP1 ROLES IN ANGIOGENESIS.	106
FIGURE 13: ISOLATION OF ECS FROM BRAIN TISSUE VIA FLUORESCENCE-ACTIVATED CELL SORTING (FACS).	113
FIGURE 14: DIFFERENTIAL GENE EXPRESSION CELL MOTILITY-ASSOCIATED TRANSCRIPTS IN ECS FROM POSTNATAL NRP1FL/FL +CRE COMPARED TO CONTROL BRAINS.	114
FIGURE 15: NRP1 REGULATES ERK1/2 PHOSPHORYLATION IN HDMEC.	117
FIGURE 16: NRP1 LOSS CAUSES ERK1/2 ACTIVATION IN RETINAL ECS.	119
FIGURE 17: NRP1 LOSS CAUSES ERK1/2 ACTIVATION IN AORTIC ECS.	120
FIGURE 18: NRP1 REGULATES THE EXPRESSION OF SRF AND MRTFA TRANSCRIPTION FACTORS.	122
FIGURE 19: LOSS OF NRP1 INDUCES SRF EXPRESSION IN POSTNATAL RETINA.	124
FIGURE 20: NRP1 REGULATES SRF EXPRESSION IN AORTIC ECS.	125

FIGURE 21: NRP1 REGULATES THE EXPRESSION OF SRF TARGETED GENES.	129
FIGURE 22: NRP1 AND PSFK ARE LOCALISED ON THE CELL PERIPHERY OF HUVEC.	140
FIGURE 23: NRP1 LOCALISES ON THE CELL PERIPHERY OF HDMEC.	142
FIGURE 24: NRP1 PROMOTES VEGF165-INDUCED SFK ACTIVATION IN HDMEC.	144
FIGURE 25: NRP1 LOSS IMPAIRS VEGF165-INDUCED SFK ACTIVATION IN HDMEC.	147
FIGURE 26: VEGFR2 AND NRP1 ARE REQUIRED FOR VEGF165-INDUCED SFK ACTIVATION.	150
FIGURE 27: ABL1 MEDIATES NRP1-DEPENDENT SFK ACTIVATION.	152
FIGURE 28: ABL KINASES ARE REQUIRED FOR VEGF165-INDUCED SFK ACTIVATION.	154
FIGURE 29: DOUBLE KNOCKDOWN FOR ABL1 AND ABL2 ABOLISHED CRKL ACTIVATION AND REDUCED PSFK.	156
FIGURE 30: LOSS OF NRP1 IMPAIRS VEGF-INDUCED FAK ACTIVATION IN HDMEC.	158
FIGURE 31: NCD LOSS IMPAIRS VEGF164-INDUCED SFK ACTIVATION IN THE MOUSE.	160
FIGURE 32: NCD LOSS DOES NOT AFFECT CDH5 LOCALISATION IN THE MOUSE.	162
FIGURE 33: SCHEMATIC REPRESENTATION OF NRP1 ROLE IN PERMEABILITY.	171
FIGURE 34: SCHEMATIC REPRESENTATION OF NRP1 ROLES IN VESSEL GROWTH AND PERMEABILITY.	174

ABBREVIATIONS

A	alanine
AJ	adherens junctions
ALK1 (or ACVRL1)	Activin a receptor like type 1
AMD	age related macular degeneration
Arf6	ADP-ribosylation factor 6
BBB	blood-brain barrier
Bcar1	Breast cancer anti-estrogen resistance 1
BECS	Brain Endothelial Cells
bp	base
BSA	bovine serum albumin
CAV-1	Caveolin-1
CDH5	VE-cadherin
cDNA	complementary DNA
ChIP	chromatin immunoprecipitation
CRKL	CRK like proto-oncogene
Csf1	Colony stimulating factor 1
DAPI	4'-6'diamidino-2-phenylindole
Diap1	Diaphanous homolog 1 (Drosophila)
DMEM	Dulbecco's modified eagle medium
DNA	deoxyribonucleic acid
DNase	deoxyribonuclease
dNTP	deoxynucleoside triphosphate
DTT	dithiothreitol

E	embryonic day
ECs	endothelial cells
ECM	extracellular matrix
EDTA	ethyldiaminotetraacetic acid, disodium salt
EGF	Epidermal Growth Factor
EGR1	Early Growth Response 1
Enah	Enabled homolog (Drosophila)
ENG	endoglin
eNOS	endothelial Nitric Oxide Synthase
FA	focal adhesion
FACS	fluorescence-activated cell sorting
F-actin	filamentous-actin
FAK	Focal Adhesion Kinase
FAT	focal adhesion targeting
FBS	foetal bovine serum
Fgf2	Fibroblast growth factor 2
FLNA	Filamin A
FMO	fluorescence-minus-one
FN	fibronectin
FOS	FBJ murine osteosarcoma viral oncogene homolog
GEFs	guanine nucleotide exchange factors
h	hour
HCl	hydrochloric acid
HDMEC	Human Dermal Microvascular Endothelial Cell
Hgf	Hepatocyte growth factor
HUVEC	Human Umbilical Vein Endothelial Cell

IB4	Isolectin B4 (<i>bandeirea simplicifolia</i>)
ICAM2	Intercellular Adhesion Molecule 2
Igf1	Insulin-like growth factor 1
ITGB1	Integrin Beta 1
Itga4	Integrin alpha 4
Itgb3	Integrin beta 3
JAMs	junctional adhesion molecules
JUN	Jun proto-oncogene
kb	kilobase
l	litre
LIMK	LIM domain kinase
Limk1	LIM-domain containing, protein kinase
M	molar
m	milli
MACS	magnetic-activated cell sorting
MAPK	Mitogen-activated protein kinase
min	minute
MLEC	Mouse Lung Endothelial Cell
Mmp2	Matrix metalloproteinase 2
mRNA	messenger RNA
MRTFs	Myocardin-related Transcription Factors
MYH10	Myosin heavy chain 10
MYH9	Myosin Heavy Chain 9
MYL9	Myosin light chain 9
Mylk	Myosin, light polypeptide kinase
NEAA	non-essential amino acids

NGS	normal goat serum
NO	nitric oxide
NRP1/2	Neuropilin 1/2
PBS	phosphate buffered saline
PBT	1X PBS + Triton X-100
PCR	polymerase chain reaction
PECAM1	Platelet Endothelial Cell Adhesion Molecule 1
PFA	paraformaldehyde
PI3K	Phosphoinositide 3-kinase
Ptk2	PTK2 protein tyrosine kinase 2
Ptk2b	PTK2 protein tyrosine kinase 2 beta
Ptpn1	Protein tyrosine phosphatase, non-receptor type 1
PXN	Paxillin
qRT-PCR	quantitative real-time PCR
RAP	retinal angiomatous proliferation
RGC	retinal ganglion cells
RNA	ribonucleic acid
RNAse	ribonuclease
Rock1	Rho-associated coiled-coil containing protein kinase 1
rpm	rotations per minute
RT	room temperature
SDS	sodium dodecyl sulphate
SEMA3	class III Semaphorin
SFKs	SRC family kinases
SH2D2A (or TSA _d)	SH2 domain-containing protein 2A
Sh3pxd2a	SH3 and PX domains 2A

SMC	Smooth Muscle Cell
SNP	single-nucleotide polymorphism
SRF	Serum Response Factor
TAE	tris acetate EDTA
TCF	Ternary Complex Factor
TF	transcription factor
TGFB1	Transforming Growth Factor Beta 1
TGFBR1	Transforming Growth Factor Beta Receptor 1
TGFBR2	Transforming Growth Factor Beta Receptor 2
TJ	tight junctions
TLN	Talin
Tris	tris (hydroxymethyl) aminomethane
VEGF	Vascular Endothelial Growth Factor
Vegfa	Vascular endothelial growth factor A
VE-PTP	Vascular Endothelial Protein Tyrosine Phosphatase
(v/v)	volume to volume ratio
VVOs	vesiculo-vacuolar organelles
WASP	Wiskott-Aldrich syndrome protein
(w/v)	weight to volume ratio
Y	tyrosine
ZO-1	zona occludens protein 1
ZO-2	zona occludens protein2
μ	micro

Chapter 1 Introduction

The cardiovascular system is the first organ system to develop during embryogenesis in vertebrates. Vasculogenesis enables the creation of new blood vessels from angioblasts, whilst angiogenesis subsequently expands these blood vessels, through vessel sprouting, into a vast network capable of sustaining tissue metabolism. Angiogenic vessel sprouts are composed of endothelial tip cells that lead the growing sprouts and endothelial stalk cells that form the lumen and proliferate [e.g.(Gerhardt et al., 2003)]. In addition to expanding the vasculature by infiltrating host tissues, the vessel sprouts have to fuse to each other to add new perfused circuits to the expanding plexus. Vascular endothelial growth factor (VEGF) signalling and extracellular matrix (ECM) signalling via integrins are thought to be coordinated to control endothelial cells (ECs) behaviour, especially during angiogenesis when the blood vessels need to invade into tissues.

Under physiological conditions, angiogenesis occurs during embryonic and perinatal development. In contrast, the endothelium is usually quiescent in adults and becomes proliferative again only in specific circumstances, for example in the cycling uterus and during pregnancy, or during wound healing and other pathological conditions [reviewed in (Chung and Ferrara, 2011, Hoeben et al., 2004)]. For example, in diseases with tissue ischemia, such as diabetic retinopathy, wet age-related macular degeneration (AMD) or cancer, hypoxic cells trigger the formation of new blood vessels to increase their supply of nutrients and oxygen, which typically involves upregulation of VEGF (Chung and Ferrara, 2011). However, an excess of VEGF also increases vascular permeability to pathological levels, and accordingly, it was first identified as a vascular permeability factor (Senger et al., 1983).

The transmembrane protein neuropilin (NRP) 1 is expressed in the vascular endothelium to modulate responses to promote angiogenesis and vascular permeability. Here, I will introduce VEGF and I will describe the role of NRP1 in angiogenesis and permeability. Also, I will explain NRP1's possible links with transcription networks in ECs, including its interaction with several distinct ligands and other receptors that regulate endothelial cell behaviour.

1.1 VEGF: isoforms and receptors

Several different molecules stimulate the proliferation or migration of the ECs that line all blood vessels and also form the heart endocardium. Amongst these, the vascular endothelial growth factor VEGFA (referred to in short as VEGF) is essential for all stages of cardiovascular development or vascular pathology (Ruhrberg, 2003). VEGF exists in three major forms that are produced by alternative splicing and termed VEGF121, VEGF165 and VEGF189 in humans (or VEGF120, VEGF164 and VEGF188 in mice). The name refers to the number of amino acids in the mature protein (Ruhrberg, 2003). The VEGF isoforms have a differential affinity for extracellular matrix (ECM) scaffolds, allowing them to establish growth factor gradients for blood vessel guidance (Ruhrberg et al., 2002). Thus, growth factor and matrix signals are coordinated to ensure proliferation and migration of ECs during physiological angiogenesis.

VEGF is a key mediator of both physiological and pathological angiogenesis and a validated target for anti-angiogenesis therapy in the clinic (Welti et al., 2013, Kim and D'Amore, 2012). However, long-term anti-VEGF treatment has been proposed to pose likely risks, as pre-clinical studies for several different eye diseases revealed excessive neuronal cell death in the retina after VEGF blockade (Saint-Geniez et al., 2008, Nishijima et al., 2007). These considerations highlight the need to identify effective anti-angiogenesis therapies that are based on VEGF independent targets and can be used in combination with or independently of anti-VEGF therapy to improve outcome for patients.

All VEGF isoforms bind the receptor tyrosine kinases VEGFR1 (also known as FLT1) and VEGFR2 (also called KDR or FLK1). VEGFR2 is the pre-dominant signalling receptor in ECs and induces differentiation, proliferation and survival of ECs; in contrast, VEGFR1 mainly serves as a VEGF trap to modulate local VEGF bioavailability and fine tune growth factor stimulation (Koch et al., 2011). VEGF165 also binds NRP1, a non-catalytic transmembrane protein, and induces complex formation with VEGFR2 (Koch et al., 2011). Most models suggest that complex formation of NRP1 and VEGFR2 after VEGF165 binding enhances VEGFR2 signalling in ECs [e.g. (Soker et al., 2002a, Whitaker et al., 2001)]. This complex is

indeed required for arteriogenesis (Lanahan et al., 2013a), but appears to be dispensable for physiological and pathological angiogenesis (Fantin et al., 2014, Gelfand et al., 2014). As of the start of my thesis research, the specific role of NRP1 in angiogenesis therefore was not yet defined.

1.2 Domain structure of NRP1 and NRP2

The neuropilins NRP1 and NRP2 are single pass transmembrane glycoproteins with a large extracellular domain of 840 amino acid residues, a short transmembrane domain and a cytoplasmic tail of 40 residues [reviewed in (Schwarz and Ruhrberg, 2010)]. NRP1 is thought to lack catalytic activity, but its intracellular domain interacts with an adaptor protein named synectin or GIPC1 [reviewed in (Schwarz and Ruhrberg, 2010)] to promote endocytic trafficking (Salikhova et al., 2008, Ballmer-Hofer et al., 2011, Lanahan et al., 2013a). Initially, NRP1 expression was discovered in neurons as an adhesion receptor (Schwarz and Ruhrberg, 2010), but its specific angiogenic adhesion ligands have not yet been identified. Subsequently, NRP1 was shown to be a receptor for the class 3 semaphorin SEMA3A, a secreted glycoprotein that regulates axon guidance, and then as a receptor for an isoform of VEGF termed VEGF165 [reviewed in (Schwarz and Ruhrberg, 2010)] (**Fig. 1**). NRP2 has 44% homology to NRP1, a similar domain organisation and binding sites for SEMA3F and VEGF145 [reviewed in (Schwarz and Ruhrberg, 2010)].

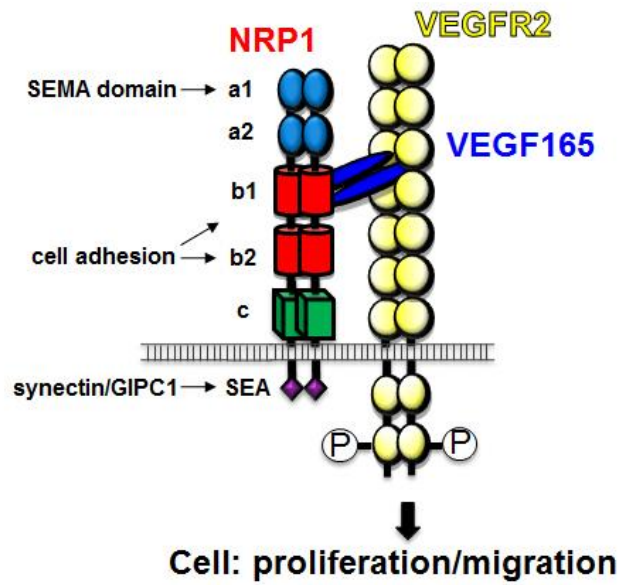


Figure 1: NRP1 domains and its interaction with VEGFR2.

NRP1 is a transmembrane protein and contains a mosaic of extracellular domains with distinct ligand specificities and a cytoplasmic tail that binds syndectin through the SEA motif. VEGF165 binds NRP1 and induces complex formation with VEGFR2 to promote cell proliferation and survival.

1.3 Essential role for NRP1 in developmental angiogenesis

During embryonic development and in the early postnatal period, NRP1 is prominent on developing blood vessels, for example in the hindbrain and retina (Fantin et al., 2013b, Fantin et al., 2011). A role for NRP1 in vasculature was initially identified through its transgenic overexpression in mice, which increased the number of capillaries, but also caused haemorrhages (Kitsukawa et al., 1995). Subsequently, loss of NRP1 was shown to impair vessel sprouting into the brain and spinal cord of mice (Fantin et al., 2013a, Gerhardt et al., 2004, Kawasaki et al., 1999). The morpholino-mediated knockdown of either of the two zebrafish NRP1 homologs, *Nrp1a* or *Nrp1b*, was also reported to impair vessel sprouting and arteriovenous patterning (Lee et al., 2002, Martyn and Schulte-Merker, 2004, Wang et al., 2006a), although these observations were subsequently questioned when a transgenic *Nrp1a*-mutant fish was created by programmable site-specific nucleases and found to not have a phenotype (Kok et al., 2015).

During angiogenesis, NRP1 is not only expressed in endothelial cells, but also in other cell types; for example, neural progenitors and tissue macrophages express NRP1 alongside sprouting vessels in the mouse embryo hindbrain (Fantin et al., 2010, Fantin et al., 2013a). The brain vessel defects of NRP1 knockouts might therefore be due to an additive effect of NRP1 loss from both endothelial and non-endothelial cells. However, experiments using Cre-LoxP technology in mice to create cell-type specific *Nrp1* null mutants revealed that NRP1 is exclusively required in endothelial rather than non-endothelial cells for brain angiogenesis (Fantin et al., 2013a, Fantin et al., 2013b). Interestingly, incomplete endothelial Cre-LoxP recombination in these experiments resulted in mosaic hindbrain vessels containing both NRP1-positive and NRP1-negative endothelial cells, with NRP1-retaining cells being enriched in the tip, but not stalk cell position (Fantin et al., 2013a) (**Fig. 2**). These observations predict a role for NRP1 during sprouting angiogenesis in endothelial cell migration, as this is a tip cell function, but not proliferation, which is a stalk cell function. In agreement with this idea, NRP1 is not essential for endothelial cell proliferation in the developing yolk sac, even though it is required for yolk sac angiogenesis, as least in C57/Bl6 mice (Jones et al., 2008). In addition to its role in developmental angiogenesis, NRP1 has been implicated in

tumour angiogenesis, with NRP1 expression reported for both tumour vasculature and cancer cells [reviewed in (Raimondi and Ruhrberg, 2013)].

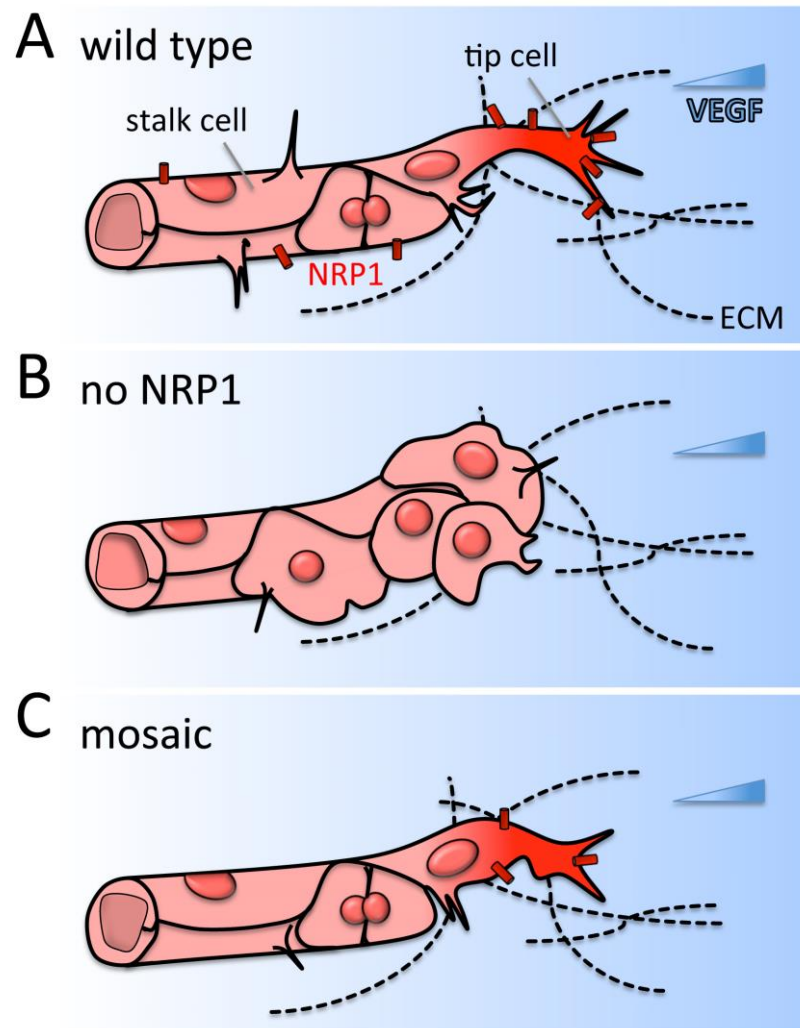


Figure 2: Role of NRP1 in angiogenesis.

(A) NRP1 is expressed in tip and stalk cells of the vessel that extend filopodia to migrate towards VEGF and ECM signals. (B) Lack of endothelial NRP1 leads to the formation of vessels with impaired filopodia and blind-ended vascular tufts. (C) Mosaic targeting of endothelial NRP1 showed that cells that express NRP1 adopt a tip rather than a stalk position in vessel sprouts [figure taken from a book chapter (Brash et al., 2017)]

1.4 NRP1 ligands in angiogenesis: SEMA3A

Even though SEMA3A can bind NRP1 on embryonic blood vessels, mice lacking SEMA3A or semaphorin signalling through both neuropilins have normal embryonic angiogenesis in all organs examined [e.g. (Vieira et al., 2007, Gu et al., 2005, Bouvree et al., 2012)]. Moreover, mice lacking both SEMA3A and VEGF165 have similar defects in brain vascular patterning as mice lacking VEGF165 only (Vieira et al., 2007). These findings suggest that SEMA3A and semaphorin signalling through neuropilins are not essential for angiogenesis in mouse embryos (Vieira et al., 2007, Gu et al., 2003). However, studies in chick and fish have suggested that SEMA3A signalling through NRP1 regulates vascular development (Acevedo et al., 2008, Shoji et al., 2003, Torres-Vazquez et al., 2004). Thus, exogenous SEMA3A inhibits VEGF-induced angiogenesis in the chick chorioallantoic membrane by inhibiting the VEGF-induced activation of the focal adhesion kinase FAK and the cellular homolog of the ROUS sarcoma kinase, SRC, two intracellular proteins that promote angiogenesis via cytoskeletal remodelling (Acevedo et al., 2008). Moreover, morpholino-induced knockdown of the *sema3a1* or *sema3a2* homologs in fish inhibits intersomitic vessel sprouting (Shoji et al., 2003, Torres-Vazquez et al., 2004). Accordingly, different conclusions regarding the role of semaphorin signalling have been reached depending on the species studied, with no obvious role for SEMA3A signalling in developmental angiogenesis in mice. In contrast, SEMA3A plays an important role in the murine lymphatic system by promoting lymphatic valve development through its interaction with NRP1 and PLXNA1 (Bouvree et al., 2012, Jurisic et al., 2012).

Despite being dispensable for developmental angiogenesis, SEMA3A regulates pathological angiogenesis in mice, for example in mice with oxygen-induced retinopathy (OIR). In this model, neonatal mice are exposed to a high oxygen atmosphere for 5 days and then returned to normoxia; hyperoxia causes vessel regression in the retina, and the resulting vasculature is unable to sustain retinal metabolism on return to normoxia, causing inflammation and the upregulation of excessive and abnormal vessel growth. Under these conditions, SEMA3A is secreted from neurons in the avascular retina in response to the cytokine IL-1 β and creates a repulsive barrier that forces sprouting vessels to grow ectopically towards the

vitreous. In agreement with these findings, endothelial cells treated with conditioned medium from hypoxic retinal ganglion cells (RGC), which secrete SEMA3A, show cytoskeletal rearrangements and loss of stress fibres (Joyal et al., 2011). In contrast, SEMA3A inhibition enabled normal neovascularisation within the hypoxic retina in this model, promoting regeneration of neural tissue and improving retinal function (Joyal et al., 2011).

SEMA3A also regulates tumour angiogenesis in cancer models. Initially, SEMA3A expression induces endothelial cell apoptosis, which correlates with inhibition of tumour angiogenesis and cancer growth, but SEMA3A subsequently supports vascular normalisation by promoting pericyte coverage of tumour vessels and reducing vessel leakiness (Casazza et al., 2011, Maione et al., 2009). SEMA3A can also indirectly induce the maturation of tumour vessels by recruiting NRP1-expressing monocytes, which then secrete growth factors such as TGF β and PDGF β to attract pericytes involved in vessel maturation (Carrer et al., 2012, Zacchigna et al., 2008).

1.5 NRP1 ligands in angiogenesis: VEGF165

As NRP1 was first identified as a co-receptor for the VEGF receptor tyrosine kinase VEGFR2 in endothelial cells upon VEGF165 stimulation (Soker et al., 1998), the exclusive explanation for the angiogenic defects of *Nrp1* knockout mice was initially thought to be disrupted VEGF signalling [reviewed in (Raimondi et al., 2016)] Several lines of evidence were obtained that support this hypothesis, including *in vitro* studies of porcine aortic endothelial cells (PAE), which endogenously lack VEGFR2 and NRP1, but can be transfected with expression plasmids for one or both of these receptors to establish the relative contribution of both receptors to VEGF signalling (Soker et al., 1998). In these cells, VEGF-stimulated, VEGFR2-mediated activation of the extracellular signal-regulated kinase 1/2 (ERK1/2) and p38MAPK signalling and chemotaxis was enhanced by NRP1 (Becker et al., 2005, Soker et al., 1998). In cultured embryoid bodies, VEGF also requires NRP1 to activate p38 MAPK kinase, whose inhibition attenuates angiogenesis (Kawamura et al., 2008). To test the relevance of VEGF binding to NRP1 for angiogenesis, knock-in mice expressing NRP1 carrying a tyrosine (Y) 297 substitution to alanine (A) were

generated [*Nrp1*^{Y297A/Y297A} mice; (Fantin et al., 2014)]. This mutation had previously been shown to disrupt VEGF binding to NRP1 (Herzog et al., 2011a). Unexpectedly, the *Nrp1*^{Y297A/Y297A} mice lacking VEGF binding to NRP1 had much milder angiogenesis defects than full *Nrp1* knockouts or endothelial-specific *Nrp1* knockouts (Fantin et al., 2014). In fact, the knockin *Nrp1*^{Y297A} mutation additionally caused a reduced NRP1 expression by approximate 40%, and it is likely that the mild embryonic angiogenesis defects of *Nrp1*^{Y297A/Y297A} mouse embryos are at least partly caused by low NRP1 expression levels rather than defective VEGF binding to NRP1 (Fantin et al., 2014). Another study using mice with a different point mutation (D320K mutation) in the VEGF164 binding site and normal NRP1 expression showed normal embryonic angiogenesis when VEGF binding to NRP1 is lost (Gelfand et al., 2014).

The absence of severe angiogenesis defects in *Nrp1*^{Y297A/Y297A} and *Nrp1*^{D320K/D320K} embryos agreed with prior findings in *Vegfa*^{120/120} mouse embryos, which lack VEGF164 because they express only the VEGF120 isoform. Thus, the *Vegfa*^{120/120} mutation causes a milder reduction in vessel branching together with increased vascular diameter in the embryonic day (E) mouse 12.5 brain, rather than the near complete loss of vessel branching seen in *Nrp1*-null mutants (Ruhrberg et al., 2002, Gerhardt et al., 2004). In fact, the vascular defects in *Vegfa*^{120/120} mouse embryo hindbrains are more likely caused by changes in the extracellular localisation of different VEGF isoforms rather than isoform-specific signalling through NRP1. Thus, VEGF120 lacks the domains that confer extracellular matrix binding in VEGF165 and the larger VEGF189 isoform, but are important to establish VEGF gradients for chemotaxis and vessel sprouting (Ruhrberg et al., 2002, Gerhardt et al., 2003).

Even though *Nrp1*^{Y297A/Y297A} and *Nrp1*^{D320K/D320K} mice have only mild defects or not in embryonic angiogenesis, they have angiogenesis and arteriogenesis defects in the perinatal retina and heart (Fantin et al., 2014, Gelfand et al., 2014), suggesting a role in postnatal vascular development. Moreover, VEGF165 binding to NRP1 may be important for pathological neovascularisation, as the OIR response of mouse pups is attenuated in *Nrp1*^{Y297A/Y297A} mice and their tumour growth is delayed (Fantin et al., 2014). In summary, these findings suggest that VEGF165 binding to NRP1 is largely

dispensable for embryonic angiogenesis, but may be important for postnatal developmental and pathological angiogenesis. The analysis of vascular defects in *Nrp1*^{Y297A/Y297A} and *Nrp1*^{D320K/D320K} mice together with the comparison of full *Nrp1* knockout and *Vegfa*^{120/120} mice suggested that NRP1 additionally functions in angiogenesis in a VEGF-independent pathway.

1.6 NRP1 ligands in angiogenesis: unidentified adhesion molecules

NRP1 was first described as an adhesion molecule (Takagi et al., 1995) in the nervous system. It is not known whether NRP1 controls the interactions of blood vessels with their environment through the regulation of adhesive intercellular interactions or the control of cell-matrix adhesion during angiogenesis *in vivo*, but the domains that enable NRP1 to modulate adhesion to unidentified proteins on neighbouring cell have been shown to reside in the b1 and b2 domains (Shimizu et al., 2000).

In vitro studies support the idea that NRP1 promotes intercellular adhesion through homophilic interactions (West et al., 2005) or heterophilic adhesion *in trans* (Takagi et al., 1995). There are several candidate adhesion partners for NRP1 such as L1CAM and NrCAM. L1CAM associates with NRP1 in neurons, and NrCAM overlaps functionally with L1CAM in the nervous system and has also been identified in two screens for genes upregulated during angiogenesis (Castellani et al., 2002, Aitkenhead et al., 2002, Glienke et al., 2000). However, preliminary data in the Ruhrberg lab suggest that mice lacking L1CAM and NrCAM do not have angiogenesis defects (J. M. Vieira and C. Ruhrberg, unpublished observations). *In vitro* studies on ECs showed that NRP1 increases cell-matrix attachment (Murga et al., 2005), but others reported that blocking NRP1 function *in vitro* does not impair endothelial cell adhesion to fibronectin (FN) (Pan et al., 2007a). One report showed that NRP1 enhances FN assembly by promoting integrin turnover in a mechanism depending on its cytoplasmic domain (Valdembri et al., 2009).

1.7 NRP1 signalling in endothelial cells: association with co-receptors

Because NRP1 is a non-catalytic transmembrane protein, it interacts with co-receptors to transduce downstream signals. Thus, in neurons, NRP1 associates with

plexins to transduce semaphorin signals [reviewed in (Schwarz and Ruhrberg, 2010)], whilst in endothelial cells, NRP1 interacts with VEGFR1 or VEGFR2 (Soker et al., 1998). In circumstances where endothelial cells respond to class 3 semaphorins, it is therefore expected that a plexin co-receptor should be involved in signal transduction. This has, for example, been proposed for SEMA3A/NRP1-mediated vascular permeability signalling (Acevedo et al., 2008). Interestingly, NRP1 can also form a tripartite complex with PLXND1 and VEGFR2 to transduce semaphorin signals in neurons (Bellon et al., 2010, Cariboni et al., 2015), but such a complex has not yet been demonstrated in endothelial cells. Instead, in VEGF165-stimulated endothelial cells NRP1 is thought to preferentially complex with VEGFR2 via a VEGF165 bridge.

Conceptually, VEGF165-bound NRP1 may interact with VEGFR2 in *cis*, when the same endothelial cell co-expresses both receptors, or in *trans*, when one endothelial cell expresses VEGFR2 and another endothelial or non-endothelial cell expresses NRP1. Accordingly, it has been suggested that endothelial VEGFR2 interacts with NRP1 on tumour cells *in trans* (Soker et al., 2002b). A recent study with PAE cells showed that NRP1/VEGFR2 *trans* interaction decreases the activation of endothelial VEGFR2, prevents VEGFR2 endocytosis and suppresses tumour angiogenesis; in contrast, *cis* interaction induces rapid NRP1/VEGFR2 complex formation and initiation of signal transduction through PLC γ and ERK1/2 (Koch et al., 2014). Moreover, this pathway was important for tumour initiation by regulating the early steps in tumour vascularisation, but was not important at the later stages of tumour vascularisation (Koch et al., 2014). In contrast, our recent work in the mouse embryo hindbrain angiogenesis excluded the possibility of a *trans* interaction between non-endothelial NRP1 and endothelial VEGFR2 in developmental angiogenesis; thus, hindbrain vessels express VEGFR2, but loss of NRP1 function from neural progenitors or macrophages did not impair angiogenesis in this organ [see above; (Fantin et al., 2013a)].

Whilst VEGF165 is the main VEGF isoform that binds NRP1, VEGF121 can also bind NRP1, at least *in vitro* and with much lower affinity (Parker et al., 2012, Pan et al., 2007b). Unlike VEGF165, VEGF121 binding to NRP1 cannot induce the formation of an extracellular bridge between NRP1 and VEGFR2 to enhance

VEGFR2 signal transduction [e.g. (Prahst et al., 2008, Becker et al., 2005, Soker et al., 2002b, Soker et al., 1998)]. Moreover, the physiological or pathological significance of low affinity VEGF₁₂₁-binding to NRP1 is unknown. Importantly, expression of VEGF₁₂₀ at the expense of VEGF₁₆₄ in mice causes similar defects as loss of NRP1 in the nervous system [e.g. (Erskine et al., 2011)], arguing against an essential physiological role for VEGF₁₂₀ binding to NRP1 in mice.

1.8 NRP1 as a regulator of TGF β signalling

The cytokines TGF β ₁, TGF β ₂ and TGF β ₃ regulate migration, proliferation and apoptosis in various cell types (Deininger et al., 2005). Studies in T-cells suggest that the latent and activated forms of TGF β ₁ bind to NRP1 at the site that also interacts with VEGF₁₆₅, and that soluble NRP1 activates latent TGF β ₁ (Glinka and Prud'homme, 2008). In breast cancer cells, NRP1 also interacts with the TGF β receptors TGF β R1 and TGF β R2 to activate their effectors SMAD2 and SMAD3 (Glinka et al., 2011). In contrast, two recent studies suggested that NRP1 dampens endothelial TGF β signalling via both the SMAD2/3 and the SMAD1/5/8 pathways (Aspalter et al., 2015, Hirota et al., 2015). In particular, it was demonstrated that NRP1-mediated suppression of TGF β signalling promotes the tip cell phenotype and therefore blood vessel growth during retinal angiogenesis (Aspalter et al., 2015). Moreover, DLL4 in endothelial tip cells activates notch signalling in neighbouring endothelial cells to downregulate NRP1 and thereby induces excessive TGF β signalling and stalk cell behaviour (Aspalter et al., 2015). Endothelial NRP1 loss also increases TGF β signalling via SMAD2/3 in the mouse embryo hindbrain (Hirota et al., 2015). Interestingly, *in vitro* and genetic mouse studies suggest that neuroepithelial integrin β 8 interacts with endothelial NRP1 in *trans* and reduces endothelial SMAD2/3 activation by maintaining TGF β at the inactive latent form (Hirota et al., 2015). It is not known whether these opposing roles can be explained by a direct integrin-NRP1 interaction, their competition for binding to latent TGF β and/or additional roles for NRP1 in regulating TGF β receptor activation, receptor levels or the expression of TGF β pathway genes.

1.9 NRP1 associates with the cytoplasmic adaptor synectin to regulate VEGFR2 trafficking for VEGF-induced arteriogenesis

In vitro studies suggested that the NRP1 cytoplasmic tail and its interactor synectin are required for complex formation between NRP1 and VEGFR2 (Prahst et al., 2008). To understand the mechanistic role of the NRP1 interaction with VEGFR2, PAE cells lacking endogenous VEGFR2 expression were co-transfected with expression vectors for VEGFR2 and several different, fluorophore-linked RAB proteins. The analysis of co-localisation of the over-expressed proteins showed that synectin binding to the NRP1 cytoplasmic tail promotes VEGF165-stimulated VEGFR2 trafficking into different subsets of endocytic vesicles distinguished by specific RAB proteins (Ballmer-Hofer et al., 2011). Another study showed that cultured arterial endothelial cells from mice lacking the NRP1 cytoplasmic tail showed an enrichment of VEGFR2 in RAB5+ endosomes and decreased entry of VEGFR2 into EAA1+ endosomes after VEGF165 stimulation, and this defect was associated with reduced ERK1/2 signalling (Lanahan et al., 2013a). This NRP1-cytoplasmic tail dependent pathway was essential for the formation of a normal number of arterioles in several different organs examined (Lanahan et al., 2013a). In contrast, the cytoplasmic NRP1 tail is dispensable for both developmental and pathological angiogenesis in mice (Fantin et al., 2011, Lanahan et al., 2013a).

Whilst the NRP1 cytoplasmic tail is dispensable for angiogenesis in mice (Fantin et al., 2011), different results have been obtained in zebrafish studies. Thus, NRP1 lacking the SEA motif of the cytoplasmic domain (Wang et al., 2006a) cannot rescue the defective dorsal migration of intersomitic vessels after *Nrp1* knockdown with morpholinos, and knockdown of synectin with morpholinos causes similar defects (Chittenden et al., 2006). It has not been resolved why intersomitic sprouting in fish might be compromised by loss of the NRP1 cytoplasmic tail, but appears normal in mice. One possibility may be that these vessels in the fish have a stronger arterial character and/or depend on specific VEGFR2 trafficking pathways that are regulated by NRP1. Alternatively, morpholino-induced toxicity may have caused defects in vascular development in these studies that are unrelated to the function of the targeted gene (Kok et al., 2015).

1.10 VEGFR2-independent NRP1 signalling in endothelial cells

Tissue culture studies have suggested that NRP1 promotes cell motility independently of VEGFR2. For example, fusion of the extracellular domain of the epidermal growth factor (EGF) receptor to the transmembrane and cytoplasmic domains of NRP1 creates a chimeric receptor that promotes the migration of EGF-stimulated endothelial cells (Wang et al., 2003). Another study shows that loss of NRP1, but not VEGFR2, inhibits ECs adhesion and spreading of HUVEC on FN (Murga et al., 2005). Also, the cytoplasmic NRP1 domain promotes FN fibrillogenesis in arterial ECs by regulating endosomal trafficking of activated $\alpha 5\beta 1$ integrin (Valdembri et al., 2009) and is involved in ABL1-mediated FN fibrillogenesis in myofibroblasts (Yaqoob et al., 2012). However, NRP1 cytoplasmic domain-mediated signal transduction pathways or integrin endocytosis are unlikely to play major roles in angiogenesis, because genetic mouse studies showed that this NRP1 domain is dispensable for physiological and pathological angiogenesis (Fantin et al., 2011, Lanahan et al., 2013a). Surprisingly, the intracellular pathways that may be regulated by NRP1 in a VEGF/VEGFR2-independent fashion have not yet been defined.

1.11 Integrin activation and signalling mechanisms

Integrins are family of transmembrane proteins that are heterodimers of one α and one β chain (Humphries et al., 2006). There are 24 distinct integrin heterodimers, which are formed by different combinations of 18 α and 8 β subunits (Hynes, 2002). Each heterodimer has a large extracellular domain, a transmembrane domain and a short cytoplasmic domain; the extracellular domain binds proteins such as ECM glycoproteins, including collagens, fibronectins and laminins (Hynes, 2002).

As ECM receptors, integrins promote cell attachment and migration by modulating cell-matrix contacts and the actin cytoskeleton (Arnaout et al., 2005). They have no kinase activity, but they provide a link between ECM and actin cytoskeleton. They get activated by a combination of internal signals, which induce conformational changes of integrins, and external signals, i.e. ligands that bind to the receptors. More specifically, the transmembrane and cytoplasmic domains of the subunits are closely associated when integrins are in an inactive, stable state (Arnaout et al., 2007). Then,

in response to intracellular signals, talin and kindlin proteins bind to the β subunit of the heterodimer and activate integrins at an intermediate stage (Calderwood et al., 2003, Montanez et al., 2008). At this stage, the cytoplasmic and transmembrane subunits of the integrins are separated and the extracellular domain is extended to bind to the ligand (Wegener and Campbell, 2008). This conformational change is also known as affinity modulation and occurs before avidity modulation, which is the final step of activation, when the integrins bind to the ligands and cluster at the plasma membrane (Plow et al., 2014).

Upon activation, integrins associate to filamentous (F)-actin, regulate focal adhesion growth, actin polymerization and cytoskeletal dynamics. Different focal adhesion proteins mediate the linkage between integrins and actin and can be divided into groups depending on their binding to integrins or the actin cytoskeleton. Thus, proteins such as talin, filamin and α -actinin bind directly to integrins and F-actin, while others like kindlin, paxillin and FAK bind to integrins and indirectly associate with the actin cytoskeleton. Also, there are proteins such as vinculin, which do not bind to integrins, but are important regulators of focal adhesions (Legate et al., 2009). In addition to regulating focal adhesions, integrins mediate the activation of RHO-GTPases to promote actin remodelling. Below I describe in detail molecules that are involved in focal adhesion formation, cytoskeletal dynamics and signal transduction downstream of integrins.

Paxillin (PXN)

Paxillin is a focal adhesion protein that is detected at the early focal adhesions. Studies have shown that paxillin links talin and α integrins, creating a stable interaction between integrins and the actin cytoskeleton (Alon et al., 2005).

Focal adhesion kinase (FAK)

FAK is an ubiquitously expressed protein tyrosine kinase that is composed of an N-terminal FERM domain that binds to integrins and growth factors receptors, a kinase domain, proline rich regions and the C-terminal focal adhesion targeting (FAT) domain which contains paxillin and talin binding sites (Schaller, 2001). FAK is a

signalling protein that has been shown to bind to β integrins *in vitro* via its N-terminal domain (Schaller et al., 1995), but evidence from *in vivo* studies has shown that FAK associates with integrins indirectly by binding to integrin-associated proteins such as paxillin (Hayashi et al., 2002). While FAK is dispensable for the initial connection of integrins to the actin cytoskeleton and the formation of the first focal adhesion (FA), it is required to promote the maturation and the turnover of focal adhesion (Parsons, 2003, Ilic et al., 1995). It is known that FAK mediates the phosphorylation of α -actinin, which increases its affinity for actin (Izaguirre et al., 2001).

FAK can be activated via either ECM stimuli or growth factors, and this leads to tyrosine phosphorylation of FAK and activation of downstream signals. The C-terminal domain of FAK contains two proline-rich regions that function as binding sites for SRC-homology (SH)3 domain containing proteins (Mitra et al., 2005). The most well characterised phosphorylation site of FAK is the autophosphorylation site of FAK at the Y397 (Toutant et al., 2002), which then binds SH2 domain containing proteins such as SRC family kinases (SFKs), phospholipase $C\gamma$ (PLC γ), p120RasGAP, the p85 subunit of phosphatidylinositol 3-kinase (PI3K) and others (Schaller, 2001).

One of the first events that have been described after integrin activation and growth factor stimulation is the association of the FAK with the SFKs. The binding of the FAK Y397 phosphorylation site to SRC mediates its conformational activation, which leads to FAK transactivation and maximal catalytic activity (Schlaepfer et al., 2004). Indeed, after SRC binding to FAK, SRC mediates the transactivation of FAK at Y576 and Y577 for FAK maximal activation (Hanks et al., 2003).

Two of the best characterised downstream targets of the FAK/SRC complex are p130Cas and paxillin (Hanks et al., 2003, Turner, 2000). More specifically, SRC binding mediates the phosphorylation of other FAK residues, which then promote the binding of other SH3-containing proteins such as p130Cas to the C-terminal proline rich regions of FAK (Hanks et al., 2003). Also, the FAK/SRC complex mediates the phosphorylation of paxillin, which then promotes the binding of the adaptor protein

CRK to it, probably regulating focal adhesion turnover and cell motility (Turner, 2000).

SRC family kinases (SFKs)

The SRC family of tyrosine kinases consists of eight members: LYN, HCK, LCK, BLK, SRC, FYN, YES1, and FGR (Parsons and Parsons, 2004). One family member, SRC, is a non-receptor tyrosine kinase that is constitutively associated with the cytoplasmic domain of $\beta 3$ integrins (de Virgilio et al., 2004) and is activated immediately after integrin ligation and clustering (Legate et al., 2009). When SRC is in a fully active configuration, the activation loop residue Y397 is phosphorylated, while the C-terminal tyrosine Y508 is dephosphorylated (Ingleby, 2008). SRC can be activated after binding to FAK, but also through direct interaction with the cytoplasmic domains of β integrins (Arias-Salgado et al., 2003).

ABL

It has been shown that integrins mediate the activation of ABL kinase after cell adhesion. More specifically, studies on fibroblasts have shown that adhesion on FN increases ABL activation and triggers the translocation of ABL from the nucleus to focal adhesions (Lewis et al., 1996a).

ABL is a non-receptor tyrosine kinase with binding domains for F-actin and DNA (Sato et al., 2012). In an inactive stage, F-actin binds to ABL and inhibits its kinase activity (Woodring et al., 2001). Cell attachment and spreading cause dissociation of ABL and F-actin, which then leads to increased ABL activation. ABL can be activated by different factors such as SFKs (Furstoss et al., 2002) or by binding to the intracellular domain of activated integrins (Sato et al., 2012, Woodring et al., 2003). The activated ABL is then localised to specific F-actin sites such as lamellipodia, membrane ruffles and focal adhesion sites (Plattner et al., 1999, Ting et al., 2001) to promote actin remodelling. After cell attachment and activation of ABL, the inhibitory effect of F-actin on ABL kinase activity might be neutralised in attached cells.

RHO-GTPases

Integrin activation can also promote actin remodelling via RHO-GTPases (Schwartz and Shattil, 2000). RHO-GTPases cycle between a GTP-bound active and a GDP-bound inactive state to regulate F-actin remodelling for filopodia extension and directional migration (Heasman and Ridley, 2008). The activity of RHO-GTPases is promoted by guanine nucleotide exchange factors (GEFs) that catalyse the exchange of GDP for GTP and inhibited by GTPase-activating proteins (GAPs) that promote GTP hydrolysis to GDP (Schwartz and Shattil, 2000). Each integrin-associated RHO-GTPase controls particular aspects of actin cytoskeleton dynamics. For instance, RAC promotes lamellipodia and RHOA actin stress fibres formation (Heasman and Ridley, 2008), whilst CDC42 stimulates filopodia extension (Lamallice et al., 2004).

CDC42 regulates cell polarity by directly binding to the Wiskott-Aldrich syndrome protein (WASP), which then activates the actin-related protein 2/3 complex (ARP2/3) and induces filopodia formation, reorientation of the microtubule-organizing centre and the Golgi in front of the nucleus (Jaffe and Hall, 2005). Binding of the activated RAC to the WAVE protein can also lead to activation of the ARP2/3 complex and the lamellipodia formation (Sadok and Marshall, 2014). Whilst CDC42 and RAC both activate the ARP2/3 complex, studies have shown that CDC42-induced filopodia formation occurs first and is followed by RAC-mediated lamellipodia formation (Guillou et al., 2008).

RHOA regulates cell contractility by activating the RHO-associated coiled-coil-containing protein kinase (ROCK) and promoting the phosphorylation of the regulatory light chain of myosin II (Sadok and Marshall, 2014). ROCK also phosphorylates the LIM domain kinase (LIMK), leading to inhibition of cofilin activity and actin filament stabilisation (Maekawa et al., 1999). RHOA can also activate the formin mDia to promote actin polymerization and microtubule stability (Fukata et al., 2003). Thus, in response to integrin activation, RHO-GTPases activate downstream signals to promote actin polymerisation and cell migration.

RHO-GTPases activity can be regulated by FAK and ABL kinases. In particular, FAK phosphorylation is linked to RHOA activation and the formation of stress fibres (Schlaepfer et al., 2004). For example, FAK activates the p190 Rho GEF in neurons to regulate axonal branching and synapse formation (Rico et al., 2004). Also, FAK phosphorylates the CDC42 effector N-WASP (Wu et al., 2004), which controls actin polymerisation through the activation of the ARP2/3 complex (Pollard, 2007). FAK phosphorylation of N-WASP, does not affect N-WASP activity, but its subcellular localisation which therefore can affect cell migration (Wu et al., 2004).

In addition to FAK, ABL1 can also induce RHO-GTPases activation. Indeed, EGF-stimulated fibroblasts showed increased ABL activation, which then induces phosphorylation of an important regulator of RAC activity, the RAS-RAC GEF SOS1 (Sini et al., 2004). In addition to the fact that ABL kinase can regulate RHO-GTPases activation directly through GEFs, it can also regulate their activity indirectly through the phosphorylation of ABL adaptor proteins. Thus, ABL-dependent CRKII phosphorylation (Feller et al., 1994) can mediate the activation of RAC and its cellular localisation (Abassi and Vuori, 2002).

1.12 Integrins and angiogenesis and their interaction with NRP1

Integrins are important regulators of angiogenesis, as integrin global or EC-specific knockout integrin mice showed vascular defects [i.e. (Tanjore et al., 2008) (Stenzel et al., 2011b)]. The $\alpha 5\beta 1$ integrin is the main FN receptor, and both integrin subunits are expressed in ECs *in vitro* and *in vivo* (Mettouchi and Meneguzzi, 2006). Loss of $\beta 1$ integrin in ECs blocks angiogenesis in mouse embryos and leads to embryonic lethality before E10.5 (Tanjore et al., 2008). Also, $\alpha 5$ -null mouse embryos showed reduced vessel branching in the cranial plexus due to impaired FN organisation (Francis et al., 2002). Inhibition of $\alpha v\beta 3$ integrin also impairs angiogenesis in chick embryos (Brooks et al., 1994). Also, studies using the retina as a model to study postnatal angiogenesis, showed that mice the endothelial deletion of *Itgb1* induces hypersprouting in postnatal retinas, while the global deletion of *Itga2* and *Itgb3* did not affect postnatal angiogenesis, and *Itga3* deletion slightly decreased the vascular density of angiogenic retina (Stenzel et al., 2011b). In addition, mice with an endothelial specific deletion of *Itgb1* displayed decreased radial vessel outgrowth,

but also increased ECs proliferation as well as increased filopodia formation and length, explaining the hypersprouting phenotype (Yamamoto et al., 2015). Another study had shown that deletion of astrocytic FN reduces radial endothelial migration during vascular plexus formation, while increases number of filopodia and branchpoints and downregulates signalling downstream of VEGFR2 through PI3K and AKT (Stenzel et al., 2011c).

NRP1 interacts with integrins *in vitro*, including the $\beta 1$ and $\beta 3$ integrin subunits (Valdembri et al., 2009, Fukasawa et al., 2007). The interaction of NRP1 with $\alpha v\beta 3$ integrin negatively regulates VEGF-mediated angiogenesis by limiting the NRP1 and VEGFR2 interaction, as demonstrated in endothelial cell wound closure assay *in vitro*, aortic ring microvessel sprouting *ex vivo* and growth factor-induced angiogenesis in $\beta 3$ -null mice (Robinson et al., 2009). Indeed, the combined effect of $\beta 3$ inhibition and NRP1 blockade reduces VEGF-mediated angiogenesis more than inhibiting each molecule individually (Robinson et al., 2009). In human umbilical artery ECs *in vitro*, NRP1 interacts with integrin $\alpha 5\beta 1$ to regulate integrin endocytosis and recycling to organise FN deposition (Valdembri et al., 2009). Whether this pathway is important for angiogenesis or arteriogenesis was not demonstrated. However, it was shown to rely on the NRP1 cytoplasmic domain and synectin, which are dispensable for angiogenesis (Fantin et al., 2011) but required for arteriogenesis (Lanahan et al., 2013a), arguing that a role for this NRP1-mediated integrin recycling pathway in arteriogenesis is more likely. Also, an *in vivo* study in embryonic brain showed that *in trans* NRP1 interaction with integrin $\beta 8$ regulates cerebral angiogenesis; this study showed that endothelial NRP1 suppresses TGF β activation and controls sprouting angiogenesis by forming an intercellular complex with neuroepithelial integrin $\beta 8$ (Hirota et al., 2015).

1.12.1 Possible links between NRP1 and RHO -GTPases via integrin-mediated ABL1 activation

In cancer cells, the extracellular NRP1 domain directly interacts with integrins (Fukasawa et al., 2007). Activated integrins recruit SFKs and FAK to regulate focal adhesion assembly and the actin cytoskeleton (Michael et al., 2009). Both kinases can activate downstream signals and phosphorylate two non-receptor tyrosine

kinases, p130CAS (Guo and Giancotti, 2004) and ABL1 (Lewis and Schwartz, 1998b) as well as the focal adhesion-associated protein paxillin (Schaller and Schaefer, 2001). Studies have shown that the integrin subunits $\beta 1$ and $\beta 2$ can both associate with ABL1 to promote cell adhesion and migration (Cui et al., 2009, Baruzzi et al., 2010).

For example, studies in bone marrow-derived macrophages showed that integrin's association with ABL1 and SFKs promotes cell migration by regulating the activity of CDC42 and RAC1 (Baruzzi et al., 2010). In cancer cells, CDC42 also promotes $\beta 1$ integrin transcription (Reymond et al., 2012a), suggesting a positive feedback loop for ECM-induced cell motility. In endothelial cells, CDC42 is essential for vascular network assembly in the embryoid body model of vasculogenesis and directional ECs migration (Qi et al., 2011). Surprisingly, however, it had not previously been investigated if the integrin interactor NRP1 is required to regulate CDC42, RAC or RHOA activity in ECs.

1.12.2 The role of CDC42 in filopodia formation and sprouting angiogenesis

During angiogenesis, the highly polarised endothelial tip cells can be distinguished from neighbouring stalk cells by clusters of numerous long filopodia that are thought to detect microenvironmental cues for directional migration (De Smet et al., 2009). Filopodia are highly dynamic cellular protrusions that contain parallel bundles of F-actin and can extend from lamellipodia (Mattila and Lappalainen, 2008). In addition to sensing growth factors, filopodia can adhere to the ECM and form focal contacts that link the cytoskeleton to the ECM to promote forward movement. The filopodia regulator CDC42 is activated by VEGF signalling in cultured ECs (Lamallice et al., 2004). Agreeing with a role for CDC42 in endothelial actin dynamics, both general and endothelial-specific CDC42 deletions disrupt blood vessel formation at the stage of vasculogenesis during mouse development (Jin et al., 2013, Chen et al., 2000). However, the resulting early embryonic lethality of these mutants has precluded the demonstration that CDC42 controls endothelial filopodia formation, tip cell function and sprouting angiogenesis *in vivo*. Moreover, at the time I started my PhD it was not known whether VEGF and/or ECM cues are important for CDC42 regulation during

vessel sprouting and whether NRP1 regulates CDC42-dependent actin polymerisation.

1.13 The Serum Response Factor (SRF) and its co-factors

Serum Response Factor (SRF) is a member of the MADS (MCM1, Agamous, Deficiens, SRF) family of transcription factors that acts together with two families of signal regulated co-factors. SRF recruits co-activators of the myocardin family (myocardin-related transcription factors, MRTFs) in response to RHO-actin signalling (Wang et al., 2002a, Pipes et al., 2006a) or the ternary complex factor (TCF) family (Hipskind et al., 1991, Buchwalter et al., 2004) in response to mitogen-activated protein kinase (MAPK) phosphorylation (Gineitis and Treisman, 2001). Thus, SRF can regulate a wide range of genes encoding myogenic contractile and cytoskeletal proteins as well as genes involved in cell growth and survival. The TCF and MRTF cofactors compete for binding to the same region of SRF (Zaromytidou et al., 2006, Wang et al., 2004).

SRF has been described to bind the CArG box in the promoters of target genes, such as the early-transcribed genes *Fos* (FBJ murine osteosarcoma viral oncogene homolog) and *Egr1* (early growth response 1)(Miwa and Kedes, 1987, Norman et al., 1988, Treisman, 1995). Microarray studies revealed 150 genes with CArG boxes that can be transcriptionally regulated by SRF (Sun et al., 2006a, Selvaraj and Prywes, 2004b, Tullai et al., 2004). Other studies using chromatin immunoprecipitation (ChIP) in combination with human promoter microarrays identified around 200 putative SRF binding sites in the human genome (Cooper et al., 2007).

SRF target genes are involved in essential cell functions, and for this reason studies with *Srf* global or tissue-specific deletion showed severe phenotypes (Arsenian et al., 1998, Parlakian et al., 2005). During embryogenesis, SRF is highly expressed in skeletal, cardiac and vascular smooth muscle tissue. In adult mice, SRF is expressed in higher levels in skeletal and cardiac muscles and in lower levels in liver, lung and spleen (Belaguli et al., 1997). Studies using *Srf* null mice showed that these mice were embryonic lethal before gastrulation with severe defect in mesoderm formation and no expression of developmental marker genes such as *Bmp2/4* (bone morphogenetic protein 2/4) or *Shh* (sonic hedgehog) (Arsenian et al., 1998). Other

studies pointed out the importance of SRF in the cardiovascular system by describing defects in mice with *Srf* specific deletion in cardiac myocytes. These mice exhibited lethal cardiac defects between E10.5 and E13.5, and showed thin myocardium and defective trabeculation in the embryonic heart. Also, the expression of gene markers that are important for the heart development such as *Nkx2.5*, *Gata4*, *myocardin*, and *Fos* was decreased, suggesting a role of SRF in cardiac morphogenesis (Parlakian et al., 2004). In adults, conditional specific deletion of *Srf* in cardiac myocytes, showed heart failure and the mice died 10 weeks after the *Srf* specific deletion. The mice showed early alterations in the cardiac gene expression program, differences in the architecture of cardiomyocytes and developed cardiomyopathy (Parlakian et al., 2005). Other studies that described mice with *Srf* deletion in vascular smooth muscle cell (SMC), displayed similar embryonic heart defects with mice lacking *Srf* expression in cardiomyocytes (Miano et al., 2004), suggesting that the promoter that had been used to control *Cre* recombinase induces recombination in both SMC and cardiomyocytes (Lepore et al., 2005).

1.13.1 The SRF co-factors MRTFs and TCFs

The myocardin family of co-activators consists of myocardin, which is highly expressed in smooth and cardiac muscle cells, MRTFA and MRTFB (also known as MKL1 and MKL2 respectively), which are expressed more ubiquitously (Kuwahara et al., 2005, Nakamura et al., 2010, Olson and Nordheim, 2010a). The MRTFs contain the RPEL domains that form a complex with monomeric G-actin, the SAP and leucine zipper (LZ) domains that facilitate the function as SRF coactivators and the B1 domains that are involved in the nuclear import of the MRTFs (Wang et al., 2002b). *In vitro* studies have shown that MRTFB is not as potent transcriptional co-activator as MRTFA (Wang et al., 2002b).

MRTFs are expressed in embryos and adult mice, and the genetic deletion of either *Mrtfa* or *Mrtfb* causes distinct phenotypes. MRTFA is expressed together with myocardin in the human heart and aorta (Wang et al., 2002b, Du et al., 2004) and during embryonic development is enriched in mesenchymal, muscle and epithelial cells (Pipes et al., 2006b). MRTFA is the most ubiquitously expressed of the MRTFs and plays a crucial role in RHO-actin signal transduction from the cytoplasm to the

nucleus (Miralles et al., 2003). Surprisingly, mice lacking MRTFA are viable and fertile, but *Mrtfa*^{-/-} dams exhibit defects in lactation due to impairments in mammary myoepithelial cells (Li et al., 2006a, Sun et al., 2006b). These findings suggest that MRTFA is required for differentiation and survival of the myoepithelial cells during lactation (Li et al., 2006b). MRTFB is highly expressed in the heart and brain of adult mouse (Wang et al., 2002b) and during embryogenesis is detected in the embryonic dorsal aorta and the cardiac neural crest cells (Li et al., 2005). In contrast to the phenotype observed in *Mrtfa* null mice, global deletion of *Mrtfb* results in embryonic lethality due to cardiovascular defects observed with abnormal branchial arch arteries and thin myocardium (Sodroski et al., 1984). The *Mrtfb* null mice died at mid-gestation at E14.5 and displayed cardiac outflow tract defects (Aquino et al., 2006).

Under steady state conditions, MRTFs are in an inactive state in the cytoplasm, where they form a complex with monomeric actin, i.e. G-actin (Posern et al., 2004, Miralles et al., 2003, Posern et al., 2002). However, after stimulation of actin polymerisation via the RHOA/ROCK/cofilin pathway (Hill et al., 1995), the G-actin is polymerised into F-actin, and MRTFA is released from actin and translocates to the nucleus to bind SRF to regulate gene transcription (Kuwahara et al., 2005, Miralles et al., 2003). Also, growth factor stimulation acts via RHO and ERK1/2-dependent mechanisms to regulate MRTFA phosphorylation at different sites and thus to control MRTFA nuclear import into or export from the nucleus (Miralles et al., 2003, Muehlich et al., 2008).

At least 26 phosphorylation sites were identified in MRTFA by mass spectrometric analysis after serum stimulation in fibroblasts (Panayiotou et al., 2016). For example, MRTFA phosphorylation by ERK1/2 at residue S549 promotes nuclear export (Miralles et al., 2003) by mediating its binding to G-actin (Muehlich et al., 2008). However, ERK1/2-mediated S98 phosphorylation inhibits G-actin/MRTFA interaction and promotes MRTFA nuclear accumulation, while S33 phosphorylation promotes nuclear export (Panayiotou et al., 2016).

Study has shown that MRTFs act solely in complex with SRF (Medjkane et al., 2009). Gene ontology analysis of the MRTF/SRF target genes in serum stimulated

fibroblasts showed that many target genes were involved in cell adhesion, cell motility, extracellular matrix synthesis, F-actin remodelling and microtubules dynamics (Esnault et al., 2014). Also, this study showed that the MRTFA/SRF complex can target and regulate other transcription factors such as AP1 and the ERF family of chromatin regulators. Interestingly, the target genes of the MRTF/SRF complex overlap with the gene signatures associated with cancer cell invasiveness and metastasis, mechanotransduction through the YAP/TAZ pathway and response to FAK and TGF β signalling (Esnault et al., 2014).

Activation of TGF β signalling can also promote RHOA-dependent MRTFA translocation to the nucleus and thereby formation of the MRTFA/SRF complex. In addition, TGF β canonical pathway phosphorylates SMAD3, which translocates to the nucleus and form another complex with MRTFA. Accordingly, TGF β signalling can regulate the transcription of genes related to actin polymerisation and adherens junctions (Morita et al., 2007). This mechanism can be disturbed by the nuclear export of MRTFA, mediated by nuclear G-actin presence (Vartiainen et al., 2007) or by ERK1/2 phosphorylation-induced TCF activation, which displaces MRTFA from the promoter of target genes (Wang et al., 2004).

The TCF family of ETS transcription factors (E26 transformation-specific) consists of ELK1, ELK3 (NET) and ELK4 (SAP1), which are under the control of the MAPK signalling pathway (Buchwalter et al., 2004). Growth factor stimulation or vascular injury induces MAPK signalling cascade and activation of ERK1/2, which promotes TCF translocation to the nucleus and thereby formation of a TCF/SRF complex (Parmacek, 2007). This complex binds to an Ets binding site located next to a CarG box in the promoter of the target genes to promote the transcription of growth related genes (Shore et al., 1996). Studies using TCF-deficient mouse embryonic fibroblasts, showed decreased expression of genes involved in metabolism, DNA repair, cell cycle and proliferation, while MRTFA/SRF target gene expression was increased (Gualdrini et al., 2016, Esnault et al., 2014). These findings suggest that TCFs not only mediate the ERK1/2 signalling, but also negatively regulate the genes involved in cell adhesion, contractility and motility by inhibiting the MRTFA/SRF interaction. Thus, the relative levels of MRTF and TCF co-factors can control the balance between proliferative and contractile-related events (Gualdrini et al., 2016) (**Fig. 3**).

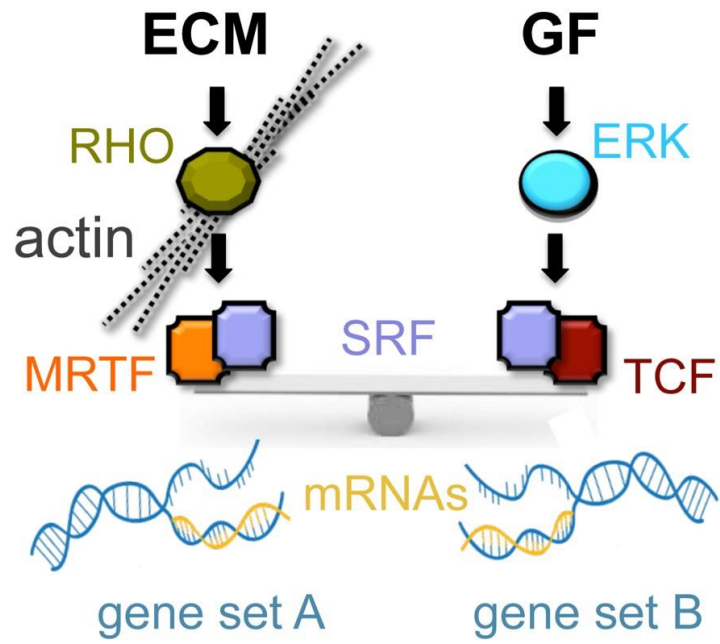


Figure 3: Balance between proliferative and contractile-related events via the SRF and cofactors.

The seesaw represents balancing of extracellular matrix (ECM) and growth factors (GF) signalling at the cells surface and corresponding downstream balance of actin- (gene set A) vs. MAPK-regulated (gene set B) SRF signalling.

1.14 The role of SRF in postnatal and pathological angiogenesis

In vitro studies have shown that in response to VEGF, SRF can be activated through the RHOA and MAPK pathways and translocate to the nucleus to bind the CARG region of genes in ECs. Thus, SRF is required for VEGF-induced angiogenesis (Chai et al., 2004).

In mouse embryos, SRF is expressed in ECs of small vessels, capillaries and arterioles, but not in ECs of large vessels (Franco et al., 2008). In the mouse hindbrain, SRF is detected in both tip and stalk cells. *Tie1-Cre* endothelial deletion of *Srf* leads to aneurysm and hemorrhage of small vessels in the limb buds, head and tail of mouse embryos which leads to embryonic lethality at E14.5 (Franco et al., 2008). More specifically, embryos with an endothelial *Srf* deletion showed defects in sprouting angiogenesis with reduced vascular branching, filopodia formation and defective ECs junctions. Also, ECs lacking SRF expression showed decreased expression of genes for transcription factors, cytoskeletal and junctional proteins or genes involved in signalling pathways such as TGF β , VEGF, Notch, angiopoietin etc. (Franco et al., 2008). In agreement, another study using *Tie2-Cre⁺ Srf^{fl/fl}* embryos showed cerebrovascular hemorrhaging and severe vascular defects within the yolk sac that led to embryonic death at E14.5 (Holtz and Misra, 2008). Also, the hearts of the mutant embryos were smaller than in wildtypes and dysmorphic (Holtz and Misra, 2008). Immunostaining showed ECs with disruptive cell-cell junctions and E-cadherin staining pattern in yolk sac tissues of mutant embryos (Holtz and Misra, 2008).

In addition to the important role for SRF in embryogenesis, endothelial SRF is required for postnatal angiogenesis. Indeed, studies have shown that it is strongly expressed in tip and stalk ECs in the postnatal mouse retina, where it regulates sprouting angiogenesis (Franco et al., 2013, Weinl et al., 2013). Postnatal endothelial *Srf* deletion impairs survival and causes hypovascularisation and severe retina angiopathy (Franco et al., 2013). More specifically, mice lacking postnatal endothelial SRF expression showed reduced radial migration, number of branching points and filopodia formation of retinal ECs. SRF deficient retinas also showed ECs junctions with different morphology compared to control (more linear structure) and

decreased expression of the myosin heavy chain 10 (Myh10) and myosin light chain 9 (My19) contractile proteins (Franco et al., 2013). Also, *in vitro* studies using HUVEC showed that the MRTF/SRF complex regulates the expression of MYL9 as well as the MYH9 contractile protein (Franco et al., 2013). These observations might explain the migratory defects observed in the postnatal retina of mice lacking endothelial SRF.

In agreement with the idea that the MRTF co-factors and their regulated proteins are responsible for the migratory defects observed in *Srf* mutants, the EC-specific genetic ablation of either *Srf* or *Mrtfa/Mrtfb* causes similar defects in postnatal retinal angiogenesis, including decreased radial outgrowth, fewer branching points and defects in filopodia formation (Weinl et al., 2013). Interestingly, mice with a deletion of the other SRF co-factors of the TCF family, *Elk1* and *Elk4*, displayed normal vascularization of the postnatal retina, including radial outgrowth, sprouting and filopodia formation (Weinl et al., 2013). Taken together, the overlapping phenotypic characteristics of the EC-specific *Srf* with *Mrtfa/Mrtfb* but not *Tcf* knockout mice strongly suggest that the MRTFs are the relevant SRF cofactors for retinal angiogenesis.

Postnatal retina angiogenesis of wildtype mice reaches completion by P25 (Fruttiger, 2002). SRF is an important regulator of vascularisation not only for the early stages of retinal angiogenesis, but also for the later ones and the adult retina (Franco et al., 2013, Weinl et al., 2013). Retinas of P12 and P21 *Srf* mutant mice, showed vascular defects with balloon-like sprouts at the vascular front and lacked the intermediate and deeper vascular layers (Franco et al., 2013). In agreement, another study that used P10 and P17 mouse retina showed large avascular zones in the peripheral retina, large clusters of tip cells in the angiogenic front and an absence of deep plexi in *Srf* mutant ECs (Weinl et al., 2013). *Srf* deletion in adult ECs elicited intraretinal neovascularisation (Weinl et al., 2013), which is characteristic of a retinal vascular pathology known as adult intraretinal age-related macular degeneration (AMD) that is described in patients with retinal angiomatous proliferation (RAP) (Yannuzzi et al., 2012).

Another study showed that endothelial *Srf* deletion can also affect tumour angiogenesis (Franco et al., 2013). They injected lung carcinoma cells into 3 month old wildtype and endothelial specific *Srf* knockout mice and compared the size of the tumours that developed 12 and 24 days after the injection. They showed that endothelial *Srf* deletion decreased tumour angiogenesis and increased necrotic regions within the tumour mass (Franco et al., 2013). Thus, lack of SRF in ECs impairs tumour angiogenesis, which then affects the oxygenation of the tumour and therefore inhibits its growth.

1.15 The role of SRF and MRTFA in vascular homeostasis

Studies have shown that SRF is not only important to regulate the expression of contractile proteins during development, but also that excessive SRF is pathogenic, indicating its requirement for vascular homeostasis (Olson and Nordheim, 2010a). SRF-regulated genes such as *Anf* (atrial natriuretic factor), *Acta1* (skeletal a-actin), *Actc1* (cardiac a-actin), *a-MHC* (a-myosin heavy chain), and *b-MHC* have been shown to change during cardiac hypertrophy and cardiomyopathy, suggesting that SRF may play a role in the cardiac function (Argentin et al., 1994, Chien, 1992, Colucci, 1997, Durand, 1999). Overexpressing SRF in cardiomyocytes under the a-MHC promoter caused dysregulation of several SRF-dependent cardiac genes and developed cardiomyopathy (Zhang et al., 2001). Some of the genes that have an SRF-binding site were upregulated and others downregulated, and these changes in the expression of cardiac markers occurred much earlier than the overt development of cardiomyopathy. At the 6th week of age, transgenic mice showed upregulation of *Fos*, *Jun*, *Anf*, *b-MHC* and *Acta1* and downregulation of *a-MHC* and *Actc1*, suggesting that SRF regulates the transcription of those genes together with other co-factors. SRF transgenic mice developed hypertrophy and cardiomyopathy at around the 20th week of age, probably due to the dysfunction of the SRF-regulated genes (Zhang et al., 2001). Indeed, studies have showed that animal models with cardiomyopathy and patients with heart failure showed increased expression of the SRF-regulated gene *Anf* (Chien, 1992, Arai et al., 1993). Therefore, increased expression of SRF can lead to cardiac dysfunction and vascular pathology.

Moreover, other studies have shown that SRF protein levels were increased by 20% in the hearts of old adult compared to young rats, suggesting a possible link between SRF expression and myocardial aging (Lu et al., 1998). Studies have used mice with mild SRF overexpression in the heart that reaches 50% to mimic the aging process. They showed increased expression of SRF-targeted genes such *Acta1* and *Anf* but no obvious morphological changes. After 6 months of age, the transgenic mice showed increased heart to body weight ratio, myocyte size, a slight increase of the ventricular wall thickness and cardiac fibrosis (Zhang et al., 2003b). These changes observed in SRF transgenic mice were very similar to the defects observed in aging heart (Olivetti et al., 1991). The heart of older mice showed a myocardium with few but bigger myocytes, slightly thicker ventricular wall and more fibroblast-produced collagen (Zhang et al., 2003a). Thus, the age-associated increase in SRF expression in the heart of older rats or mice might contribute to morphological or functional changes observed in aging heart.

In addition to the *in vivo* studies described above, microarray experiments using the SRF transgenic mice revealed changes in gene expression of 200 SRF-modulated genes that have also been altered in hearts with cardiac ischemia or aortic constriction. These genes encoded for a wide range of proteins that were involved in different cell functions such as cytoskeleton, transcription, metabolism, ion transport, ECM components and others (Zhang et al., 2011). However, all the studies so far have described a role of SRF-expressed in cardiomyocytes for cardiac pathology, but little is known about the contribution of the endothelial SRF to vascular homeostasis in the heart or other vessels.

Studies have shown that MRTFA expression is upregulated in injured femoral arteries in dedifferentiated VSMCs during vascular remodelling. Also, MRTFA gene expression is upregulated in aortic tissues in the atherosclerotic lesion of *Apoe*^{-/-} mice. *Apoe*^{-/-} mice lacking MRTFA expression or mice treated with an inhibitor that blocks MRTFA translocation to the nucleus (CCG1423) showed smaller atherosclerotic lesion in the aortas (Tibbs, 1987). In agreement with the *in vivo* mouse data, genetic studies have identified a single-nucleotide polymorphism (SNP) in the promoter of the human MRTFA that increases MRTFA expression and is associated with coronary artery disease (Hinohara et al., 2009). These findings

suggest that MRTFA might be therapeutic target to treat vascular diseases such as atherosclerosis. However, further work is required to investigate the specific role of endothelial MRTFA to vascular homeostasis.

Overall, it has not yet been investigated whether a NRP1-dependent transcriptional network exists in ECs and whether NRP1 controls genes involved in cytoskeletal remodelling or cell survival through the regulation of SRF, MRTF or TCF. Also, it is not known whether NRP1 regulates the activity or/and the expression of transcription factors such as SRF and its cofactors or other members of the MAPK that can act as transcriptional regulators. So far, studies have shown a crucial role of endothelial SRF for angiogenesis, but it has not been examined the role of the EC-expressed SRF, MRTF and TCF for vascular homeostasis.

1.16 Vascular permeability

Major organs such as kidneys, heart and lungs and large vessels supply the capillaries with nutrients to mediate the molecular exchange of gases, water, sugars, salts and small amount of plasma proteins less than 40 kDa between the tissues and the circulating blood (Nagy et al., 2008). This process is characterised by diffusion, which is driven by the molecular concentration gradient across the vascular endothelium (Nagy et al., 2008). In addition, regulated vascular permeability is essential for the health of normal tissues to mediate the exchange of blood constituents with surrounding tissues. Whilst it is normally maintained at a basal level, it is transiently upregulated during injury to promote wound healing. In addition, vascular permeability can be pathological when increased excessively in acute or chronic conditions (Nagy et al., 2008).

For example, growth factors and cytokines can induce vascular hyperpermeability which leads to disruption of the vascular barrier, leakage of large molecules and cells and the development of inflammation and oedema in inflammatory diseases or cancer (Claesson-Welsh, 2015). Below I describe the characteristics of basal vascular permeability in different organs and also the mechanisms of acute and chronic vascular hyperpermeability.

1.16.1 Basal vascular permeability

The level of the basal permeability is organ-specific and it may also vary in response to other physiological stimuli such as exercise (Nagy et al., 2008). For example the brain vasculature forms a very tight barrier, which is called the blood-brain barrier (BBB) in order to maintain neural homeostasis. This highly impermeable ECs barrier is maintained by the cross-talk with surrounding cells such as pericytes and astrocytes. The BBB has ECs with adherens junctions, high-resistance tight junctions and abundant basement membrane (Paolinelli et al., 2011). ECs in other organs such as pancreas, kidneys or all the endocrine glands contain fenestrae on the surface, which are circular pores in the plasma membrane that allow rapid transport of nutrients across the endothelium (Tse and Stan, 2010). The fenestrated endothelia are characterised by the presence of fenestral diaphragms, which consist of the plasmalemmal vesicle protein-1 (PV1) and PV1 loss leads to leakage of plasma proteins (Stan et al., 2012).

1.16.2 Acute and chronic vascular hyperpermeability

Rapid increases in vascular hypermeability occur in response to a number of factors, such as histamine, semaphorins or VEGFA (Miles and Miles, 1952a, Acevedo et al., 2008, Senger et al., 1983). Whilst basal permeability occurs in capillaries, acute vascular hypermeability takes place in post-capillary venules that are characterised by a cuboidal endothelium (Majno et al., 1961) and chronic vascular hypermeability in abnormal enlarged, newly form vessels (Nagy et al., 2008). The vascular leakage in acute vascular hypermeability is a rapid and self-limited process that last up to 30 min and results in influx of plasma proteins into the tissue (Nagy et al., 2008). The vascular leakage in chronic hyperpermeability is observed in diseases such as cancer and chronic inflammatory diseases like rheumatoid arthritis, psoriasis or neovascular eye diseases (Nagy et al., 1995, Stewart, 2012). In pathological conditions such as cancer and AMD, persistent VEGF upregulation triggers the formation of new, enlarged leaky vessels (Liao and Johnson, 2007). The amount and the composition of the extravasated liquid is different compared to the one at basal permeability. In acute and chronic vascular leakage, there is an increased number of plasma proteins

in the extravasated fluid, including fibrinogen and clotting factors that cause tissue swelling and oedema (Nagy et al., 2008).

1.17 The mechanisms of vascular permeability

Two main mechanisms that cause disruption of the endothelial barrier are the transcellular and the paracellular permeability routes. The first one occurs across the cell body and the latter one between the cells (Tse and Stan, 2010).

1.17.1 The transcellular mechanism

The transcellular mechanism is the vesicular transport of molecules across the endothelium through transcytosis and the formation of transendothelial channels from caveolae and vesiculo-vacuolar organelles (VVOs) (Claesson-Welsh, 2015). Endothelial transcytosis is a constitutive process of vesicular transport that can be upregulated in response to pathological stimuli (Predescu et al., 2007). Transcytosis is mediated by caveolae, which are lipid raft microdomains that form “cave-like” structures in the plasma membrane (Predescu et al., 2007). Caveolae contain the caveolin-1 (CAV-1) protein, which after phosphorylation mediated by SFKs, is recruited to the membrane and oligomerises to form caveolae (Sargiacomo et al., 1995). Caveolae contain approximately a volume of fluid equal to the 20% of an EC interior volume (Frokjaer-Jensen, 1991) and have a diameter of approximately 70nm. VVOs offer an alternative transendothelial route for plasma extravasation upon exposure to permeability factors such as histamine and VEGF (Feng et al., 1996). They consist of hundreds of vesicles and vacuoles that create grape-like clusters of 80–200 nm diameter and can traverse from the luminal to the basal side of ECs (Tse and Stan, 2010). At the beginning, it was thought that many individual caveolae form the VVOs. However, studies have since shown that the CAV-1 protein was not expressed regularly in VVOs, and mice lacking CAV-1 showed absence of caveolae structures but presence of VVOs in the endothelium (Feng et al., 1999). Interestingly, mice lacking CAV-1 expression showed increased permeability, suggesting that probably VVOs mediate this function (Schubert et al., 2002).

1.17.2 The paracellular mechanism

The paracellular pathway is the main mechanism that regulates the extravasation of plasma proteins and blood during acute and chronic permeability. There are two types of intercellular junctions responsible for endothelial cell-cell contact: the adherens junctions (AJ) and tight junctions (TJ) (Mehta and Malik, 2006). The AJ are found in the most of the microvascular structures, while the TJ are present in some tissues such as brain and retina that create the BBB and the blood-retinal barrier (BRB) respectively (Hawkins and Davis, 2005, Gardner et al., 1999). In both types of junctions, adhesion is mediated by transmembrane proteins that promote homophilic interactions and form a pericellular structure along the cell-cell borders (Dejana, 2004).

Vascular endothelial (VE)-cadherin is believed to be the most important protein in regulating the function of AJs (Carmeliet et al., 1999). The extracellular domain of VE-cadherin interacts with VE-cadherin of neighbouring cells, while the cytoplasmic tail binds to actin cytoskeleton via catenins to stabilise the junctions and regulate the junctional opening (Rudini and Dejana, 2008). Also, VE-cadherin interacts with growth factors receptors such as VEGFR2 to promote cell survival and inhibit growth in confluent ECs monolayers (Dejana, 2004). In addition, it co-precipitates with signalling molecules such as SFKs (Weis et al., 2004a) or interacts with phosphatases like the vascular endothelial protein tyrosine phosphatase (VE-PTP), which decreases VE-cadherin phosphorylation and thereby regulates vascular permeability (Nawroth et al., 2002). Other proteins that may associate or interact with the AJs are E-cadherin, junctional adhesion molecules (JAMs) and platelet-endothelial cell adhesion molecule (PECAM-1) (Dejana, 2004).

The endothelial tight junctions are similar to AJs, but are composed of TJ proteins including occludin, claudins (3/5) and JAM-A (Hawkins and Davis, 2005). These proteins can interact with the zona occludens proteins ZO-1 and ZO-2, which mediate the interaction with the actin cytoskeleton, other PDZ-domain containing proteins or signalling mediators to regulate vascular permeability (Matter and Balda, 2003).

1.18 The molecular mechanisms of VEGF-induced vascular permeability: VEGFR2 and its interactors

VEGFR2 plays a crucial role in VEGF-induced vascular permeability in different organs such as brain, lung and skin [e.g. (Hudson et al., 2014, Murohara et al., 1998, Sun et al., 2012)]. VEGFR2 controls vascular permeability through its interactions with cell-cell adhesion molecules, integrins or by regulating cytoplasmic transduction molecules (Weis and Cheresh, 2005).

1.18.1 VEGFR2 activation and its interaction with transmembrane proteins

VEGF binding to VEGFR2 leads to phosphorylation of VEGFR2 at Y949 (Y951 in human VEGFR2), which serves as a binding site for the adaptor protein SH2 domain-containing protein 2A (SH2D2A, also known as TSAAd), which then mediates SFKs recruitment to the receptor (Sun et al., 2012). Mice lacking TSAAd or lack the VEGFR2 Y949 site showed high-resistance endothelial cell junctions and did not display VEGF-induced hyperpermeability (Sun et al., 2012, Li et al., 2016). More specifically, the vasculature of the mice carried the VEGFR2 Y949 mutation was sensitive to inflammatory cytokines such as histamine but not to VEGF164, suggesting that the pY949-dependent SFK activation is specifically required for VEGF-induced vascular permeability (Li et al., 2016).

Moreover, in cultured endothelial cells under flow conditions VEGFR2 associates with the VE-cadherin transmembrane protein (Shay-Salit et al., 2002) to regulate cell-cell junctional integrity. *In vitro* studies showed that upon VEGF stimulation, VE-cadherin is phosphorylated and the complexes between VE-cadherin, VEGFR2 and β -catenin are dissolved. VE-cadherin is then internalised, leading to loosening cell-cell contacts in ECs (Esser et al., 1998). In agreement, *in vivo* experiments using heart lysates prepared from adult mice injected with VEGF showed that the proposed complex is dissociated rapidly in response to VEGF stimulation (Weis et al., 2004a).

The VEGFR2 cooperation with integrins may also affect vascular leakage (Robinson et al., 2004, Eliceiri et al., 2002). Studies have shown that mice lacking integrin β 3 expression showed increased VEGF-induced plasma extravasation and increased levels of VEGFR2 expression compared to wildtypes. They showed that increased

levels of VEGFR2 led to an increased sensitivity to VEGF-induced vascular leakage, suggesting that $\beta 3$ integrin influences vascular permeability via the regulation of VEGFR2 expression (Robinson et al., 2004). Another study showed that VEGF stimulation led to the formation of a FAK/ $\alpha v\beta 5$ complex in both cultured endothelial cells *in vitro* and blood vessels *in vivo* (Eliceiri et al., 2002). They also showed that integrin $\beta 5$ -deficient mice had significant decreased VEGF-induced vascular permeability compared to control littermates. These findings support the idea that the VEGF-induced formation of the FAK/ $\alpha v\beta 5$ complex may be an important mechanism for coordinating growth factors with integrin signalling during VEGF-mediated vascular leakage (Eliceiri et al., 2002).

NRP1 has also been shown to be involved in VEGF-induced vascular leak [e.g. (Acevedo et al., 2008)] (for further detail, see below, section 1.19).

1.18.2 Cytoplasmic mediators of vascular permeability

Many cytoplasmic proteins are activated in response to VEGF-induced vascular permeability. Many of those are kinases such as SFKs, ABL1/2, FAK, AKT but also non-kinases proteins like the endothelial nitric oxide synthase (eNOS).

As mentioned above, SFKs are important regulators of VEGF-induced vascular permeability. The SFK members SRC and YES1 have been reported to be tyrosine phosphorylated in response to VEGF (Eliceiri et al., 1999, Scheppke et al., 2008). *In vivo* studies using mice deficient for SRC and YES1 showed reduced VEGF-induced vascular leakage in an assay that measures the extravasation of Evan's blue dye in the dermis after VEGF injection (Eliceiri et al., 1999). In agreement, another study showed that VEGF injection or laser-induced vascular permeability failed to augment retinal vascular permeability in *Src* and *Yes* knockout mice (Scheppke et al., 2008). Also, activated SRC has been suggested to phosphorylate VE-cadherin on Y685 upon VEGF stimulation and to dissociate VE-cadherin from β -catenin, leading to disruption of the junctions and vascular leakage (Weis et al., 2004a, Wallez et al., 2007). However, it was not distinguished whether the activation was exclusive to SRC or also affected YES1.

VEGF can activate FAK at Y397, Y407 and Y861 (Abu-Ghazaleh et al., 2001, Herzog et al., 2011b) and VEGF-induced FAK Y397 phosphorylation occurs independently of SRC activation (Liang et al., 2010). Studies using pharmacological inhibition of FAK or genetic deletion in ECs showed reduced VEGF-induced vascular permeability downstream of the VEGFR2 or SFKs activation *in vivo* (Chen et al., 2012). They showed that VEGF promotes FAK activation and localisation to cell-cell junction, where it binds to VE-cadherin via its FERM domain and phosphorylates β -catenin, leading to dissociation of the complex and junctional breakdown (Chen et al., 2012). On another study they also showed that FAK mediates VEGF-dependent VE-cadherin phosphorylation at Y658 site (Jean et al., 2014).

The ABL kinases ABL1 and ABL2 (also known as ARG) are activated in response to VEGF to mediate vascular permeability (Chislock and Pendergast, 2013, Aman et al., 2012). Studies using Imatinib treatment or the genetic deletion of ABL kinases (Abl1^{ECKO}; Arg^{+/-}) showed decreased VEGF-induced vascular leakage compared to controls in Miles assays (Chislock and Pendergast, 2013, Aman et al., 2012). It has also been shown that ABL2 partially compensates for ABL1 in VEGF164-induced vascular leakage in the Miles assays (Chislock and Pendergast, 2013). Also, biochemical studies in HUVEC demonstrated that VEGF activates ABL via the phosphoinositide 3-kinase (PI3K). Then the activated ABL reduces the activity of mitogen-activated protein kinases (ERK1/2, JNKs and p38) by a negative feedback mechanism that involves adaptor proteins (Anselmi et al., 2012). However, whether this ABL-dependent mechanism is important for vascular permeability, needs to be tested.

It has been shown that AKT functions in a key pathway downstream of VEGF to mediate vascular permeability (Six et al., 2002). Also, VEGF mediates nitric oxide (NO) production through the direct phosphorylation of the endothelial nitric oxide synthase (eNOS) by AKT (Fulton et al., 1999). In vascular permeability, NO production is used for S-nitrosylation of the β -catenin at the residue Cys619 to promote the dissociation of the VE-cadherin/ β -catenin complex and to cause endothelial barrier disruption (Thibeault et al., 2010). In support of the findings that showed the importance of eNOS for vascular permeability, mice mutated at the

AKT-mediated phosphorylated site of eNOS showed reduced VEGF-induced vascular permeability (Fukumura et al., 2001).

1.19 Role of NRP1 in VEGF-induced vascular permeability

NRP1 has also been implicated in vascular permeability signalling (Raimondi et al., 2016). Intradermal vascular leakage induced by VEGF164, is defective in mice lacking endothelial NRP1 expression, even though they retain VEGFR2 (Acevedo et al., 2008, Wang et al., 2015a). Agreeing with an important role for NRP1 in VEGF164-induced vascular permeability, a peptide blocking VEGF164 binding to NRP1 inhibits serum albumin leak in a mouse model of diabetic retinal injury (Wang et al., 2015a), and function-blocking antibodies for NRP1 suppress intradermal vascular leak induced by VEGF164 injection (Teesalu et al., 2009), as well as VEGF164-induced pulmonary vascular leak (Becker et al., 2005). However, other studies have argued against an important role for NRP1 in VEGF-induced vascular permeability, with one study showing that an antibody blocking VEGF164 binding to NRP1 impaired corneal neovascularisation, but not VEGF164-induced intradermal vascular permeability in mice (Pan et al., 2007a), and another study finding that NRP1 deletion does not impair VEGF164-induced permeability of retinal vasculature (Cerani et al., 2013).

The relative importance of VEGFR2 and NRP1 for VEGF-induced vascular permeability signalling has therefore remained unclear. Moreover, it is not known whether NRP1 function may intersect with signal transduction molecules such as ABL kinase or SFKs and whether these kinases operate in a regulatory hierarchy to convey permeability signals.

Aims of the study

NRP1 is a transmembrane protein that is essential for blood vessel growth in development and disease. Yet, it is not well understood how NRP1 activation affects endothelial cell behaviour to enhance blood vessel growth, and how this pathway may be exploited for therapeutic benefit to stimulate vessel growth in ischemic tissues. In particular, it has remained controversial if NRP1 mainly acts to promote VEGF signalling through the receptor tyrosine kinase VEGFR2, or if it has other roles that synergise with VEGFR2 pathways to promote effective tissue vascularisation. The aims of this study are to (a) investigate how NRP1 modulates the endothelial cells response to ECM components (**Chapter 3**); (b) determine whether NRP1 regulates the activity or nuclear translocation of transcriptional regulators and, if so, identify NRP1-dependent target genes (**Chapter 4**); and (c) understand how NRP1 promotes VEGF₁₆₄-induced vascular permeability (**Chapter 5**). This knowledge will increase our understanding of the mechanisms of blood vessel formation and vascular permeability and may, in the long run, benefit translational research aimed at developing novel proangiogenic therapies.

Chapter 2 Materials and Methods

2.1 Materials

2.1.1 General Laboratory Materials

All chemicals were obtained from Sigma Aldrich, except where indicated otherwise. Glassware was obtained from VWR International and plastic items were purchased from Corning or Nunc.

2.1.2 General Laboratory Solutions

Water was used after purification by a Milli-Ro 15 Water Purification System (Millipore) and, where necessary, water was further purified using the Milli-Q reagent Grade Water Ultrafiltration System (Millipore). RNase and DNase-free water was supplied by Sigma and absolute ethanol, methanol and isopropanol were obtained from Fischer Scientific.

2.2 Cell Culture Methods

2.2.1 Cell lines and culture

Primary Human Dermal Microvascular Endothelial Cells (HDMEC) are isolated from the adult skin (Promocell, UK). As the dermis contains both blood and lymphatic capillaries, the primary HDMEC I used comprise blood and lymphatic microvascular endothelial cells. The cells were isolated from female donor at the age of 30-40 years old. HDMEC were cultured in MV2 media with supplements (Promocell, UK) in the incubator (Heraeus) at 37°C and 5% CO₂. HDMEC were transfected with 20µM SMARTpool siRNA targeting NRP1, ABL1, ABL2 and KDR (Dharmacon, USA) or *Silencer*[®] negative control siRNA (Applied Biosystems, UK) using Lipofectamine RNAiMAX (Life Technologies) and Optimem (Invitrogen).

For some experiments I also used Primary Human Umbilical Vein Endothelial Cells (HUVEC), which were isolated from the vein of the umbilical cord of a single donor (Promocell, UK). HUVEC were cultured in EBM-2 media (Lonza) containing 10%

foetal bovine serum (Life Technologies), ECGS (Sigma) and hydrocortisone (Lonza).

Mouse lung endothelial cells (MLEC) were isolated from mice between one and two months of age by magnetic-activated cell sorting (MACS) with rat anti-platelet endothelial cell adhesion molecule 1 (PECAM1) and rat anti-intercellular adhesion molecule 2 (ICAM2) antibodies (BD Biosciences). More specifically, lungs from three mice were isolated, minced with blades and incubated at 37 °C for 45 min with collagenase type II (Worthington). After digestion, the solution was sequentially passed through syringes connected to 19G, 21G and 23G needles and through a 40 µm filter to create single cell suspension, centrifuged for 8 min at 4 °C and the pellet was incubated for 10 min at RT with 0.1% BSA containing anti-rat Dynabeads (Invitrogen) pre-incubated with anti-PECAM1 antibodies. Finally, the samples were washed 5x times with growth media using the magnetic separator DynaMag™-2 Magnet (Thermo Fisher Scientific). MLEC were cultured on 10 µg/ml FN in DMEM-GlutaMAX supplemented with 20% foetal bovine serum (FBS), non-essential amino acids (NEAA) (Life Technologies), heparin and ECGS (Sigma) and four days later were detached using Tryple (Gibco), sorted using anti-ICAM2 pre-incubated beads (as described before) and seeded in T25 flask for expansion.

In some experiments in Chapter 3, transfected HDMEC were serum-starved overnight 56h after transfection and then were detached with 0.5% trypsin (Sigma) and plated on 10 µg/ml FN (Sigma) for indicated times. In other experiments, I additionally stimulated cells with 5 ng/ml VEGF165 for 15 min (R&D Systems). Also, untransfected cells were treated with vehicle (DMSO) or 10 µM Imatinib (Cambridge Bioscience), a concentration known to effectively target ABL kinases (Chislock and Pendergast, 2013), 30 min before plating on FN or stimulating both with FN and VEGF165; for the same experiments, I also treated untransfected cells for 30 min with 7.5 µM ML141, which was previously shown to efficiently block CDC42 association with GTPγS and the CDC42 substrate PAK1; it was also shown to decrease the amount of GTP-CDC42 by >95% in EGF-stimulated 3T3 cells and has excellent selectivity over other RHO family GTPases (Hong et al., 2013). Also, MLEC from *Nrpl*^{cyto/cyto} and wild type lungs were serum-starved for 5 hours with DMEM-GlutaMAX, 0.1% FBS and NEAA and seeded or not on 10 µg/ml FN for 1h.

In Chapter 5, cells were starved for 5h and stimulated with 50 ng/ml VEGF165 (Preprotech; for HDMEC) or VEGF164 (for MLEC) for the indicated times. In some experiments, HDMEC were transfected with siRNAs or incubated with inhibitors dissolved in DMSO or the same concentration of DMSO 72h or 30 min prior to VEGF165 stimulation, respectively. The following inhibitors were used: 10 μ M Imatinib (Cambridge Bioscience, 10 μ M PP2 (Sigma), 0.1 μ M PTK/ZK (Vatalanib; Selleckchem).

2.2.2 Immunofluorescence

In some experiments described in Chapter 3, HDMEC were serum-starved overnight 56h after transfection, detached, plated on glass coverslips into 24-well plates that had been coated overnight with 10 μ g/ml FN or were stimulated both with FN and 5 ng/ml VEGF165. In Chapter 5, HUVEC were plated on glass coverslips, starved for 5h and stimulated with 50 ng/ml of VEGF165 for the indicated times. Also, MLEC were seeded on plastic coverslips (Thermo Fisher Scientific), starved for 5h and stimulated with 50 ng/ml of VEGF164 to study SFK activation or with 100 ng/ml VEGF164 to check VE-cadherin (CDH5) rearrangements for the indicated times. In other experiments in Chapter 4, HDMEC were detached 48h after the transfection and plated on glass coverslips without coating and were left to grow overnight in complete MV2 media.

ECs were fixed for 15 min in 4% (w/v) formaldehyde (PFA), which was prepared freshly from paraformaldehyde in 1X PBS or thawed from frozen aliquot, permeabilised in PBS containing 0.25% Triton X-100 for 2 min, blocked with 0.1% BSA (First Link UK Ltd) in PBS for a minimum of 30 min and then stained overnight at 4°C with primary antibodies such as rabbit anti-phospho (p) PXN (pPXN), anti-pp44/42 MAPK (pERK1/2) and anti-pSRC416 (pSFK) (Cell Signalling), rabbit anti-CDH5 (gift from Patrick Turowski, UCL), mouse anti-human NRP1 (R&D Systems), goat anti-human CDH5 (Santa Cruz) or rabbit anti-SRF and goat anti-MRTFA (Santa Cruz) in blocking solution. Then, the coverslips were washed 3 times with 1X PBS for 10 min at RT and were incubated with Alexa Fluor 647, Alexa Fluor 594 or Alexa Fluor 488–conjugated goat anti–rabbit and anti–mouse or donkey FAB anti–goat antibodies (Jackson Immuno Research or

Thermofisher) or Alexa488 or 633-conjugated phalloidin (Thermofisher) diluted in the blocking solution for 1h at RT in the dark. Following the staining with the secondary antibodies, the coverslips were washed 3 times with 1X PBS for 10 min at RT, stained with DAPI at a concentration of 10 $\mu\text{g/ml}$ (Sigma) for 1min at RT and post-fixed with 4% PFA for 5 min. Using fine forceps, the coverslips were removed from the 24-well plate and mounted on a glass Superfrost Plus slides (VWR International) using Mowiol solution. Mowiol solution was made up by incubating 6 g of glycerol and 2.4 g of Mowiol 4-88 (Calbiochem) in 6 ml of water for 2h at RT and then adding 12 ml of Tris (0.2 M, pH 8.5) and 2.5% (w/v) DABCO, and incubating for several hours at 55°C until dissolved. Finally, the samples were imaged on an LSM700 confocal microscope (Zeiss) and Images were processed with Photoshop CS4 (Adobe Inc.).

2.2.3 Cell migration assay

HDMEC were transfected with siRNA, serum starved overnight and then plated onto FN-coated transwell inserts (8.0 μm pores, 10 mm diameter; Nunc) that had been pre-incubated with MV2 containing 0.5% BSA. After 4 h, cells on the upper face of the insert were removed with a cotton bud, while transmigrated cells on the underside were fixed with 4% formaldehyde in PBS for 10 min and stained with 0.1% crystal violet solution for 10 min. Images were acquired with a phase-contrast light microscope using a c-plan 10 \times /0.22objective (Leica). Transmigrated cells in duplicate inserts were counted in a minimum of five different fields per insert in three independent experiments.

2.2.4 CDC42 pull down assay, immunoprecipitation and immunoblotting

In Chapter 3, in order to isolate the GTP-bound form of CDC42, two different pull down assays were performed according to the manufacturer's instructions using glutathione agarose beads that were bound to either the p21-binding domain of PAK1 (Millipore) or the CDC42-binding domain of WASP (Cytoskeleton) via a GST tag. Immunoblotting of the eluted proteins with an antibody specific for CDC42 (Millipore) identified GTP-bound CDC42. For this experiment, I serum-starved HDMEC overnight, detached and plated them on tissue culture plastic coated with 10

$\mu\text{g/ml}$ FN for 30 minutes; in some experiments, I additionally stimulated for 15 min with 5 ng/ml VEGF165. Also, HDMEC were transfected with siRNA targeting NRP1, ABL1 or control siRNA prior to plating; in other experiments, cells were treated with vehicle or ML141, as described above. HDMEC were then lysed according to the manufacturer's instructions; 350 μg protein was incubated with 10 μg beads at 4°C for 60 minutes. The bead supernatant was collected as the input control, while the bead pellet was washed and then boiled for 5 minutes in 40 μl 2.5x Laemmli sample buffer to elute bound protein. CDC42 activation was calculated as the ratio between CDC42 and GST, detected by immunoblotting after pull down, or GAPDH, detected by immunoblotting in the input lysate (bead supernatant). For immunoprecipitation, HDMEC were lysed in 50 mM Tris pH 8.0 containing 50 mM KCl and 1% (v/v) Triton X-100 as well as protease inhibitor cocktail 2 and phosphatase inhibitor cocktail (Sigma) and incubated with goat anti-NRP1 (AF566, R&D Systems) or control goat IgG (Santa Cruz Biotechnology). For immunoblotting, heat-denatured samples were transferred to nitrocellulose membrane (Whatman, USA) after electrophoretic separation. I used the following antibodies for immunoblotting: mouse anti-CDC42 (cat. no. 17-441, Millipore) and anti-GST (cat. no. G1160, Sigma), rabbit anti-NRP1 (cat. no. D62C6, Cell Signaling), anti-pCRKL-Y207 (cat. no. 3181, Cell Signaling) and anti-GAPDH (cat. no. ab9485, Abcam) followed by appropriate HRP-conjugated secondary antibodies (Sigma).

In Chapter 3 and 5, HDMEC and MLEC were lysed and immunoblotted as described before for the following primary antibodies: rabbit anti-pPXN, anti-VEGFR2, anti-pVEGFR2-Y1175, anti-SRC, anti-pSRC-Y416 (pSFK), anti-pERK1/2 T202/Y204, anti-ERK1/2, anti-pCRKL-Y207, anti-NRP1, anti-FAK and anti-pFAK-Y397 (Cell Signalling Technology), rabbit anti-GAPDH (Abcam), goat anti-CDH5 and rabbit anti-CRKL (Santa Cruz Biotechnology) (**Table 3**).

In Chapter 4, ECs were lysed and incubated with rabbit anti-NRP1, anti-pp44/42 MAPK (pERK1/2) (Cell Signalling) or goat anti-MRTFA and rabbit anti-SRF (Santa Cruz Biotech) rabbit anti-GAPDH (Abcam) followed by HRP-conjugated secondary antibodies (Sigma) (**Table 3**).

2.2.5 Gene expression analyses (qRT-PCR)

2.2.5.1 RNA extraction

mRNA from HDMEC was extracted 72h after the transfection using the RNeasy Mini kit (Qiagen) according to manufacturer's instructions. ECs were collected in 350 μ l of RLT lysis buffer containing β -mercaptoethanol (10 μ l/ml). An equal volume of 70% (v/v) ethanol was added to lysates and solutions were transferred to individual spin columns. RNA was transferred to membranes by centrifuging columns at 8000 rpm for 15 s. Subsequently, membrane-bound RNA was washed with 700 μ l of RW1 buffer and then twice with 500 μ l of RPE buffer. Finally, RNA was eluted in 30 μ l of RNase free water.

2.2.5.2 Reverse transcription

First strand cDNA synthesis was performed using the SuperScript Transcriptase III or IV kit (Invitrogen). For each reaction 250 ng of RNA, 250 ng of random primers, 1 μ l of 10 mM dNTPs were mixed and the volume was adjusted to 13 μ l with water. The mixtures were heated to 65°C for 5 min and chilled on ice for 1 min. 4 μ l of 5X First-Strand Buffer, 1 μ l of 0.1 M DTT, 1 μ l of RNaseOUT and 1 μ l of the enzyme SuperScript III or IV (200 units/ μ l) were added to each sample. Subsequently, samples were incubated for 10 min at 25°C, 50 min at 42°C and 10 min at 70°C. Finally, cDNA quality and concentration was determined using a NanoDrop 1000 spectrometer (Thermo Scientific). cDNA was stored at -20°C.

2.2.5.3 qRT-PCR

qRT-PCR was performed on a 96-well plate using a 7900HT Fast Real-Time PCR System (Applied Biosystems). For each reaction, 50 ng of sample cDNA and 1 μ l each of 10 μ M the forward and reverse oligonucleotide primers, which were designed using the Primer3 software and synthesised to order by Sigma (**Table 1**) were added to 12.5 μ l of Power SYBR Green PCR Master Mix (Applied Biosystems) and diluted with RNase-free water to a volume of 25 μ l. For each gene, the reaction was run in triplicate and for each primer pair a no-template control was included.

After a 10 min enzyme activation step at 95°C, 40 PCR cycles consisting of a 15 s denaturation step at 95°C followed by an annealing and extension step at 60°C were carried out. Data was collected using the Sequence Detector Software (SDS version 2.2; Applied Biosystems) and the presence of primer dimer formation was excluded by examining dissociation curves and DNA amplification in no-template controls. Data analysis was performed using the DART-PCR software (Peirson et al., 2003).

Table 1: Primers designed for RT-PCR of human ECs

Gene	Primer	Sequence
<i>GAPDH</i>	F	5'-ACCCAGAAGACTGTGGATGG-3'
	R	5'- TTCAGCTCAGGGATGACCTT-3'
<i>MYL9</i>	F	5'-TCGCAATGTTTGACCAGTCC-3'
	R	5'-CCGGTACATCTCGTCCACTT-3'
<i>GUS</i>	F	5'-AAACGATTGCAGGGTTTCAC-3'
	R	5'-CTCTCGTCGGTGACTGTTCA-3'
<i>ITGB1</i>	F	5'-TCCTTGAATTGCTGACCTTG-3'
	R	5'-GGCATCGATGATTAGCTGGA-3'
<i>CDH5</i>	F	5'-TACCAGGACGCTTTCACCAT-3'
	R	5'-AAAGGCTGCTGGAAAATGGG-3'
<i>SRF</i>	F	5'-ACCAGATGGCTGTGATAGGG-3'
	R	5'-GCGGATCATTCACTCTTGGT-3'
<i>ACTB</i>	F	5'-GATGAGATTGGCATGGCTTT-3'
	R	5'-CACCTTCACCGTTCCAGTTT-3'
<i>MYH9</i>	F	5'-AAGGAGACCAAGGCTCTGTC-3'
	R	5'-CTTCCAGCTGCGTCTTCATC-3'

<i>ABL1</i>	F 5'-GAGGGCGTGTGGAAGAAATA-3'
	R 5'-GGTAGCAATTTCCCAAAGCA-3'
<i>FLNA</i>	F 5'-TCAAGGTCCCTGTGCATGAT-3'
	R 5'-CATCAGCGTTGTCTACCACG-3'
<i>TLN1</i>	F 5'-GCATCCTGAAGACTGCGAAG-3'
	R 5'-TCGTTGCACTGATGAGGTCT-3'
<i>EGR1</i>	F 5'-AGCCCTACGAGCACCTGAC-3'
	R 5'-GGTTGGCTGGGGTAACTG-3'
<i>FOS</i>	F 5'-TGACTGATACTCCAAGCGGA-3'
	R 5'-CAGGTCATCAGGGATCTTGCA-3'
<i>JUN</i>	F 5'-AACGTGACAGATGAGCAGGA-3'
	R 5'-CTGGGTTGAAGTTGCTGAGG-3'
<i>ABL2</i>	F 5'-TGGTGCGAGAAAGTGAGAGT -3'
	R 5'-CTTGGGTGCTGGGTAGTGTA-3'
<i>TGFB1</i>	F 5'-GACTCTCCACCTGCAAGACC-3'
	R 5'-GACTGGCGAGCCTTAGTTTG-3'
<i>TGFB2</i>	F 5'-TCGCTCATCTCCACAGTGAC-3'

	R 5'-CACACAGGCAACAGGTCAAG-3'
<i>ALK5</i>	F 5'CCGTTTGTATGTGCACCCTC-3'
	R 5'GTGAATGACAGTGCGGTTGT-3'
<i>ENG</i>	F 5'-TCCATTGTGACCTTCAGCCT-3'
	R 5'-CTTGGATGCCTGGAGAGTCA-3'
<i>ALK1</i>	F 5'-GCTTCATCGCCTCAGACATG-3'
	R 5'-TTGCCCTGTGTACCGAAGAT-3'

2.3 Mouse Methods

2.3.1 Animal Maintenance and Husbandry

All animal procedures were performed in accordance with institutional and UK Home Office guidelines. Mice were mated in the evening, and the morning of vaginal plug formation was counted as embryonic (E) 0.5 days. Laura Denti and Dr Valentina Senatore performed mouse husbandry.

2.3.2 Genetic mouse strains

2.3.2.1 Tissue-specific gene targeting

To delete genes in specific tissues, a genetic approach based on the *Cre/lox* recombination system was used [reviewed in (Nagy, 2000)]. This method utilises the properties of the enzyme CRE recombinase, which was initially discovered in the P1 bacteriophage. This enzyme catalyses the recombination between its two 34 bp recognition sites, which are called *loxP* (locus of recombination) sites (Hamilton and Abremski, 1984). By flanking a DNA sequence with these sites, the enzyme is able to bind and create either an inversion or deletion of the sequence depending on the orientation of the *loxP* sites. This recombination can be made tissue-specific by creating a *Cre* transgene under the control of a tissue-specific promoter. Thus, the enzyme will only be expressed and sequence deletion will only occur in the cell type of interest.

2.3.2.2 Temporary regulated *Cre* activation

For temporal activation of CRE in ECs, I used mice containing the *Pdgfb-iCre-ERT2-Egfp* transgene. This transgene consists of a codon-improved *Cre* (*iCre*) gene fused to a murine oestrogen receptor mutant gene (*ERT2*) under the control of the endothelial *Pdgfb* promoter. Unlike the endogenous mouse oestrogen receptor, which binds to 17 α -oestradiol, the CRE-ERT2 recombinase binds to the synthetic compound 4-hydroxytamoxifen (Danielian et al., 1998). CRE-ERT2 is sequestered within the cytoplasm by the cytoplasmic protein HSP90 (Mattioni et al., 1994, Picard, 1994); however, upon tamoxifen binding to the receptor, this interaction is prevented and

thus allows the enzyme to translocate to the nucleus. Therefore, *Cre*-mediated DNA recombination will only occur once 4-hydroxytamoxifen, or its precursor tamoxifen, has been administered to the mouse.

For tamoxifen-induced, endothelial specific targeting of *Nrp1*, I used mice carrying two floxed conditional *Nrp1* null alleles (*Nrp1^{fl/fl}*) together with one copy of the *Pdgfb-iCre-ERT2-Egfp* on a C57/B16 background (Fantin et al., 2013a). Tamoxifen (Sigma) was dissolved in peanut oil at 2 mg/ml, and 0.1 mg was administered to mouse pups on postnatal (P) day 2 and P3 via subcutaneous injections, followed by intraperitoneal injections on P4 and P5. Injections were carried out by Dr Alessandro Fantin.

2.3.2.3 Generation of *Nrp1^{cyto/cyto}* mice

Mice lacking NRP1 cytoplasmic domain (*Nrp1^{cyto/cyto}*) were engineered by Dr Quentin Schwarz, in Prof Ruhrberg's team, using gene targeting. A premature stop codon was introduced into the last exon of a *Nrp1* cDNA immediately downstream of the predicted transmembrane domain to prevent translation of the cytoplasmic domain (amino acid residues 885-923). The mutated exon was inserted into the BACPAC clone RP23-298G15 (Children's Hospital Oakland Research Institute CHORI, Oakland, California, USA) by ET recombineering. The construct was electroporated into a hybrid male ES cell line that contains both a 129vEvTac and a C57BI/6 genome (line D, established from 129S6/C57B1/6J F1 blastocysts by the Gene Targeting and Transgenic Facility of the University of Connecticut Health Center, Farmington, USA). Neomycin selection identified gene targeted clones. To identify ES cells carrying the neomycin cassette, EcoRI-digested genomic DNA was screened in 96-well plates by Southern blot analysis with an external 3' probe. Homologous recombination was confirmed using an external 5' probe on SspI-digested genomic DNA. The targeted ES cells were aggregated with CD1 embryos at the 8-cell stage. The resulting chimeric males were mated to CD1 females to determine if the targeted ES cells had contributed to the germline, i.e. if pups with black eyes were born. A germline-transmitting male (2E2) was then mated to a female carrying a targeted X-linked *Hprt^{Cre}* transgene (The Jackson Laboratory) to delete the neo cassette in the germline. The F1 offspring were genotyped by PCR to

distinguish wild type and heterozygous littermates. Finally, heterozygous offspring were backcrossed to C57B1/6 mice (Charles River Laboratories) for 6 generations. Southern blotting and PCR were used to confirm the presence of the mutated knock-in allele in the progeny of the first heterozygous intercross.

2.3.3 Genotyping of mouse strains

Genotyping was performed by Ms Denti and Dr Senatore. DNA was extracted from adult ear punches using a previously published method (Laird et al., 1991). Briefly, cells were lysed by incubating them overnight at 55°C with gentle agitation in 500 µl of lysis buffer (100 mM Tris-HCl pH 8.5, 5 mM EDTA, 0.2% SDS, 200 mM NaCl) with freshly added proteinase K (100 µg/ml). After the enzymatic digestion, DNA was precipitated by adding 1 ml of 100% ethanol, and collected following a 3 min centrifugation at 13000 rpm. DNA was resuspended in 70% ethanol and collected following another centrifugation. Subsequently, DNA was air-dried for 10 min at RT and reconstituted in 100 µl TBE buffer (2 mM Tris pH 8.0, 0.2 mM EDTA) for 5-30 min at 55°C.

The genomic DNA was amplified by PCR using primers specific to the DNA sequence of interest (i.e. *Nrp1*) on a BioRad C1000 Touch Thermal Cycler. Per PCR reaction, 2 µl of DNA were added to 8 µl Megamix (Microzone, containing Taq polymerase, 1.1X reaction buffer, 220 µM dNTPs, loading dye) and 0.1 µg of both the forward and reverse primer using the relevant annealing temperature and number of amplification cycles (**Table 2**).

The PCR products were analysed using electrophoresis through a 2% (w/v) agarose (BDH Electran) gel containing 2 µl of nucleic acid staining solution RedSafe (iNtRON) in TAE buffer (40 mM Tris-acetate, 1 mM EDTA, pH 8.0). For each reaction, a negative control consisting of 2 µl sterile water and a positive control comprising 2 µl of previously validated DNA were used instead of the DNA of interest.

Table 2: PCR cycling parameters used in genotyping

Genes	Hot Start	Denaturing	Annealing	Extension	Cycles	End
<p><u>Nrp1^{cyto}</u>: CytoF 5'-CCTTTTGATGGACATGTGACCTGTAGC-3'</p> <p>CytoR 5'-CACCAGGTCTGATTGAAGAGAAGG-3'</p>	94°C, 2 min	94°C, 40s	60°C, 45 s	72°C, 1min	35	72°C, 5min
<p><u>Nrp1, Nrp1^{fl}</u>: NRP1Neo 5'-CGTGATATTGCTGAAGAGCTTGGC-3'</p> <p>NRP1F 5'-CAATGACACTGACCAGGCTTATCATC-3'</p> <p>NRP1R 5'-GATTTTATGGTCCCGCCACATTGTC-3'</p>	94°C, 3min	94°C, 40s	66°C, 1min	72°C, 1min	35	72°C, 5min

2.3.4 Whole mount immunolabelling and imaging of mouse retinas and aortas

P6-P7 mouse retinas and aortas were immunolabelled as described (Fantin et al., 2013b, Pitulescu et al., 2010). Dr Alessandro Fantin performed retinal dissections as it has been outlined in (Pitulescu et al., 2010) and together we performed dissection of aortas as it has been described in (Corada et al., 2013).

Some retinas and aorta samples were fixed in 4% PFA for 2 h at 4°C and used immediately for staining or stored for short-term at 4°C with 1X PBS. Other samples were fixed in 4% PFA for 2 h at 4°C followed by 100% methanol overnight at -20°C. Following fixation, all samples were washed twice with 1X PBS for 5 min at RT to remove any residual PFA or methanol. Subsequently, the samples were blocked for 1h using a blocking solution consisting of either 10% (v/v) NGS (Normal Goat Serum) in 1X PBT (1X PBS + 0.1% (v/v) Triton X-100) or 100% (v/v) serum free block (Dako). After blocking, the primary antibodies were diluted in the blocking solution and the samples were incubated overnight at 4°C. The antibody solution was removed and the samples were washed 3 times with 1X PBT for 10 min each at RT. Secondary antibodies raised against the host animal of the primary antibody were diluted 1:200 in the blocking solution. Samples were incubated with secondary antibody solution for 1h at RT in the dark to protect fluorophores. More specifically, the postnatal retinas and aortas were immunolabelled using rabbit anti-pp44/42 MAPK (ERK1/2) (Cell Signaling), rabbit anti-SRF (Santa Cruz Biotech) or goat anti-rat NRP1 (cat. no. AF566, R&D Systems) and rat anti-CD144 (BD Bioscience) followed by Alexa Fluor 594- or 488-conjugated goat anti-rabbit or anti-rat or by Alexa Fluor 647-conjugated donkey anti-goat Fab fragment (Jackson Immuno) (**Tables 3,4**). Subsequently, the samples were washed 3 times with 1X PBS for 10 min, stained with DAPI for 3 min to visualise the nuclei and post-fixed for 10 min with 4% PFA at RT. The samples were flatmounted in Mowiol with a glass cover slip.

Samples were imaged with a LSM710 laser scanning confocal microscopes (Zeiss, Jena, Germany) and confocal z-stacks through the labelled tissue were acquired using 10x and 40x objectives. Images were processed with Photoshop CS4 (Adobe Inc.).

Table 3: List of antibodies used for immunoblotting and immunofluorescence

Antibodies	Origin	Supplier	Dilution
mouse PECAM1 (CD31)	rat	BD Pharmingen	1:100
mouse ICAM2 (CD102)	rat	BD Pharmingen	1:100
mouse Cdh5 (CD144)	rat	BD Pharmingen	1:1.000 IB 1:200 IF
human phospho-Paxillin (pPXN)	rabbit	Cell Signaling Technology	1:1.000 IB 1:50 IF
human phospho-p44/42 MAPK (pERK1/2)	rabbit	Cell Signaling Technology	1:1.000 IB 1:200 IF
rat p44/42 MAPK (ERK1/2)	rabbit	Cell Signaling Technology	1:1.000 IB
human Src	rabbit	Cell Signaling Technology	1:1.000 IB
human phospho-SrcTyr416 (pSFK)	rabbit	Cell Signaling Technology	1:1.000 IB 1:200 IF
mouse Neuropilin-1 (NRP1)	human	R&D Systems	1:200 IF
human CDH5	goat	Santa Cruz Biotechnology	1:2.000 IB 1:200 IF
human SRF (H-300)	rabbit	Santa Cruz Biotechnology	1:1.000 IB 1:200 IF
human CRKL	rabbit	Santa Cruz Biotechnology	1:2.000 IB

human MRTFA	goat	Santa Cruz Biotechnology	1:500 IB 1:200 IF
mouse/rat Neuropilin-1 (NRP1)	goat	R&D Systems	1:200 IF
human CDC42	mouse	Merck Millipore	1:500 IB
Glutathione-S-Transferase (GST)	mouse	Sigma-Aldrich	1: 2.000IB
mouse NRP1	rabbit	Cell Signaling Technology	1:1.000 IB
human phospho-CrkLTyr207 (pCRKL)	rabbit	Cell Signaling Technology	1:1.000 IB
human GAPDH	rabbit	Abcam	1: 2.000IB
human FAK	rabbit	Cell Signaling Technology	1:1.000 IB
human phospho-FAKTyr397 pFAK	rabbit	Cell Signaling Technology	1:1.000 IB
human phospho-VEGF Receptor 2Tyr1175 (pVEGFR2)	rabbit	Cell Signaling Technology	1:1.000 IB
human VEGF Receptor 2 (VEGFR2)	rabbit	Cell Signaling Technology	1:1.000 IB

Table 4: List of the secondary antibodies used for immunofluorescence

Secondary antibodies	Supplier
Alexa488/594/647- conjugated goat anti-mouse IgG	Jackson ImmunoResearch Laboratories
Alexa488/594/647- conjugated goat anti-rabbit IgG	Jackson ImmunoResearch Laboratories
Alexa488/594- conjugated goat anti-rat IgG	Jackson ImmunoResearch Laboratories
Alexa488/594/647- conjugated donkey anti-goat Fab fragment	Thermofisher Scientific (Invitrogen)
Alexa488/633- conjugated phalloidin	Thermofisher Scientific (Molecular Probes)

2.3.5 Fluorescence-activated cell sorting (FACS)

Tissues were isolated and homogenised in ice-cold RPMI1640 medium (Life Technologies) containing 5% (v/v) FBS, 2.38 g/L HEPES and 1.5 g/L sodium hydrogen carbonate according to their tissue-specific requirements. Thus, brain tissue from P7 mice was homogenised using a scalpel, 21 G and 23 G needle syringes and re-suspended in RPMI media as described above containing collagenase (Worthington). The samples were incubated in the water bath for 20 min and then centrifuged at 1200 rpm for 5 min. The supernatant was removed and the sample was re-suspended in RPMI buffer. To generate single cell suspensions, homogenates were passed through a 70 µm filter. Cell suspensions were incubated with Fc block (BD Biosciences) for 5 min at RT to prevent non-specific binding of antibodies. Samples were stained using the following directly conjugated antibodies (BD Biosciences): PECAM-APC, IB4-FITC and DAPI to identify live cells. Labelled cells were analysed with a BD Influx cell sorter (BD Biosciences). Unstained samples and fluorescence-minus-one (FMO) samples, stained with all the fluorochromes minus one fluorochrome, were used to identify appropriate fluorescence voltage and gate parameters. Cells that were double positive for IB4 and PECAM were collected in RLT buffer for RNA extraction and stored in -80°C.

2.3.6 RNA extraction from ECs collected by FACS sorting

Total RNA was extracted from samples using the RNeasy Micro kit (Qiagen) according to manufacturer's instructions. ECs were collected after FACS sorting in 350 µl of RLT lysis buffer containing β-mercaptoethanol (10 µl/ml). An equal volume of 70% (v/v) ethanol was added to lysates and solutions were transferred to individual spin columns. RNA was transferred to membranes by centrifuging columns at 8000 rpm for 15 s. Subsequently, membrane-bound RNA was washed with 350 µl of RW1 buffer. Genomic DNA was removed by digestion with DNase 1 solution for 15 min at RT and a subsequent wash with 350 µl of RW1 buffer. Membrane-bound RNA was first washed with 500 µl of RPE buffer and then 80% (v/v) ethanol. Finally, RNA was eluted in 14 µl of RNase free water.

2.3.7 RT² Profiler PCR Array

Brain endothelial cells (BECs) from P7 mice were collected with FACS sorting. mRNA was extracted as described above and the cDNA was synthesized using the RT² First Strand Kit. For each reaction 60 ng of RNA, 2 µl of buffer GE were mixed and the volume was adjusted to 10 µl with water (genomic DNA elimination mix). The mixtures were heated to 42°C for 5 min and chilled on ice for 1 min. 4 µl of 5X Buffer BC3, 1 µl of Control P2, 2 µl of RE3 Reverse Transcriptase Mix were added to each sample and the volume was adjusted to 10 µl with water (Reverse-transcription mix). 10 µl reverse-transcription mix were added to each tube containing 10 µl genomic DNA elimination mix. Subsequently, samples were incubated for 15 min at 42°C and then the reaction was immediately stopped with incubation at 95°C for 5 min. 91 µl of RNase free water was added to each sample.

qRT-PCR was performed on a 96-well RT² Profiler PCR Array plate ('Mouse Cell motility' Array, Qiagen; see **Table 5**). For each plate, 60 ng of cDNA (diluted in a volume of 102 µl) from four pooled brains added to 1350 µl of RT² SYBR Green Mastermix (Qiagen) and 1248 µl RNase free-water, and the resulting solution was split equally amongst the wells. Expression values for genes examined using the RT² Profiler PCR Array plate were calculated manually using the online Qiagen expression analysis software and normalised using *Actb* expression as a reference.

Table 5: Cell motility related genes in RT² Profiler PCR Array

Symbol	Description
2900073G15 Rik	RIKEN cDNA 2900073G15 gene
Actn1	Actinin, alpha 1
Actn3	Actinin alpha 3
Actn4	Actinin alpha 4
Acr2	ARP2 actin-related protein 2 homolog (yeast)
Acr3	ARP3 actin-related protein 3 homolog (yeast)
Akt1	Thymoma viral proto-oncogene 1
Arf6	ADP-ribosylation factor 6
Arhgdia	Rho GDP dissociation inhibitor (GDI) alpha
Arhgef7	Rho guanine nucleotide exchange factor (GEF7)
Baiap2	Brain-specific angiogenesis inhibitor 1-associated protein 2
Bcar1	Breast cancer anti-estrogen resistance 1
Capn1	Calpain 1
Capn2	Calpain 2
Cav1	Caveolin 1, caveolae protein
Cdc42	Cell division cycle 42 homolog (<i>S. cerevisiae</i>)
Cfl1	Cofilin 1, non-muscle
Crk	V-crk sarcoma virus CT10 oncogene homolog (avian)
Csf1	Colony stimulating factor 1 (macrophage)
Ctn	Cortactin
Diap1	Diaphanous homolog 1 (<i>Drosophila</i>)
Dpp4	Dipeptidylpeptidase 4
Egf	Epidermal growth factor
Egfr	Epidermal growth factor receptor
Enah	Enabled homolog (<i>Drosophila</i>)
Ezr	Ezrin
Fap	Fibroblast activation protein
Fgf2	Fibroblast growth factor 2
Hgf	Hepatocyte growth factor
Igf1	Insulin-like growth factor 1
Igf1r	Insulin-like growth factor 1 receptor
Ilk	Integrin linked kinase
Itga4	Integrin alpha 4
Itgb1	Integrin beta 1 (fibronectin receptor beta)
Itgb2	Integrin beta 2
Itgb3	Integrin beta 3
Limk1	LIM-domain containing, protein kinase
Mapk1	Mitogen-activated protein kinase 1
Met	Met proto-oncogene
Mmp14	Matrix metalloproteinase 14 (membrane-inserted)
Mmp2	Matrix metalloproteinase 2
Mmp9	Matrix metalloproteinase 9

Symbol	Description
Msn	Moesin
Myh10	Myosin, heavy polypeptide 10, non-muscle
Myh9	Myosin, heavy polypeptide 9, non-muscle
Mylk	Myosin, light polypeptide kinase
Pak1	P21 protein (Cdc42/Rac)-activated kinase 1
Pak4	P21 protein (Cdc42/Rac)-activated kinase 4
Pfn1	Profilin 1
Pik3ca	Phosphatidylinositol 3-kinase, catalytic, alpha polypeptide
Plaur	Plasminogen activator, urokinase receptor
Plcg1	Phospholipase C, gamma 1
Pld1	Phospholipase D1
Prkca	Protein kinase C, alpha
Pten	Phosphatase and tensin homolog
Plk2	PTK2 protein tyrosine kinase 2
Plk2b	PTK2 protein tyrosine kinase 2 beta
Ptpn1	Protein tyrosine phosphatase, non-receptor type 1
Pxn	Paxillin
Rac1	RAS-related C3 botulinum substrate 1
Rac2	RAS-related C3 botulinum substrate 2
Rasa1	RAS p21 protein activator 1
Rdx	Radixin
Rho	Rhodopsin
Rhoa	Ras homolog gene family, member A
Rhob	Ras homolog gene family, member B
Rhoc	Ras homolog gene family, member C
Rnd3	Rho family GTPase 3
Rock1	Rho-associated coiled-coil containing protein kinase 1
Sh3pxd2a	SH3 and PX domains 2A
Src	Rous sarcoma oncogene
Stat3	Signal transducer and activator of transcription 3
Svil	Supervillin
Tgfb1	Transforming growth factor, beta 1
Timp2	Tissue inhibitor of metalloproteinase 2
Tln1	Talin 1
Vasp	Vasodilator-stimulated phosphoprotein
Vcl	Vinculin
Vegfa	Vascular endothelial growth factor A
Vim	Vimentin
Wasf1	WASP family 1
Wasf2	WAS protein family, member 2
Wasl	Wiskott-Aldrich syndrome-like (human)
Wipf1	WAS/WASL interacting protein family, member 1
Actb	Actin, beta
B2m	Beta-2 microglobulin
Gapdh	Glyceraldehyde-3-phosphate dehydrogenase
Gusb	Glucuronidase, beta
Hsp90ab1	Heat shock protein 90 alpha (cytosolic), class B member 1
MGDC	Mouse Genomic DNA Contamination
RTC	Reverse Transcription Control
RTC	Reverse Transcription Control
RTC	Reverse Transcription Control
PPC	Positive PCR Control
PPC	Positive PCR Control
PPC	Positive PCR Control

2.4 Statistical analysis

To determine if two data sets were significantly different, the P-value was calculated by performing a two-tailed unpaired t-test for the *in vivo* experiments and either paired or unpaired t-test for the *in vitro* experiments, depending on the experimental conditions. $P < 0.05$ was considered significant. The graphs and the statistical analysis were carried out using Microsoft Excel (Microsoft).

Chapter 3 NRP1 promotes actin remodelling via ABL1 and CDC42

3.1 Introduction

NRP1 is a non-catalytic receptor for the VEGF₁₆₅ isoform of VEGF that complexes with VEGFR2 to potentiate signal transduction [e.g. (Mamluk et al., 2002, Koch et al., 2011)]. Thus, the NRP1 cytoplasmic tail recruits a trafficking complex that directs VEGFR2 along an endocytic pathway that prevents receptor dephosphorylation to augment mitogen-activated protein kinase (MAPK) signalling via ERK1 and ERK2 (Lanahan et al., 2013a, Salikhova et al., 2008, Ballmer-Hofer et al., 2011). This NRP1 function is essential for arteriogenesis, which depends on luminal vessel growth, but dispensable for angiogenesis, driven by vessel sprouting, branching and fusion (Lanahan et al., 2013a, Fantin et al., 2011).

Studies from our lab showed that the hindbrain of E12.5 mice that express NRP1 with a mutation at the VEGF₁₆₄ binding site and reduced NRP1 expression (Y297A mutation) showed milder angiogenesis defects compared to *Nrp1*^{-/-} mice (Fantin et al., 2014). During the course of my PhD research, another study was published using mice with a different point mutation (D320K mutation) in the VEGF₁₆₄ binding site and normal NRP1 expression; their analysis showed normal embryonic angiogenesis when VEGF binding to NRP1 is lost (Gelfand et al., 2014). These findings show that VEGF binding to NRP1 is dispensable for embryonic development and suggests that NRP1 can contribute to angiogenesis independently of VEGFR2.

It is known that NRP1 is able to interact with extracellular matrix (ECM) receptors of the integrin family independently of VEGFR2 (Valdembri et al., 2009, Fukasawa et al., 2007, Murga et al., 2005). More specifically, studies in human umbilical artery ECs showed that the NRP1 cytoplasmic domain promotes the internalisation of active $\alpha 5 \beta 1$ integrin to enhance ECs spreading on FN (Valdembri et al., 2009). Also, in cancer cells, a NRP1 interaction with integrin $\beta 1$ promotes cell adherence and invasion (Fukasawa et al., 2007). In HUVEC, NRP1 promotes adhesion to low concentrations of extracellular matrix proteins, including FN, independently of VEGFR-2 (Murga et al., 2005). However, NRP1 does not appear to be required for adhesion to the FN concentrations usually used for adhesion assays and tissue culture, even though it still promotes motility and migration on this substrate

(Raimondi et al., 2014). Yet, the intracellular pathways that are regulated by NRP1 in a VEGF/VEGFR2-independent fashion have not been defined. Moreover, the relative significance of NRP1 for VEGF/VEGFR2-dependent versus integrin ligand-stimulated, but VEGFR2-independent processes for angiogenesis *in vivo* has not been determined.

Here, I have used primary ECs as a model to show how NRP1 controls actin cytoskeleton remodelling independently of VEGFR2. The first part of the Chapter, which describes how NRP1 mediates PXN phosphorylation via ABL1 in HDMEC (**Fig. 4 and 5**), includes experiments performed by Dr Claudio Raimondi and myself and has been published [(Raimondi et al., 2014); see Appendix]. Dr Raimondi designed these experiments and I carried out experiments such as immunoblotting and immunostaining under his supervision, while I was also responsible for the cell culture. This work was also validated in a mouse model of endothelial NRP1 deficiency *in vivo* by Dr Fantin, published in the same paper and other [(Raimondi et al., 2014) and (Fantin et al., 2015); see Appendix].

3.2 Results

3.2.1 NRP1-dependence of ECM-induced angiogenesis

3.2.1.1 NRP1 promotes actin remodelling of FN-stimulated ECs independently of VEGFR2

To examine whether NRP1 promotes ECM-induced angiogenesis, Dr Raimondi in the lab and I used HDMEC, because dermal vasculature naturally undergoes extensive angiogenesis during wound healing. I transfected these primary cells with a previously validated small interference (si) RNA that targets NRP1 or VEGFR2 or with a control nonsense siRNA (Nayak and Cooper, 2012). Cells were detached and seeded on FN for 240 min (**Fig. 4A**). Western blot analysis confirmed that the knockdown for NRP1 and VEGFR2 was effective (**Fig. 4B**). Phalloidin staining of F-actin showed that NRP1-deficient HDMEC adopted an abnormal round morphology with abundant cortical actin. In contrast, control cells appeared elongated and contained stress fibres typical of adherent cells (**Fig. 4C**). VEGFR2 protein levels were slightly, but significantly decreased in NRP1-deficient cells (**Fig. 4B**). However, cytoskeletal defects in NRP1-deficient cells were not caused by low VEGFR2 expression, because cells transfected with siRNA targeting VEGFR2 spread well on FN and assembled many stress fibres (**Fig. 4C**). Quantitation of phalloidin-positive, filopodia-like microspikes in HDMEC seeded for 30, 60, 120 and 240 min on FN, confirmed that NRP1, but not VEGFR2 downregulation significantly impaired microspike extension (**Fig. 4D**). Strikingly, addition of VEGF165, known to bind both VEGFR2 and NRP1, did not rescue the cytoskeletal defects of FN-stimulated HDMEC lacking NRP1 (data not shown, experiment performed by Dr Raimondi). NRP1 therefore functions independently of VEGF165 and VEGFR2 to regulate ECM-induced actin remodelling in ECs.

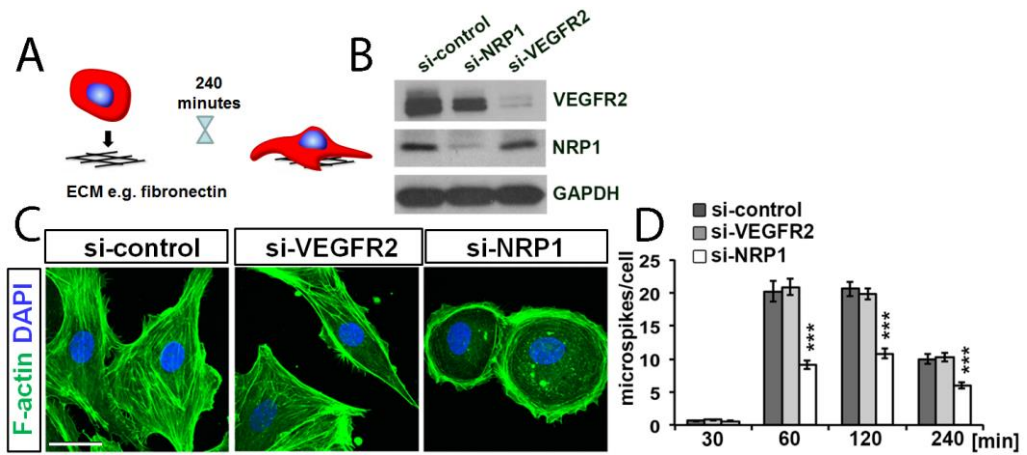


Figure 4: NRP1 promotes FN-induced actin remodelling and filopodia extension in primary ECs.

HDMEC transfected with control, VEGFR2 or NRP1 siRNA were plated on FN for 240 minutes (A) before immunoblotting (B) or fluorescent labelling (C) with the F-actin marker phalloidin (green) and the nuclear counterstain DAPI (blue). Scale bar 20 μm . Quantification (D) of actin microspikes of cells seeded for the indicated time on FN; mean \pm SEM of ≥ 30 cells from 3 independent experiments (***) P < 0.001; unpaired t-test)

3.2.1.2 NRP1 is required for ECM-induced PXN phosphorylation and focal adhesion localisation in ECs and EC migration

Because pPXN is recruited to focal adhesions to promote their turnover during cell migration (Zaidel-Bar et al., 2007, Pasapera et al., 2010), I examined pPXN protein level and localisation in FN-stimulated HDMEC by immunostaining. In control cells, pPXN was present in focal adhesions at the end of F-actin stress fibres, correlating with an elongated cell shape (**Fig. 5A**). Moreover, FN-stimulated control HDMEC displayed the hallmarks of polarised cells. In contrast, HDMEC lacking NRP1 displayed a characteristic rounded morphology with abundant cortical actin; moreover, correlating with the lack of stress fibres, pPXN levels were significantly decreased, with remaining pPXN being localised mainly to the cell periphery (**Fig. 5A**). Notably, VEGF165-induced PXN phosphorylation was unaffected by NRP1 loss (data not shown, experiment performed by Dr Raimondi). These findings demonstrate that NRP1 promotes PXN phosphorylation downstream of ECM activation independently of VEGF165. Impaired actin remodelling in NRP1-deficient ECs on FN predicts defective cell motility. A transwell assay measuring FN-induced haptotaxis demonstrated reduced migration of NRP1-deficient compared to control cells on FN, but VEGFR2 knockdown did not affect FN-induced migration (data not shown, experiment performed by Dr Raimondi). NRP1 deficiency therefore impairs ECM-induced EC migration independently of VEGFR2.

3.2.1.3 ABL1 kinase is essential for ECM-induced PXN phosphorylation and EC migration

As NRP1 lacks catalytic activity, it requires a partner kinase to promote FN-induced PXN phosphorylation. A good candidate is the cell adhesion-associated kinase ABL1, which interacts with PXN in FN-stimulated fibroblasts (Lewis and Schwartz, 1998b) as well as with the integrin β subunits $\beta 1$ and $\beta 2$ (Baruzzi et al., 2010, Cui et al., 2009). Furthermore, the PXN Y118 residue that is phosphorylated in a NRP1-dependent fashion resides in an ABL1 phosphorylation consensus site (Cujec et al., 2002), and ABL1 is an effector of NRP1 and integrins in tumour matrix remodelling (Yaqoob et al., 2012). To investigate ABL1 function in FN-stimulated ECs, we used

two independent, but complementary methods, the siRNA-mediated knockdown of ABL1 and the pharmacological inhibition of ABL1 kinase activity.

We found that targeting ABL1 caused a phenotype similar to NRP1 knockdown. Thus, immunostaining revealed significantly reduced pPXN levels, with residual pPXN accumulating in the cell periphery (**Fig. 5A,C**). ABL1 knockdown was confirmed by qPCR (**Fig. 5B**). Moreover, there was a conspicuous absence of pPXN-positive focal adhesion contacts in areas where stress fibres terminate in control cells, but abundant cortical actin, correlating with impaired cell spreading and a round, rather than elongated cell shape, as observed after NRP1 knockdown. Hence, ABL1 may affect NRP1-dependent pPXN upregulation by directly promoting PXN phosphorylation.

To examine if ABL1 kinase activity was required for FN-induced PXN phosphorylation, we treated HDMEC with Imatinib (Glivec), a small molecule inhibitor that effectively targets ABL1, but not VEGFR2 (Buchdunger et al., 2002, Anselmi et al., 2012), and has been approved for therapy in cancers with upregulated ABL1 kinase activity (Druker et al., 1996). As observed in siABL1-transfected cells, Imatinib-treated HDMEC formed few stress fibres, but abundant cortical actin, and they adopted a round shape with reduced cell spreading; moreover, they had low pPXN phosphorylation, with residual pPXN in the cell periphery rather than in areas where stress fibres normally terminate in focal adhesions (**Fig. 5A**). The quantitation of pixel intensities in immunostaining (**Fig. 5D**) confirmed significantly reduced PXN phosphorylation in Imatinib-treated compared to control cells.

As PXN phosphorylation promotes the turnover of focal adhesions that serve as traction points during cell migration (Zaidel-Bar et al., 2007), ABL1 loss would be predicted to impair EC migration on FN. In agreement, a transwell assay showed a 40% reduction in haptotactic migration after ABL1 knockdown (**Fig. 5E**), which was similar to the reduction observed after NRP1 knockdown. NRP1 and ABL1 therefore similarly regulate PXN phosphorylation, actin remodelling and cell migration in FN-stimulated ECs.

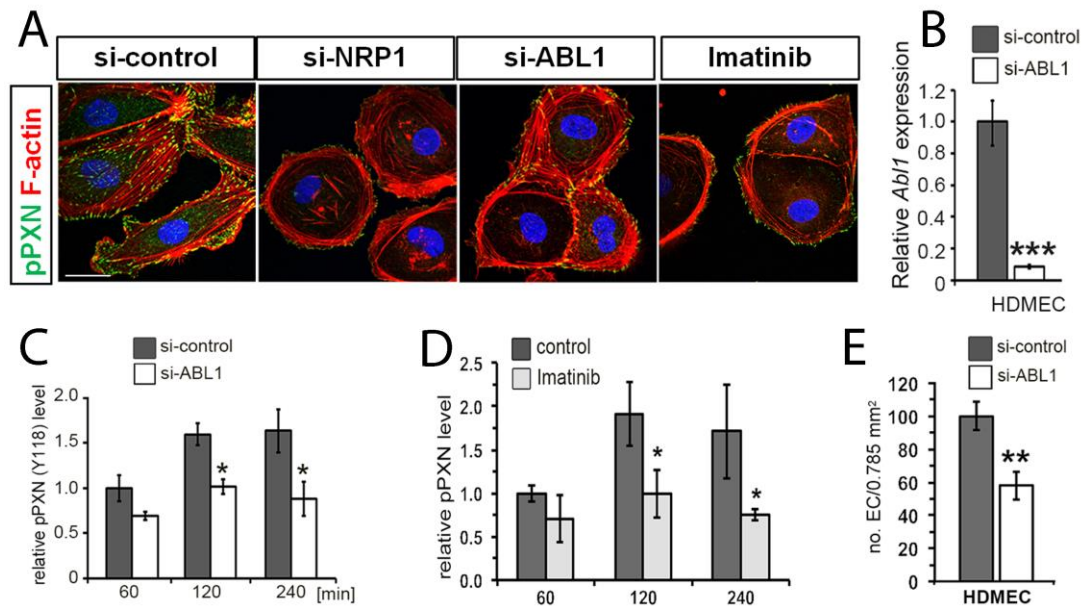


Figure 5: NRP1 promotes FN-induced PXN phosphorylation via ABL1 kinase in primary ECs.

(A) HDMEC were transfected with NRP1 or ABL1 or control siRNA and treated with 10 μ M Imatinib or vehicle and then seeded on FN for 4h before staining for F-actin (red), pPXN (green) and DAPI (blue). Scale bar 20 μ m.

(B) *Abl1* expression in HDMEC after ABL1 knockdown (*** $P < 0.001$)

(C,D) pPXN pixel intensity was quantified and expressed as fold change in siABL or Imatinib treated cells at the indicated time points relative to control cells at 60 min (mean \pm SD of 4 independent experiments). Asterisks indicate P values for control relative to si-NRP1 transfected cells: (* $P < 0.05$; paired t-test)

(E) HDMEC transfected with control or ABL1 siRNA were plated on FN-coated transwells and the percentage of transmigrated HDMEC determined after 240 min in knockdown relative to control cells (mean \pm SEM in 4 independent experiments). Asterisks indicate P values for control relative to si-NRP1 transfected cells: (** $P < 0.01$; paired t-test)

3.2.2 NRP1 cytoplasmic domain is not required for ECM-induced PXN phosphorylation

Prior studies have shown that *Nrp1*^{cyto/cyto} mice are viable and display normal developmental and pathological angiogenesis, with the only reported vascular growth abnormalities seen in arterial patterning; thus these mice have an increased number of artery-vein crossings in the retina and impaired arteriolar formation in several organs (Fantin et al., 2011, Lanahan et al., 2013b). Here, MLEC from wild type or *Nrp1*^{cyto/cyto} lungs were seeded for 1h on FN before lysis or lysed before seeding. Immunoblotting showed that phosphorylated PXN was similarly activated 1h after FN stimulation in wild type and *Nrp1*^{cyto/cyto} cells, suggesting that the cytoplasmic domain of NRP1 is not required for ECM-induced PXN phosphorylation (2 independent experiments) (**Fig. 6**). It is instead possible that NRP1 interacts with an integrin receptor upon FN stimulation to mediate ABL-dependent paxillin phosphorylation and actin remodelling.

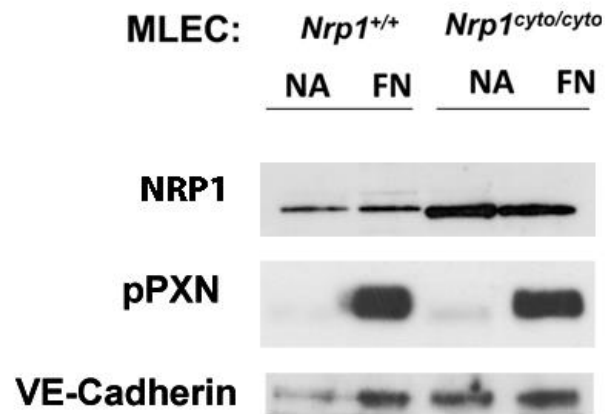


Figure 6: The NRP1 cytoplasmic domain is not required for ECM-induced PXN phosphorylation.

MLEC from *Nrp1*^{cyto/cyto} and wildtype lungs were serum-starved and stimulated with FN for 1 hour before lysis or lysed before plating on FN (non-adherent, NA). Lysate was used for immunoblotting with the indicated antibodies. N= 2 independent experiments.

3.2.3 NRP1 regulates CDC42 activity to promote filopodia formation in ECs

In order to investigate how NRP1 modulates cytoskeleton remodelling and filopodia formation, which are both required for tip cell formation, I examined whether it affects CDC42 activation, as this small RHO-GTPase promotes actin remodelling and filopodia formation in other cell types.

3.2.3.1 NRP1 enables CDC42-dependent actin dynamics and filopodia extension in ECM-stimulated ECs

To compare the effect of NRP1 loss and CDC42 inhibition on actin remodelling, I used phalloidin staining to visualise F-actin after NRP1 knockdown or treatment with ML141, a validated allosteric inhibitor with exquisite specificity for CDC42 over other small RHO-GTPases (Hong et al., 2013). I found that many control cells (transfected with si-control or treated with vehicle) had assumed an elongated appearance with irregular edges and numerous stress fibres after 2 hours on FN, typical of motile cells (**Fig. 7A,C**). In contrast, NRP1 knockdown caused many cells to adopt a rounded morphology with few stress fibres (**Fig. 7B**), as shown above (**Fig. 4C**). ML141-treated cells presented a similar phenotype to cell lacking NRP1 (**Fig 7D**). Higher magnification images showed that the altered morphology of NRP1-deficient and ML141-treated cells correlated with reduced cell protrusive activity compared to control cells (**Fig. 7A', B', D'**). Moreover, quantitative analysis confirmed that both NRP1 knockdown and CDC42 inhibition significantly reduced the number of actin-positive, filopodia-like microspikes extending from the cell periphery in HDMEC plated on FN for 1 hour. The relative reduction in microspike number was similar in ML141-treated compared to NRP1 knockdown HDMEC on FN (**Fig. 7E**).

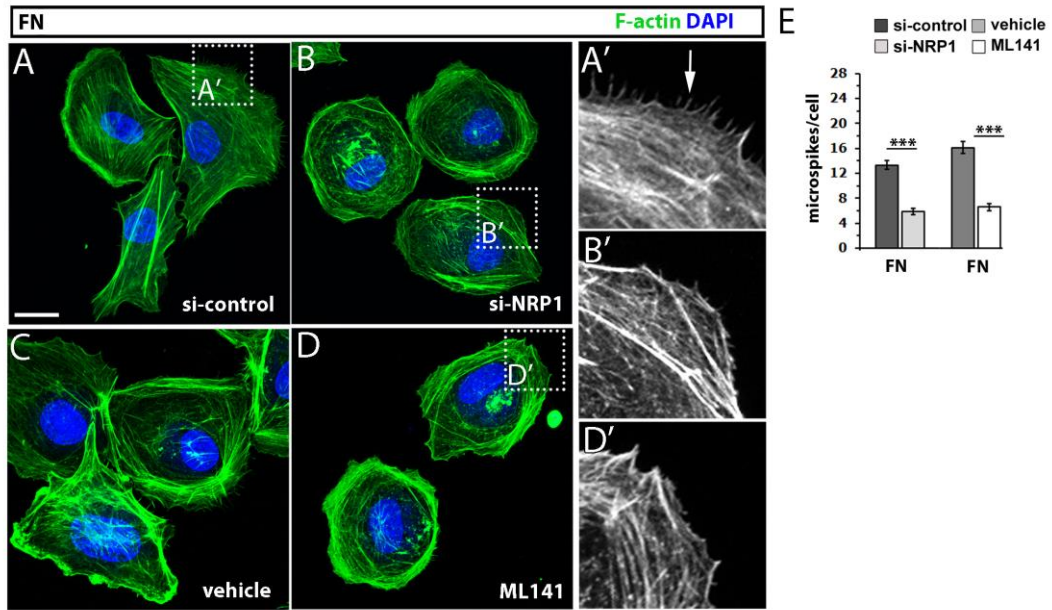


Figure 7: NRP1 and CDC42 are required for ECM-induced actin remodelling in ECs.

HDMEC were serum-starved and treated with vehicle or ML141 for 30 minutes or transfected with si-control or si-NRP1 and serum starved.

(A-D) HDMEC were detached, plated on FN for 2 hours and stained with phalloidin (green) to label F-actin and DAPI (blue) to visualise cell nuclei. Scale bar 20 μm. Higher magnification images of the boxed areas in (A, B, D) are shown in (A', B', D'). Arrowhead indicates filopodia extension (A').

(E) Microspike quantitation after NRP1 knockdown or CDC42 inhibition and plating for 1 hour on FN, shown as mean microspike number per cell ± SEM; $n \geq 42$ cells from 3 independent experiments for each condition; asterisks indicate P values for control relative to si-NRP1 or ML141 treated cells: (***) $P < 0.001$; unpaired t-test

3.2.3.2 NRP1 is required for ECM-induced CDC42 activation in ECs

To measure levels of GTP-bound, i.e. activated CDC42, I used a pull down assay with the p21-binding domain of the p21-activated protein kinase PAK1 (Benard et al., 1999). This experiment showed that FN stimulation for 30 minutes efficiently activated CDC42 in HDMEC (**Fig. 8A**). Moreover, the CDC42 inhibitor ML141 effectively targeted this FN-dependent CDC42 activation, confirming specificity of the assay (**Fig. 8A**). I next transfected HDMEC with control si-RNA (si-control) or NRP1 si-RNA (si-NRP1), stimulated them with FN and compared levels of total and activated CDC42 with this method. Whilst NRP1 knockdown did not affect the overall level of CDC42 (**Fig. 8B**), it efficiently inhibited FN-induced CDC42 activation (**Fig. 8C**).

In a parallel approach, I measured levels of GTP-bound, activated CDC42 by performing pull down assays with the CDC42 binding domain of Wiskott-Aldrich syndrome protein (WASP) fused to GST (GST-WASP) (Kolluri et al., 1996). These experiments confirmed that FN stimulation increases CDC42 activation in HDMEC (**Fig. 8D**, first two lanes) and that NRP1 was required for normal CDC42 activation after FN stimulation (**Fig. 8D**, middle lanes), as shown with the GST-PAK1 assay (**Fig. 8C**). As expected, ML141 inhibited CDC42 activation in this assay (**Fig. 8D**, last two lanes), similar to the GST-PAK1 assay (**Fig. 8A**).

The quantitative analysis of GTP-bound, activated CDC42 confirmed that ML141 treatment significantly decreased CDC42 activation, as expected (**Fig. 8E**, left hand graph; mean fold change relative to control \pm SD: control 1 ± 0.1 vs. ML141 0.37 ± 0.17 , $P < 0.05$). Moreover, there was a significant decrease in CDC42 activation in HDMEC transfected with si-NRP1 compared to si-control cells (**Fig. 8E**, right hand graph; mean fold change relative to control \pm SD: si-control 1 ± 0.11 , si-NRP1 0.34 ± 0.24 , $P < 0.05$; $n=3$ independent experiments). For the quantifications, I pooled data from experiments performed using GST-PAK1 or GST-WASP beads.

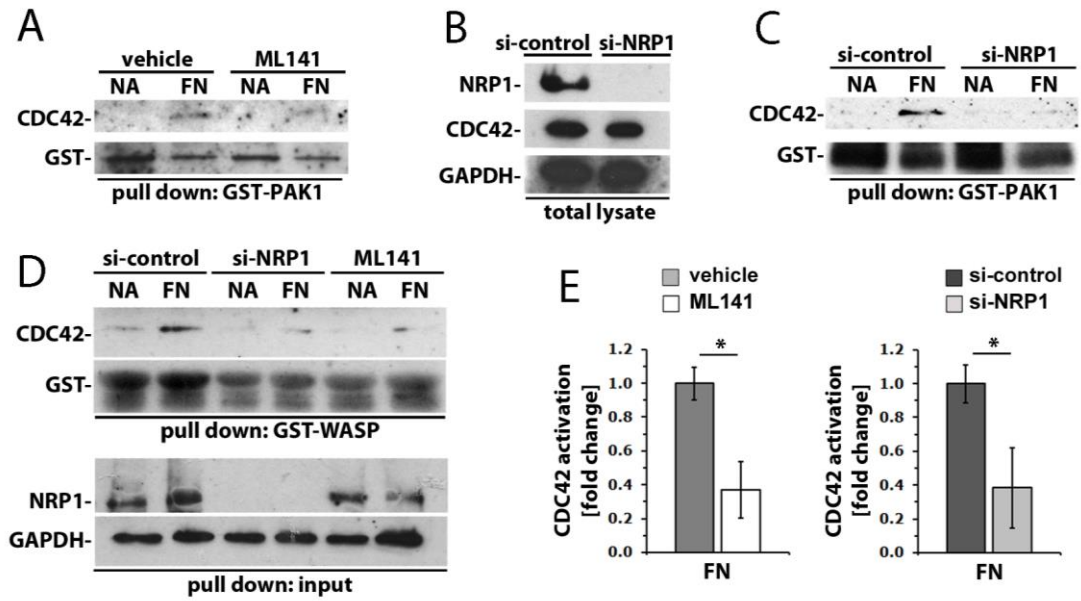


Figure 8: NRP1 enables ECM-induced CDC42 activation.

(A-D) HDMEC were serum-starved and treated with vehicle or ML141 for 30 minutes (A,D) or transfected with si-control or si-NRP1 and serum starved (B-D); protein lysates of non-adherent (NA) cells or adherent cells after 30 minutes on FN (A) were incubated with PAK1-GST (A, C) or WASP-GST (D, upper panel) beads and immunoblotted or used directly for immunoblotting (B, D, bottom panel).

(E) Activated CDC42 was normalised to GST input and expressed as mean fold change relative to control \pm SD; 3 independent experiments; asterisks indicate *P* values for control relative to si-NRP1 or ML141 treated cells: (**P*<0.05; paired t-test)

3.2.3.3 NRP1 promotes ECM-induced CDC42 activation and filopodia extension independently of VEGF

HDMEC transfected with control siRNA or siNRP1 and cells treated with ML141 or vehicle were seeded for 2h on FN, stimulated for 15 min with 5 ng/ml of VEGF and stained for F-actin and DAPI (**Fig. 9A-D**). Higher magnification shows decreased number of filopodia in ECs lacking NRP1 or treated with ML141 (**Fig. 9A', B', D'**). Additional VEGF stimulation of HDMEC further increased the number of microspikes in cells plated on FN compared to cells plated on FN without VEGF stimulation (**Fig. 6E** compare dark grey columns). VEGF addition also increased the number of microspikes in NRP1-depleted ECs on FN (**Fig. 9E**, compare light grey columns). Yet, the relative reduction in the number of microspikes between si-control and si-NRP1 cells was similar in both FN only and FN+VEGF conditions (**Fig. 9E**, red arrows). Surprisingly, however, ML141 treatment was less effective than NRP1 knockdown in reducing the microspike number of cells plated on FN and stimulated with VEGF compared to cells on FN without VEGF stimulation (**Fig. 9F**). This observation raised the possibility that VEGF can stimulate microspike formation in both CDC42-dependent and CDC42-independent pathways, although this idea was not investigated further in the present study.

GST-PAK1 assay showed that CDC42 activation was also reduced in cells lacking NRP1 when VEGF was provided as an additional stimulus to FN (**Fig. 9G**). Pull down assay using the GST-WASP beads confirmed the above observations (**Fig. 9H**). Thus, NRP1 enables CDC42 activation and CDC42-dependent actin dynamics and filopodia extension in ECM-stimulated ECs, independently of VEGF signalling.

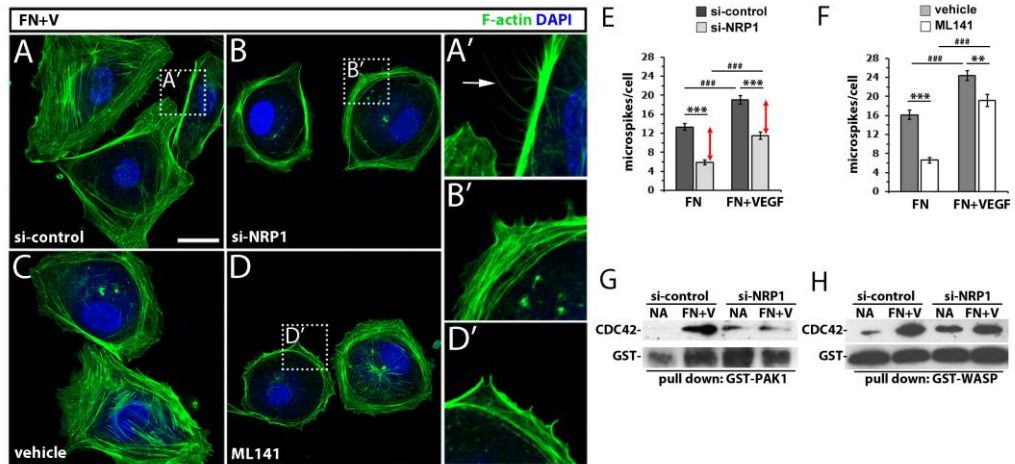


Figure 9: NRPI is required for ECM-induced actin remodelling and CDC42 activation in ECs independently of VEGF.

HDMEC were serum-starved and treated with vehicle or ML141 for 30 minutes or transfected with si-control or si-NRP1 and serum starved.

(A-D) HDMEC were detached, plated on FN for 2 hour, additionally stimulated for 15min with 5ng/ml VEGF165 and stained with phalloidin (green) to label F-actin and DAPI (blue) to visualise cell nuclei. 3 independent experiments; Scale bar 20 μ m. Higher magnification images of the boxed areas in (A, B, D) are shown in (A', B', D').

(E,F) Microspike quantitation after NRP1 knockdown or CDC42 inhibition and plating for 1 hour on FN, shown as mean microspike number per cell \pm SEM; $n \geq 42$ cells for each condition; asterisks indicate *P* values for control relative to si-NRP1 or ML141 treated cells, (***P*<0.01, ****P*<0.001; unpaired t-test); hash tags indicate *P* values for FN without VEGF stimulation (FN) relative to cells on FN with additional VEGF stimulation (FN+VEGF): (### *P*<0.001; unpaired t-test). Red arrows indicate the similar relative reduction in microspike number on FN compared to FN+VEGF.

(G,H) Protein lysates of non-adherent (NA) cells or adherent cells after 30 minutes on FN (A), additionally stimulated for 15 min with 5 ng/ml VEGF165, were incubated with PAK1-GST (G) or WASP-GST (H) beads and immunoblotted; 3 independent experiments.

3.2.3.4 ABL1 is required for NRP1-dependent CDC42 activation

The phenotype of HDMEC after CDC42 inhibition or NRP1 knockdown resembled the cellular phenotype caused by ABL1 knockdown, including a rounded cell shape, increased cortical actin, reduced stress fibre and impaired microspike formation (**Fig. 7**). Moreover, similar to CDC42 activation (**Fig. 8**), ABL1 activation depends on NRP1 in FN-stimulated ECs. I therefore examined if ABL1 was upstream of CDC42 activation in FN-stimulated ECs. For this experiment, I transfected HDMEC with control si-RNA (si-control) or si-RNA targeting ABL1 (si-ABL1), stimulated the cells with FN and then performed GST-WASP pull down assays for activated CDC42 (**Fig. 10A**). This experiment demonstrated that ABL1 loss attenuated FN-induced CDC42 activation (**Fig. 10A** upper panel, **10B**; mean fold change relative to control \pm SD: si-control 1 ± 0.28 vs. si-ABL1 0.38 ± 0.2 , $P < 0.05$; $n=3$ independent experiments). ABL1 knockdown was confirmed by reduced phosphorylation of CRKL (pCRKL; **Fig. 10A**, lower panel), a known ABL1 kinase target (Lewis et al., 1996b). The similar loss of CDC42 activation after ABL1 or NRP1 knockdown (compare **Fig. 8E** with **Fig. 10B**) is consistent with the idea that ABL1 is upstream of CDC42 activation in NRP1-mediated ECM signalling.

Previous experiments performed by Dr Raimondi showed that NRP1 forms a complex with ABL1 [not shown; see (Raimondi et al., 2014), Appendix]. Considering that ABL1 is involved in NRP1-dependent CDC42 activation, I therefore examined whether NRP1 and CDC42 also form a complex. Indeed, I found that CDC42 co-immunoprecipitated with NRP1 in HDMEC both before and during FN stimulation (**Fig. 10C**).

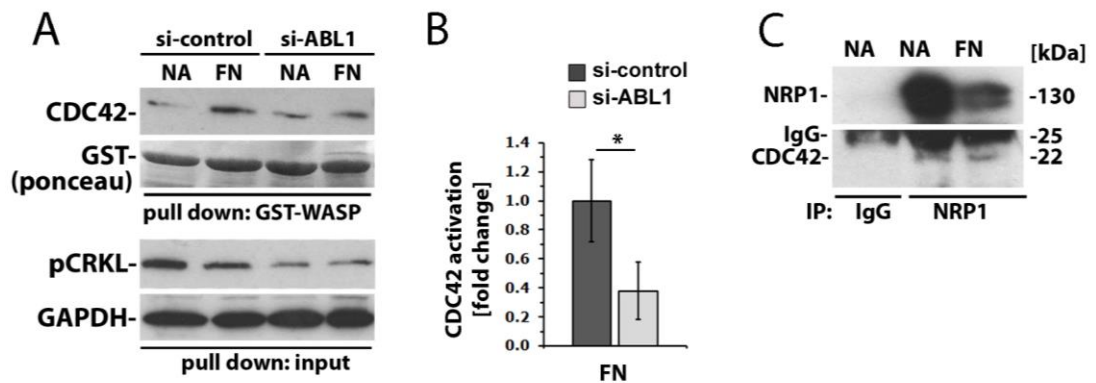


Figure 10: ABL1 enables CDC42 activation in ECM-stimulated ECs.

(A,B) After transfection with si-control or si-ABL1, lysates from NA and A HDMEC were incubated with WASP-GST beads followed by immunoblotting (A, upper panel) or used directly for immunoblotting (A, bottom panel). GST and GAPDH immunoblotting confirmed similar input of GST-beads and lysate. (B) Activated CDC42 was normalised to GST input and expressed as mean fold change relative to control \pm SD; 3 independent experiments; asterisks indicate *P* values (**P*<0.05; paired t-test).

(C) Lysates from NA and A HDMEC were immunoprecipitated with control IgG or NRP1 antibody, followed by immunoblotting for NRP1 and CDC42 to reveal complex formation of endogenous NRP1 with CDC42. The 25 kDa IgG band is indicated.

3.2.4 CDC42 is dispensable for FN-induced PXN phosphorylation

I investigated next whether FN-induced CDC42 activation is important for PXN phosphorylation to understand whether CDC42 and PXN act in the same pathway or in parallel pathways. For these experiments, I again used HDMEC.

First, HDMEC transfected with si-control and si-NRP1 or treated with ML141 or vehicle were seeded for 2 hours on FN and then stained for phalloidin and pPXN. Immunostaining showed reduced pPXN in treated and si-NRP1 transfected cells compared to controls; also, pPXN localised to the periphery of ECs treated with the CDC42 inhibitor, similar to cells lacking NRP1 (**Fig. 11A**).

Second, immunoblotting of cells treated with ML141 or vehicle and either seeded on FN for 30 min or not seeded and lysed in suspension showed that the ML141 treatment reduced baseline pPXN levels prior to FN stimulation. Whereas FN-stimulated ML141-treated cells showed reduced pPXN levels 30 min after FN stimulation compared to control cells, the non-adherent treated cells already had reduced baseline pPXN (**Fig. 11B**). Indeed, quantification showed that the fold change of FN stimulated cells relative to non-adherent cells of treated and untreated samples is similar (**Fig. 11B**, red arrows). Thus, ML141 treatment only affected baseline, but not FN-induced PXN phosphorylation.

Even though NRP1 and ABL1 are both upstream of both PXN and CDC42 activation in ECM stimulated signalling pathways, the best explanation for my findings is that NRP1 regulates PXN and CDC42 activity via ABL1 through parallel and synergistic pathways to control actin remodelling.

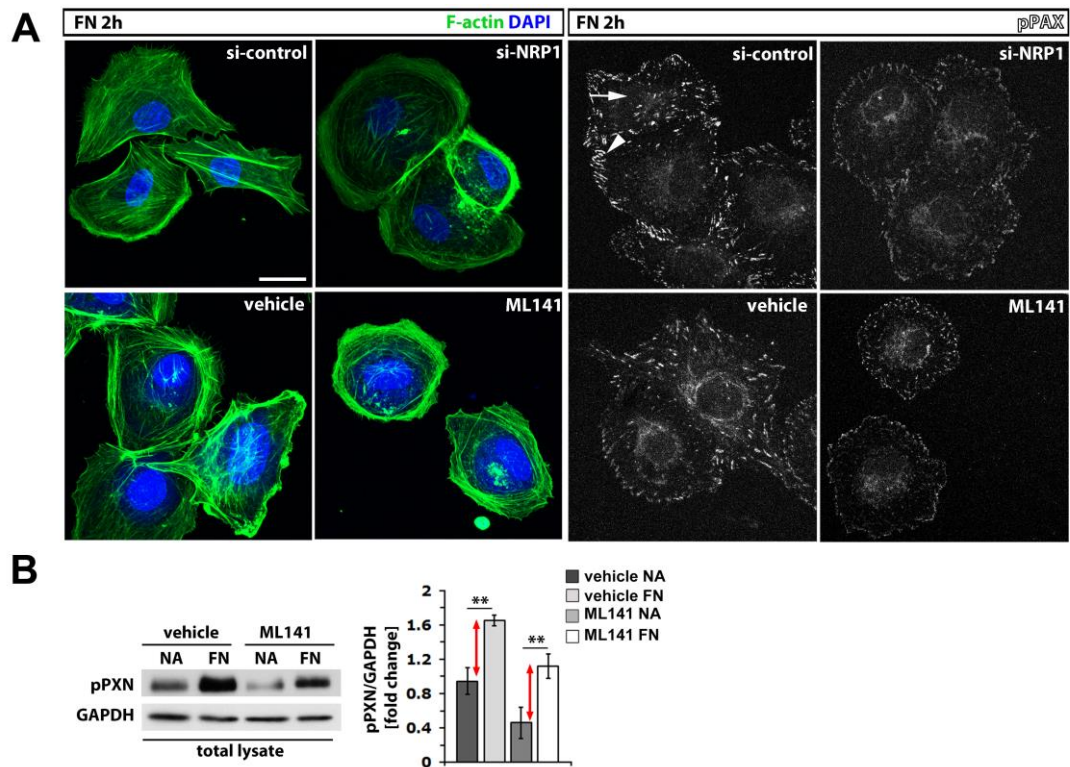


Figure 11: CDC42 is dispensable for FN-induced PXN phosphorylation.

(A,B) HDMEC were serum-starved and treated with vehicle or ML141 for 30 minutes or transfected with si-control or si-NRP1 and serum starved. (A) HDMEC were detached, plated on FN for 2 hours and stained with phalloidin (green) to label F-actin, DAPI (blue) to visualise cell nuclei and pPXN (grey) to detect focal adhesion proteins. Arrows indicate focal adhesion sites. 3 independent experiments. (B) Cells were treated for 30 min with ML141 or vehicle and protein lysates were collected from non-adherent (NA) cells or adherent cells after 30 minutes on FN. Immunoblotting was performed for the indicated antibodies. pPXN levels were normalised to GAPDH and values were expressed as fold change of FN-stimulated cells (treated with vehicle or ML141) relative to NA cells; 3 independent experiments; asterisks indicate *P* values for cells stimulated with FN relative to NA cells, ***P*<0.01; paired t-test. Red arrows indicate the similar reduction in PXN phosphorylation in cells treated with ML141 compared to vehicle-treated cells.

3.3 Discussion

In vertebrates, organ formation and homeostasis require the delivery of oxygen and nutrients through blood vessel networks, which form in response to signals provided by the vascular endothelial growth factor VEGF (Ruhrberg, 2003). However, it is poorly understood how VEGF signalling is integrated with other signalling pathways to ensure that processes such as vasculogenesis, angiogenesis or arteriogenesis take place in appropriate contexts (Carmeliet and Jain, 2011). I have shown here that the VEGF receptor NRP1 has an unexpected role in a non-VEGF driven angiogenesis pathway that is activated by ECM signals. Taken together with results obtained by Dr Fantin in the retinal angiogenesis model, this work shows that the NRP1-regulated ECM pathway synergises with the known VEGF pathway involving NRP1 together with VEGFR2 to promote angiogenesis (**Fig. 12**).

The co-activation of VEGF-induced and ECM-stimulated signalling pathways likely benefits ordered blood vessel growth in complex tissues. Thus, it was previously shown that endothelial tip cells extend filopodia to sense VEGF gradients and to align themselves along matrix templates for directional migration (Ruhrberg et al., 2002, Gerhardt et al., 2003, Uemura et al., 2006, Stenzel et al., 2011b). Filopodia also act as anchorage points for ECM attachment, likely generating tension to pull cells forward as they become motile (De Smet et al., 2009). During retinal angiogenesis, vessel sprouts headed by filopodia-studded tip cells migrate towards astrocyte-localised VEGF in the retinal periphery (Gerhardt et al., 2003, Ruhrberg et al., 2002). Here, I have shown that NRP1 promotes actin remodelling and filopodia formation in ECs in response to ECM signals, independently of VEGF (**Fig. 9**). Also, Dr Fantin has described a more severe phenotype in the *Nrp1*^{-/-} hindbrain compared to hindbrain of mice that express NRP1 lacking VEGF binding, with severe vascular defects including decreased number of filopodia in the former, but not the latter (Fantin et al., 2014). These findings corroborate that NRP1 is involved in VEGF independent pathways to promote angiogenesis *in vivo*, in agreement with the *in vitro* work presented here, which has identified NRP1 regulation of a VEGF-independent ECM pathway.

The process of VEGF/ECM-driven radial migration is accompanied by lateral

branching and sprout fusion to add perfused loops to the expanding vessel network. Dr Fantin has shown that mice lacking endothelial NRP1 have decreased radial migration, number of tip cells and branchpoints compared to controls (Fantin et al., 2015). Given my finding that NRP1 promotes integrin-mediated signal transduction pathways involved in filopodia formation and cell migration, it is therefore interesting to consider which specific integrin might be involved. However, there is no known integrin mutation that causes the same phenotype as endothelial NRP1 loss. Mice with an endothelial specific postnatal deletion of *Itgb1* displayed decreased radial outgrowth, but increased sprouting at the angiogenic front and increased filopodia formation in the mouse retina (Yamamoto et al., 2015). Whereas the endothelial deletion of *Itgb1* induces hypersprouting in postnatal mice, the global deletion of *Itga2* and *Itgb3* did not affect postnatal angiogenesis, and *Itga3* deletion slightly decreased the vascular density of angiogenic retina (Stenzel et al., 2011b).

A study in embryonic brain showed that NRP1 intercellular interaction with integrins on adjacent cells regulates cerebral angiogenesis. More specifically, this study showed that neuroepithelial $\beta 8$ integrin can activate the latent form of TGF β . When endothelial NRP1 forms intercellular complexes with neuroepithelial $\beta 8$ integrin, the activation of TGF β latent form is prevented. Therefore, using this intercellular interaction, NRP1 suppresses TGF β signalling in endothelial cells and controls sprouting angiogenesis in the brain (Abu-Ghazaleh et al., 2001). Integrin $\beta 8$ is also expressed in endothelial cells, however the intracellular interaction with NRP1 in angiogenesis has not been investigated yet. Moreover, whether NRP1's association with integrins also regulates TGF β signalling in the retina for radial migration or lateral branching and fusion of vessels is not yet understood. Even though NRP1's ability to interact with integrins is clear, we still need to define whether NRP1 interacts with integrins directly to promote these processes, or they occur indirectly via interaction with other proteins.

As described here, *in vitro* models of EC signalling have demonstrated that NRP1 promotes integrin ligand-induced EC motility in a VEGFR2-independent mechanism that involves ABL1-dependent PXN phosphorylation and CDC42 activation (**Fig. 8 and 10**), which correlates with defective focal adhesion and actin remodelling (**Fig 4 and 5**). As ABL1 can interact with the integrin subunits $\beta 1$ and $\beta 2$ (Baruzzi et al.,

2010, Cui et al., 2009), NRP1 is present in a complex with ABL1 (Raimondi et al., 2014), and the NRP1 cytoplasmic domain is not required for PXN phosphorylation (**Fig. 6**), NRP1 likely promotes ABL1 activation indirectly via integrin-associated proteins to exert its downstream signalling effects. Studies have shown that ABL1 can be activated by binding to the cytoplasmic region of the integrins, by other kinases or by adaptor proteins (Bradley and Koleske, 2009). In particular, it has been shown that the adaptor proteins ABI and CRK can be phosphorylated by ABL and then in turn they bind to the ABL C-terminus to transactivate it. Thus, NRP1 may play a role in the activation of integrins by affecting their conformation or clustering. Then the activated integrins can either activate ABL1 directly or through the recruitment of adaptor proteins or other kinases such as SFKs.

My results showed that CDC42 and PXN activation can be regulated by ABL in parallel pathways, possibly through the recruitment of different adaptor proteins (**Fig. 11**). Interestingly, different ABL adaptor proteins mediate the assembly of different multimolecular complexes to control actin dynamics. More specifically, it has been shown that the ABL adaptor protein ABI synergises with CDC42 to activate N-WASP at the maximal level by binding simultaneously at distinct sites of N-WASP (Innocenti et al., 2005). Other studies have shown that ABL phosphorylates paxillin (Lewis and Schwartz, 1998a) or that FAK phosphorylates paxillin and mediates the recruitment of another adaptor protein CRK that localises paxillin at the focal adhesion sites (Schaller and Parsons, 1995). Additional work is required to investigate how ABL1 is activated in order to regulate actin dynamics and induction of downstream signalling mechanisms.

Experiments with the embryoid body model of vasculogenesis had been carried out prior to my research and had suggested that CDC42 is essential for blood vessel assembly by vasculogenesis, which takes place prior to angiogenesis (Qi et al., 2011). However, the early embryonic lethality of both constitutive and endothelial-specific CDC42 knockout mice due to defective vasculogenesis (Jin et al., 2013, Chen et al., 2000) had previously precluded the investigation of CDC42 in tip cell function and therefore sprouting angiogenesis in the mouse. I have circumvented this limitation by targeting CDC42 activation with an allosteric inhibitor that displays exquisite selectivity for CDC42 over other small RHO-GTPases (Hong et al., 2013).

Thus, using a pharmacological approach with ML141, I found that CDC42 inhibition impaired ECM-induced actin cytoskeleton remodelling and the extension of filopodia-like microspikes similarly to endothelial NRP1 knockdown in primary ECs (**Fig. 7**). While the majority of the cells treated with the ML141 showed a phenotype similar to ECs lacking NRP1 expression, some cells had more severe actin disruptions, presumably because CDC42 is a target of several different signalling pathways, some of which NRP1-independent.

Consistent with a role for NRP1 in CDC42 activation in ECs (**Fig. 8**), NRP1 is enriched on tip cells and their filopodia *in vivo* (Fantin et al., 2013a) and CDC42 co-immunoprecipitates with NRP1 *in vitro* both before and during FN stimulation (**Fig. 10**). Studies on retina angiogenesis, as described by Dr Fantin, showed that both ECs NRP1 deletion or CDC42 inhibition with ML141, reduced vascular network density at P6, with sprouts at the vascular front appearing longer and larger, and fewer lateral connections between neighbouring vessels (Fantin et al., 2015). More specifically, quantitative analysis demonstrated significant reduction in tip cell density and the number of vascular branchpoints at the vascular front in both NRP1-targeted and ML141-treated retinas (Fantin et al., 2015). In agreement with a role for CDC42 in filopodia formation in ECs during blood vessels morphogenesis, another study recently showed that CDC42 activation is required to promote the extension of lateral filopodia and the formation of blood vessel lumen during angiogenesis (Abraham et al., 2015).

Another study was published shortly after ours and used mice with an inducible deletion of endothelial CDC42 (CDC42^{Cad5KO}) to study CDC42 function in postnatal blood vessels (Barry et al., 2015). They showed that mice lacking Cdc42 during the postnatal days P0-P4 showed decreased filopodia formation and defects in sprouting of retinal blood vessels, but normal vascular extension, similar to findings made in our lab by Dr Fantin with the ML141 inhibitor. In addition, CDC42^{Cad5KO} retinas also had increased numbers of vessels at the retina centre (Barry et al., 2015). The differences in the results could be explained by the fact that genetic deletion of CDC42 is more effective method than the use of an inhibitor, which blocks specifically CDC42 activity but likely did not completely abolish it.

Strikingly, the pharmacological CDC42 inhibition affected actin cytoskeleton similarly to the pharmacological inhibition of ABL kinases, which are also activated in a NRP1-dependent fashion after stimulating ECs with FN (**Fig. 5 and 7**). Specifically, Dr Raimondi and I have shown that ABL1 knockdown in primary human ECs impaired ECM-induced and NRP1 dependent actin cytoskeleton remodelling and filopodia extension in ECs (**Fig. 5**). Interestingly, prior observations had suggested that ABL kinases function upstream of CDC42 in myeloid cells after lysophosphatidic acid stimulation (Baruzzi et al., 2010). In agreement, we found that ABL1 is also required for CDC42 activation in ECM-stimulated ECs (**Fig. 10**). Also, Dr Fantin showed similar defects in vascular network complexity, with decreased number of tip cells and branchpoints, in postnatal retinas from mice treated with ML141 or Imatinib (Fantin et al., 2015). Together, these findings suggesting that CDC42 and ABL kinases operate in a shared angiogenic tip cell pathway.

However, a small, but significant decrease in NRP1 protein levels that has been observed after ABL1 knockdown (Raimondi et al., 2014), and this may also contribute to reduced CDC42 activation. Whereas Dr Raimondi demonstrated that ABL1 forms a complex with NRP1 (Raimondi et al., 2014), I found that NRP1 forms a complex with CDC42 (**Fig. 10C**). Accordingly, it is likely that the NRP1/ABL1 complex has a direct role in CDC42 activation, perhaps by localising CDC42 to sites of actin remodelling. It is known that ECM signals or growth factors that affect F-actin remodelling can induce ABL kinase activation and subsequently promote relocalisation of ABL to F-actin specific sites such as lamellipodia, membrane ruffles and focal adhesion sites (Plattner et al., 1999, Ting et al., 2001). ABL1 is a tyrosine kinase whose C-terminal region contains different functional domains, including an actin-binding domain (Sato et al., 2012). In non-adherent cells, F-actin binding to ABL at the actin-binding domain inhibits its kinase activity (Woodring et al., 2001). This interaction positions ABL at sites where it can promote actin remodelling immediately after its activation by cell adhesion (Woodring et al., 2003). After adhesion of the cells to the substrate, ABL dissociates from F-actin and is activated by different factors such as SRC kinases (Furstoss et al., 2002) and mediates cell spreading and actin remodelling (Woodring et al., 2003).

In either scenario, the surprising similarity of phenotypes caused by ABL or CDC42

inhibition distinguishes ECM-induced NRP1 signalling functionally from VEGF-induced NRP1 signalling, which instead appears to be more important for chemotactic guidance and vascular extension (Fantin et al., 2014, Gelfand et al., 2014), likely by potentiating VEGFR2 signalling in both tip and stalk cells. In agreement, Dr Fantin's data showed that NRP1 loss severely inhibited vascular extension, but this phenotype was not observed after CDC42 inhibition. Instead, mice lacking VEGF binding to NRP1 recapitulated the vascular extension defects caused by endothelial NRP1 loss in mouse retina. But the reduction in vascular branching that has been described for retinas with endothelial NRP1 loss, ABL or CDC42 inhibition was only mild in mice lacking VEGF binding to NRP1 (Fantin et al., 2015). Thus, both NRP1 functions may cooperate to ensure that angiogenic growth factor guidance and ECM-stimulated migration are coordinated to ensure the ordered vascularisation of developing organs.

The novel pro-angiogenic NRP1 function we have identified differs fundamentally from prior models, which proposed that endothelial NRP1 acts exclusively as a VEGF co-receptor to enhance VEGFR2 signalling (Soker et al., 1998). The existence of an ECM-driven and ABL1- and CDC42-dependent, but VEGF and VEGFR2-independent role for NRP1 in angiogenesis may help explain why blood vessel growth is affected more severely by loss of NRP1 than loss of NRP1-binding VEGF isoforms (Ruhrberg et al., 2002, Gerhardt et al., 2004), why the loss of VEGF binding to NRP1 causes milder embryonic vascular defects than loss of NRP1 (Fantin et al., 2014), and why anti-NRP1 and anti-VEGF treatments synergise to block angiogenesis-dependent tumour growth (Pan et al., 2007a). In addition, it has been described that NRP1 suppresses TGF β signalling to promote the tip cell phenotype and therefore blood vessel growth during retinal angiogenesis by inhibition of both SMAD2/3 and SMAD1/5/8 pathways (Aspalter et al., 2015, Hirota et al., 2015). Accordingly, NRP1 acts in at least two angiogenesis-relevant pathways in addition to the classical pathway of acting as a VEGFR2 co-receptor to promote MAPK signalling. In summary, this study identified endothelial NRP1 as a trimodal regulator of vascular morphogenesis that regulates angiogenesis by suppressing TGF β or mediating ECM and VEGF signals.

In conclusion, here I showed that ECM-induced ABL1- and CDC42- mediated signal

transduction and therefore paxillin phosphorylation and actin remodelling during angiogenesis. Thus, targeting NRP1-mediated ABL1 and/or CDC42 signalling might therefore provide novel therapeutic opportunities to enhance the efficacy of current anti-angiogenic therapies that focus on manipulating VEGF signalling through VEGFR2, for example to inhibit tumour angiogenesis or neovascular eye disease (**Fig. 12**). In particular, the FDA-approved ABL1/2 inhibitor Imatinib might provide a complementary treatment to improve the responsiveness of patients to anti-angiogenic therapies, for example in metastatic colon cancer or AMD.

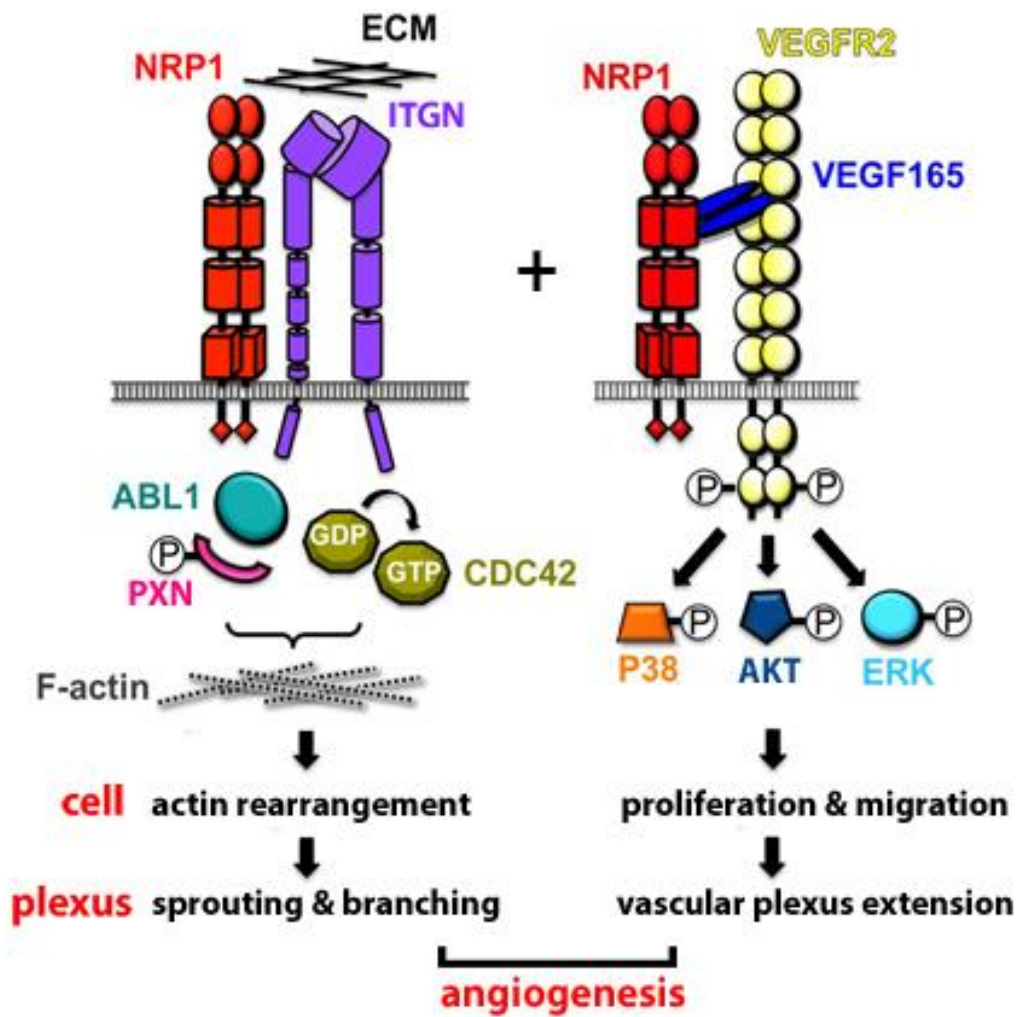


Figure 12: Schematic representation of NRP1 roles in angiogenesis.

NRP1 enables the ECM-dependent activation of ABL1 and CDC42 in addition to its classical role as a VEGFR2 co-receptor in VEGF signalling for ERK1/2 and P38 and potentially the AKT pathway activation.

Chapter 4 NRP1 regulates gene transcription

4.1 Introduction

In Chapter 3, I showed that NRP1 controls actin remodelling and filopodia formation via CDC42. It is known that RHO-GTPases regulate the transcription of several genes involved in actin remodelling (Sotiropoulos et al., 1999). In particular, studies in cancer cells have shown that p38 MAPK promotes the transcription of integrins in a CDC42-dependent manner (Reymond et al., 2012b). Moreover, the SRF and MRTFA transcription factors have previously been reported to act downstream of RHO-GTPases, in particular RHOA, and loss of SRF or MRTFA impairs filopodia formation and angiogenesis (Franco and Li, 2009, Weinl et al., 2013), similar to the phenotype induced by loss of NRP1. However, it had not yet been investigated whether NRP1 also contributes to actin remodelling by regulating transcription networks for ECs migration *in vitro* or angiogenesis *in vivo*. It has also been shown that RHOA kinase induces the translocation of phosphorylated ERK1/2 to the nucleus and thus indirectly controls the transcription of cell proliferation- and growth-related target genes (Chai et al., 2004). However, it has not been examined whether NRP1 can also regulate ERK1/2 to modulate a transcription network that is involved in cell proliferation and survival. Thus, I was keen to investigate whether NRP1 regulates gene transcription during angiogenesis and to identify putative NRP1-regulated transcription factors that are involved in controlling vascular growth or homeostasis, with particular focus on the SRF pathway and MAPK regulation of gene transcription.

4.2 Results

4.2.1 Differential gene expression in postnatal brains of mice lacking endothelial NRP1

I first investigated whether NRP1 regulates actin remodelling and cell motility by controlling the expression of angiogenesis-related genes. To investigate whether NRP1 loss alters gene transcription programmes during angiogenesis, Dr Fantin and I carried out FACS to isolate ECs for expression analysis, using postnatal brains of tamoxifen-treated *Nrp1^{fl/fl}* mice lacking *Cre* (wild type) or expressing *Pdgfb-iCre-ER^{T2}-Egfp* (mutant). Dr Fantin was responsible for the tamoxifen injections, and we together performed brain dissections and sample preparation for the FACS experiment.

Four brain samples from each genotype on postnatal day (P) 7 were labelled for the vessel markers IB4 and PECAM, subjected to FACS and only the double positive ECs collected for RNA isolation (**Fig. 13A**). The cDNA from four brains from each genotype was pooled in order to have sufficient template. Using this method, more ECs were isolated from wildtype compared to the mutant brains. Accordingly, the amount of the cDNA available for the subsequent expression analyses was slightly different for the two groups, with 60 ng of cDNA available from the wildtype brains and 50 ng from the NRP1 mutants. As quantification showed that the number of the double positive ECs was higher for the wildtype compared to NRP1 mutant brains (**Fig. 13B**), there may be decreased ECs proliferation in NRP1 mutant brains. However, this was not investigated further.

As ECs lacking NRP1 expression show decreased motility and migration compared to control ECs, I investigated whether they differentially expressed cell motility-related genes by using a 96-well qRT-PCR array plate containing primer pairs to amplify 84 different cell motility-associated transcripts (full list of genes in **Table 3**). In addition, the array plates contained primers for ‘housekeeping’ genes to normalise expression values between samples as well as those for experimental controls, including lack of genomic DNA contamination, efficiency of reverse transcription and positive PCR template controls.

The five housekeeping genes used in the array were *Actb*, *B2m* (encoding *beta-2 microglobulin*), *Gapdh*, *Gusb* (encoding *glucuronidase beta*) and *Hsp90ab1* (encoding *heat shock protein 90αb1*). The housekeeping genes *Actb*, *Hsp90ab1*, *Gapdh* and *B2m* had less than one cycle of difference in the Ct (cycle threshold) value between the control and mutant group. I decided that the best housekeeping genes to be used for normalisation of gene expression were those that showed small differences in the Ct values that reflected the difference in the amount of cDNA that was used for the mutant and control group (because I had not adjusted the input for the lower yield from mutant ECs). Therefore, I used *Actb* as the housekeeping gene for normalising expression values across the qRT-PCR array (**Fig. 14**) and then validated that similar results were obtained after normalisation with the other housekeeping genes *Hsp90ab*, *Gapdh* and *B2m* (data not shown). *Gusb* was not used for normalisation, as the Ct values of this gene were similar for both control and mutant, even though the initial amount of cDNA used for the assay was slightly different between the two groups. Providing a positive control for the validity of the experimental procedure, *Nrp1* expression was reduced by 98% in mutant compared to control brain ECs (**Fig. 14B**).

I initially analysed the data using a very stringent approach, in which a gene was considered differentially expressed if the fold change in gene expression was more than twice or less than half in mutants compared to control samples ($\geq 2x$ or $\leq 0.5x$ in mutants compared to controls). These thresholds were recommended by the array's manufacturer as guidance for establishing candidate genes for further analysis. By applying this threshold I took into consideration only genes that were amplified up to 35 cycles in control ECs, 9/84 genes were differentially expressed in mutants compared to controls (**Fig. 14A**). I then classified the differentially expressed cell motility-related genes into two categories, those that are upregulated (**Fig. 14C**) and those that are downregulated (**Fig. 14D**). Interestingly, described below are four genes that were only expressed either in the control ECs or ECs from mutants.

Expression of five transcripts that encode transcriptional regulators were upregulated in mutant ECs at least 2.0-fold compared to control ECs. The expression of the gene encoding membrane receptor, *Bcar1* was increased in mutant compared to control ECs (**Fig. 14C**). The *Bcar1* gene encodes the breast cancer anti-estrogen resistance 1

protein that is also known as CAS or p130Cas; it is an SFK substrate involved in cell migration, survival and invasion (Sawada et al., 2006). It was expressed after 31 cycles in control ECs and upregulated 2.1-fold in *Nrp1^{fl/fl} +Cre* ECs relative to *Nrp1^{fl/fl} -Cre* ECs. Another gene encoding the epidermal growth factor (EGF) receptor (EGFR) was not obviously expressed in normal brain ECs, but was amplified only in ECs lacking NRP1 after 35 cycles.

Mmp2, *Mylk* and *Rock1* were upregulated in mutant ECs (**Fig. 14C**; *Mmp2* 6.8-fold change, *Mylk* 2.1-fold change, *Rock1* 4-fold change in mutants compared to controls). The *Mmp2* encodes a member of the MMP family of enzymes that cleave ECM components (Gomes et al., 2012). *Mylk* and *Rock1* encode the myosin light chain kinase MYLK and the RHO-associated coiled-coil containing protein kinase 1, respectively, which regulate actin-myosin contractility and actin polymerisation (Van Aelst and D'Souza-Schorey, 1997).

The expression of the *Igf1* gene encoding the insulin-like growth factor 1 (IGF1) was increased in *Nrp1^{fl/fl} +Cre* ECs 2.8-fold compared to *Nrp1^{fl/fl} -Cre* ECs (**Fig. 14C**), even though its expression is typically low in ECs (Kern et al., 1989, Bach, 2015). *Igf1* is known to promote EC migration by activating the *Igfr1* receptor and thereby MAPK signalling (Bach, 2015). There was no difference in the expression of the *Igfr1* receptor between the two groups examined. Various other growth factors were poorly expressed in control ECs and downregulated further in ECs from mutants, including the *Egf*, *Fgf2* and the *Hgf* genes, which encode EGF, the fibroblast growth factor FGF2 and the hepatocyte growth factor HGF, respectively (**Fig. 14A**). These genes amplified only after 35 cycles and were not detectable in mutant ECs. An *in vitro* study using HDMEC has previously identified autocrine EGF production and showed that EC-secreted EGF increased the motility of cancer cells (Zhang et al., 2014). These observations are interesting, because FGF2-induced angiogenesis in the mouse cornea relies on a mechanism by which endogenous FGF2 expression controls endothelial autocrine expression of VEGF (Seghezzi et al., 1998). In agreement, *Vegfa* expression was strongly reduced in mutant compared to control ECs (**Fig. 14D**; *Vegfa* 0.08-fold change in mutants compared to controls). Studies in HUVEC showed that the combined treatment with exogenous VEGFA and HGF promotes EC proliferation and migration through the activation of MAPK pathways (Sulpice et al.,

2009). However, it is not known whether this synergism would also apply to autocrine HGF.

The qPCR assay also suggested that transcripts encoding molecules involved in integrins signalling were downregulated in *Nrp1^{fl/fl} + Cre* samples. For example, the expression of *Itgb3*, *Ptk2b* (FAK2) and *Pxn*, encoding integrin beta 3, the protein tyrosine kinase 2 beta (PTK2B) and paxillin, respectively, was decreased in brain ECs lacking NRP1 (**Fig. 14D**; *Itgb3* 0.25-fold change, *Ptk2b* 0.48-fold change, *Pxn* 0.43-fold change in mutants compared to controls). These data raise the possibility that NRP1-deficient ECs may have a reduced response to integrin stimulation.

Due to the limited amount of cDNA obtained from each brain, I had to pool four brains of each genotype. Given this approach, I considered that a fold change in gene expression of more than 1.5-fold and less than 0.67-fold in mutants relative to controls might also reflect a relevant change in gene expression (**Table 6**). By applying this threshold, 18/84 genes were found to be differentially expressed. Thus, by narrowing the threshold, an additional 9 genes showed differential expression between the two groups. The downregulated genes in this group were *Arf6*, *Csf1*, *Diap1* and *Ptpn1*, encoding the ADP-ribosylation factor 6, the colony stimulating factor 1 (CSF1), the diaphanous homolog 1 and the protein tyrosine phosphatase (non-receptor type 1), respectively (**Table 6**; *Arf6* 0.62-fold change, *Csf1* 0.66-fold change, *Diap1* 0.58-fold change, *Ptpn1* 0.62-fold change in mutants compared to controls). A prior study has shown that exogenous CSF1 promotes tumour angiogenesis by induction of VEGF from skeletal muscles (Okazaki et al., 2005). Whether endogenous endothelial CSF1 regulates angiogenesis or vascular homeostasis needs to be examined. Also proteins that are involved in RHO-GTPase signalling mechanism are affected in ECs lacking NRP1 expression. Thus, the small GTPase ARF6 regulates EC membrane trafficking and motility, and its expression is associated with increased capillary density in a mouse model of angiogenesis (Ikeda et al., 2005). The DIAP1 protein operates downstream of RHOA and is required for the formation of stress fibres and stabilisation of microtubules at the cell cortex (Watanabe et al., 1997).

The upregulated genes in this group were *Enah*, *Itga4*, *Limk1*, *Ptk2* and *Sh3pxd2a*, encoding the enabled homolog, integrin alpha 4, the LIM-domain containing protein kinase (LIMK1), PTK2 and SH3 and PX domain-containing protein 2A (**Table 6**; *Enah* 1.61-fold change, *Itga4* 1.55-fold change, *Limk1* 1.51-fold change, *Ptk2* 1.67-fold change, *Sh3pxd2a* 1.85-fold change in mutants compared to controls). The LIMK1 operates downstream of RHOA/ROCK1 pathway and controls actin filament dynamics and therefore cell motility (Maekawa et al., 1999). The ENAH and SH3PXD2A proteins are involved in lamellipodial and filopodial dynamics (Gertler et al., 1996) and in ECM degradation (Diaz et al., 2009) respectively.

Taken together, these findings suggest that numerous transcripts associated with cell motility are regulated in a NRP1-dependent mechanism in the endothelium of the mouse postnatal brain. Further work is required to validate the results obtained with the qRT-PCR array at transcription and protein level and to determine the mechanisms by which NRP1 suppresses or activates the expression of EC genes.

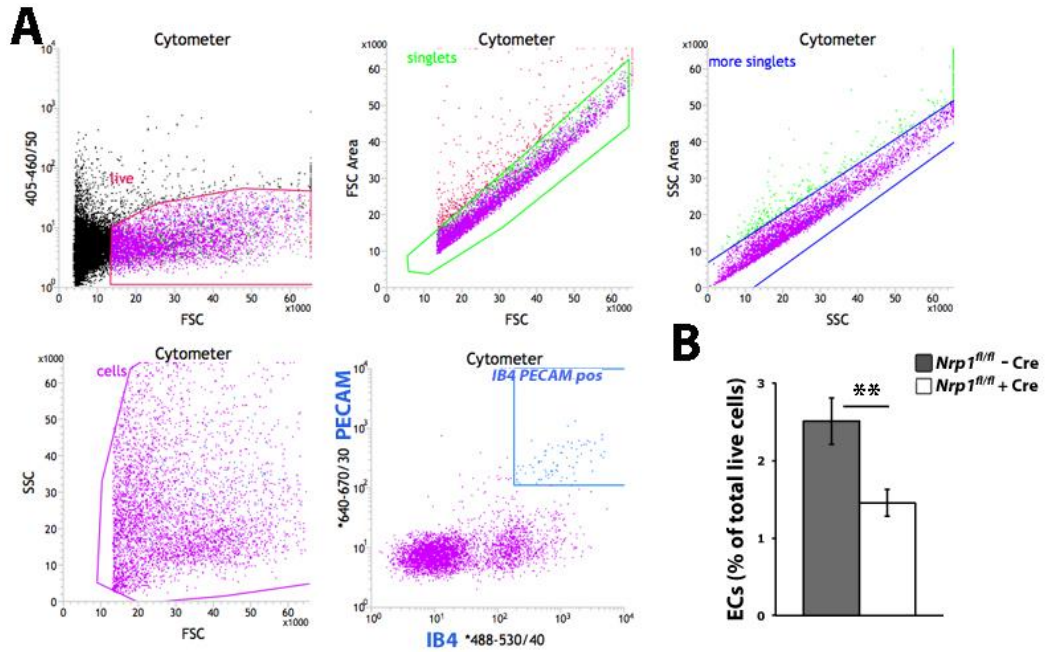


Figure 13: Isolation of ECs from brain tissue via fluorescence-activated cell sorting (FACS).

(A) Endothelial cells from brains of *Nrp1^{fl/fl}* mice lacking *Cre* or containing *Pdgfb-iCre-ERT2-Egfp* on postnatal (P) day 7 were labelled with DAPI to distinguish dead from live cells (purple) and with the vessel markers IB4 and PECAM to collect the double positive stained ECs (blue). (B) The number of double positive stained ECs from the brains of *Nrp1^{fl/fl} -Cre* and *Nrp1^{fl/fl} +Cre* mice was expressed as percentage (%) of ECs relative to the total number of live cells during the FACS experiment; mean±SEM. For the quantification, data from 3 FACS experiments were pooled together and a total number of n≥10 samples from each genotype were used. (**P < 0.01; unpaired t-test)

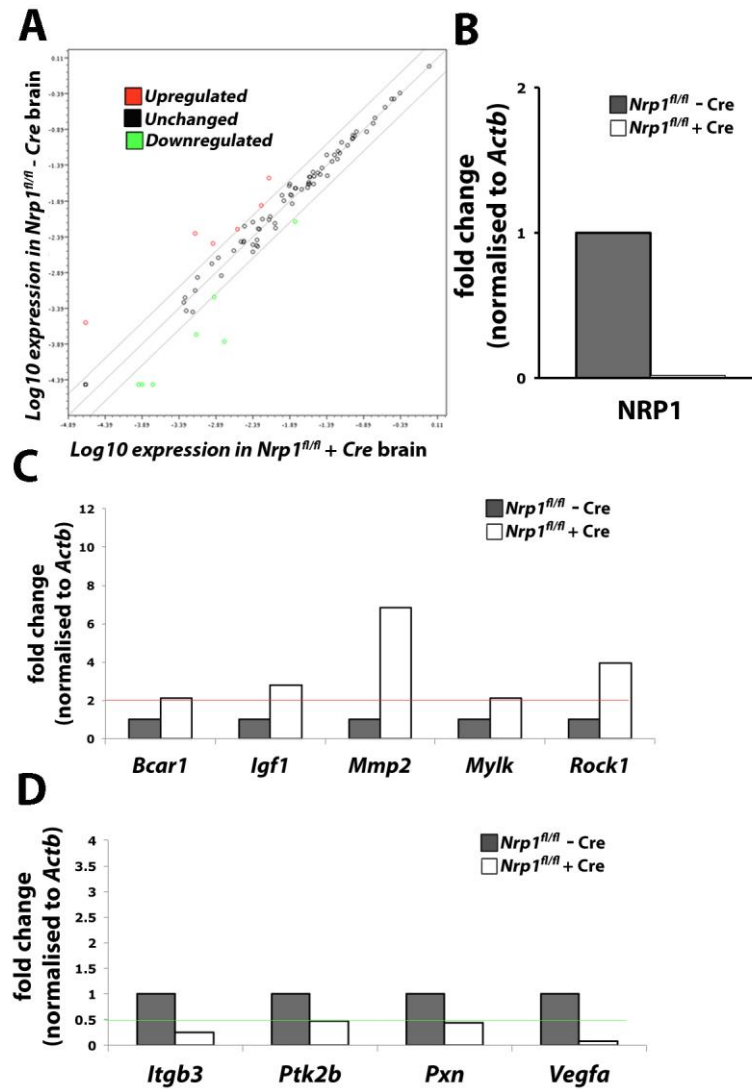


Figure 14: Differential gene expression cell motility-associated transcripts in ECs from postnatal *Nrp1^{fl/fl}* + Cre compared to control brains.

(A) Scatter plot indicating differentially and non-differentially expressed genes between tamoxifen-treated *Nrp1^{fl/fl}* mice lacking *Cre* or expressing *Pdgfb-iCre-ERT2-Egfp*, normalised to *Actb*. Red and green dots represent genes that are up- or downregulated in ECs from *Nrp1^{fl/fl}* + *Cre* brains, respectively. Black dots are non-differentially expressed genes, are those that are not $\geq 2x$ or $\leq 0.5x$ expressed in *Nrp1^{fl/fl}* + *Cre* brain EC. Middle diagonal line represents equal gene expression levels between both genotypes, whilst parallel, flanking diagonal lines demark the $\geq 2x$ and $\leq 0.5x$ thresholds. (B) qPCR shows effective NRP1 knockout in the brain ECs of *Nrp1^{fl/fl}* mice expressing *Pdgfb-iCre-ERT2-Egfp* (*Nrp1^{fl/fl}* + *Cre*). (C-D) Differentially expressed transcripts that are either upregulated (C) or downregulated in ECs from *Nrp1^{fl/fl}* + *Cre* brains (D). Red and green dotted lines demark the $\geq 2x$ and $\leq 0.5x$ thresholds.

Table 6: Differentially expressed genes in qRT-PCR array. The data were displayed as fold change of gene expression in mutants compared to controls, using as a threshold values that were $\geq 1.5x$ or $\leq 0.67x$

Gene	Description	Fold change (<i>Nrp1^{fl/fl} +Cre</i> / <i>Nrp1^{fl/fl} -Cre</i>)
<i>Mmp2</i>	Matrix metalloproteinase 2	6.8223
<i>Rock1</i>	Rho-associated coiled-coil containing protein kinase 1	3.9617
<i>Igf1</i>	Insulin-like growth factor 1	2.7873
<i>Bcar1</i>	Breast cancer anti-estrogen resistance 1	2.1172
<i>Mylk</i>	Myosin, light polypeptide kinase	2.0966
<i>Sh3pxd2a</i>	SH3 and PX domains 2A	1.8503
<i>Ptk2</i>	PTK2 protein tyrosine kinase 2	1.6675
<i>Enah</i>	Enabled homolog (Drosophila)	1.6058
<i>Itga4</i>	Integrin alpha 4	1.5544
<i>Limk1</i>	LIM-domain containing, protein kinase	1.5174
<i>Csf1</i>	Colony stimulating factor 1 (macrophage)	0.6637
<i>Arf6</i>	ADP-ribosylation factor 6	0.6251
<i>Ptpn1</i>	Protein tyrosine phosphatase, non-receptor type 1	0.6248
<i>Diap1</i>	Diaphanous homolog 1 (Drosophila)	0.5774
<i>Ptk2b</i>	PTK2 protein tyrosine kinase 2 beta	0.4819
<i>Pxn</i>	Paxillin	0.4373
<i>Itgb3</i>	Integrin beta 3	0.2494
<i>Vegfa</i>	Vascular endothelial growth factor A	0.0845

4.2.2 NRP1-dependent signalling regulates ERK1/2 activation

I next investigated whether NRP1 loss affects ERK1/2 activation, because it regulates the transcription of genes involved in cell migration, survival or proliferation. For these experiments, HDMEC transfected with siRNA control and siRNA for NRP1 were grown under normal culture conditions, seeded on glass coverslips and fixed 72h after the transfection.

Immunostaining showed that NRP1 downregulation increased ERK1/2 phosphorylation in the cytoplasm and the nucleus (**Fig. 15A**). Immunoblotting and quantification of pERK1/2 pixel intensity normalised to GAPDH confirmed this result (**Fig. 15B**, si-NRP1 relative to si-control: pERK1/2 19.84-fold change). These findings agree with prior work from our lab, which showed, but did not specifically focus on, an increased ERK1/2 activation in NRP1-deficient HDMEC (Raimondi et al., 2014).

Further work should define the amount of phosphorylated ERK1/2 that translocates to the nucleus versus the amount that remains in the cytoplasm in order to describe its role as a transcriptional regulator and define the interactions with other co-factors.

These findings raise the possibility that NRP1 regulates the activity of transcription regulators. I have therefore begun to examine ERK1/2 regulation by NRP1 *in vivo*.

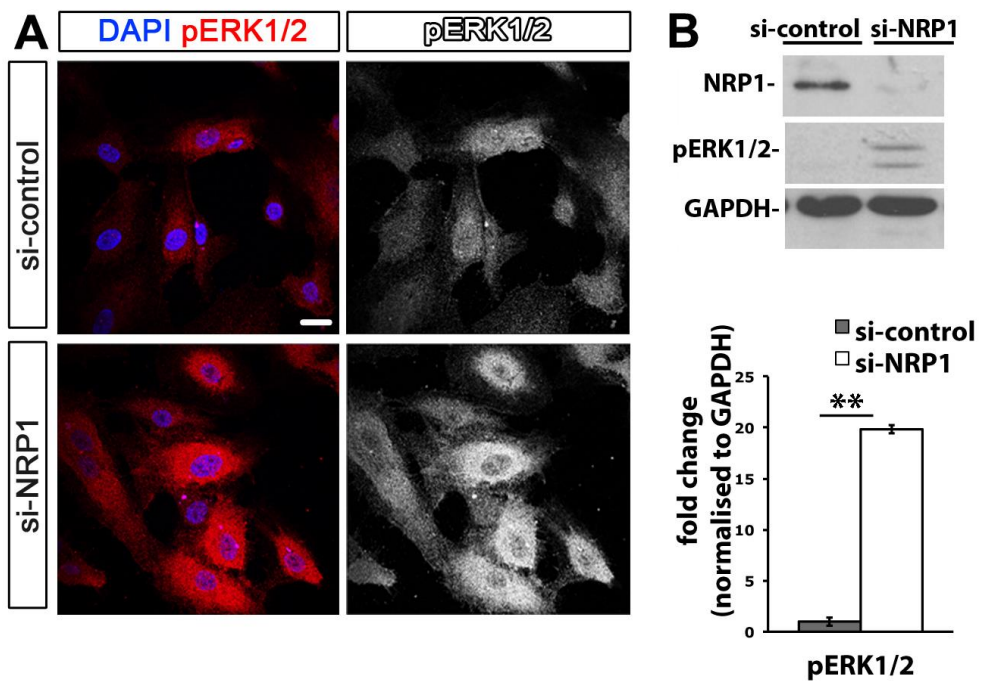


Figure 15: NRP1 regulates ERK1/2 phosphorylation in HDMEC.

(A) HDMEC transfected with siRNA control or NRP1, seeded on glass coverslips and stained for pERK1/2 (green) and DAPI (blue). 3 independent experiments; Scale bar: 10 μ m

(B) Immunoblotting for pERK1/2(T202/Y204) and quantification of pERK1/2 levels were quantified as pixel intensity relative to GAPDH and values expressed as fold change \pm SEM relative to control, 3 independent experiments (** P < 0.01; paired t-test)

To investigate whether lack of NRP1 induces ERK1/2 phosphorylation *in vivo*, I obtained tissues from P6 and P7 littermate mice with conditional *Nrp1*-null (floxed) alleles (*Nrp1^{f/f}*) expressing a tamoxifen-inducible *Cre* transgene under the control of the endothelial *Pdgfb* promoter (*Pdgfb-iCreER-Egfp*) or littermate controls lacking the *Cre* transgene (Fantin et al., 2013a). The tamoxifen injections from perinatal day (P) 2 to P5 and retina dissections were performed by Dr Fantin, while the aorta dissections were performed by both of us. In agreement with my findings in HDMEC, pERK1/2 staining was increased in the VE-cadherin (CDH5)-positive ECs of NRP1 knockout retinas (**Fig. 16**) and aortas (**Fig. 17A, B**, *Nrp1^{f/f} + Cre*: pERK1/2 22.59-fold change) compared to control littermates. Whereas I have three independent aorta experiments to show that the difference between mutant and control ECs is significant, additional experiments are required for the retinas to also obtain statistical significant result for this tissue. Importantly, the *in vivo* data agree with the *in vitro* data I have obtained and suggest that NRP1 negatively regulates the activation of ERK1/2, which is an important regulator of transcription of genes involved in cell survival and proliferation.

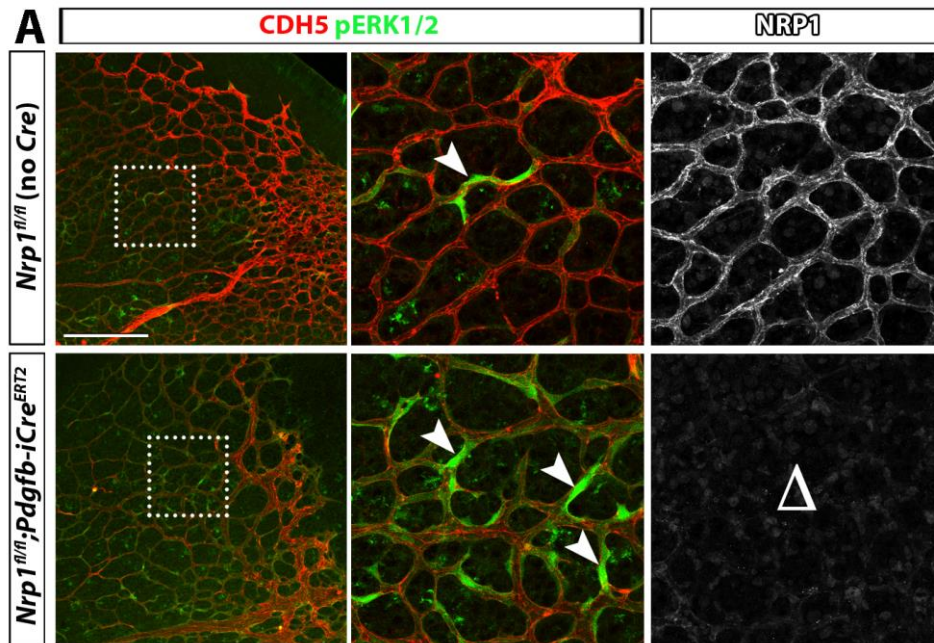


Figure 16: NRP1 loss causes ERK1/2 activation in retinal ECs.

Retinal vasculature from *Nrp1*^{fl/fl} mice lacking *Cre* or expressing *Pdgfb-iCre-ERT2-Egfp* after daily tamoxifen injection from P2 to P5, was immunostained with the indicated antibodies. Triple labelling for NRP1, the vascular marker CDH5 and pERK1/2 shows endothelial NRP1 knockdown (Δ) and an increased number of ECs with high pERK1/2 levels (arrowheads). Scale bar 50 μ m; 2 independent experiments

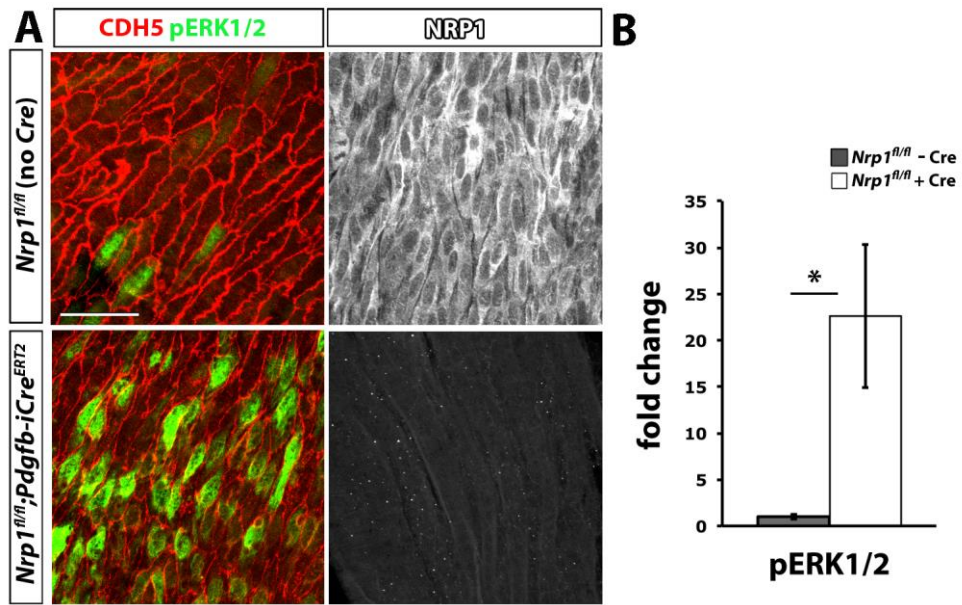


Figure 17: NRP1 loss causes ERK1/2 activation in aortic ECs.

(A) P6 aorta from littermate $Nrp1^{fl/fl}$ mice lacking Cre or expressing Pdgfb-iCre-ERT2-Egfp after daily tamoxifen injection from P2 to P5, were stained for CDH5 (VE-cadherin) (red) and pERK1/2 (green). NRP1 staining of the aorta from another $Nrp1^{fl/fl}$ mice lacking or expressing Cre showed endothelial NRP1 knockdown in the mutant. Scale bar 10 μ m; (B) Quantification of pERK1/2 levels were quantified as pixel intensity and values expressed as fold change \pm SEM relative to control. 3 independent experiments; (* $P < 0.05$; unpaired t-test)

4.2.3 NRP1 regulates the expression of the SRF and MRTFA transcription factors and targeted genes

4.2.3.1 NRP1 suppresses SRF and MRTFA expression in HDMEC

To determine whether NRP1 regulates SRF or its interactors, I transfected HDMEC grown in complete media with si-control or siNRP1 and then performed immunoblotting or immunostaining for these proteins 72h after the transfection. My analysis showed that SRF levels were mildly and MRTFA levels prominently increased in HDMEC lacking NRP1 expression (**Fig. 18A**, si-NRP1 relative to si-control: SRF 3.08-fold change, MRTFA 17.32-fold change). Immunostaining of NRP1-deficient cells confirmed increased MRTFA levels compared to control cells and accumulation of MRTFA mostly in the cytoplasm (**Fig. 18B**). Additionally, staining of cells lacking NRP1 expression showed mildly increased SRF levels in the cytoplasm compared to control cells (**Fig. 18B**). Also, the cells in the NRP1 knockdown samples showed uniformly high levels of nuclear localisation of SRF, whereas the cells in the control samples had variable levels of nuclear SRF, with some cells having higher and others having lower nuclear levels (**Fig. 18B**). These findings suggest that NRP1 negatively regulates SRF and MRTFA levels. Further work is required to describe the distribution of these transcription factors in the nucleus and the cytoplasm of control versus ECs lacking NRP1 expression.

Even though loss of either NRP1 or SRF impairs angiogenesis, my observations argue against the possibility that NRP1 controls angiogenesis via SRF. Specifically, I show that NRP1-deficient cells with defective actin remodelling (described in Chapter 3) and cell migration (Raimondi et al., 2014) show increased SRF levels, even though the lack of endothelial SRF impairs angiogenesis by affecting the transcription of genes involved in cell migration and actin remodelling (Franco et al 2013). However, my findings do not exclude the possibility that NRP1 may dampen SRF activity to control endothelial functions other than angiogenesis, such as vascular homeostasis.

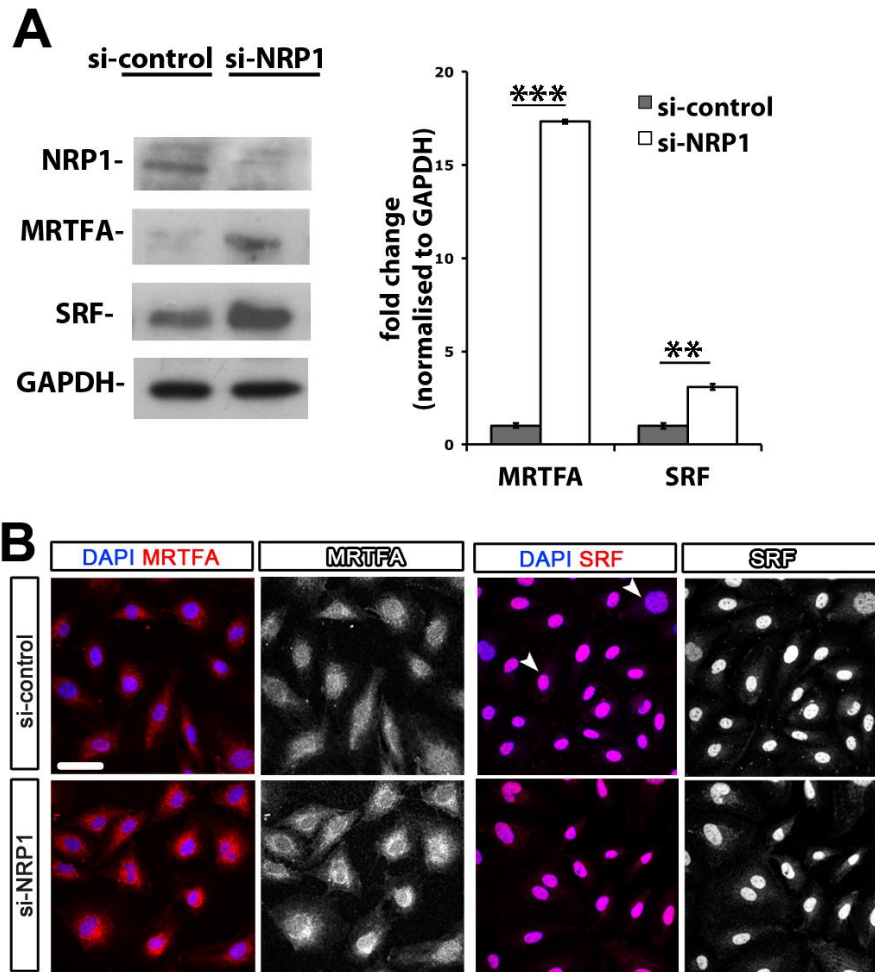


Figure 18: NRP1 regulates the expression of SRF and MRTFA transcription factors.

(A) HDMEC transfected with si-RNA control or NRP1 were lysed and incubated with the indicated antibodies. MRTFA and SRF levels were quantified as pixel intensity relative to GAPDH and values expressed as fold change \pm SEM relative to control, 5 independent experiments; (** $P < 0.01$, *** $P < 0.001$; paired t-test)

(B) HDMEC transfected with si-RNA control or NRP1 were seeded on glass coverslips and stained 72h after the transfection with antibodies for the transcription factors MRTFA or SRF (red) and DAPI. Arrowheads indicate nuclei with variable levels of SRF. Scale bar 20 μ m.

4.2.3.2 NRP1 regulates SRF expression in vivo

To investigate whether my *in vitro* results on HDMEC are relevant *in vivo*, I studied the SRF expression pattern in retinas and aortas obtained from P6 and P7 littermate *Nrp1^{fl/fl}* mice lacking *Cre* or expressing *Pdgfb-iCre-ERT2-Egfp* (**Figs. 19, 20**). The knockdown of NRP1 was effective, as shown by NRP1 staining of retina from tamoxifen-induced mice expressing *Pdgfb-iCre-ERT2-Egfp* (**Fig. 19A**). SRF appeared to be significantly increased in the retina of the mutants, with more intense staining in both the cytoplasm and the nucleus of CDH5 positive ECs compared to wildtype mice (n=3 each). Images confirmed increased SRF expression in the tip cells at the vascular sprouting regions of wild type mice, while SRF expression was even higher in tip and stalk cells at the vascular front of NRP1 mutant retinas (**Fig. 19A, B**, *Nrp1^{fl/fl} +Cre*: SRF 1.86-fold change). Aortic regions showed a significant increase of SRF expression in NRP1 mutants compared to controls (n=5 each) (**Fig. 20A, B**, *Nrp1^{fl/fl} +Cre*: SRF 3.99-fold change).

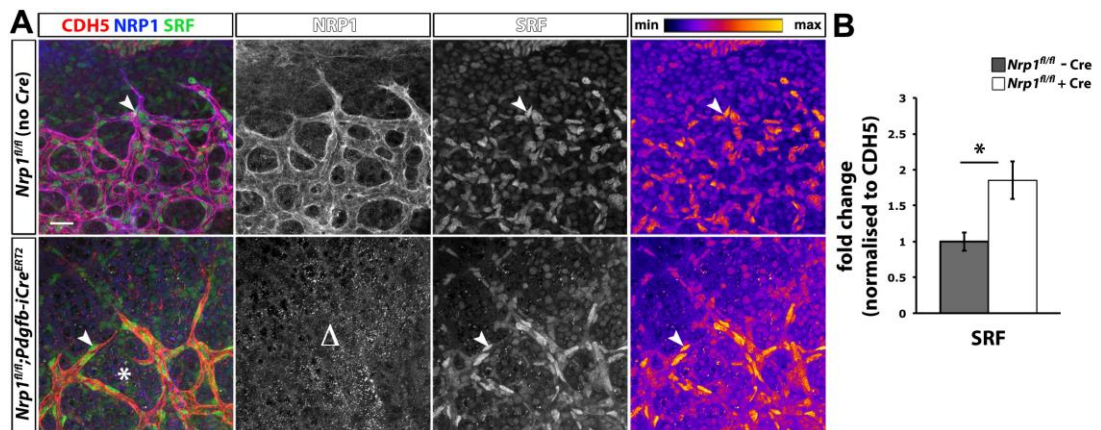


Figure 19: Loss of NRPI induces SRF expression in postnatal retina.

(A) P6 retinas from littermate $Nrp1^{fl/fl}$ mice lacking *Cre* or expressing *Pdgfb-iCre-ERT2-Egfp* after daily tamoxifen injection from P2 to P5 were stained for CDH5 (red), SRF (green) and NRP1 (blue). Note reduced vascular density (*) of CDH5+ vessels and endothelial NRP1 knockdown (Δ). Arrows indicate examples of SRF+ EC nuclei; higher SRF levels (yellow colour in the far right panels) in mutants compared to control vasculature. Scale bar 20 μ m.

(B) SRF levels were quantified as pixel intensity relative to CDH5 and values expressed as fold change \pm SEM relative to control. 3 independent experiments; (* $P < 0.05$; unpaired t-test)

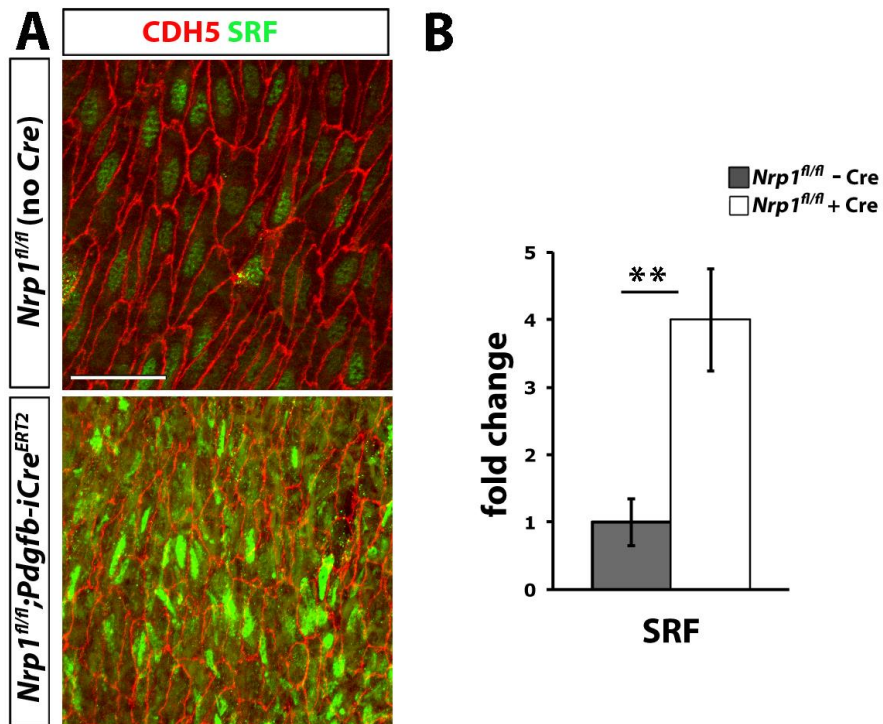


Figure 20: NRPI regulates SRF expression in aortic ECs.

(A) P6 aortas from littermate *Nrp1^{fl/fl}* mice lacking *Cre* or expressing *Pdgfb-iCre-ERT2-Egfp* after daily tamoxifen injection from P2 to P5 were stained for CDH5 (red) and SRF (green). Scale bar 10 μ m.

(B) SRF levels were quantified as pixel intensity and values expressed as fold change \pm SEM relative to control. 5 independent experiments; (**P < 0.01; unpaired t-test)

4.2.3.3 *NRP1* controls *SRF*-targeted genes

The *SRF*-regulated genes fall into two groups: genes that are regulated mainly by *RHOA* via the *MRTFA*/*SRF* complex and encode myogenic contractile and cytoskeletal proteins; and genes that are modulated by *MAPK* signalling via the *TCF*/*SRF* complex and encode early transcribed genes and other genes involved in cell growth, proliferation and survival (Pipes et al., 2006b, Buchwalter et al., 2004). In order to investigate whether *NRP1* regulates *SRF*-targeted genes that have been linked to the *MRTFA*- vs. *TCF*-regulated groups, I transfected HDMEC with si-control or si-*NRP1* and extracted RNA 72h after the transfection for quantitative real-time (q) PCR. In contrast to the mouse brain ECs analysis (see section 4.2.1), for these *in vitro* experiments I used *GUS* as a housekeeping gene because its expression values were unchanged in the different experimental groups compared to other housekeeping genes, such as *ACTB* and *CDH5* (**Fig. 21**). Thus, gene expression was normalised to *GUS* and the expression levels in si-*NRP1* samples were shown as fold change relative to si-control samples.

I first examined whether *NRP1* regulates the transcription of *MRTFA*/*SRF* target genes identified in smooth muscle cells (SMCs) or ECs of mouse embryos (Franco et al., 2008, Olson and Nordheim, 2010b). qPCR showed that HDMEC deficient for *NRP1* had significantly increased *SRF* and *MYL9* gene expression, in agreement with their increased *SRF* protein levels (**Fig. 21A**, si-*NRP1* relative to si-control: *SRF* 1.68-factor fold change, *MYL9* 2.40-factor fold change). This relationship agrees with prior studies in HUVEC, which showed that *SRF* loss leads to downregulation of *MYL9* levels (Franco et al 2013). However, the transcription of other reported *MRTFA*/*SRF* target genes, including *ACTB*, *CDH5*, *MYH9*, *FLNA* and *TALIN*, was largely unaffected (**Fig. 21A**, si-*NRP1* relative to si-control: *ACTB* 1.15-fold change, *CDH5* 1.00-fold change, *MYH9* 0.95-fold change, *FLNA* 0.98-fold change, *TALIN* 1.37-fold change). Moreover, the expression of the reported *MRTFA*/*SRF* target *ITGB1* was significantly reduced in HDMEC lacking *NRP1* (**Fig. 21A**, si-*NRP1*: *ITGB1* 0.50-fold change).

Thus, my qPCR results suggest that only the *MRTFA*/*SRF* target *MYL9* is upregulated in *NRP1*-deficient ECs, even though they upregulate *SRF*. While *ACTB*,

CDH5 and *ITGB1* gene transcription was decreased in mouse embryos lacking endothelial SRF (Franco et al., 2008) here I show that only *ITGB1* transcription is impaired in si-NRP1 samples. Although *MYH9*, *FLNA* and *TALIN* have been described to be MRTFA/SRF targets in SMCs, the expression of these genes was not affected in NRP1-deficient ECs (Olson and Nordheim, 2010b). Together, these findings show that some of the suggested MRTFA/SRF target genes may be differentially regulated in embryonic ECs compare to ECs in adults or in different cell types such as ECs vs SMCs. Also, the increased ERK1/2 activity detected in si-NRP1 samples (**Fig. 21**) can induce TCF translocation to the nucleus but also may cause MRTFA export to the cytoplasm, as it has been suggested for fibroblasts, affecting indirectly the transcription of MRTFA/SRF target genes.

Next, I examined whether NRP1 regulates the transcription of TCF/SRF target genes. The expression of several early-transcribed genes was significantly affected in ECs lacking NRP1; in particular, *FOS*, *EGR1* and *JUN* expression increased in si-NRP1 samples compared to controls (**Fig. 21B**, si-NRP1 relative to si-control: *c-FOS* 6.7-fold change, *EGR1* 12.56-fold change, *JUN* 4.28-fold change). The upregulation of early-transcribed genes in si-NRP1 samples with increased SRF levels agrees with studies in fibroblasts, which showed SRF-dependent upregulation of *FOS* and *EGR1* (Selvaraj and Prywes, 2004a).

As prior studies in mouse embryos lacking endothelial SRF expression showed downregulation of the TGF β receptors *Alk1*, *Tgfbri* and *Eng* (Franco et al., 2008). I also examined whether NRP1 knockdown-associated increase in SRF levels also affected the transcription of TGF β -related genes. However, I found that HDMEC lacking NRP1 expression showed significantly decreased expression of *ALK1* and *TGFBR2* and increased expression of *TGFB1* (**Fig. 21C**, si-NRP1 relative to si-control: *ALK1* 0.51-factor fold change, *TGFBR2* 0.75-factor fold change, *TGFB1* 1.6-factor fold change). Moreover, the *TGFBRI* and *ENG* levels did not change significantly (**Fig. 21C**, si-NRP1 relative to si-control: *TGFBRI* 1.12-fold change, *ENG* 1.28-fold change). These findings suggest that TGF β signalling is probably regulated differently by SRF and cofactors during embryogenesis and in adults. Still it remains unknown whether SRF interacts with the MRTFA or the TCFs cofactors or other transcription factors to regulate TGF β signalling in ECs.

Further work is therefore warranted to understand why NRP1-induced SRF upregulation affects some, but not all known SRF targets, and to investigate whether transcriptional modulation by NRP1 involves the MAPK or RHOA pathway that operate upstream of TCF/SRF and MRTFA/SRF complexes respectively. In particular, future work is required to test whether RHOA activity is altered in ECs lacking NRP1 expression, as I have done for CDC42, to compare the relative balance of the RHOA and the ERK1/2 pathways. Then, further work might use inhibitors that target specifically either ERK1/2 or RHOA activity to define how different SRF-target genes are regulated by the different signalling pathways in ECs.

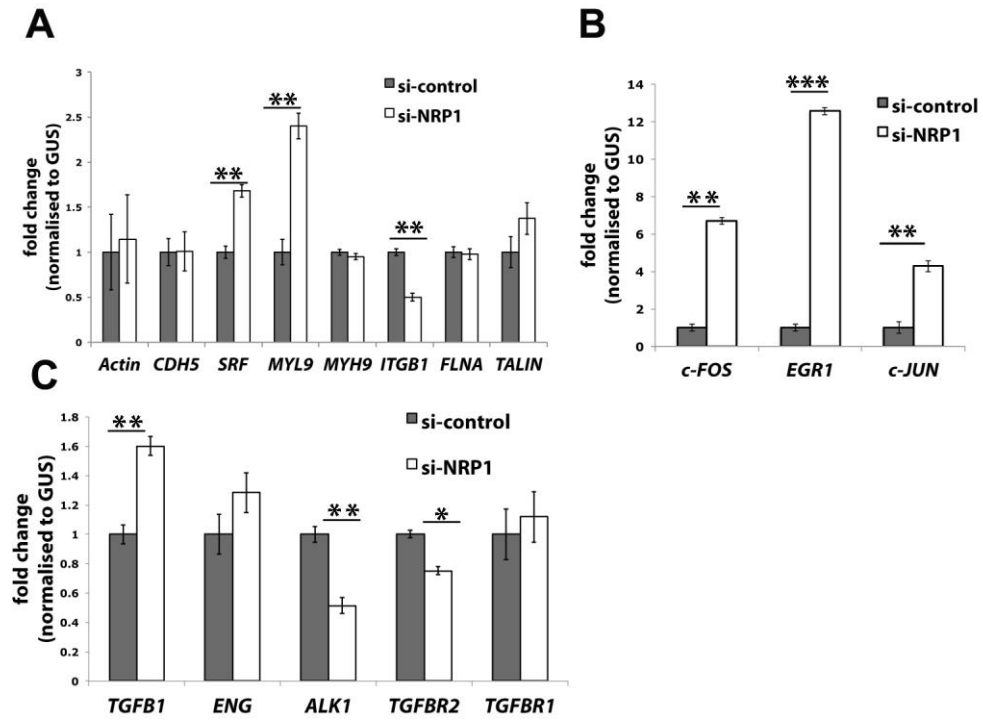


Figure 21: NRP1 regulates the expression of SRF targeted genes.

(A-C) qPCR expression analysis of the indicated SRF-targeted genes in HDMEC lacking NRP1 compare to si-control, normalised to *GUS*; expression levels are shown as fold change \pm SEM relative to control. Transcription regulation of SRF/MRTFA related genes (A), early-transcribed genes (B) and TGF β -related genes (C) more than 3 independent experiments each (* $P < 0.05$; ** $P < 0.01$, *** $P < 0.001$; paired t-test)

4.3 Discussion

NRP1 regulates EC behaviour through several different mechanisms. In Chapter 3, I have shown that NRP1 regulates angiogenic actin remodelling and EC migration via an ECM-dependent signalling pathway. In this Chapter, I have examined whether NRP1 regulates cell motility-related genes and the levels of transcription regulators in ECs during angiogenesis *in vivo* and whether NRP1 also modulates the activity of transcriptional regulators and their target genes under normal endothelial growth conditions *in vitro*.

Analysis of a qPCR array showed that 18 of the 84 genes related to growth factor and cell motility pathways that were analysed, were differentially expressed in ECs of postnatal NRP1-deficient mouse compared to wildtype brain (**Table 6**). Interestingly, from those 84 genes, some were only expressed in normal ECs and some other only in ECs lacking NRP1. These findings suggest that NRP1 regulates the transcription of cell motility genes during angiogenesis.

Prior studies have shown that the EGF, FGF2, HGF, VEGFA and IGF1 are pro-angiogenic growth factors that support EC proliferation and migration based on paracrine or autocrine mechanisms (Moller et al., 2001, Ferrucci et al., 2014, Aparicio et al., 2005, Kaga et al., 2012, Taylor and Alexander, 1993). Specifically, I found that *Egf*, *Fgf2*, *Hgf* were expressed at low levels in control ECs and downregulated further in ECs from mutants (**Fig. 14A**). Also, the expression of *Vegfa* was decreased in mutant ECs, while was only amplified after 32 cycles in control ECs (**Fig. 14D**). Together these results suggest that several endogenously expressed growth factors in ECs are downregulated in NRP1-deficient ECs. *Igf1* was also expressed at low levels in control ECs, but it was upregulated in ECs lacking NRP1 (**Fig. 14C**). In contrast to the *Egf* gene expressed only in control ECs, the gene for its receptor *Egfr* was only expressed in mutant ECs (**Fig. 14A**). Prior *in vivo* and *in vitro* studies have shown that primary ECs normally express the ERBB3 receptor from the EGFR family, while tumour ECs express the EGFR receptor that responds to EGF to enhance endothelial cell proliferation (Amin et al., 2006). Thus, ECs from NRP1 mutant express genes that are upregulated in ECs under pathological conditions. Together these data suggest that NRP1 may control the transcription of

growth factors and growth factor receptors during angiogenesis. Further work is required to test the expression levels of these growth factors in other mouse ECs such as LECs and in human ECs.

The qPCR array showed that the expression of integrins or other genes that are involved in actin remodelling was altered in NRP1 mutant ECs during angiogenesis. Indeed, the *Itga4* gene expression was upregulated, while *Itgb3* gene expression was downregulated in mutant ECs (**Fig. 14, Table 6**). A prior study on HUVEC showed that the inflammatory cytokines IL-1 β and TNF- α induce ITGA4 expression and cause ITGA4-dependent inhibition of cell spreading and migration after binding of ITGA4 at a distinct site near the C-terminus of FN (Weinlander et al., 2008). These findings raise the possibility that *Itga4* upregulation in mutant ECs contributes to the decreased migration of ECs lacking NRP1 (Raimondi et al., 2014). In contrast, as a prior *in vivo* study showed that mice lacking *Itgb3* expression do not have angiogenesis defects (Stenzel et al., 2011a), the decreased *Itgb3* expression in NRP1 mutant ECs does not explain the angiogenesis defects of NRP1-deficient retinas (Fantin et al., 2015).

The expression of the focal adhesion proteins *Ptk2b* (also known as *Fak2*) and *Pxn* was decreased in mutant ECs (**Fig. 14, Table 6**). As HDMEC lacking NRP1 expression showed reduced PXN phosphorylation in response to FN respectively (**Fig. 5**), further work is required to test whether reduced phosphorylation is due to in part to impaired transcription.

Instead, the *Rock1*, *Mylk*, *Ptk2* (also known as *Fak1*) and *Limk1* genes were upregulated in mutants (**Fig. 14C, Table 6**). These changes may reflect an attempt of NRP1-deficient ECs to activate gene-regulatory compensation mechanism to counter the reduced activation of signalling pathways involved in actin remodelling and cell migration (see Chapter 3).

As my results showed that NRP1 regulates transcription of genes in angiogenesis (**Fig. 14**), I examined whether NRP1 controls the activity or expression of transcription regulators. Thus, I first tested the activity of the MAPKs ERK1/2, which are known to control transcription of genes involved in cell proliferation and

survival (Robinson and Cobb, 1997) but also indirectly affect the transcription of genes involved in cell migration by mediating the MRTFA export from the nucleus (Panayiotou et al., 2016). My *in vitro* and *in vivo* results showed increased ERK1/2 activation (**Fig. 15-17**). In agreement, mass spectrometry analysis performed for us by Cell Signalling Technology using lysates from ECs transfected with control siRNA or si-NRP1 showed increased phosphorylation of ERK1/2 (ERK1: 5.5-fold change, ERK2: 3.1-fold change in si-NRP1 samples compared to control) (**Table 7**). As ERK1/2 can be activated by growth factors but also in response to inflammation (Lu and Xu, 2006), future work should investigate whether NRP1 normally suppresses growth factor activity or inflammatory signalling in ECs by restricting the ERK1/2 pathway. Also, I should examine whether NRP1-dependent ERK1/2 phosphorylation regulates the activity of other transcription factors and whether NRP1 controls other transcription regulators such p38 in ECs also independently of ERK1/2.

As the ERK1/2 MAPK pathway is known to regulate SRF target gene expression (Miano et al., 2007), I then tested whether NRP1 controls the transcription or the protein levels of SRF and its co-factors. Although I have not yet examined how NRP1 loss affects the expression of TCFs such as ELK1, I found that HDMEC lacking NRP1 showed increased SRF expression and protein levels and additionally MRTFA protein upregulation (**Fig. 18**). This finding suggests that NRP1 controls the transcription and maybe also the stability of SRF and MRTFA. In agreement during angiogenesis, staining of postnatal retinas showed SRF in tip and stalk cells in the sprouting region of the retinal vasculature, and SRF levels appeared to be higher in both the cytoplasm and the nucleus of ECs in *Nrp1^{fl/fl} + Cre* compared to mice *Nrp1^{fl/fl} - Cre* (**Fig. 19**). Also, SRF staining was increased in the postnatal aorta of NRP1 mutant compared to wildtype mice (**Fig. 20**). Even though the knockdown of SRF has been shown to impair VEGF-induced migration and *in vitro* angiogenesis (Franco et al., 2008), my results suggest that impaired filopodia extension in NRP1-deficient ECs is not due to loss of SRF. Therefore, loss of SRF expression in endothelial tip cells is not likely a mechanism to explain the role of NRP1 in angiogenesis. Nevertheless, the increased SRF level in mutant ECs raises the possibility that NRP1 might have a role in restricting SRF-regulated endothelial functions other than angiogenesis. In agreement with this idea, prior studies have

implicated upregulation of SRF in vascular pathology, as described in the next paragraph.

More specifically, studies showed that SRF upregulation promotes a hypercontractile phenotype in cerebral vascular SMCs (VSMCs) of small cerebral arteries, which can lead to cerebral amyloid angiopathy (CAA) or Alzheimer's disease (AD) (Bell et al., 2009). Also, studies using transgenic mice with cardiac-specific SRF overexpression showed changes in the expression of SRF target genes, causing cardiac hypertrophy, cardiomyopathy and fibrosis (Zhang et al., 2001). Interestingly, mice lacking NRP1 in cardiomyocytes and VSMCs also develop cardiomyopathy (Wang et al., 2015b). Furthermore, SRF expression increases in the heart of old compared to young rats by 20%, suggesting that raised SRF levels can contribute to age-associated diseases and functional senescence (Zhang et al., 2003b). Moreover, MRTFA is upregulated in aortic atherosclerotic lesions of *Apoe*^{-/-} mice (Minami et al., 2012), raising the possibility that an increased MRTFA level promotes pathological vascular remodelling. Thus, NRP1 may restrict SRF and MRTFA expression to maintain vascular homeostasis. Future work should therefore investigate whether NRP1-dependent endothelial SRF overexpression can cause vascular dysfunction and pathology *in vivo*, possibly in conjunction with MRTFA. To determine the NRP1-dependent mechanism that suppresses SRF and MRTFA upregulation, I could investigate pathways involved in vascular pathology and age-associated diseases. For example, the TGF β canonical pathway that is activated in vascular pathology (Singh and Ramji, 2006), can be suppressed by NRP1 in angiogenic ECs (Aspalter et al., 2015). Previous studies showed that HDMEC transfected with SRF siRNA had decreased phosphorylation of ERK1/2, suggesting that SRF is upstream of this MAPK pathway (Franco et al., 2008), without though excluding the possibility of a feedback loop.

As SRF expression and protein levels are upregulated in si-NRP1 samples, I then tested whether the transcription of SRF target genes was also increased. SRF regulates genes related to actin remodelling, metabolism and various other signalling pathways, such as TGF β signalling (Franco et al., 2008, Zhang et al., 2011). I first tested genes that are known to be targets of the MRTFA/SRF complex downstream of the RHOA pathway in embryonic ECs, SMSs or fibroblasts and then genes that

are regulated by the TCF/SRF complex in response to ERK1/2 activation. Finally, I examined genes that are SRF targets in ECs, but it is not known whether they are transcriptionally regulated by MRTFA or TCF factors.

Mice lacking SRF in ECs downregulate genes that have also been shown to be MRTFA/SRF targets in SMCs (Olson and Nordheim, 2010b), such as *ACTB* and *CDH5* (Franco et al., 2008). However, I found that the transcription of *ACTB* and *CDH5* was not affected by NRP1 knockdown in HDMECs grown under normal culture conditions (**Fig. 21**). Another prior study performed SRF knockdown in HUVEC and found that it reduces the proteins and expression levels of genes encoding myosin heavy and light chains genes, i.e. *MYL9*, *MYH9* and *MYH10* (Franco et al., 2013). Of these, *MYH9* levels were not affected in NRP1-deficient ECs and the expression of *MYL9* was instead increased under normal culture conditions (**Fig. 21**). These findings do not support the idea that NRP1 promotes the expression of known SRF/MRTFA targets. However, another MRTFA/SRF target gene, *ITGB1*, was reduced in HDMEC lacking NRP1 (**Fig. 21**). The analysis of further MRTFA targets would therefore be important to establish whether NRP1 regulates transcription in ECs via the SRF/MRTFA.

Even though a prior study has shown that MRTFA/SRF acts downstream of RHOA pathway to increase *ITGB1* transcription in mesenchymal stem cells (Zhang et al., 2015), another study in cancer cells showed that CDC42 promotes *ITGB1* transcription (Reymond et al., 2012a). Thus, reduction of *ITGB1* gene expression is consistent with impaired CDC42 activation (**Fig. 8**) and impaired cell migration of ECs lacking NRP1 (Raimondi et al., 2014). These data raise the possibility that CDC42 rather than the RHOA-dependent MRTFA/SRF pathway is more likely to regulate *ITGB1* transcription in NRP1-deficient ECs, possible through different transcription factors. Thus, future experiments should define precisely the molecular mechanism of NRP1-dependent *ITGB1* transcriptional regulation by using inhibitors to selectively target transcription regulators upstream of *ITGB1*.

Overall, my data thus far suggest that NRP1 is not required to negatively regulate the SRF/MRTFA pathway in ECs, even though SRF and MRTFA are both upregulated in NRP1-deficient ECs.

Providing an alternative to RHOA-dependent MRTFA/SRF-mediated transcription regulation, ERK1/2 activation has previously been shown to induce TCF translocation to the nucleus, whereby its binding to SRF promotes the transcription of early transcribed genes and other genes involved in proliferation and survival (Buchwalter et al., 2004). For example, it is known that ERK1/2 regulates the transcription of the early-transcribed genes *FOS* and *EGR1* (Shaw and Saxton, 2003). In agreement with increased ERK1/2 activation (**Fig. 15**), I observed an upregulation of both genes in ECs lacking NRP1 (**Fig. 21**). However, I still need to test whether the NRP1-dependent regulation of the early-transcribed genes is controlled via ERK1/2 in ECs. This would be important, because *EGR1* is expressed at high levels in human atherosclerotic lesions (Khachigian, 2016) and primary VSMCs increase *FOS* expression, which controls cyclin A upregulation and increases proliferation of VSMCs upon serum stimulation (Rivard et al., 2000). As early-transcribed genes are involved in the regulation of vascular homeostasis, future work is needed to investigate whether NRP1 suppresses the transcription of these genes to maintain vascular homeostasis.

ERK1/2 also regulates the expression of other genes, for example *MMP2* (Boyd et al., 2005), which I also found to be upregulated in NRP1 mutant ECs (**Fig. 14**). *MMP2* is known to activate TGF β (Wang et al., 2006b), which then activates TGF β signalling (Zhang, 2009). Therefore, future work should test whether ERK1/2 regulates *MMP2* in a NRP1-dependent manner and whether such upregulation leads to increase *MMP2* activity as well.

NRP1 loss also affects SRF target genes, for which it is still not known whether are regulated by MRTFA or TCF co-factors. For example, *Alk1*, *Tgfbr1* and *Eng* are SRF targets. I found that the expression of 2 TGF β receptors is affected by lack of NRP1 in ECs. In particular, *ALK1* is downregulated (**Fig. 21**). As SRF^{ECKO} embryos, have reduced *Alk1* expression (Franco et al., 2008), *ALK1* downregulation in NRP1-efficient ECs agrees with a role for NRP1 in SRF-mediated transcription. However, the prior study did not find an effect on *Tgfbr2* expression levels, whereas I observed a significant reduction of *Tgfbr2* expression in NRP1-deficient cells (**Fig. 21**). Even though *Eng* and *Tgfbr1* genes were also downregulated in SRF^{ECKO} embryos, while my data showed no difference in *ENG* and *TGFBR1* transcription levels between

cells transfected with siNRP1 and control cells (**Fig. 21**). *Tgfb1* expression was not affected in SRF^{ECKO} embryos (Franco et al., 2008), but my data showed that ECs lacking NRP1 expression had increased *TGFB1* expression (**Fig. 21**). These again could suggest that SRF recruits different co-factors (MRTFA vs TCF or other) to regulate the transcription of genes involved in TGF β signalling. Also, it would be interesting to check whether NRP1-dependent regulation of TGF β -related genes would affect TGF β signal transduction.

Future experiments should determine how NRP1 helps to balance the transcription of genes that promote vessel growth through roles in EC migration vs. EC proliferation and to maintain vascular homeostasis. It would also be interesting to define the mechanism by which NRP1 might regulate transcription through ERK1/2 and RHO-GTPases. Thus, further research is required to show how ERK1/2 is activated in ECs lacking NRP1 upstream of TCF/SRF and to define whether NRP1 regulates RHOA activity upstream of the MRTFA/SRF transcription regulatory complex. Also, future work using specific inhibitors or siRNAs, will help to assign the NRP1-regulated SRF targets to the MRTFA vs TCF pathways downstream of ECM and growth factors stimuli and establish the consequence of pathway skewing on EC phenotypes.

Finally, as the NRP1-dependent differentially expressed genes will have binding sites for transcription factors other than SRF, MRTFA and TCF, I cannot exclude the possibility that NRP1 also regulates the transcription of these and other genes not examined here via additional or alternative transcription regulators. An interesting candidate would be p38 (Raimondi et al., 2014).

Table 7: Phosphorylation of ERK1/2 in siNRP1 samples. Mass spectrometry analysis using HDMEC transfected with siRNA for NRP1 or control, revealed the levels of pERK1/2 phosphorylation 72h after transfection. The values in siNRP1 samples were presented as fold change relative to control.

Protein Name	Phosphorylated residue	Fold Change in siNRP1
ERK1	§202 and/or §204	5.5
ERK2	§185 and/or §187	3.1

Chapter 5 NRP1 regulates VEGF-165 induced vascular permeability

5.1 Introduction

To resolve conflicting ideas in the literature on the relative importance of NRP1 and VEGFR2 in VEGF164-induced vascular permeability at the time I started my PhD (see section 1.19), Dr Fantin and I worked together to define the specific role of NRP1 in this pathway. Whereas Dr Fantin performed the *in vivo* experiments to define genetic requirements for VEGFR2 and NRP1, I carried out mechanistic *in vitro* studies to elucidate the downstream signalling mechanisms. More specifically, Dr Fantin used Miles assay to measure the extravasation of Evans Blue-labelled serum albumin after intradermal injection of VEGF164 [e.g. (Zhang, 2009, Miles and Miles, 1952b, Senger et al., 1983)] in mouse mutants lacking VEGFR2 or NRP1 in ECs, or lacking the VEGF binding or cytoplasmic domains of NRP1 in all cells. Dr Fantin's experiments showed that VEGFR2, NRP1, the NRP1 VEGF binding domain and the NRP1 cytoplasmic domain (NCD) are all required for VEGF164-induced vascular permeability. To understand the signalling mechanism by which NRP1 and VEGFR2 cooperate to promote vascular leakage in response to VEGF164, I used confluent HUVEC, HDMEC and MLEC monolayers as tissue culture models amenable to biochemical studies. In the following sections, I will describe my observations in these models and relate them to Dr Fantin's findings, which have been published recently (Fantin et al., 2017).

5.2 Results

5.2.1 NRP1 and SFK are localised in cell-cell contact areas of HUVEC after VEGF165 stimulation

Immunostaining of confluent HUVEC showed NRP1 localisation to the cell periphery of serum starved ECs, in which it accumulated in cell-cell contact areas 5 min after VEGF165 stimulation and from which it was internalised 30 min later (**Fig. 22**, upper panel). I also performed immunostaining with an antibody raised against the phosphorylated tyrosine Y419 of activated SRC that also recognises the phosphorylated forms of other SFKs due to high sequence conservation around the phosphosite (amino acid sequence alignment performed with CLUSTAL OMEGA; unpublished data from James Brash in the Ruhrberg team). I will therefore refer to the proteins detected by this antibody not as phosphorylated (p) SRC, but pSFK. I found that VEGF165 induced pSFK 5 min after stimulation and that pSFK localised in cell-cell contact areas of serum-starved HUVEC (**Fig. 22**, lower panel).

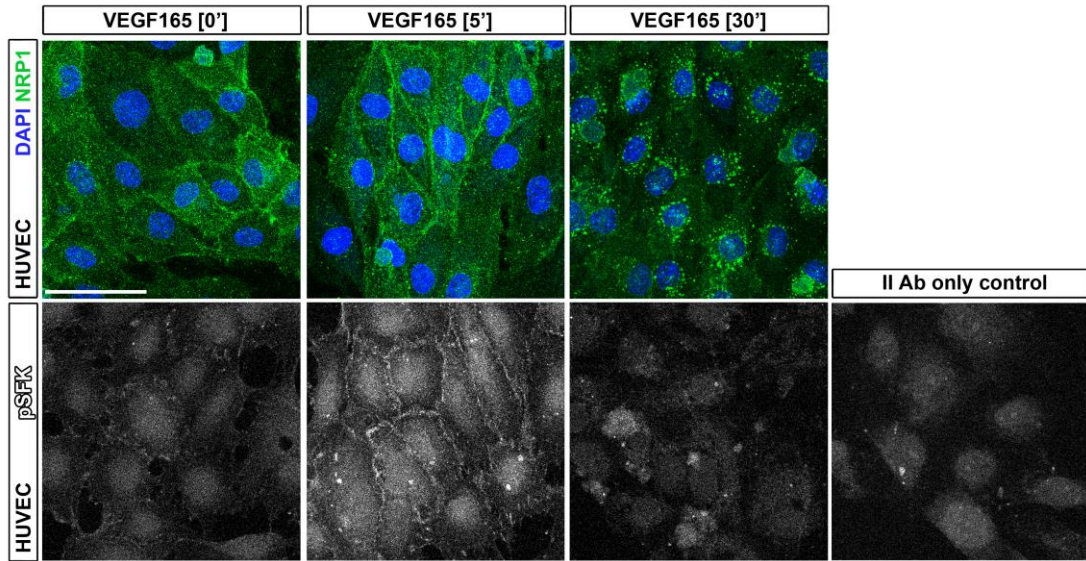


Figure 22: NRP1 and pSFK are localised on the cell periphery of HUVEC.

Immunostaining of confluent HUVEC cultures in serum starved conditions with antibodies for NRP1 together with DAPI to visualise cell nuclei (upper panel) and pSFK in grey scale (lower panel). The cells were serum starved for 5h and stimulated for 5 and 30 min with 50 ng/ml VEGF165 (2 independent experiments). Scale bar: 50 μ m.

5.2.2 NRP1 localises on the cell-cell contact areas of HDMEC

Even though I initially used HUVEC for my studies, a recent study showed that confluent HDMEC express more claudin 5, a EC tight junction protein, and that they showed higher transendothelial electric resistance (TEER) than HUVEC (Kluger et al., 2013). Moreover, prior studies have shown that VEGF165 also induces SFK activation in HDMEC, and that activated SFK localises at cell junctions 7 min after VEGF165 stimulation (Sun et al., 2012). Considering these findings, HDMEC are likely a better model to study permeability *in vitro* (Kluger et al., 2013). I therefore used HDMEC for the following experiments to understand the molecular mechanism by which VEGF165 induces vascular leakage.

Working together with Dr Senatore for NRP1 staining on ECs, we first examined whether NRP1 localises in the cell periphery of confluent HDMEC, as would be expected if it played a role in permeability induction. Thus, immunostaining of confluent, non-permeabilised HDMEC in normal growth conditions showed NRP1 localisation on the cell surface, including areas of cell-cell contact (**Fig. 23A**), similar to my observations in HUVEC (**Fig. 22**). Moreover, immunostaining for NRP1 and an intracellular epitope of CDH5 confirmed localisation of a NRP1 subset to areas of cell-cell contact in HDMEC (**Fig. 23B**), similar to the pattern observed in skin and retinal vasculature *in vivo* (data not shown, performed by Dr Fantin).

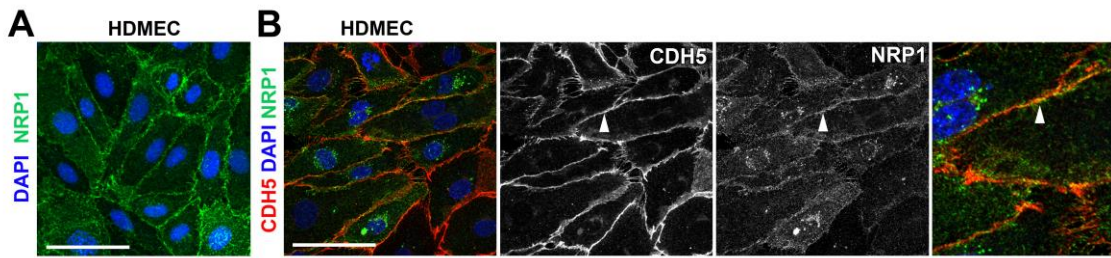


Figure 23: NRP1 localises on the cell periphery of HDMEC.

(A,B) Immunostaining of confluent HDMEC cultures in growth medium under non-permeabilising conditions with an antibody specific for human NRP1 (A) or under permeabilising conditions with antibodies for CDH5 and NRP1 together with DAPI to visualise cell nuclei (B) (3 independent experiments). Single channels in (B) are shown separately in grey scale, and the boxed area is shown in higher magnification on the right hand side. 3 independent experiments; Scale bar: 50 μ m.

5.2.3 NRP1 promotes VEGF165-induced SFK activation in HDMEC

To examine the requirement of NRP1 for VEGF165-mediated pSFK induction, I transfected HDMEC with siRNA that targets NRP1 or a control siRNA (Raimondi et al., 2014, Fantin et al., 2015). After 72 hours of transfection, the cells were starved for 5 hours and stimulated with 50 ng/ml of VEGF165 for 5 or 15 min. Immunostaining showed that levels of pSFK in si-control samples peaked at 5 and 15 min after VEGF165 stimulation, with an enrichment of pSFK at the cell periphery (**Fig. 24A**). Accordingly, HDMEC monolayers represent a suitable model to investigate NRP1-mediated permeability signalling via SFKs. Indeed, ECs lacking NRP1 expression showed decreased pSFK at 5 and 15 min compared to control cells (**Fig. 24A'**).

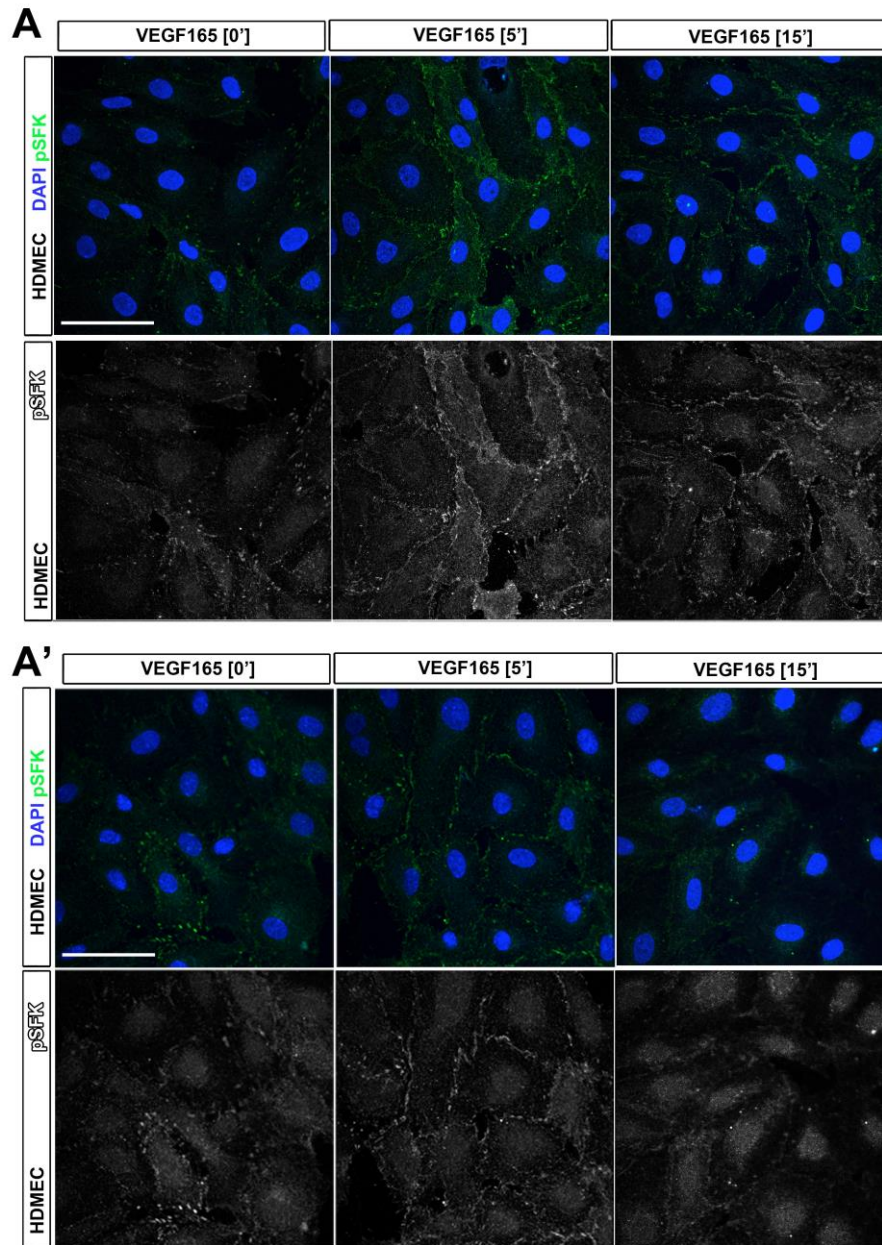


Figure 24: NRP1 promotes VEGF165-induced SFK activation in HDMEC.

(A,A') HDMEC transfected for 72h with si-control (A) or si-NRP1 (A'), were serum starved for 5h and then stimulated for 5 or 15 min with 50 ng/ml VEGF165. The ECs were stained with an antibody for pSFK (green) and DAPI (blue) to visualise cell nuclei. 3 independent experiments; Scale bar 50 μ m.

Immunoblotting validated NRP1 knockdown efficiency and reduced phosphorylation of the VEGFR2 Y1175 (pVEGFR2) and the ERK1/2 T202/Y204 (pERK) residues after VEGF165 stimulation in NRP1-deficient compared to NRP1-expressing ECs (**Fig. 25A**), as previously attributed to impaired VEGFR2 trafficking (Lanahan et al., 2013a, Raimondi et al., 2014). VEGFR2 Y1175 is one of the major VEGF-A-dependent autophosphorylation sites, and together with ERK1/2 activation is important for ECs proliferation (Takahashi et al., 2001). Quantification of VEGFR2 Y1175 activation as pVEGFR2/tVEGFR2 ratio showed that VEGFR2 activation is additionally significantly reduced at 5, but not 15 min (**Fig. 25A,B**). This experiment therefore confirmed that I was able to successfully stimulate VEGFR2 signalling in HDMEC, and that NRP1 enhances the VEGFR2 response, as expected. HDMEC lacking NRP1 expression also showed decreased total VEGFR2 protein and transcription levels (Raimondi et al., 2014). This finding suggests that lack of NRP1 affects VEGFR2 transcription in addition to VEGFR2 Y1175 phosphorylation.

As loss of the Y1175 residue is early embryonic lethal (Sakurai et al., 2005), it is not known whether it is involved in VEGF-induced permeability. In contrast, it has recently been shown that the Y951 residue is required for VEGF-induced permeability (Sun et al., 2012). Thus, we further tested whether VEGF165-induced VEGFR2 Y951 phosphorylation was reduced in NRP1-deficient HDMEC compared to control cells (data not shown, experiments performed by James Brash). This residue is essential to recruit SH2D2A (also known as T cell-specific adaptor, TSAd), which then recruits SRC to VEGFR2 for vascular permeability signalling (Sun et al., 2012, Li et al., 2016).

Immunoblotting further showed that VEGF165 stimulation increased pSFK levels in control HDMEC, but this response was attenuated in HDMEC lacking NRP1 (**Fig. 25A**), similar to the pattern observed with immunostaining (**Fig. 23**). As total SRC levels were increased in NRP1-deficient cells (**Fig. 25A**), reduced SFK activation was not explained by reduced SRC expression. However, I would like to perform additional experiments to also examine the total levels of other SFKs that are expressed in HDMEC, including YES1 and FYN. Quantification demonstrated a significant reduction in SFK activation 10 and 15 min after VEGF165 stimulation in HDMEC lacking NRP1 compared to controls (**Fig. 25C**; for quantifications I pooled

data produced by J. Brash and myself; note that we normalised pSFK to GAPDH rather than the total level of any individual SFK, because the pSFK antibody recognises the phosphorylated forms of several SFKs).

Together, these findings suggest that endothelial NRP1 is essential for VEGF165-induced SFK activation. Future work should examine which SFKs are expressed by HDMEC and might use knockdown studies to determine which specific SFKs are modulated by NRP1-dependent VEGF165 activation of VEGFR2 signalling.

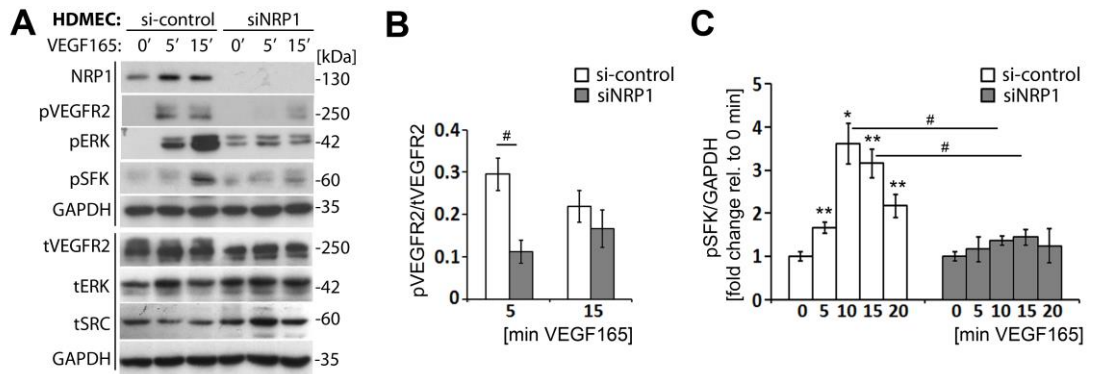


Figure 25: NRP1 loss impairs VEGF165-induced SFK activation in HDMEC.

(A) Confluent HDMEC cultures transfected with si-control or siNRP1 were serum-starved and treated with VEGF165 for the indicated times before lysates were used for immunoblotting with the indicated antibodies. (B, C) Quantification of pVEGFR2 Y1175 (B) and pSFK (C) induction relative to tVEGFR2 and GAPDH, respectively, at the indicated times after VEGF165 treatment. Each of the two vertical lines indicates a group of immunoblots from a single gel, with both gels containing aliquots of the same protein. Data for si-control and siNRP1 treated cells are expressed as fold change, mean \pm SEM, for VEGF165 treatment at different time points relative to 0 min; 4 independent experiments; asterisks indicate significant P values for pVEGFR2 and pSFK induction after VEGF165 treatment (*p<0.05, **p<0.01; paired t-test). Hash tags indicate significant P values for reduced pSFK levels in siNRP1 versus si-control at the corresponding time points (#p<0.05; unpaired t-test).

5.2.3.1 NRP1 and VEGFR2 are both required for VEGF165-dependent SFK and ABL activation. VEGFR2 kinase activity is required for VEGF165-induced SFK activation

I next asked whether VEGFR2 kinase activity was required for SFK activation by treating HDMEC with PTK/ZK (Vatalanib), a highly specific VEGFR2 inhibitor that abolishes VEGFR2 signalling by blocking the VEGF-induced autophosphorylation of VEGFR2 (Wood et al., 2000). Important for my experiments, this inhibitor does not directly target SRC or ABL kinases (VEGFR2 k_d 62 nM; SRC, YES1, ABL1 or ABL2 k_d not detected under normal assay conditions, i.e. >10 μ M; (Davis et al., 2011, Wodicka et al., 2010)). Immunoblotting confirmed that PTK/ZK impaired VEGF165-induced VEGFR2 activation (**Fig. 26A**). PTK/ZK also abrogated pSFK induction (**Fig. 26A,B**). These findings are consistent with prior work suggesting a role for VEGFR2 in SFK activation (Sun et al., 2012, Li et al., 2016).

5.2.3.2 VEGFR2 and NRP1 cooperate for VEGF165-induced ABL activation

It has been reported that VEGF165 stimulation activates ABL1 and ABL2 in human ECs *in vitro*, and that ABL kinase activation is essential for VEGF164-induced vascular permeability in the Miles assay (Anselmi et al., 2012, Chislock and Pendergast, 2013, Aman et al., 2012). Also, Dr Raimondi and I have shown that NRP1 interacts with ABL1 in normal growth conditions and that it mediates FN-induced PXN activation in HDMEC (Raimondi et al., 2014). However, it has not previously been examined whether NRP1 or VEGFR2 also contribute to SFK activation in an ABL kinase-dependent manner.

To determine whether VEGFR2 is involved in ABL kinase activation, I examined the VEGF165-induced phosphorylation of CRKL, an ABL kinase target whose phosphorylation on Y207 is widely used as readout of ABL kinase activation (Sattler and Salgia, 1998). HDMEC stimulated with VEGF165 showed increased pCRKL levels 5 and 15 min after VEGF165 treatment, but not in PTK/ZK-treated cells (**Fig. 26A,B'**). This observation confirms that VEGFR2 is upstream of ABL activation.

NRP1 knockdown cells also showed impaired VEGF165-mediated pSFK induction

and decreased pCRKL levels (**Fig. 26A,C**). In contrast to PTK/ZK treatment, however, NRP1 knockdown reduced pCRKL levels at baseline, i.e. prior to VEGF165 stimulation (**Fig. 26C**). Also different to PTK/ZK treatment, NRP1 knockdown did not prevent the VEGF165-induced pCRKL increase, although pCRKL levels remained significantly lower in NRP1-deficient compared to control cells at all times (**Fig. 26C**), suggesting that CRKL can also be activated in a NRP1-independent manner.

As neither VEGFR2 inhibition of NRP1 knockdown affected total CRKL levels (**Fig. 26A**), my findings shown that VEGF165-induced ABL kinase activation depends on VEGFR2 completely and on NRP1 partially. However, it still remains unknown whether VEGFR2, after complex formation with NRP1, can directly phosphorylate ABL kinases or whether another kinase mediates this function.

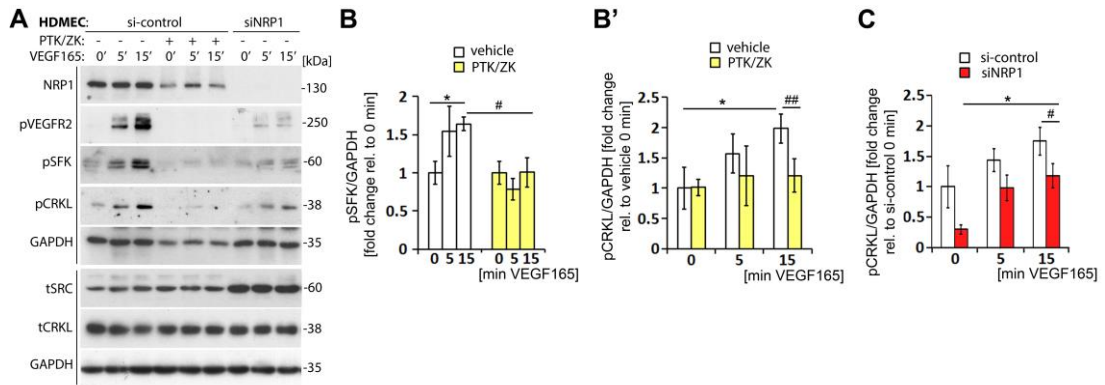


Figure 26: VEGFR2 and NRP1 are required for VEGF165-induced SFK activation.

(A-C) Confluent HDMEC cultures transfected with si-control or siNRP1 were serum-starved and treated with VEGF165 for the indicated times. Cultures were also treated with vehicle (-) or PTK/ZK (+) for 30 min prior to VEGF165 stimulation. Lysates were used for immunoblotting with the indicated antibodies (A), followed by quantification of pSFK levels (B) and pCRKL levels (B',C) relative to GAPDH. Each of the two vertical lines indicates a group of immunoblots from a single gel, with both gels containing aliquots of the same protein. In B, data are expressed as fold change, mean±SEM, in VEGF165-treated cells at 5 and 15 min relative to 0 min; in B' and C, data are expressed as fold change, mean±SEM, in VEGF165-treated cells at 5 and 15 min relative to control cells at 0 min; 4 independent experiments; asterisks indicate P values for induction after VEGF165 treatment (*p<0.05, **p<0.01, ***p<0.001; paired t-test); hash tags indicate significant P values for different treatments at corresponding time points (#p<0.05, ##p<0.01, ###p<0.001; unpaired t-test).

5.2.4 ABL1 mediates NRP1-dependent SFK activation

As NRP1 is required for both SFK and ABL kinase activation, but itself does not have kinase activity, I sought to determine whether NRP1-bound ABL1 is required for pSFK and pCRKL induction by VEGF165. For this experiment, I transfected HDMEC with a previously validated siRNA for ABL1 (Raimondi et al., 2014). Similar to NRP1 knockdown, ABL1 knockdown inhibited pSFK induction after VEGF165 stimulation (**Fig. 27A**). Also, total SRC levels were increased in ABL1-deficient cells, similar to NRP1-deficient cells, suggesting that reduced SFK activation was not explained by reduced SRC expression (**Fig. 27A**). Quantification demonstrated a significant reduction in pSFK activation 5 and 15 min after VEGF165 stimulation in HDMEC lacking ABL1 compared to controls (**Fig. 27A,B**). Moreover, ABL1 knockdown decreased overall pCRKL levels at baseline, but knockdown did not prevent the VEGF165-induced increase in pCRKL levels (**Fig. 27A,B'**). Again, decreased CRKL activation could not be explained by reduced CRKL levels, as CRKL total levels were similar between the two groups (**Fig. 27A**). The finding that pSFK induction is severely compromised and that pCRKL induction is similarly reduced in cells lacking NRP1 or ABL1 is consistent with the idea that NRP1-dependent ABL1 activation is required for pSFK activation. However, even though strongly required for pSFK induction, NRP1 cannot be the sole regulator of ABL kinase-dependent pCRKL induction, because VEGF165 can still induce CRKL activation independently of NRP1.

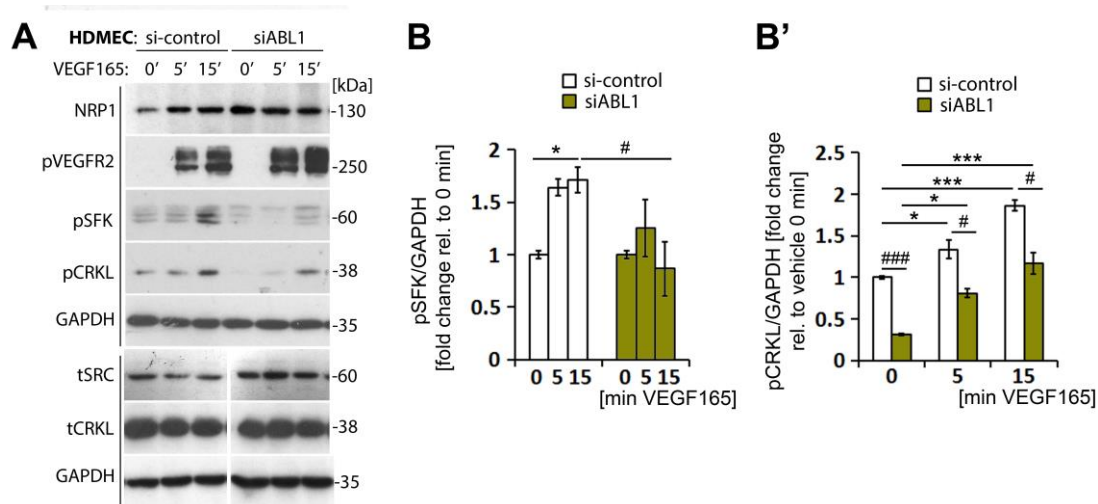


Figure 27: ABL1 mediates NRPI-dependent SFK activation.

(A-B') Confluent HDMEC cultures transfected with si-control or siABL1 were serum-starved and treated with VEGF165 for the indicated times. Lysates were used for immunoblotting with the indicated antibodies (A), followed by quantification of pSFK levels (B) and pCRKL levels (B') relative to GAPDH. Each of the two vertical lines indicates a group of immunoblots from a single gel, with both gels containing aliquots of the same protein. The spacer line (A, bottom) separates lanes 4-6 (left) from lanes 1-3 (right) of immunoblots from the same gel. In B, data are expressed as fold change, mean±SEM, in VEGF165-treated cells at 5 and 15 min relative to 0 min; in B', data are expressed as fold change, mean±SEM, in VEGF165-treated cells at 5 and 15 min relative to control cells at 0 min; 4 independent experiments; asterisks indicate P values for induction after VEGF165 treatment (*p<0.05, **p<0.01, ***p<0.001; paired t-test); hash tags indicate significant P values for different treatments at corresponding time points (#p<0.05, ##p<0.01; ###p<0.001; unpaired t-test).

5.2.5 ABL kinases are required for both VEGF165-induced CRKL and SFK activation

Based on the fact that NRP1 and ABL1 are not the only regulators of ABL kinase-dependent pCRKL induction in VEGF165-stimulated HDMEC, I next asked whether ABL2 cooperates with ABL1 to activate CRKL and SFK. For this experiment, I treated HDMEC with Imatinib, which efficiently blocks both ABL1 and ABL2, but not SRC, YES1 or VEGFR2 (ABL1 k_d 1 nM and ABL2 k_d 10 nM vs. SRC, YES1 and VEGFR2 k_d not detected under normal assay conditions, i.e. >10 μ M; ABL1 IC_{50} 0.025-0.2 μ M vs. SRC IC_{50} >100 μ M; (Davis et al., 2011, Deininger et al., 2005, Buchdunger et al., 1996). As expected, Imatinib inhibited pCRKL induction by blocking both ABL1 and ABL2 activation, suggesting that ABL2 synergises with ABL1 for VEGF165-induced CRKL phosphorylation (**Fig. 28A, B'**).

Imatinib also significantly impaired VEGF165-induced SFK activation, despite its poor specificity for SFKs (**Fig. 28A, B**). PP2, a dual SFK and ABL kinase inhibitor (Tatton et al., 2003), also impaired pSFK induction and additionally suppressed baseline SFK phosphorylation (**Fig. 28A**). In contrast, neither inhibitor impaired VEGFR2 activation (**Fig. 28A**). These findings suggest that ABL kinase activity is required for VEGF165-induced SFK activation downstream of VEGFR2.

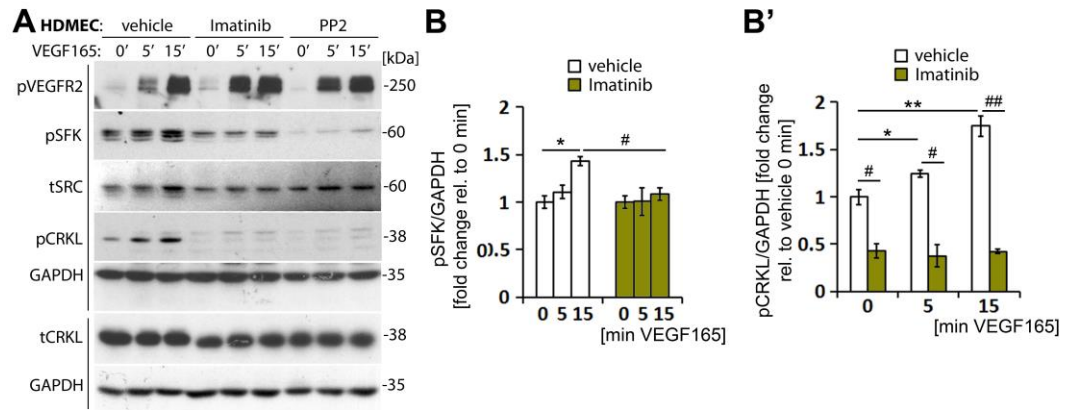


Figure 28: ABL kinases are required for VEGF165-induced SFK activation.

(A-B') Confluent HDMEC cultures were serum-starved and treated with vehicle, Imatinib or PP2 for 30 min prior to VEGF165 stimulation for the indicated times. Lysates were used for immunoblotting with the indicated antibodies (A), followed by quantification of pSFK levels (A) and pCRKL levels (B') relative to GAPDH. Each of the two vertical lines indicates a group of immunoblots from a single gel, with both gels containing aliquots of the same protein. In B, data are expressed as fold change, mean±SEM, in VEGF165-treated cells at 5 and 15 min relative to 0 min; in B', data are expressed as fold change, mean±SEM, in VEGF165-treated cells at 5 and 15 min relative to control cells at 0 min; 3 independent experiments; asterisks indicate P values for induction after VEGF165 treatment (*p<0.05, **p<0.01; paired t-test); hash tags indicate significant P values for different treatments at corresponding time points (#p<0.05, ##p<0.01; unpaired t-test).

As described above, Imatinib targets both ABL1 and ABL2 and therefore abolished pCRKL (**Fig. 28A**). In contrast, ABL1 knockdown leaves ABL2 activity intact and therefore should not completely abrogate pCRKL; in agreement, I observed that pCRKL levels were significantly reduced, but not abrogated, in HDMEC lacking ABL1 compared to controls (**Fig. 27A**).

To demonstrate that ABL2 partially compensates for ABL1 and to further confirm the data I obtained with the Imatinib treatment, I also performed a double knockdown for ABL1 and ABL2 (**Fig. 29A,B**). As expected, this abolished pCRKL activation, similar to Imatinib treatment (**Fig. 28A**). Double knockdown of ABL1 and ABL2 as well as Imatinib treatment also significantly reduced VEGF165-induced pSFK levels (**Fig 29 and Fig. 28A**). In contrast to the established role for SFK activation in vascular permeability, it has not been examined whether CRKL activation is important for this endothelial response. Future work is needed to determine whether CRKL activation also contributes to vascular permeability.

Together, the results from the inhibitor and knockdown approaches, which agree with each other, are consistent with the idea that ABL kinase and SFK activation operate in the same VEGF165-driven, NRP1- and VEGFR2-mediated pathway, with a relatively more important role of ABL1 than ABL2 for SFK activation.

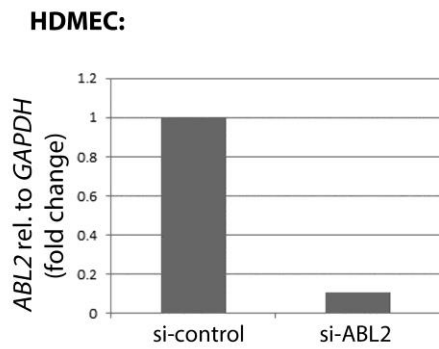
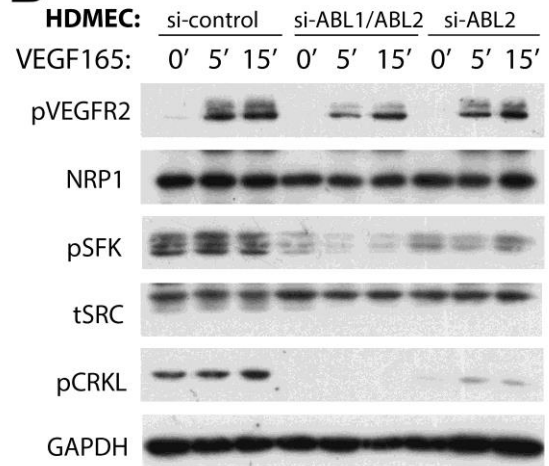
A**B**

Figure 29: Double knockdown for ABL1 and ABL2 abolished CRKL activation and reduced pSFK.

(A) qPCR analysis shows efficient reduction of ABL2 mRNA levels after treatment with ABL2-specific siRNA (n=1). (B) Confluent HDMEC cultures transfected with si-control or si-ABL1 and si-ABL2 or si-ABL2 were treated with VEGF165 for the indicated times and lysates used for immunoblotting with the indicated antibodies (3 independent experiments).

5.2.6 NRP1 is required for VEGF-induced FAK activation

Prior studies have shown that SFK-mediated FAK activation regulates adherens junctions' dynamics by promoting the dissociation of CTNNB1 (β -catenin) from CDH5 (Chen et al., 2012). As loss of NRP1 impaired SFK activation, I wanted to examine whether VEGF165-induced FAK activation is also regulated by NRP1. I found that HDMEC lacking NRP1 expression showed reduced phosphorylation of the Y397 residue in FAK (n=4 independent experiments) compared to controls (**Fig. 30A,B**). These findings agree with our model, in which NRP1 is important for VEGF165-induced permeability signalling in pathways that requires SFK activation, which was previously shown to operate upstream of FAK (Chen et al., 2012).

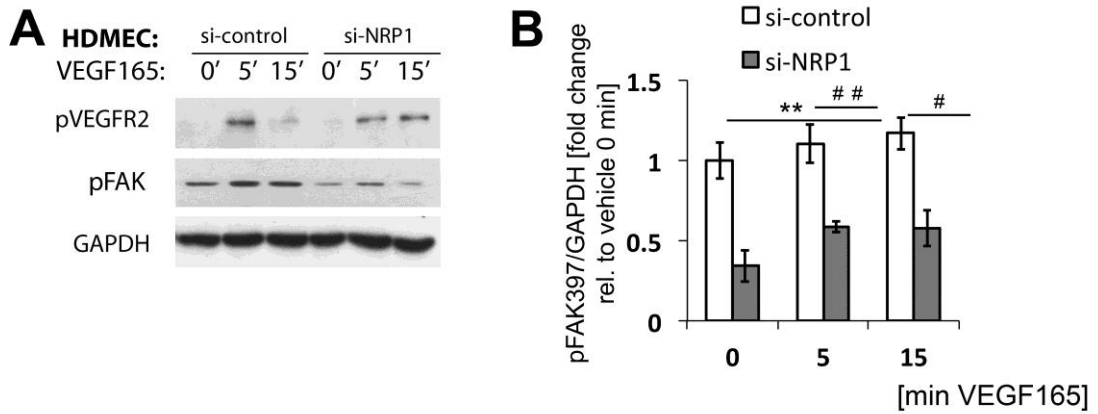


Figure 30: Loss of NRP1 impairs VEGF-induced FAK activation in HDMEC.

(A-B) Confluent HDMEC cultures transfected with si-control or siNRP1 were treated with VEGF165 for the indicated times. Lysates were used for immunoblotting with the indicated antibodies (A). Quantification of pFAK Y397 levels relative to GAPDH (4 independent experiments) (B). The data are expressed as fold change, mean±SEM, in VEGF165-treated cells at 5 and 15 min relative to control cells at 0 min; 4 independent experiments; asterisks indicate P values for induction after VEGF165 treatment (*p<0.05, **p<0.01; paired t-test); hash tags indicate significant P values for different treatments at corresponding time points (#p<0.05, ##p<0.01; unpaired t-test).

5.2.7 VEGF164-induced SFKs activation via ABL kinase relies on the NCD

I next determined whether the NCD was required for endothelial pSFK induction. Immunostaining and immunoblotting of confluent primary mouse lung EC (MLEC) confirmed that VEGF164 increased pVEGFR2 and pSFK levels in ECs from wildtype, but not *Nrp1^{cyto/cyto}* mice (**Fig. 31A,B**). ECs from *Nrp1^{cyto/cyto}* mice showed slightly reduced VEGFR2 phosphorylation (**Fig. 31C**); this agrees with finding in HDMEC lacking NRP1 expression (**Fig. 13**). Notably, VEGFR2 total levels were similar in ECs from *Nrp1^{cyto/cyto}* mice and control mice, different from HDMEC lacking NRP1 expression, as the total VEGFR2 level was decreased (compare **Fig. 31** with **Fig. 25**). NCD loss also impaired VEGF164-induced CRKL activation in MLEC (**Fig. 31C**), as observed in HDMEC lacking NRP1 expression altogether (**Fig. 26**). Although *Nrp1^{cyto/cyto}* mice showed reduced SFK and CRKL activity, total SRC and CRKL levels were similar for the wild type mice and the mutants (**Fig. 31B,C**). Together, these findings suggest that the NCD enables VEGF164-induced ABL kinase and SFK activation in ECs. Complementary work performed by Dr Senatore and J. Brash confirmed that VEGF164 induced SFK activation was impaired in NCD-deficient primary mouse brain EC (BEC) and in ear dermis lysates of VEGF164 injected NCD-deficient mice (data not shown). Experiments in three different models therefore showed that NCD loss impairs VEGF164-induced SFK activation in ECs.

In addition, immunoblotting showed that the NCD is required for VEGF164-induced FAK activation. Thus, experiments using MLEC showed reduced phosphorylation of the Y397 residue in FAK from *Nrp1^{cyto/cyto}* mutants (n=2 independent experiments) compared to controls (**Fig. 31D**). This agrees with my prior experiments, which showed that HDMEC lacking NRP1 expression have decreased FAK phosphorylation (see above, **Fig. 30**). Moreover, these findings raise the possibility that FAK activation occurs in the same NRP1-regulated pathway as SFK. This would agree with prior literature, which showed that SFKs operate upstream of FAK activation, as pharmacological inhibition of FAK activity in HUVEC or a FAK genetic deletion did not impair the VEGF-induced SFK activation (Chen et al., 2012).

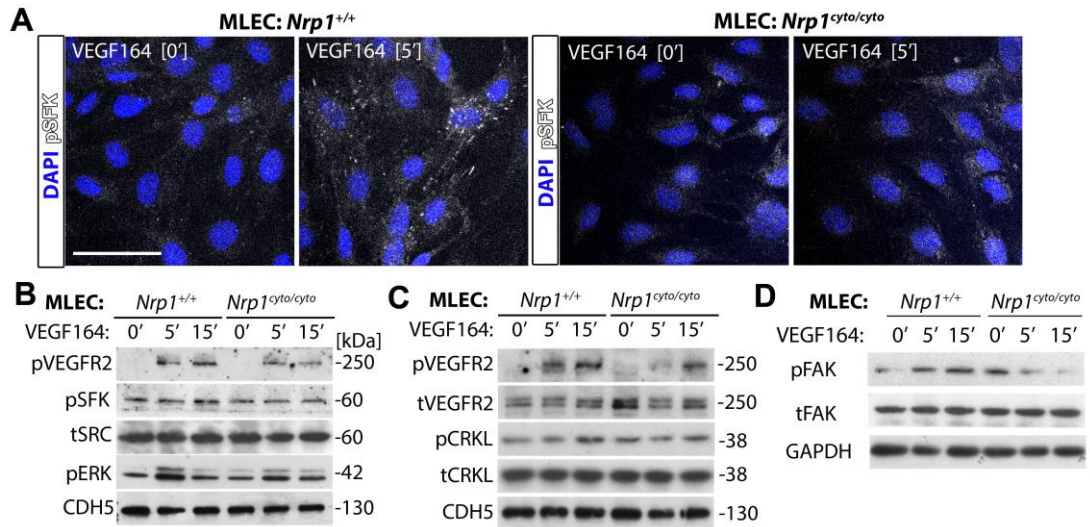


Figure 31: NCD loss impairs VEGF164-induced SFK activation in the mouse.

(A-D) Confluent MLEC from *Nrp1*^{cyto/cyto} and wildtype lungs were serum-starved and treated with VEGF164 for the indicated times and immunostained under permeabilising conditions using an antibody for pSFK (A) or lysed for immunoblotting with the indicated antibodies (B,C,D); cells were counterstained with DAPI. 2 independent experiments each. Scale bar: 50 μ m.

5.2.8 CDH5 localisation in MLEC from wild type and *Nrp1*^{cyto/cyto} mice

Prior studies have shown that VEGF164 stimulation can cause CDH5 (VE-cadherin) rearrangements that result in a “zig-zag” pattern on the cell surface of confluent MLEC monolayers (Sun et al., 2012). I therefore investigated whether VEGF164 stimulation differentially affects CDH5 rearrangements in MLEC isolated from wild type mice versus *Nrp1*^{cyto/cyto} mutants. For this analysis, I serum starved confluent MLEC from wild type mice and *Nrp1*^{cyto/cyto} mutants and then stimulated them with 100 ng/ml of VEGF164 for the indicated times (3 independent experiments) before immunostaining them for CDH5 (**Fig. 32**). Even though VEGF164-induced VE-cadherin rearrangements in MLEC has been described by Sun and colleagues, I could not detect obvious differences between stimulated and unstimulated cells in my experiments (Sun et al., 2012). Moreover, I did not observe obvious VE-cadherin rearrangements 10 min after VEGF164 stimulation compared to unstimulated cells, as unstimulated and stimulated samples both showed variable CDH5 staining pattern. Indeed, both wild type and mutant monolayers of unstimulated cells showed areas with the “zig-zag” pattern previously reported to be typical of wild type cells after VEGF164 stimulation [compare Fig. 32 in this report with Fig. 6 in (Sun et al., 2012)]. Even though the morphology of *Nrp1*^{cyto/cyto} mutant ECs was slightly different to that of wild type ECs, they also showed a similarly variable CDH5 pattern and no obvious changes in this pattern after VEGF164 stimulation (**Fig. 32**). The reasons for the different results obtained in my studies and those of the Claesson-Welsh lab are presently not clear, but possible explanations are provided in the discussion (section 5.3).

As the MLEC monolayer has high TEER level, suggesting the presence of tight junctions, I could use MLEC as a model to test other junctional markers such as ZO-1 or Claudin 5 or to test VE-cadherin phosphorylation in the future.

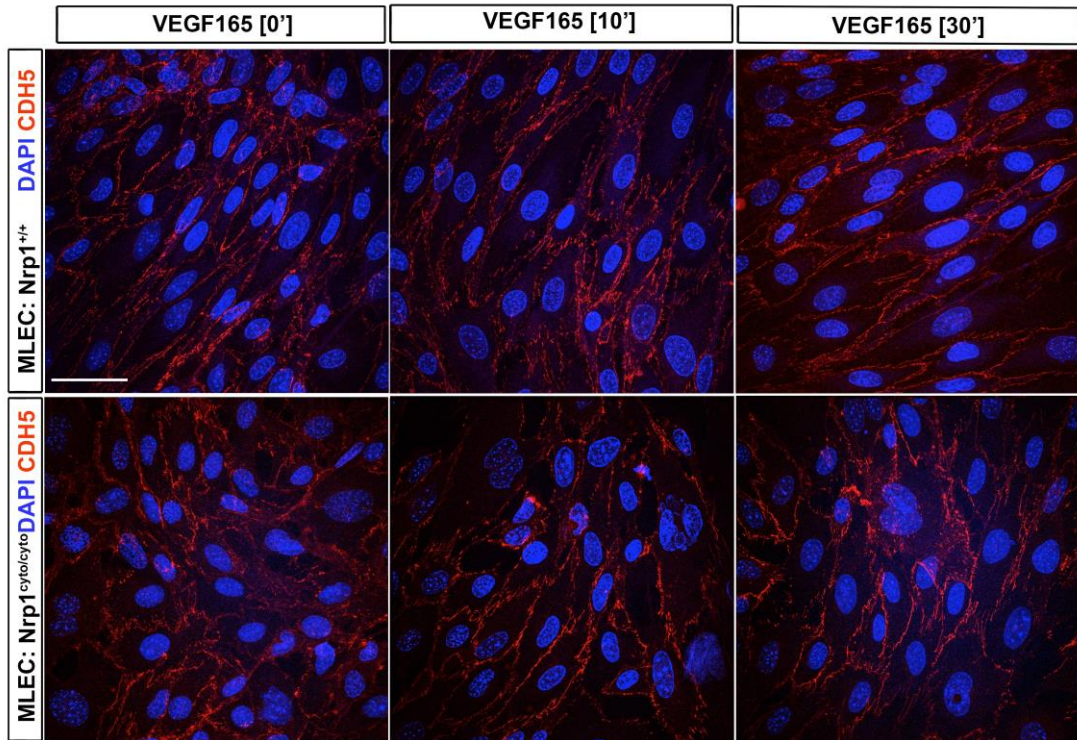


Figure 32: NCD loss does not affect CDH5 localisation in the mouse.

Confluent MLEC from *Nrp1^{cyto/cyto}* and wildtype lungs were serum-starved and treated with VEGF164 for the indicated times and immunostained under permeabilising conditions using an antibody for CDH5 and stained with DAPI. (3 independent experiments each); Scale bar: 20 μ m.

5.3 Discussion

NRP1 is a multifunctional protein with several distinct roles in regulating EC functions (Lampropoulou and Ruhrberg, 2014, Raimondi et al., 2016). Whereas VEGF165-binding to NRP1 and complex formation with VEGFR2 were originally thought to drive angiogenesis, it was subsequently shown that VEGF164 binding to NRP1 makes only a small contribution to physiological angiogenesis in mice (Gelfand et al., 2014, Fantin et al., 2014). Findings from our lab (described in Chapter 3) together with other studies showed that NRP1 instead promotes postnatal angiogenesis through essential roles in extracellular matrix-induced actin cytoskeleton remodelling and TGF β -modulated delta-notch signalling (Aspalter et al., 2015, Raimondi et al., 2014). The VEGF164-bound NRP1-VEGFR2 complex recruits GIPC1 to promote its trafficking into signalling endosomes, where it sustains pro-arteriogenic ERK1/2 signalling (Lanahan et al., 2013a). In contrast, it had not previously been examined whether VEGF164 binding to NRP1 or the NRP1 cytoplasmic domain or NCD-binding proteins contribute to VEGF164-induced vascular permeability, and it was not known whether NRP1 plays a role in SFK and ABL activation for VEGF164-induced vascular permeability.

Thus, Dr Fantin and I investigated the role of NRP1 in vascular permeability *in vivo* and *in vitro*, respectively. Together, our data show that NRP1 binds VEGF164 to promote VEGF164/VEGFR2-induced SFK activation for vascular permeability. Our findings agree with earlier work in endothelial NRP1 mouse mutants, which had identified an essential role for NRP1 in VEGF164-induced vascular leakage (Acevedo et al., 2008). Whilst prior work did not determine why VEGFR2 is insufficient for vascular permeability induction, the *in vitro* data presented here showed that NRP1 is required as a VEGFR2 co-receptor to enable ABL-dependent SFK activation (**Fig. 26, 27**). Moreover, the finding that NRP1 regulates vascular permeability through ABL kinase activation also agrees and extends genetic studies implicating ABL kinases in VEGF164-induced vascular permeability (Chislock and Pendergast, 2013, Aman et al., 2012) by identifying the receptor complex that mediates ABL kinase activation.

The work I carried out in the lab, in conjunction with James Brash's bioinformatics

analysis, also revealed additional interesting information on the question whether SRC mediates vascular permeability signalling, as suggested in the literature in several studies [e.g. (Sun et al., 2012, Weis et al., 2004b)]. In particular, the Claesson-Welsh lab suggested that VEGF- induced vascular leakage is mediated by SRC through its binding to the TSA adaptor protein that mediates VEGFR2 binding (Sun et al., 2012). Considering that the SFK antibody I have used for my experiments recognises the phosphorylated forms of several closely related SFKs, including SRC, YES1 and FYN, we cannot be sure which SFK was predominantly activated and functional in the experiments described in this chapter. Moreover, the antibody that has been used for studies in Claesson-Welsh lab [see methods in (Sun et al., 2012)] is the rabbit (polyclonal) anti-Src pY418 (Invitrogen) that also cross react with the YES1 and FYN proteins. Future work is therefore required to define which members of the SFK family are activated by VEGF in a NRP1- and VEGFR2-dependent manner to induce vascular permeability. This is particularly important, because two different SFK members, SRC and YES1, have previously been reported to be tyrosine phosphorylated in response to VEGF, and mice lacking either kinase were found to have reduced VEGF₁₆₄-induced vascular leakage (Eliceiri et al., 1999, Scheppeke et al., 2008).

A prior study used SU6656 to investigate the regulatory hierarchy of SRC and ABL kinase activation in ECs after VEGF₁₆₄ stimulation placed SRC upstream of ABL kinases (Chislock and Pendergast, 2013). However, this inhibitor targets both SRC and YES1 as well as VEGFR2, which resides at the top of this signalling cascade, and even targets ABL1, although to a smaller extent (remaining activity at 1 μ M: SRC 31% and YES1 12% vs. VEGFR2 51% and ABL1 77%; (Gao et al., 2013). Similarly, the SRC inhibitor PP2, which I have used here, is not selective for SRC, but has dual SFK/ABL kinase specificity (Tatton et al., 2003) and accordingly abrogated both VEGF₁₆₅-induced SFK and ABL kinase activation (**Fig. 28**). Treatment with the PP1 inhibitor (very similar to PP2) has been shown to inhibit VEGF-induced retinal vascular permeability by blocking extravasation of fluorescein conjugate dextran or albumin after VEGF intravitreal injection, similarly to the blockade of vascular leak observed in retinas of VEGF-stimulated *Src* and *Yes* knockout mice (Scheppeke et al., 2008). Prior results obtained with these inhibitors therefore support the idea that the VEGFR2-ABL-SFK axis has a key role in

VEGF164-induced permeability signalling, but they did not allow us to define the regulatory relationship of these kinases. In contrast, Imatinib does not block VEGFR2 activation (**Fig. 28**) and has high specificity for ABL kinases over SFKs (Davis et al., 2011, Deininger et al., 2005). The results with Imatinib, when combined with those acquired with the VEGFR2 inhibitor PTK/ZK, therefore conclusively show that VEGFR2 is upstream of ABL kinases, which are upstream of SFKs (**Fig. 26, 28**). These observations agree with those obtained with siRNA-mediated knockdown of ABL1 (**Fig. 27**). Hence, the finding that NRP1 cooperates with VEGFR2 to enable ABL-dependent SFK activation in an NCD-dependent fashion places several molecules previously reported to be essential for VEGF165-induced vascular permeability into a well-defined regulatory hierarchy (**Fig. 31**).

The observation that NRP1 forms a complex with ABL1 in ECs independently of VEGF165 stimulation (Raimondi et al., 2014) raises the possibility that NRP1 may use its NCD to help deliver ABL1 to VEGFR2, once VEGF164 has induced complex formation between NRP1 and VEGFR2. In this manner, NRP1-bound ABL1 would be able to phosphorylate SFKs that are recruited to VEGFR2 via SH2D2A/TSAd, the intracellular adaptor protein that binds VEGFR2 phosphorylated Y951 residue that is required for VEGF164-induced vascular permeability (Sun et al., 2012, Li et al., 2016). Supporting this idea, SFK activation by ABL kinases would require spatial proximity of both types of proteins, because ABL kinases depend on the interaction with their substrates to overcome intramolecular autoinhibition (Wang, 2014), and such proximity would be instilled when VEGF164 tethers the VEGFR2/TSAd/SFK and NRP1/ABL1 complexes to each other by forming a bridge between its two receptors (**Fig. 33**). This model of higher order complex formation between several signalling components in the VEGF pathway is consistent with the strong reduction in pSFK levels after NRP1 or ABL1 knockdown (**Fig. 25, 27**). Moreover, an important role of the NCD in this pathway agrees with prior observations that the NCD enhances complex formation of NRP1 and VEGFR2 in VEGF165-stimulated ECs (Prahst et al., 2008) and promotes ABL1 function in tumour cells (Yaqoob et al., 2012). Future work should examine whether ABL kinases can regulate TSAd phosphorylation and/or SFK's recruitment to VEGFR2/TSAd complex to induce vascular permeability, or if their recruitment occurs independently of NRP1 and ABL1. Moreover, it should be examined which kinase phosphorylates ABL kinases

to activate them.

Downstream of the VEGF165-induced signal transduction cascade, different cellular mechanisms have been implicated in the induction of vascular leakage. For example, VEGF has variably been suggested to stimulate the formation of vesiculo-vacuolar organelles for transcellular leakage (Bates and Harper, 2002, Dvorak et al., 1996) or disrupt AJs between adjacent ECs to increase paracellular leakage (Dejana et al., 2008). For paracellular leakage, SFK-mediated FAK activation regulates adherens junctions dynamics by promoting the dissociation of CTNNB1 (β -catenin) from CDH5 (Chen et al., 2012). In agreement, here I show that ECs lacking NRP1 expression or lacking the cytoplasmic domain of NRP1 showed decreased FAK activity together with reduction of SFK phosphorylation (**Fig. 30, 31**). However, my CHD5 staining of confluent MLEC isolated from lungs of wildtype mice or NRP1^{cyto/cyto} mutants and stimulated with VEGF164 did not present considerable differences in the cell-cell contact areas either between unstimulated and stimulated cells, or between genotypes (**Fig. 32**). A possible reason that may explain the different results described here compared to Claesson-Welsh's published data, could be the use of another coating for the coverslips that had been used to seed the MLEC for the experiments. As for my experiments I used glass coverslips pre-coated with 6 μ g/ml FN and the Claesson-Welsh lab used collagen, my future work will include experiments with collagen to compare how the different substrates might affect the ECs monolayer. Whether the NRP1 pathway controls VEGF165-induced permeability by promoting adherens junction breakdown and/or a transcellular transport therefore remains to be further evaluated using other junctional markers, and extended to tight junction markers such as claudin 5.

In agreement with my *in vitro* data that showed that PTK/ZK treatment completely abolished ABL-dependent SFK activation (**Fig. 26**), Dr Fantin showed that mice lacking endothelial VEGFR2 expression did not respond to VEGF164 with increased vessel leakage. Also, endothelial *Nrp1* knockout mice showed a significant reduction in VEGF164-induced leakage compared to littermate controls, but, unlike endothelial *Vegfr2* knockout mice, had a residual response, and this work has now been published together with my *in vitro* findings [(Fantin et al., 2017), see Appendix]. Moreover, in agreement with the *in vitro* data that showed decreased ABL1 and SFK

activity in NRP1-deficient cells (**Fig. 25,27**), Dr Fantin demonstrated that VEGF binding to NRP1 is required for vascular permeability induction, as mice expressing a mutated form of NRP1 that lacks VEGF binding phenocopy the defective response observed in the inducible *Nrp1* knockout mice (Fantin et al., 2017). Therefore, both NRP1 and VEGFR2 are essential for VEGF164-induced vascular permeability *in vivo*, with VEGFR2 being absolutely required and NRP1 making an indispensable contribution for a robust response.

Together, my *in vitro* findings and Dr Fantin's *in vivo* findings are compatible with a model in which VEGF164 binding to NRP1 induces complex formation between NRP1 and VEGFR2 [e.g. (Soker et al., 2002b)] to create an obligate holoreceptor in which VEGFR2 is required, but depends on NRP1 to evoke a maximal permeability response to VEGF164.

The finding that VEGFR2 is indispensable for VEGF165-induced SFK activation and vascular leakage also agrees with prior permeability studies using inhibitors that have VEGFR2 as one of their targets (Murohara et al., 1998), as well as recent studies using function-blocking antibodies for VEGFR2 (Hudson et al., 2014) and a mouse knockin mutation to prevent VEGFR2 Y951 phosphorylation (Li et al., 2016).

In vivo data further showed that the cytoplasmic domain of NRP1 is required for VEGF164-induced vascular permeability, in agreement with my observation that MLEC cultures showed NCD-dependent ABL1-mediated SFK activation (**Fig. 31**). Thus, Dr Fantin demonstrated that *Nrp1*^{cyto/cyto} mice showed reduced vascular leakage compared to wildtypes littermates in response to VEGF164 stimulation.

Other studies have shown that NRP1 can convey C-end-Rule peptide-mediated leakage independently of VEGFR2 activation in a mechanism involving the NCD (Roth et al., 2016). The C-end-Rule peptide RPARPAR, binds to the NRP1 b1 pocket that also binds VEGF, but it cannot bind VEGFR2. Thus, the peptide can induce vascular leakage without affecting phosphorylation of VEGFR2 and its MAPK targets p38 and ERK1/2 or AKT. Instead, the signal was proposed to be mediated by the activation of SFKs, independently of FAK phosphorylation (Roth et al., 2016).

Interestingly, the *Nrp1*^{cyto/cyto} phenotype is ligand specific, as Miles assays using other stimuli such as SEMA3A or histamine, which have also been implicated in vascular permeability induction (Acevedo et al., 2008, Cerani et al., 2013, Miles and Miles, 1952a), induced hyperpermeability responses in *Nrp1*^{cyto/cyto} mice similar to wildtype controls. Thus, the NCD, even though required for VEGF164-induced and C-end-Rule peptide-induced SFK activation and vascular leakage, is dispensable for SEMA3A-induced vascular leakage. Taken together with the prior observation that SEMA3A induces vascular hyperpermeability via NRP1 independently of SFK activation via PI3K γ / δ -Akt pathway (Acevedo et al., 2008), the VEGF164 and SEMA3A permeability pathways appear to diverge at the level of signal transduction, despite their shared NRP1 dependence.

Other experiments from Dr Fantin showed that *Nrp1*^{cyto/cyto} mice do not exhibit any difference in baseline vascular permeability in any organ examined, for example the kidney or brain. In agreement with his *in vivo* data, I found that MLEC from wildtype and mutants had similar CHD5 levels and basal SFK activation, suggesting that there was no difference under baseline conditions (**Fig. 31**).

Even though a CHD5 zig zag pattern was previously proposed to be typical of junctional opening in response to VEGF164 stimulation (Sun et al., 2012), I unexpectedly found that CDH5 distribution in both unstimulated wild type and *Nrp1*^{cyto/cyto} MLEC cultures presented a relatively linear organisation in some, but a zig zag pattern in other cell areas (**Fig. 32**). Moreover, the CDH5 pattern did not change in response to stimulation. In the (Sun et al., 2012) paper, they show images with low and higher magnifications of selective cell areas. In the low magnification images, we can observe cell areas that are different to the area selected for high magnification presentation and analysis; also, it is not clear how they quantified changes in these cell areas.

Dr Fantin also examined whether GIPC1 (synectin), which is the only known molecule to bind to the cytoplasmic domain of NRP1, contributes to VEGF164-induced vascular leakage *in vivo*. Prior studies have shown that NRP1 promotes VEGF-164 induces VEGFR2 trafficking via GIPC1 binding to NRP1 cytoplasmic domain, and that this process promotes arteriogenic ERK1/2 signalling (Lanahan et

al., 2013a). Whereas the NRP1 cytoplasmic domain is important for both arteriogenesis and vascular permeability, he showed that GIPC1 is dispensable for VEGF164-induced vascular leakage, because mice lacking GIPC1 (Chittenden et al., 2006) showed a similar response to VEGF164 compared to controls in the Miles assay. Therefore, GIPC1 is required for normal arteriogenesis, but not for VEGF164-induced vascular hyperpermeability *in vivo*. As hyperpermeability occurs in capillaries and veins, it is conceivable that GIPC1 is not important in the ECs from these types of vessels, but mediates VEGF signalling mainly in arteries for reasons that are not yet understood.

Dr Fantin showed a residual vascular permeability response in the Miles assay with mice lacking endothelial NRP1, VEGF164-binding to NRP1 or the NCD. Thus, a low level of VEGFR2-mediated permeability signalling, independently of NRP1, may explain this residual response. A possibility to explain these observations may be that the NRP1-independent pathway can utilise the ABL1 homolog ABL2 for SFK activation. In agreement with this idea, ABL2 can be activated by VEGF165 in HUVEC lacking ABL1 expression (Chislock and Pendergast, 2013, Aman et al., 2012). Moreover, it has been shown that ABL2 partially compensates for ABL1 in VEGF164-induced vascular leakage in the Miles assay (Chislock and Pendergast, 2013). Supporting the idea that ABL2 can help convey VEGF164-induced VEGFR2-mediated signals, I show here that ABL1 knockdown or NRP1 does not completely abolish pCRKL induction, whereas the pharmacological VEGFR2 blockade with PTK/ZK or dual ABL1/ABL2 blockade with Imatinib or the double knockdown of ABL1/ABL2 abrogated both pCRKL and pSFK induction in response to VEGF165 *in vitro*. In agreement with the *in vitro* data, Imatinib treatment or the genetic deletion of ABL kinases (*Abl1*^{ECKO}; *Arg*^{+/-}) showed decreased VEGF-induced vascular leakage compared to controls in Miles assays (Chislock and Pendergast, 2013, Aman et al., 2012). It remains to be investigated how ABL2, which remains active in VEGF165-stimulated ECs after NRP1 knockdown, but not VEGFR2 inhibition, might be recruited to VEGFR2 during the permeability response.

Together, my *in vitro* data and Dr Fantin's *in vivo* data show that VEGF164-induced vascular leakage relies on both VEGFR2 and NRP1, because of an absolute requirement for VEGFR2 and a strong dependency on NRP1 to induce the activation

of two essential intracellular signal transducers for the endothelial permeability response. Moreover, my data show that SFK activation is ABL1 dependent and thereby place these effectors in a regulatory hierarchy.

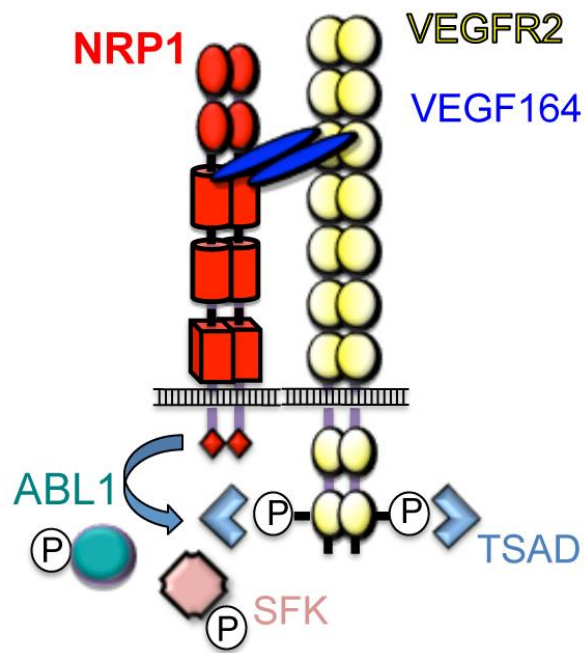


Figure 33: Schematic representation of NRP1 role in permeability.

NRP1 may use its NCD to help deliver ABL1 to VEGFR2 upon VEGF164 stimulation and the formation of a complex between NRP1 and VEGFR2. NRP1-bound ABL1 then promotes the phosphorylation of SFKs that are recruited to VEGFR2 via the adaptor protein SH2D2A/TSAd.

Chapter 6 Final Conclusions and Future work

6.1 Summary of Conclusions and Final Remarks

My aims have been to understand the role of NRP1 in angiogenesis versus vascular permeability and to investigate possible links of NRP1 with transcription networks in ECs that can affect angiogenesis and vascular homeostasis (**Fig. 34**).

It is known that the therapeutic induction of blood vessel growth by delivery of the vascular growth factor VEGF-A has the potential to alleviate tissue ischemia, but VEGF additionally increases pathological vascular hyperpermeability and therefore causes tissue-damaging oedema. A poor understanding of the molecular mechanisms that distinguish VEGF-mediated permeability from other VEGF responses has hampered the design of therapies that selectively promote VEGF-induced vessel growth or inhibit VEGF-induced vessel leak. I found that NRP1-mediated VEGF signalling pathways in blood vessel growth and hyperpermeability, have a distinct requirement for the NRP1 cytoplasmic domain (NCD), raising the possibility that these two VEGF-mediated processes might be inhibited or promoted independently of each other to help treat diseases with blood vessel dysfunction. In particular, my *in vitro* results combined with the *in vivo* data from Dr Fantin (Fantin et al., 2017) showed that loss of NCD reduces vascular permeability, but not angiogenesis. Thus, NCD may be a suitable target to inhibit vascular hyperpermeability without disrupting beneficial angiogenesis.

At the time of starting my PhD research, it was not known the molecular mechanism by which the VEGF receptor NRP1 regulates blood vessel growth independently of VEGF and VEGFR2. My PhD research has contributed to two studies that identified the molecular mechanism by which NRP1 enables endothelial cell shape changes to promote blood vessel growth. In particular, I showed that NRP1 controls actin remodelling and cell motility independently of VEGFR2 via the ECM-induced ABL1 kinase and CDC42 activation. This was an important finding for the vascular field, as NRP1 previously was mainly thought to act as a VEGFR2 co-receptor to enhance the signalling downstream of the VEGFR2 (Soker et al., 2002b). I have also contributed to a third study showing that NRP1 is an essential component of the

machinery that promotes pathological vascular hyperpermeability. Using cell culture models, I demonstrated that NRP1 has a significant role in VEGF-induced vascular permeability, with VEGFR2 absolutely required for this function and NRP1 required for a robust response. Despite a few controversial studies in the past (Acevedo et al., 2008, Cerani et al., 2013) my findings finally provide a solid demonstration of NRP1 role in VEGF-induced vascular leakage as well as new insights into the underlying molecular mechanism.

My PhD work also provide strong evidence about the role of NRP1 in the regulation of transcription networks. I showed that NRP1 modulates ECs gene transcription during angiogenesis and under normal growth conditions. In particular NRP1 controls the activity of transcription regulators such as pERK1/2, the expression of the SRF and MRTFA transcription factors and target genes that promote vessel growth and maintain vascular health. My future work will therefore further investigate if NRP1 balances gene expression programmes for distinct ECs behaviours.

Altogether, my work investigating NRP1 signalling has so far contributed to three peer-reviewed primary research paper [(Raimondi et al., 2014, Fantin et al., 2015, Fantin et al., 2017)], one peer-reviewed review article (Lampropoulou and Ruhrberg, 2014) and a book chapter (Brash et al., 2017) (see Appendix – co-authored publications). Furthermore, a manuscript outlining my findings regarding the role of NRP1 in regulating gene transcription programmes for blood vessel growth and vascular homeostasis is in preparation.

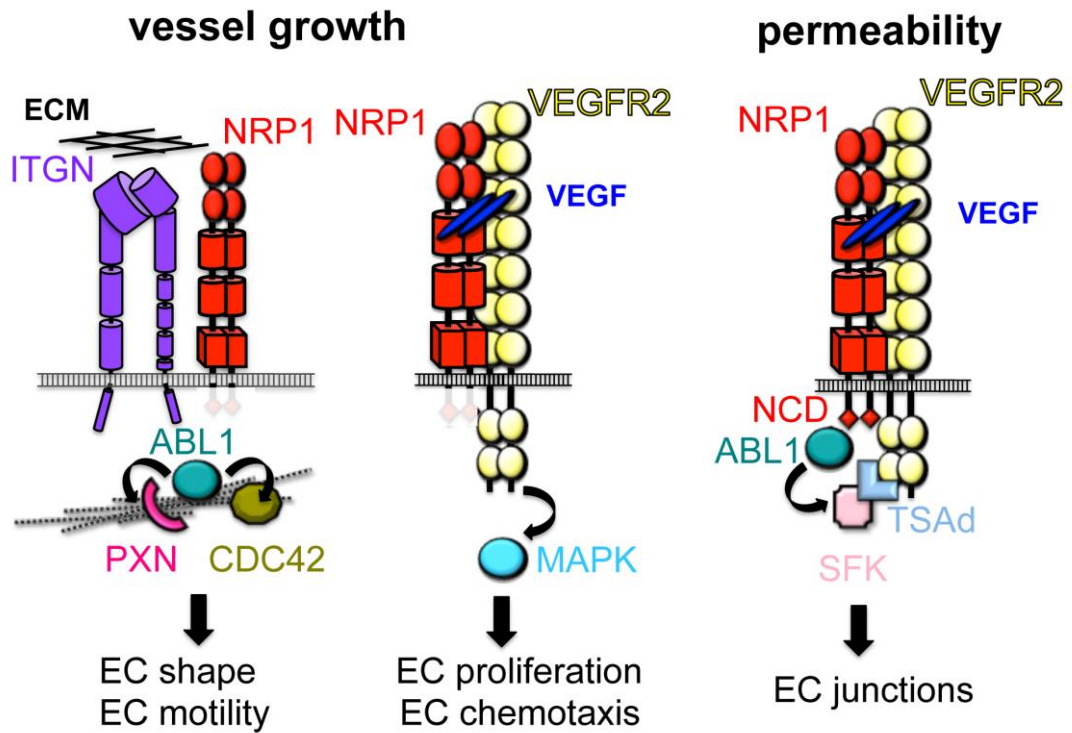


Figure 34: Schematic representation of NRP1 roles in vessel growth and permeability.

NRP1 enables ECM-dependent ABL1 and CDC42 activation in addition to its role as a VEGFR2 co-receptor to promote MAPK signalling. NRP1 uses its NCD to mediate ABL1-dependent SFK phosphorylation in response to VEGF.

6.2 Future work

6.2.1 Identify the specific integrins that interact with NRP1 in ECs and define their function in angiogenesis.

In Chapter 3, I showed that NRP1 promotes actin remodelling in response to ECM stimulus via ABL1 kinase activation and paxillin phosphorylation. However, I have not demonstrated which integrin interacts with NRP1 in ECs to promote angiogenesis. The finding that NRP1 promotes matrix signalling to enhance angiogenesis agrees with prior observations that NRP1 interacts with $\alpha 5\beta 1$ integrin (Fukasawa et al., 2007, Valdembri et al., 2009). Thus, the $\alpha 5\beta 1$ integrin together with another known endothelial FN receptor, $\alpha v\beta 3$, (Dejana et al., 1990), are possible candidate NRP1 interactors in matrix induces angiogenesis. To test this idea, I would perform co-immunoprecipitation (co-IP) experiments in control HDMEC to define the interaction with either of the two integrins with NRP1, and whether it depends on FN or not. Then, in order to confirm that NRP1 and the identified integrin are required for ABL1-mediated PXN phosphorylation, I would perform co-IPs between the integrin, ABL1 and PXN in ECs transfected with control siRNA or si-NRP1 in response to ECM stimulus. I would also need to test how NRP1 modulates integrins function by investigating changes in the activation state of the integrin. For example, I will use available antibodies for the identified integrin, such as HUTS21 antibody to detect the activated form of ITGB1 in ECs lacking NRP1 compared to control ECs upon FN stimulation. I could also investigate the effect of NRP1 loss in integrin activation with immunostaining *in vivo* using as a model to study angiogenesis the postnatal retina of mice lacking endothelial NRP1 compared to wildtype. Finally, I could examine whether NRP1 controls integrin activity by modulating their transcription.

6.2.2 Determine if NRP1 regulates RAC and RHOA RHO-GTPase activation and function in angiogenic ECs.

My data show that NRP1 promotes CDC42 activation and filopodia formation in ECs. ECs lacking NRP1 expression also showed impaired stress fibres formation, increased cortical actin and defects in cell motility, suggesting that other RHO

GTPases may also be regulated by NRP1. Prior studies have shown that RAC and RHOA are responsible for lamellipodia and stress fibres formation, respectively (Etienne-Manneville and Hall, 2002) and are involved in EC migration and angiogenesis (Fryer and Field, 2005). Thus, further work is required to test whether NRP1 controls RAC and RHOA activity downstream of ECM and/or VEGF, for example in HDMEC transfected with control siRNA or siNRP1. To extend results to ECs from other species and use an alternative method of inactivating NRP1, I could also treat primary mouse ECs, such as MLECs, with a function blocking antibody for NRP1 that the lab has previously validated for neural studies (Cariboni et al., 2011, Erskine et al., 2011). Alternatively, I could use MLECs from genetically modified mice lacking endothelial NRP1. To identify functional roles for NRP1-regulated GTPases in VEGF- and FN-induced actin remodelling in ECs, I would use small molecule inhibitors and siRNAs for these GTPases as I have done for CDC42; thus, I could treat ECs with inhibitors versus vehicle and then label ECs with immunofluorescence for focal adhesion proteins and actin, followed by analysis of lamellipodia and stress fibre formation and cell migration.

6.2.3 Examine whether NRP1 regulates different set of genes in angiogenesis and in vascular homeostasis

My results obtained from the qPCR array and the *in vitro* experiments using ECs during angiogenesis or under normal growth condition respectively, showed that NRP1 regulates transcription of various different genes. Thus, RNA sequencing of HDMEC transfected with control siRNA or siNRP1 and of BECs from mice expressing or lacking endothelial NRP1 would help to define the different gene categories that are regulated by NRP1. Thus, I would examine if more SRF target genes are regulated by NRP1, based on knowledge from other cell types (but I would also investigate changes in the expression of genes regulated by different transcription factors). To understand whether identified SRF target genes are regulated by TCF vs. MRTFA factors and therefore in response to ERK1/2 vs. RHOA activation, I would use specific inhibitors that block ERK1/2 or RHOA activity. I should also investigate pathways that may regulate SRF and MRTFA expression levels, that have been shown to be affected by NRP1 loss such as p38 (Raimondi et al., 2014). Then, I would validate my results by investigating the

importance of NRP1-dependent transcription regulation for the maintenance of vascular homeostasis using the adult aorta or retina as models. For example, I could investigate the expression pattern of the identified genes at protein level by immunostaining aortas of adult mice lacking endothelial NRP1 compared to wildtype.

6.2.4 NRP1 signalling downstream of SFK activation in response to VEGF

I showed that NRP1 is required for FAK and SFK activation in response to VEGF, whereas other studies have shown that FAK or SFK activation can induce phosphorylation of VE-cadherin, and that this leads to dissociation of VE-cadherin/ β -catenin complex and disruption of adherens junctions (Jean et al., 2014, Esser et al., 1998, Wallez et al., 2007). Thus, I would next investigate whether NRP1 regulates VE-cadherin phosphorylation and whether its loss disrupts EC junctions. For these experiments, I would use HDMEC and BEC, which have been shown by us and others to be good models to study permeability signalling *in vitro*. Immunoblotting and immunofluorescence would be used to test phosphorylation of VE-cadherin in ECs transfected with control siRNA or siNRP1, and staining of ECs with markers for adherens or tight junction such as Claudin 5 and ZO-1 would reveal junctional defects. MLECs isolated from *Nrp1*^{cyto/cyto} mice would also be used for these experiments to understand whether the NCD is required for VE-cadherin phosphorylation and the stability of the VE-cadherin/ β -catenin complex.

My experiments showed that ABL1 is upstream of SFK activation, but still I need to examine whether FAK activity is upstream or downstream of ABL and SFK in ECs. I would test this by using specific inhibitors for FAK and ABL or using siRNA in ECs. Also, the identification of good ABL antibodies would help me to validate the complex formation between those molecules and to define specific phosphorylation sites that are affected in response to VEGF in a NRP1-dependent manner.

6.2.5 Investigate the role of ABL2 in VEGF-induced vascular permeability

My *in vitro* experiments showed that Imatinib and siABL1 both reduced pSFK induction, except that the effect of Imatinib was stronger. This finding suggested that

ABL2 might also play a role in SFK induction. In agreement with this idea, the double knockdown of ABL1 and ABL2 reduced pSFK more than the single knockdown and similar to Imatinib. Future work is therefore required to examine the role of ABL2 in VEGF-induced permeability *in vivo* using Miles assay to test vascular leakage in mice lacking endothelial ABL1, ABL2 or both.

BIBLIOGRAPHY

- ABASSI, Y. A. & VUORI, K. 2002. Tyrosine 221 in Crk regulates adhesion-dependent membrane localization of Crk and Rac and activation of Rac signaling. *EMBO J*, 21, 4571-82.
- ABRAHAM, S., SCARCIA, M., BAGSHAW, R. D., MCMAHON, K., GRANT, G., HARVEY, T., YEO, M., ESTEVES, F. O., THYGESEN, H. H., JONES, P. F., SPEIRS, V., HANBY, A. M., SELBY, P. J., LORGER, M., DEAR, T. N., PAWSON, T., MARSHALL, C. J. & MAVRIA, G. 2015. A Rac/Cdc42 exchange factor complex promotes formation of lateral filopodia and blood vessel lumen morphogenesis. *Nat Commun*, 6, 7286.
- ABU-GHAZALEH, R., KABIR, J., JIA, H., LOBO, M. & ZACHARY, I. 2001. Src mediates stimulation by vascular endothelial growth factor of the phosphorylation of focal adhesion kinase at tyrosine 861, and migration and anti-apoptosis in endothelial cells. *Biochem J*, 360, 255-64.
- ACEVEDO, L. M., BARILLAS, S., WEIS, S. M., GOTHERT, J. R. & CHERESH, D. A. 2008. Semaphorin 3A suppresses VEGF-mediated angiogenesis yet acts as a vascular permeability factor. *Blood*, 111, 2674-80.
- AITKENHEAD, M., WANG, S. J., NAKATSU, M. N., MESTAS, J., HEARD, C. & HUGHES, C. C. 2002. Identification of endothelial cell genes expressed in an in vitro model of angiogenesis: induction of ESM-1, (beta)ig-h3, and NrCAM. *Microvasc Res*, 63, 159-71.
- ALON, R., FEIGELSON, S. W., MANEVICH, E., ROSE, D. M., SCHMITZ, J., OVERBY, D. R., WINTER, E., GRABOVSKY, V., SHINDER, V., MATTHEWS, B. D., SOKOLOVSKY-EISENBERG, M., INGBER, D. E., BENOIT, M. & GINSBERG, M. H. 2005. Alpha4beta1-dependent adhesion strengthening under mechanical strain is regulated by paxillin association with the alpha4-cytoplasmic domain. *J Cell Biol*, 171, 1073-84.
- AMAN, J., VAN BEZU, J., DAMANAFSHAN, A., HUVENEERS, S., ERINGA, E. C., VOGEL, S. M., GROENEVELD, A. B., VONK NOORDEGRAAF, A., VAN HINSBERGH, V. W. & VAN NIEUW AMERONGEN, G. P. 2012. Effective treatment of edema and endothelial barrier dysfunction with imatinib. *Circulation*, 126, 2728-38.
- AMIN, D. N., HIDA, K., BIELENBERG, D. R. & KLAGSBRUN, M. 2006. Tumor endothelial cells express epidermal growth factor receptor (EGFR) but not ErbB3 and are responsive to EGF and to EGFR kinase inhibitors. *Cancer Res*, 66, 2173-80.
- ANSEMI, F., ORLANDINI, M., ROCCHIGIANI, M., DE CLEMENTE, C., SALAMEH, A., LENTUCCI, C., OLIVIERO, S. & GALVAGNI, F. 2012. c-ABL modulates MAP kinases activation downstream of VEGFR-2 signaling by direct phosphorylation of the adaptor proteins GRB2 and NCK1. *Angiogenesis*, 15, 187-97.
- APARICIO, S., SAWANT, S., LARA, N., BARNSTABLE, C. J. & TOMBRANTINK, J. 2005. Expression of angiogenesis factors in human umbilical vein endothelial cells and their regulation by PEDF. *Biochem Biophys Res Commun*, 326, 387-94.
- AQUINO, J. B., HJERLING-LEFFLER, J., KOLTZENBURG, M., EDLUND, T., VILLAR, M. J. & ERNFORS, P. 2006. In vitro and in vivo differentiation of boundary cap neural crest stem cells into mature Schwann cells. *Exp Neurol*, 198, 438-49.

- ARAI, M., ALPERT, N. R., MACLENNAN, D. H., BARTON, P. & PERIASAMY, M. 1993. Alterations in sarcoplasmic reticulum gene expression in human heart failure. A possible mechanism for alterations in systolic and diastolic properties of the failing myocardium. *Circ Res*, 72, 463-9.
- ARGENTIN, S., ARDATI, A., TREMBLAY, S., LIHRMANN, I., ROBITAILLE, L., DROUIN, J. & NEMER, M. 1994. Developmental stage-specific regulation of atrial natriuretic factor gene transcription in cardiac cells. *Mol Cell Biol*, 14, 777-90.
- ARIAS-SALGADO, E. G., LIZANO, S., SARKAR, S., BRUGGE, J. S., GINSBERG, M. H. & SHATTIL, S. J. 2003. Src kinase activation by direct interaction with the integrin beta cytoplasmic domain. *Proc Natl Acad Sci U S A*, 100, 13298-302.
- ARNAOUT, M. A., GOODMAN, S. L. & XIONG, J. P. 2007. Structure and mechanics of integrin-based cell adhesion. *Curr Opin Cell Biol*, 19, 495-507.
- ARNAOUT, M. A., MAHALINGAM, B. & XIONG, J. P. 2005. Integrin structure, allostery, and bidirectional signaling. *Annu Rev Cell Dev Biol*, 21, 381-410.
- ARSENIAN, S., WEINHOLD, B., OELGESCHLAGER, M., RUTHER, U. & NORDHEIM, A. 1998. Serum response factor is essential for mesoderm formation during mouse embryogenesis. *EMBO J*, 17, 6289-99.
- ASPALTER, I. M., GORDON, E., DUBRAC, A., RAGAB, A., NARLOCH, J., VIZAN, P., GEUDENS, I., COLLINS, R. T., FRANCO, C. A., ABRAHAMS, C. L., THURSTON, G., FRUTTIGER, M., ROSEWELL, I., EICHMANN, A. & GERHARDT, H. 2015. Alk1 and Alk5 inhibition by Nrp1 controls vascular sprouting downstream of Notch. *Nat Commun*, 6, 7264.
- BACH, L. A. 2015. Endothelial cells and the IGF system. *J Mol Endocrinol*, 54, R1-13.
- BALLMER-HOFER, K., ANDERSSON, A. E., RATCLIFFE, L. E. & BERGER, P. 2011. Neuropilin-1 promotes VEGFR-2 trafficking through Rab11 vesicles thereby specifying signal output. *Blood*, 118, 816-26.
- BARRY, D. M., XU, K., MEADOWS, S. M., ZHENG, Y., NORDEN, P. R., DAVIS, G. E. & CLEAVER, O. 2015. Cdc42 is required for cytoskeletal support of endothelial cell adhesion during blood vessel formation in mice. *Development*, 142, 3058-70.
- BARUZZI, A., IACOBUCCI, I., SOVERINI, S., LOWELL, C. A., MARTINELLI, G. & BERTON, G. 2010. c-Abl and Src-family kinases cross-talk in regulation of myeloid cell migration. *FEBS Lett*, 584, 15-21.
- BATES, D. O. & HARPER, S. J. 2002. Regulation of vascular permeability by vascular endothelial growth factors. *Vascul Pharmacol*, 39, 225-37.
- BECKER, P. M., WALTENBERGER, J., YACHECHKO, R., MIRZAPOIAZOVA, T., SHAM, J. S., LEE, C. G., ELIAS, J. A. & VERIN, A. D. 2005. Neuropilin-1 regulates vascular endothelial growth factor-mediated endothelial permeability. *Circ Res*, 96, 1257-65.
- BELAGULI, N. S., SCHILDMEYER, L. A. & SCHWARTZ, R. J. 1997. Organization and myogenic restricted expression of the murine serum response factor gene. A role for autoregulation. *J Biol Chem*, 272, 18222-31.
- BELL, R. D., DEANE, R., CHOW, N., LONG, X., SAGARE, A., SINGH, I., STREB, J. W., GUO, H., RUBIO, A., VAN NOSTRAND, W., MIANO, J. M. & ZLOKOVIC, B. V. 2009. SRF and myocardin regulate LRP-mediated amyloid-beta clearance in brain vascular cells. *Nat Cell Biol*, 11, 143-53.

- BELLON, A., LUCHINO, J., HAIGH, K., ROUGON, G., HAIGH, J., CHAUVET, S. & MANN, F. 2010. VEGFR2 (KDR/Flk1) signaling mediates axon growth in response to semaphorin 3E in the developing brain. *Neuron*, 66, 205-19.
- BENARD, V., BOHL, B. P. & BOKOCH, G. M. 1999. Characterization of rac and cdc42 activation in chemoattractant-stimulated human neutrophils using a novel assay for active GTPases. *The Journal of Biological Chemistry*, 274, 13198-204.
- BOUVREE, K., BRUNET, I., DEL TORO, R., GORDON, E., PRAHST, C., CRISTOFARO, B., MATHIVET, T., XU, Y., SOUEID, J., FORTUNA, V., MIURA, N., AIGROT, M. S., MADEN, C. H., RUHRBERG, C., THOMAS, J. L. & EICHMANN, A. 2012. Semaphorin3A, Neuropilin-1, and PlexinA1 are required for lymphatic valve formation. *Circulation research*, 111, 437-45.
- BOYD, P. J., DOYLE, J., GEE, E., PALLAN, S. & HAAS, T. L. 2005. MAPK signaling regulates endothelial cell assembly into networks and expression of MT1-MMP and MMP-2. *Am J Physiol Cell Physiol*, 288, C659-68.
- BRADLEY, W. D. & KOLESKE, A. J. 2009. Regulation of cell migration and morphogenesis by Abl-family kinases: emerging mechanisms and physiological contexts. *J Cell Sci*, 122, 3441-54.
- BROOKS, P. C., CLARK, R. A. & CHERESH, D. A. 1994. Requirement of vascular integrin alpha v beta 3 for angiogenesis. *Science*, 264, 569-71.
- BUCHDUNGER, E., O'REILLY, T. & WOOD, J. 2002. Pharmacology of imatinib (STI571). *European journal of cancer*, 38 Suppl 5, S28-36.
- BUCHDUNGER, E., ZIMMERMANN, J., METT, H., MEYER, T., MULLER, M., DRUKER, B. J. & LYDON, N. B. 1996. Inhibition of the Abl protein-tyrosine kinase in vitro and in vivo by a 2-phenylaminopyrimidine derivative. *Cancer Res*, 56, 100-4.
- BUCHWALTER, G., GROSS, C. & WASYLYK, B. 2004. Ets ternary complex transcription factors. *Gene*, 324, 1-14.
- CALDERWOOD, D. A., FUJIOKA, Y., DE PEREDA, J. M., GARCIA-ALVAREZ, B., NAKAMOTO, T., MARGOLIS, B., MCGLADE, C. J., LIDDINGTON, R. C. & GINSBERG, M. H. 2003. Integrin beta cytoplasmic domain interactions with phosphotyrosine-binding domains: a structural prototype for diversity in integrin signaling. *Proc Natl Acad Sci U S A*, 100, 2272-7.
- CARIBONI, A., ANDRE, V., CHAUVET, S., CASSATELLA, D., DAVIDSON, K., CARMELLO, A., FANTIN, A., BOULOUX, P., MANN, F. & RUHRBERG, C. 2015. Dysfunctional SEMA3E signaling underlies gonadotropin-releasing hormone neuron deficiency in Kallmann syndrome. *J Clin Invest*, 125, 2413-28.
- CARIBONI, A., DAVIDSON, K., DOZIO, E., MEMI, F., SCHWARZ, Q., STOSI, F., PARNAVELAS, J. G. & RUHRBERG, C. 2011. VEGF signalling controls GnRH neuron survival via NRP1 independently of KDR and blood vessels. *Development*, 138, 3723-33.
- CARMELIET, P. & JAIN, R. K. 2011. Molecular mechanisms and clinical applications of angiogenesis. *Nature*, 473, 298-307.
- CARMELIET, P., LAMPUGNANI, M. G., MOONS, L., BREVIARIO, F., COMPERNOLLE, V., BONO, F., BALCONI, G., SPAGNUOLO, R., OOSTUYSE, B., DEWERCHIN, M., ZANETTI, A., ANGELLILO, A., MATTOT, V., NUYENS, D., LUTGENS, E., CLOTMAN, F., DE RUITER, M. C., GITTENBERGER-DE GROOT, A., POELMANN, R., LUPU, F.,

- HERBERT, J. M., COLLEN, D. & DEJANA, E. 1999. Targeted deficiency or cytosolic truncation of the VE-cadherin gene in mice impairs VEGF-mediated endothelial survival and angiogenesis. *Cell*, 98, 147-57.
- CARRER, A., MOIMAS, S., ZACCHIGNA, S., PATTARINI, L., ZENTILIN, L., RUOZI, G., MANO, M., SINIGAGLIA, M., MAIONE, F., SERINI, G., GIRAUDO, E., BUSSOLINO, F. & GIACCA, M. 2012. Neuropilin-1 identifies a subset of bone marrow Gr1- monocytes that can induce tumor vessel normalization and inhibit tumor growth. *Cancer Research*, 72, 6371-81.
- CASAZZA, A., FU, X., JOHANSSON, I., CAPPARUCCIA, L., ANDERSSON, F., GIUSTACCHINI, A., SQUADRITO, M. L., VENNERI, M. A., MAZZONE, M., LARSSON, E., CARMELIET, P., DE PALMA, M., NALDINI, L., TAMAGNONE, L. & ROLNY, C. 2011. Systemic and targeted delivery of semaphorin 3A inhibits tumor angiogenesis and progression in mouse tumor models. *Arteriosclerosis, thrombosis, and vascular biology*, 31, 741-9.
- CASTELLANI, V., DE ANGELIS, E., KENWRICK, S. & ROUGON, G. 2002. Cis and trans interactions of L1 with neuropilin-1 control axonal responses to semaphorin 3A. *Embo J*, 21, 6348-57.
- CERANI, A., TETREAU, N., MENARD, C., LAPALME, E., PATEL, C., SITARAS, N., BEAUDOIN, F., LEBOEUF, D., DE GUIRE, V., BINET, F., DEJDA, A., REZENDE, F. A., MILOUDI, K. & SAPIEHA, P. 2013. Neuron-derived semaphorin 3A is an early inducer of vascular permeability in diabetic retinopathy via neuropilin-1. *Cell Metabolism*, 18, 505-18.
- CHAI, J., JONES, M. K. & TARNAWSKI, A. S. 2004. Serum response factor is a critical requirement for VEGF signaling in endothelial cells and VEGF-induced angiogenesis. *FASEB J*, 18, 1264-6.
- CHEN, F., MA, L., PARRINI, M. C., MAO, X., LOPEZ, M., WU, C., MARKS, P. W., DAVIDSON, L., KWIATKOWSKI, D. J., KIRCHHAUSEN, T., ORKIN, S. H., ROSEN, F. S., MAYER, B. J., KIRSCHNER, M. W. & ALT, F. W. 2000. Cdc42 is required for PIP(2)-induced actin polymerization and early development but not for cell viability. *Current Biology*, 10, 758-65.
- CHEN, X. L., NAM, J. O., JEAN, C., LAWSON, C., WALSH, C. T., GOKA, E., LIM, S. T., TOMAR, A., TANCIONI, I., URYU, S., GUAN, J. L., ACEVEDO, L. M., WEIS, S. M., CHERESH, D. A. & SCHLAEPFER, D. D. 2012. VEGF-induced vascular permeability is mediated by FAK. *Dev Cell*, 22, 146-57.
- CHIEN, R. 1992. Signaling mechanisms for the activation of an embryonic gene program during the hypertrophy of cardiac ventricular muscle. *Basic Res Cardiol*, 87 Suppl 2, 49-58.
- CHISLOCK, E. M. & PENDERGAST, A. M. 2013. Abl family kinases regulate endothelial barrier function in vitro and in mice. *PLoS One*, 8, e85231.
- CHITTENDEN, T. W., CLAES, F., LANAHAN, A. A., AUTIERO, M., PALAC, R. T., TKACHENKO, E. V., ELFENBEIN, A., RUIZ DE ALMODOVAR, C., DEDKOV, E., TOMANEK, R., LI, W., WESTMORE, M., SINGH, J. P., HOROWITZ, A., MULLIGAN-KEHOE, M. J., MOODIE, K. L., ZHUANG, Z. W., CARMELIET, P. & SIMONS, M. 2006. Selective regulation of arterial branching morphogenesis by syndectin. *Dev Cell*, 10, 783-95.
- CHUNG, A. S. & FERRARA, N. 2011. Developmental and pathological angiogenesis. *Annual review of cell and developmental biology*, 27, 563-84.

- CLAESSON-WELSH, L. 2015. Vascular permeability--the essentials. *Ups J Med Sci*, 120, 135-43.
- COLUCCI, W. S. 1997. Molecular and cellular mechanisms of myocardial failure. *Am J Cardiol*, 80, 15L-25L.
- COOPER, S. J., TRINKLEIN, N. D., NGUYEN, L. & MYERS, R. M. 2007. Serum response factor binding sites differ in three human cell types. *Genome Res*, 17, 136-44.
- CORADA, M., ORSENIGO, F., MORINI, M. F., PITULESCU, M. E., BHAT, G., NYQVIST, D., BREVIARIO, F., CONTI, V., BRIOT, A., IRUELA-ARISPE, M. L., ADAMS, R. H. & DEJANA, E. 2013. Sox17 is indispensable for acquisition and maintenance of arterial identity. *Nat Commun*, 4, 2609.
- CUI, L., CHEN, C., XU, T., ZHANG, J., SHANG, X., LUO, J., CHEN, L., BA, X. & ZENG, X. 2009. c-Abl kinase is required for beta 2 integrin-mediated neutrophil adhesion. *J Immunol*, 182, 3233-42.
- CUJEC, T. P., MEDEIROS, P. F., HAMMOND, P., RISE, C. & KREIDER, B. L. 2002. Selection of v-abl tyrosine kinase substrate sequences from randomized peptide and cellular proteomic libraries using mRNA display. *Chemistry & biology*, 9, 253-64.
- DANIELIAN, P. S., MUCCINO, D., ROWITCH, D. H., MICHAEL, S. K. & MCMAHON, A. P. 1998. Modification of gene activity in mouse embryos in utero by a tamoxifen-inducible form of Cre recombinase. *Curr Biol*, 8, 1323-6.
- DAVIS, M. I., HUNT, J. P., HERRGARD, S., CICERI, P., WODICKA, L. M., PALLARES, G., HOCKER, M., TREIBER, D. K. & ZARRINKAR, P. P. 2011. Comprehensive analysis of kinase inhibitor selectivity. *Nat Biotechnol*, 29, 1046-51.
- DE SMET, F., SEGURA, I., DE BOCK, K., HOHENSINNER, P. J. & CARMELIET, P. 2009. Mechanisms of vessel branching: filopodia on endothelial tip cells lead the way. *Arterioscler Thromb Vasc Biol*, 29, 639-49.
- DE VIRGILIO, M., KIOSSES, W. B. & SHATTIL, S. J. 2004. Proximal, selective, and dynamic interactions between integrin alphaIIb beta3 and protein tyrosine kinases in living cells. *J Cell Biol*, 165, 305-11.
- DEININGER, M., BUCHDUNGER, E. & DRUKER, B. J. 2005. The development of imatinib as a therapeutic agent for chronic myeloid leukemia. *Blood*, 105, 2640-53.
- DEJANA, E. 2004. Endothelial cell-cell junctions: happy together. *Nat Rev Mol Cell Biol*, 5, 261-70.
- DEJANA, E., LAMPUGNANI, M. G., GIORGI, M., GABOLI, M. & MARCHISIO, P. C. 1990. Fibrinogen induces endothelial cell adhesion and spreading via the release of endogenous matrix proteins and the recruitment of more than one integrin receptor. *Blood*, 75, 1509-17.
- DEJANA, E., ORSENIGO, F. & LAMPUGNANI, M. G. 2008. The role of adherens junctions and VE-cadherin in the control of vascular permeability. *Journal of cell science*, 121, 2115-22.
- DIAZ, B., SHANI, G., PASS, I., ANDERSON, D., QUINTAVALLE, M. & COURTNEIDGE, S. A. 2009. Tks5-dependent, nox-mediated generation of reactive oxygen species is necessary for invadopodia formation. *Sci Signal*, 2, ra53.

- DRUKER, B. J., TAMURA, S., BUCHDUNGER, E., OHNO, S., SEGAL, G. M., FANNING, S., ZIMMERMANN, J. & LYDON, N. B. 1996. Effects of a selective inhibitor of the Abl tyrosine kinase on the growth of Bcr-Abl positive cells. *Nature medicine*, 2, 561-6.
- DU, K. L., CHEN, M., LI, J., LEPORE, J. J., MERICKO, P. & PARMACEK, M. S. 2004. Megakaryoblastic leukemia factor-1 transduces cytoskeletal signals and induces smooth muscle cell differentiation from undifferentiated embryonic stem cells. *The Journal of biological chemistry*, 279, 17578-86.
- DURAND, J. B. 1999. Genetic basis of cardiomyopathy. *Curr Opin Cardiol*, 14, 225-9.
- DVORAK, A. M., KOHN, S., MORGAN, E. S., FOX, P., NAGY, J. A. & DVORAK, H. F. 1996. The vesiculo-vacuolar organelle (VVO): a distinct endothelial cell structure that provides a transcellular pathway for macromolecular extravasation. *J Leukoc Biol*, 59, 100-15.
- ELICEIRI, B. P., PAUL, R., SCHWARTZBERG, P. L., HOOD, J. D., LENG, J. & CHERESH, D. A. 1999. Selective requirement for Src kinases during VEGF-induced angiogenesis and vascular permeability. *Mol Cell*, 4, 915-24.
- ELICEIRI, B. P., PUENTE, X. S., HOOD, J. D., STUPACK, D. G., SCHLAEPFER, D. D., HUANG, X. Z., SHEPPARD, D. & CHERESH, D. A. 2002. Src-mediated coupling of focal adhesion kinase to integrin alpha(v)beta5 in vascular endothelial growth factor signaling. *J Cell Biol*, 157, 149-60.
- ERSKINE, L., REIJNTJES, S., PRATT, T., DENTI, L., SCHWARZ, Q., VIEIRA, J. M., ALAKAKONE, B., SHEWAN, D. & RUHRBERG, C. 2011. VEGF signaling through neuropilin 1 guides commissural axon crossing at the optic chiasm. *Neuron*, 70, 951-65.
- ESNAULT, C., STEWART, A., GUALDRINI, F., EAST, P., HORSWELL, S., MATTHEWS, N. & TREISMAN, R. 2014. Rho-actin signaling to the MRTF coactivators dominates the immediate transcriptional response to serum in fibroblasts. *Genes Dev*, 28, 943-58.
- ESSER, S., LAMPUGNANI, M. G., CORADA, M., DEJANA, E. & RISAU, W. 1998. Vascular endothelial growth factor induces VE-cadherin tyrosine phosphorylation in endothelial cells. *J Cell Sci*, 111 (Pt 13), 1853-65.
- ETIENNE-MANNEVILLE, S. & HALL, A. 2002. Rho GTPases in cell biology. *Nature*, 420, 629-35.
- FANTIN, A., HERZOG, B., MAHMOUD, M., YAMAJI, M., PLEIN, A., DENTI, L., RUHRBERG, C. & ZACHARY, I. 2014. Neuropilin 1 (NRP1) hypomorphism combined with defective VEGF-A binding reveals novel roles for NRP1 in developmental and pathological angiogenesis. *Development*, 141, 556-62.
- FANTIN, A., LAMPROPOULOU, A., GESTRI, G., RAIMONDI, C., SENATORE, V., ZACHARY, I. & RUHRBERG, C. 2015. NRP1 Regulates CDC42 Activation to Promote Filopodia Formation in Endothelial Tip Cells. *Cell Rep*, 11, 1577-90.
- FANTIN, A., LAMPROPOULOU, A., SENATORE, V., BRASH, J. T., PRAHST, C., LANGE, C. A., LIYANAGE, S. E., RAIMONDI, C., BAINBRIDGE, J. W., AUGUSTIN, H. G. & RUHRBERG, C. 2017. VEGF165-induced vascular permeability requires NRP1 for ABL-mediated SRC family kinase activation. *J Exp Med*, 214, 1049-1064.
- FANTIN, A., SCHWARZ, Q., DAVIDSON, K., NORMANDO, E. M., DENTI, L. & RUHRBERG, C. 2011. The cytoplasmic domain of neuropilin 1 is

- dispensable for angiogenesis, but promotes the spatial separation of retinal arteries and veins. *Development*, 138, 4185-91.
- FANTIN, A., VIEIRA, J. M., GESTRI, G., DENTI, L., SCHWARZ, Q., PRYKHOZHII, S., PERI, F., WILSON, S. W. & RUHRBERG, C. 2010. Tissue macrophages act as cellular chaperones for vascular anastomosis downstream of VEGF-mediated endothelial tip cell induction. *Blood*, 116, 829-40.
- FANTIN, A., VIEIRA, J. M., PLEIN, A., DENTI, L., FRUTTIGER, M., POLLARD, J. W. & RUHRBERG, C. 2013a. NRP1 acts cell autonomously in endothelium to promote tip cell function during sprouting angiogenesis. *Blood*, 121, 2352-62.
- FANTIN, A., VIEIRA, J. M., PLEIN, A., MADEN, C. H. & RUHRBERG, C. 2013b. The embryonic mouse hindbrain as a qualitative and quantitative model for studying the molecular and cellular mechanisms of angiogenesis. *Nature Protocols*, 8, 418-29.
- FELLER, S. M., KNUDSEN, B. & HANAFUSA, H. 1994. c-Abl kinase regulates the protein binding activity of c-Crk. *EMBO J*, 13, 2341-51.
- FENG, D., NAGY, J. A., HIPPEL, J., DVORAK, H. F. & DVORAK, A. M. 1996. Vesiculo-vacuolar organelles and the regulation of venule permeability to macromolecules by vascular permeability factor, histamine, and serotonin. *J Exp Med*, 183, 1981-6.
- FENG, D., NAGY, J. A., PYNE, K., HAMMEL, I., DVORAK, H. F. & DVORAK, A. M. 1999. Pathways of macromolecular extravasation across microvascular endothelium in response to VPF/VEGF and other vasoactive mediators. *Microcirculation*, 6, 23-44.
- FERRUCCI, A., MOSCHETTA, M., FRASSANITO, M. A., BERARDI, S., CATAACCHIO, I., RIA, R., RACANELLI, V., CAIVANO, A., SOLIMANDO, A. G., VERGARA, D., MAFFIA, M., LATORRE, D., RIZZELLO, A., ZITO, A., DITONNO, P., MAIORANO, E., RIBATTI, D. & VACCA, A. 2014. A HGF/cMET autocrine loop is operative in multiple myeloma bone marrow endothelial cells and may represent a novel therapeutic target. *Clin Cancer Res*, 20, 5796-807.
- FRANCIS, S. E., GOH, K. L., HODIVALA-DILKE, K., BADER, B. L., STARK, M., DAVIDSON, D. & HYNES, R. O. 2002. Central roles of alpha5beta1 integrin and fibronectin in vascular development in mouse embryos and embryoid bodies. *Arterioscler Thromb Vasc Biol*, 22, 927-33.
- FRANCO, C. A., BLANC, J., PARLAKIAN, A., BLANCO, R., ASPALTER, I. M., KAZAKOVA, N., DIGUET, N., MYLONAS, E., GAO-LI, J., VAAHTOKARI, A., PENARD-LACRONIQUE, V., FRUTTIGER, M., ROSEWELL, I., MERICKSKAY, M., GERHARDT, H. & LI, Z. 2013. SRF selectively controls tip cell invasive behavior in angiogenesis. *Development*, 140, 2321-33.
- FRANCO, C. A. & LI, Z. 2009. SRF in angiogenesis: branching the vascular system. *Cell Adh Migr*, 3, 264-7.
- FRANCO, C. A., MERICKSKAY, M., PARLAKIAN, A., GARY-BOBO, G., GAO-LI, J., PAULIN, D., GUSTAFSSON, E. & LI, Z. 2008. Serum response factor is required for sprouting angiogenesis and vascular integrity. *Dev Cell*, 15, 448-61.

- FROKJAER-JENSEN, J. 1991. The endothelial vesicle system in cryofixed frog mesenteric capillaries analysed by ultrathin serial sectioning. *J Electron Microsc Tech*, 19, 291-304.
- FRUTTIGER, M. 2002. Development of the mouse retinal vasculature: angiogenesis versus vasculogenesis. *Invest Ophthalmol Vis Sci*, 43, 522-7.
- FRYER, B. H. & FIELD, J. 2005. Rho, Rac, Pak and angiogenesis: old roles and newly identified responsibilities in endothelial cells. *Cancer Lett*, 229, 13-23.
- FUKASAWA, M., MATSUSHITA, A. & KORC, M. 2007. Neuropilin-1 interacts with integrin beta1 and modulates pancreatic cancer cell growth, survival and invasion. *Cancer Biol Ther*, 6, 1173-80.
- FUKATA, M., NAKAGAWA, M. & KAIBUCHI, K. 2003. Roles of Rho-family GTPases in cell polarisation and directional migration. *Curr Opin Cell Biol*, 15, 590-7.
- FUKUMURA, D., GOHONGI, T., KADAMBI, A., IZUMI, Y., ANG, J., YUN, C. O., BUERK, D. G., HUANG, P. L. & JAIN, R. K. 2001. Predominant role of endothelial nitric oxide synthase in vascular endothelial growth factor-induced angiogenesis and vascular permeability. *Proc Natl Acad Sci U S A*, 98, 2604-9.
- FULTON, D., GRATTON, J. P., MCCABE, T. J., FONTANA, J., FUJIO, Y., WALSH, K., FRANKE, T. F., PAPAPETROPOULOS, A. & SESSA, W. C. 1999. Regulation of endothelium-derived nitric oxide production by the protein kinase Akt. *Nature*, 399, 597-601.
- FURSTOSS, O., DOREY, K., SIMON, V., BARILA, D., SUPERTI-FURGA, G. & ROCHE, S. 2002. c-Abl is an effector of Src for growth factor-induced c-myc expression and DNA synthesis. *EMBO J*, 21, 514-24.
- GAO, Y., DAVIES, S. P., AUGUSTIN, M., WOODWARD, A., PATEL, U. A., KOVELMAN, R. & HARVEY, K. J. 2013. A broad activity screen in support of a chemogenomic map for kinase signalling research and drug discovery. *Biochem J*, 451, 313-28.
- GARDNER, T. W., ANTONETTI, D. A., BARBER, A. J., LIETH, E. & TARBELL, J. A. 1999. The molecular structure and function of the inner blood-retinal barrier. Penn State Retina Research Group. *Doc Ophthalmol*, 97, 229-37.
- GELFAND, M. V., HAGAN, N., TATA, A., OH, W. J., LACOSTE, B., KANG, K. T., KOPYCINSKA, J., BISCHOFF, J., WANG, J. H. & GU, C. 2014. Neuropilin-1 functions as a VEGFR2 co-receptor to guide developmental angiogenesis independent of ligand binding. *Elife*, 3, e03720.
- GERHARDT, H., GOLDING, M., FRUTTIGER, M., RUHRBERG, C., LUNDKVIST, A., ABRAMSSON, A., JELTSCH, M., MITCHELL, C., ALITALO, K., SHIMA, D. & BETSHOLTZ, C. 2003. VEGF guides angiogenic sprouting utilizing endothelial tip cell filopodia. *The Journal of cell biology*, 161, 1163-77.
- GERHARDT, H., RUHRBERG, C., ABRAMSSON, A., FUJISAWA, H., SHIMA, D. & BETSHOLTZ, C. 2004. Neuropilin-1 is required for endothelial tip cell guidance in the developing central nervous system. *Developmental Dynamics*, 231, 503-9.
- GERTLER, F. B., NIEBUHR, K., REINHARD, M., WEHLAND, J. & SORIANO, P. 1996. Mena, a relative of VASP and Drosophila Enabled, is implicated in the control of microfilament dynamics. *Cell*, 87, 227-39.

- GINEITIS, D. & TREISMAN, R. 2001. Differential usage of signal transduction pathways defines two types of serum response factor target gene. *The Journal of biological chemistry*, 276, 24531-9.
- GLIENKE, J., SCHMITT, A. O., PILARSKY, C., HINZMANN, B., WEISS, B., ROSENTHAL, A. & THIERAUCH, K. H. 2000. Differential gene expression by endothelial cells in distinct angiogenic states. *Eur J Biochem*, 267, 2820-30.
- GLINKA, Y. & PRUD'HOMME, G. J. 2008. Neuropilin-1 is a receptor for transforming growth factor beta-1, activates its latent form, and promotes regulatory T cell activity. *J Leukoc Biol*, 84, 302-10.
- GLINKA, Y., STOILOVA, S., MOHAMMED, N. & PRUD'HOMME, G. J. 2011. Neuropilin-1 exerts co-receptor function for TGF-beta-1 on the membrane of cancer cells and enhances responses to both latent and active TGF-beta. *Carcinogenesis*, 32, 613-21.
- GOMES, L. R., TERRA, L. F., WAILEMANN, R. A., LABRIOLA, L. & SOGAYAR, M. C. 2012. TGF-beta1 modulates the homeostasis between MMPs and MMP inhibitors through p38 MAPK and ERK1/2 in highly invasive breast cancer cells. *BMC Cancer*, 12, 26.
- GU, C., RODRIGUEZ, E. R., REIMERT, D. V., SHU, T., FRITZSCH, B., RICHARDS, L. J., KOLODKIN, A. L. & GINTY, D. D. 2003. Neuropilin-1 conveys semaphorin and VEGF signaling during neural and cardiovascular development. *Developmental Cell*, 5, 45-57.
- GU, C., YOSHIDA, Y., LIVET, J., REIMERT, D. V., MANN, F., MERTE, J., HENDERSON, C. E., JESSELL, T. M., KOLODKIN, A. L. & GINTY, D. D. 2005. Semaphorin 3E and plexin-D1 control vascular pattern independently of neuropilins. *Science*, 307, 265-8.
- GUALDRINI, F., ESNAULT, C., HORSWELL, S., STEWART, A., MATTHEWS, N. & TREISMAN, R. 2016. SRF Co-factors Control the Balance between Cell Proliferation and Contractility. *Mol Cell*, 64, 1048-1061.
- GUILLOU, H., DEPRAZ-DEPLAND, A., PLANUS, E., VIANAY, B., CHAUSSY, J., GRICHINE, A., ALBIGES-RIZO, C. & BLOCK, M. R. 2008. Lamellipodia nucleation by filopodia depends on integrin occupancy and downstream Rac1 signaling. *Exp Cell Res*, 314, 478-88.
- GUO, W. & GIANCOTTI, F. G. 2004. Integrin signalling during tumour progression. *Nature reviews. Molecular cell biology*, 5, 816-26.
- HAMILTON, D. L. & ABREMSKI, K. 1984. Site-specific recombination by the bacteriophage P1 lox-Cre system. Cre-mediated synapsis of two lox sites. *J Mol Biol*, 178, 481-6.
- HANKS, S. K., RYZHOVA, L., SHIN, N. Y. & BRABEK, J. 2003. Focal adhesion kinase signaling activities and their implications in the control of cell survival and motility. *Front Biosci*, 8, d982-96.
- HAWKINS, B. T. & DAVIS, T. P. 2005. The blood-brain barrier/neurovascular unit in health and disease. *Pharmacol Rev*, 57, 173-85.
- HAYASHI, I., VUORI, K. & LIDDINGTON, R. C. 2002. The focal adhesion targeting (FAT) region of focal adhesion kinase is a four-helix bundle that binds paxillin. *Nat Struct Biol*, 9, 101-6.
- HEASMAN, S. J. & RIDLEY, A. J. 2008. Mammalian Rho GTPases: new insights into their functions from in vivo studies. *Nat Rev Mol Cell Biol*, 9, 690-701.
- HERZOG, B., PELLET-MANY, C., BRITTON, G., HARTZOULAKIS, B. & ZACHARY, I. C. 2011a. VEGF binding to NRP1 is essential for VEGF

- stimulation of endothelial cell migration, complex formation between NRP1 and VEGFR2, and signaling via FAK Tyr407 phosphorylation. *Molecular biology of the cell*, 22, 2766-76.
- HERZOG, B., PELLET-MANY, C., BRITTON, G., HARTZOULAKIS, B. & ZACHARY, I. C. 2011b. VEGF binding to NRP1 is essential for VEGF stimulation of endothelial cell migration, complex formation between NRP1 and VEGFR2, and signaling via FAK Tyr407 phosphorylation. *Mol Biol Cell*, 22, 2766-76.
- HILL, C. S., WYNNE, J. & TREISMAN, R. 1995. The Rho family GTPases RhoA, Rac1, and CDC42Hs regulate transcriptional activation by SRF. *Cell*, 81, 1159-70.
- HINOHARA, K., NAKAJIMA, T., YASUNAMI, M., HOUDA, S., SASAOKA, T., YAMAMOTO, K., LEE, B. S., SHIBATA, H., TANAKA-TAKAHASHI, Y., TAKAHASHI, M., ARIMURA, T., SATO, A., NARUSE, T., BAN, J., INOKO, H., YAMADA, Y., SAWABE, M., PARK, J. E., IZUMI, T. & KIMURA, A. 2009. Megakaryoblastic leukemia factor-1 gene in the susceptibility to coronary artery disease. *Hum Genet*, 126, 539-47.
- HIPSKIND, R. A., RAO, V. N., MUELLER, C. G., REDDY, E. S. & NORDHEIM, A. 1991. Ets-related protein Elk-1 is homologous to the c-fos regulatory factor p62TCF. *Nature*, 354, 531-4.
- HIROTA, S., CLEMENTS, T. P., TANG, L. K., MORALES, J. E., LEE, H. S., OH, S. P., RIVERA, G. M., WAGNER, D. S. & MCCARTY, J. H. 2015. Neuropilin 1 balances beta8 integrin-activated TGFbeta signaling to control sprouting angiogenesis in the brain. *Development*, 142, 4363-73.
- HOEBEN, A., LANDUYT, B., HIGHLEY, M. S., WILDIERS, H., VAN OOSTEROM, A. T. & DE BRUIJN, E. A. 2004. Vascular endothelial growth factor and angiogenesis. *Pharmacol Rev*, 56, 549-80.
- HOLTZ, M. L. & MISRA, R. P. 2008. Endothelial-specific ablation of serum response factor causes hemorrhaging, yolk sac vascular failure, and embryonic lethality. *BMC Dev Biol*, 8, 65.
- HONG, L., KENNEY, S. R., PHILLIPS, G. K., SIMPSON, D., SCHROEDER, C. E., NOTH, J., ROMERO, E., SWANSON, S., WALLER, A., STROUSE, J. J., CARTER, M., CHIGAEV, A., URSU, O., OPREA, T., HJELLE, B., GOLDEN, J. E., AUBE, J., HUDSON, L. G., BURANDA, T., SKLAR, L. A. & WANDINGER-NESS, A. 2013. Characterization of a Cdc42 protein inhibitor and its use as a molecular probe. *The Journal of Biological Chemistry*, 288, 8531-43.
- HUDSON, N., POWNER, M. B., SARKER, M. H., BURGOYNE, T., CAMPBELL, M., OCKRIM, Z. K., MARTINELLI, R., FUTTER, C. E., GRANT, M. B., FRASER, P. A., SHIMA, D. T., GREENWOOD, J. & TUROWSKI, P. 2014. Differential apicobasal VEGF signaling at vascular blood-neural barriers. *Dev Cell*, 30, 541-52.
- HUMPHRIES, J. D., BYRON, A. & HUMPHRIES, M. J. 2006. Integrin ligands at a glance. *J Cell Sci*, 119, 3901-3.
- HYNES, R. O. 2002. Integrins: bidirectional, allosteric signaling machines. *Cell*, 110, 673-87.
- IKEDA, S., USHIO-FUKAI, M., ZUO, L., TOJO, T., DIKALOV, S., PATRUSHEV, N. A. & ALEXANDER, R. W. 2005. Novel role of ARF6 in vascular endothelial growth factor-induced signaling and angiogenesis. *Circ Res*, 96, 467-75.

- ILIC, D., FURUTA, Y., KANAZAWA, S., TAKEDA, N., SOBUE, K., NAKATSUJI, N., NOMURA, S., FUJIMOTO, J., OKADA, M. & YAMAMOTO, T. 1995. Reduced cell motility and enhanced focal adhesion contact formation in cells from FAK-deficient mice. *Nature*, 377, 539-44.
- INGLEY, E. 2008. Src family kinases: regulation of their activities, levels and identification of new pathways. *Biochim Biophys Acta*, 1784, 56-65.
- INNOCENTI, M., GERBOTH, S., ROTTNER, K., LAI, F. P., HERTZOG, M., STRADAL, T. E., FRITTOLI, E., DIDRY, D., POLO, S., DISANZA, A., BENESCH, S., DI FIORE, P. P., CARLIER, M. F. & SCITA, G. 2005. Abi1 regulates the activity of N-WASP and WAVE in distinct actin-based processes. *Nat Cell Biol*, 7, 969-76.
- IZAGUIRRE, G., AGUIRRE, L., HU, Y. P., LEE, H. Y., SCHLAEPFER, D. D., ANESKIEVICH, B. J. & HAIMOVICH, B. 2001. The cytoskeletal/non-muscle isoform of alpha-actinin is phosphorylated on its actin-binding domain by the focal adhesion kinase. *J Biol Chem*, 276, 28676-85.
- JAFFE, A. B. & HALL, A. 2005. Rho GTPases: biochemistry and biology. *Annu Rev Cell Dev Biol*, 21, 247-69.
- JEAN, C., CHEN, X. L., NAM, J. O., TANCIONI, I., URYU, S., LAWSON, C., WARD, K. K., WALSH, C. T., MILLER, N. L., GHASSEMIAN, M., TUROWSKI, P., DEJANA, E., WEIS, S., CHERESH, D. A. & SCHLAEPFER, D. D. 2014. Inhibition of endothelial FAK activity prevents tumor metastasis by enhancing barrier function. *J Cell Biol*, 204, 247-63.
- JIN, Y., LIU, Y., LIN, Q., LI, J., DRUSO, J. E., ANTONYAK, M. A., MEININGER, C. J., ZHANG, S. L., DOSTAL, D. E., GUAN, J. L., CERIONE, R. A. & PENG, X. 2013. Deletion of Cdc42 enhances ADAM17-mediated vascular endothelial growth factor receptor 2 shedding and impairs vascular endothelial cell survival and vasculogenesis. *Mol Cell Biol*, 33, 4181-97.
- JONES, E. A., YUAN, L., BREANT, C., WATTS, R. J. & EICHMANN, A. 2008. Separating genetic and hemodynamic defects in neuropilin 1 knockout embryos. *Development*, 135, 2479-88.
- JOYAL, J. S., SITARAS, N., BINET, F., RIVERA, J. C., STAHL, A., ZANIOLO, K., SHAO, Z., POLOSA, A., ZHU, T., HAMEL, D., DJAVARI, M., KUNIK, D., HONORE, J. C., PICARD, E., ZABEIDA, A., VARMA, D. R., HICKSON, G., MANCINI, J., KLAGSBRUN, M., COSTANTINO, S., BEAUSEJOUR, C., LACHAPPELLE, P., SMITH, L. E., CHEMTOB, S. & SAPIEHA, P. 2011. Ischemic neurons prevent vascular regeneration of neural tissue by secreting semaphorin 3A. *Blood*, 117, 6024-35.
- JURISIC, G., MABY-EL HAJJAMI, H., KARAMAN, S., OCHSENBEIN, A. M., ALITALO, A., SIDDIQUI, S. S., OCHOA PEREIRA, C., PETROVA, T. V. & DETMAR, M. 2012. An unexpected role of semaphorin3a-neuropilin-1 signaling in lymphatic vessel maturation and valve formation. *Circ Res*, 111, 426-36.
- KAGA, T., KAWANO, H., SAKAGUCHI, M., NAKAZAWA, T., TANIYAMA, Y. & MORISHITA, R. 2012. Hepatocyte growth factor stimulated angiogenesis without inflammation: differential actions between hepatocyte growth factor, vascular endothelial growth factor and basic fibroblast growth factor. *Vascul Pharmacol*, 57, 3-9.
- KAWAMURA, H., LI, X., GOISHI, K., VAN MEETEREN, L. A., JAKOBSSON, L., CEBE-SUAREZ, S., SHIMIZU, A., EDHOLM, D., BALLMER-HOFER,

- K., KJELLEN, L., KLAGSBRUN, M. & CLAESSION-WELSH, L. 2008. Neuropilin-1 in regulation of VEGF-induced activation of p38MAPK and endothelial cell organization. *Blood*, 112, 3638-49.
- KAWASAKI, T., KITSUKAWA, T., BEKKU, Y., MATSUDA, Y., SANBO, M., YAGI, T. & FUJISAWA, H. 1999. A requirement for neuropilin-1 in embryonic vessel formation. *Development*, 126, 4895-902.
- KERN, P. A., SVOBODA, M. E., ECKEL, R. H. & VAN WYK, J. J. 1989. Insulinlike growth factor action and production in adipocytes and endothelial cells from human adipose tissue. *Diabetes*, 38, 710-7.
- KHACHIGIAN, L. M. 2016. Early growth response-1 in the pathogenesis of cardiovascular disease. *J Mol Med (Berl)*, 94, 747-53.
- KIM, L. A. & D'AMORE, P. A. 2012. A brief history of anti-VEGF for the treatment of ocular angiogenesis. *The American Journal of Pathology*, 181, 376-9.
- KITSUKAWA, T., SHIMONO, A., KAWAKAMI, A., KONDOH, H. & FUJISAWA, H. 1995. Overexpression of a membrane protein, neuropilin, in chimeric mice causes anomalies in the cardiovascular system, nervous system and limbs. *Development*, 121, 4309-18.
- KLUGER, M. S., CLARK, P. R., TELLIDES, G., GERKE, V. & POBER, J. S. 2013. Claudin-5 controls intercellular barriers of human dermal microvascular but not human umbilical vein endothelial cells. *Arterioscler Thromb Vasc Biol*, 33, 489-500.
- KOCH, S., TUGUES, S., LI, X., GUALANDI, L. & CLAESSION-WELSH, L. 2011. Signal transduction by vascular endothelial growth factor receptors. *The Biochemical Journal*, 437, 169-83.
- KOCH, S., VAN MEETEREN, L. A., MORIN, E., TESTINI, C., WESTROM, S., BJORKELUND, H., LE JAN, S., ADLER, J., BERGER, P. & CLAESSION-WELSH, L. 2014. NRP1 presented in trans to the endothelium arrests VEGFR2 endocytosis, preventing angiogenic signaling and tumor initiation. *Developmental cell*, 28, 633-46.
- KOK, F. O., SHIN, M., NI, C. W., GUPTA, A., GROSSE, A. S., VAN IMPEL, A., KIRCHMAIER, B. C., PETERSON-MADURO, J., KOURKOULIS, G., MALE, I., DESANTIS, D. F., SHEPPARD-TINDELL, S., EBARASI, L., BETSHOLTZ, C., SCHULTE-MERKER, S., WOLFE, S. A. & LAWSON, N. D. 2015. Reverse genetic screening reveals poor correlation between morpholino-induced and mutant phenotypes in zebrafish. *Dev Cell*, 32, 97-108.
- KOLLURI, R., TOLIAS, K. F., CARPENTER, C. L., ROSEN, F. S. & KIRCHHAUSEN, T. 1996. Direct interaction of the Wiskott-Aldrich syndrome protein with the GTPase Cdc42. *Proc Natl Acad Sci U S A*, 93, 5615-8.
- KUWAHARA, K., BARRIENTOS, T., PIPES, G. C., LI, S. & OLSON, E. N. 2005. Muscle-specific signaling mechanism that links actin dynamics to serum response factor. *Molecular and cellular biology*, 25, 3173-81.
- LAMALICE, L., HOULE, F., JOURDAN, G. & HUOT, J. 2004. Phosphorylation of tyrosine 1214 on VEGFR2 is required for VEGF-induced activation of Cdc42 upstream of SAPK2/p38. *Oncogene*, 23, 434-45.
- LAMPROPOULOU, A. & RUHRBERG, C. 2014. Neuropilin regulation of angiogenesis. *Biochem Soc Trans*, 42, 1623-8.
- LANAHAN, A., ZHANG, X., FANTIN, A., ZHUANG, Z., RIVERA-MOLINA, F., SPEICHINGER, K., PRAHST, C., ZHANG, J., WANG, Y., DAVIS, G.,

- TOOMRE, D., RUHRBERG, C. & SIMONS, M. 2013a. The Neuropilin 1 Cytoplasmic Domain Is Required for VEGF-A-Dependent Arteriogenesis. *Developmental Cell*, 25, 156-68.
- LANAHAN, A., ZHANG, X., FANTIN, A., ZHUANG, Z., RIVERA-MOLINA, F., SPEICHINGER, K., PRAHST, C., ZHANG, J., WANG, Y., DAVIS, G., TOOMRE, D., RUHRBERG, C. & SIMONS, M. 2013b. The neuropilin 1 cytoplasmic domain is required for VEGF-A-dependent arteriogenesis. *Dev Cell*, 25, 156-68.
- LEE, P., GOISHI, K., DAVIDSON, A. J., MANNIX, R., ZON, L. & KLAGSBRUN, M. 2002. Neuropilin-1 is required for vascular development and is a mediator of VEGF-dependent angiogenesis in zebrafish. *Proceedings of the National Academy of Sciences of the United States of America*, 99, 10470-5.
- LEGATE, K. R., WICKSTROM, S. A. & FASSLER, R. 2009. Genetic and cell biological analysis of integrin outside-in signaling. *Genes Dev*, 23, 397-418.
- LEPORE, J. J., CHENG, L., MIN LU, M., MERICKO, P. A., MORRISEY, E. E. & PARMACEK, M. S. 2005. High-efficiency somatic mutagenesis in smooth muscle cells and cardiac myocytes in SM22alpha-Cre transgenic mice. *Genesis*, 41, 179-84.
- LEWIS, J. M., BASKARAN, R., TAAGEPERA, S., SCHWARTZ, M. A. & WANG, J. Y. 1996a. Integrin regulation of c-Abl tyrosine kinase activity and cytoplasmic-nuclear transport. *Proc Natl Acad Sci U S A*, 93, 15174-9.
- LEWIS, J. M., BASKARAN, R., TAAGEPERA, S., SCHWARTZ, M. A. & WANG, J. Y. 1996b. Integrin regulation of c-Abl tyrosine kinase activity and cytoplasmic-nuclear transport. *Proceedings of the National Academy of Sciences of the United States of America*, 93, 15174-9.
- LEWIS, J. M. & SCHWARTZ, M. A. 1998a. Integrins regulate the association and phosphorylation of paxillin by c-Abl. *J Biol Chem*, 273, 14225-30.
- LEWIS, J. M. & SCHWARTZ, M. A. 1998b. Integrins regulate the association and phosphorylation of paxillin by c-Abl. *The Journal of Biological Chemistry*, 273, 14225-30.
- LI, J., CHEN, K., ZHU, L. & POLLARD, J. W. 2006a. Conditional deletion of the colony stimulating factor-1 receptor (c-fms proto-oncogene) in mice. *Genesis*, 44, 328-35.
- LI, J., ZHU, X., CHEN, M., CHENG, L., ZHOU, D., LU, M. M., DU, K., EPSTEIN, J. A. & PARMACEK, M. S. 2005. Myocardin-related transcription factor B is required in cardiac neural crest for smooth muscle differentiation and cardiovascular development. *Proc Natl Acad Sci U S A*, 102, 8916-21.
- LI, S., CHANG, S., QI, X., RICHARDSON, J. A. & OLSON, E. N. 2006b. Requirement of a myocardin-related transcription factor for development of mammary myoepithelial cells. *Molecular and cellular biology*, 26, 5797-808.
- LI, X., PADHAN, N., SJOSTROM, E. O., ROCHE, F. P., TESTINI, C., HONKURA, N., SAINZ-JASPEADO, M., GORDON, E., BENTLEY, K., PHILIPPIDES, A., TOLMACHEV, V., DEJANA, E., STAN, R. V., VESTWEBER, D., BALLMER-HOFER, K., BETSHOLTZ, C., PIETRAS, K., JANSSON, L. & CLAESSEON-WELSH, L. 2016. VEGFR2 pY949 signalling regulates adherens junction integrity and metastatic spread. *Nat Commun*, 7, 11017.
- LIANG, W., KUJAWSKI, M., WU, J., LU, J., HERRMANN, A., LOERA, S., YEN, Y., LEE, F., YU, H., WEN, W. & JOVE, R. 2010. Antitumor activity of

- targeting SRC kinases in endothelial and myeloid cell compartments of the tumor microenvironment. *Clin Cancer Res*, 16, 924-35.
- LIAO, D. & JOHNSON, R. S. 2007. Hypoxia: a key regulator of angiogenesis in cancer. *Cancer Metastasis Rev*, 26, 281-90.
- LU, X. G., AZHAR, G., LIU, L., TSOU, H. & WEI, J. Y. 1998. SRF binding to SRE in the rat heart: influence of age. *J Gerontol A Biol Sci Med Sci*, 53, B3-10.
- LU, Z. & XU, S. 2006. ERK1/2 MAP kinases in cell survival and apoptosis. *IUBMB Life*, 58, 621-31.
- MAEKAWA, M., ISHIZAKI, T., BOKU, S., WATANABE, N., FUJITA, A., IWAMATSU, A., OBINATA, T., OHASHI, K., MIZUNO, K. & NARUMIYA, S. 1999. Signaling from Rho to the actin cytoskeleton through protein kinases ROCK and LIM-kinase. *Science*, 285, 895-8.
- MAIONE, F., MOLLA, F., MEDA, C., LATINI, R., ZENTILIN, L., GIACCA, M., SEANO, G., SERINI, G., BUSSOLINO, F. & GIRAUDO, E. 2009. Semaphorin 3A is an endogenous angiogenesis inhibitor that blocks tumor growth and normalizes tumor vasculature in transgenic mouse models. *J Clin Invest*, 119, 3356-72.
- MAJNO, G., PALADE, G. E. & SCHOEFL, G. I. 1961. Studies on inflammation. II. The site of action of histamine and serotonin along the vascular tree: a topographic study. *J Biophys Biochem Cytol*, 11, 607-26.
- MAMLUK, R., GECHTMAN, Z., KUTCHER, M. E., GASIUNAS, N., GALLAGHER, J. & KLAGSBRUN, M. 2002. Neuropilin-1 binds vascular endothelial growth factor 165, placenta growth factor-2, and heparin via its b1b2 domain. *J Biol Chem*, 277, 24818-25.
- MARTYN, U. & SCHULTE-MERKER, S. 2004. Zebrafish neuropilins are differentially expressed and interact with vascular endothelial growth factor during embryonic vascular development. *Developmental dynamics : an official publication of the American Association of Anatomists*, 231, 33-42.
- MATTER, K. & BALDA, M. S. 2003. Signalling to and from tight junctions. *Nat Rev Mol Cell Biol*, 4, 225-36.
- MATTLA, P. K. & LAPPALAINEN, P. 2008. Filopodia: molecular architecture and cellular functions. *Nat Rev Mol Cell Biol*, 9, 446-54.
- MATTIONI, T., LOUVION, J. F. & PICARD, D. 1994. Regulation of protein activities by fusion to steroid binding domains. *Methods Cell Biol*, 43 Pt A, 335-52.
- MEDJKANE, S., PEREZ-SANCHEZ, C., GAGGIOLI, C., SAHAI, E. & TREISMAN, R. 2009. Myocardin-related transcription factors and SRF are required for cytoskeletal dynamics and experimental metastasis. *Nat Cell Biol*, 11, 257-68.
- MEHTA, D. & MALIK, A. B. 2006. Signaling mechanisms regulating endothelial permeability. *Physiol Rev*, 86, 279-367.
- METTOUCHI, A. & MENEGUZZI, G. 2006. Distinct roles of beta1 integrins during angiogenesis. *Eur J Cell Biol*, 85, 243-7.
- MIANO, J. M., LONG, X. & FUJIWARA, K. 2007. Serum response factor: master regulator of the actin cytoskeleton and contractile apparatus. *Am J Physiol Cell Physiol*, 292, C70-81.
- MIANO, J. M., RAMANAN, N., GEORGER, M. A., DE MESY BENTLEY, K. L., EMERSON, R. L., BALZA, R. O., JR., XIAO, Q., WEILER, H., GINTY, D. D. & MISRA, R. P. 2004. Restricted inactivation of serum response factor to the cardiovascular system. *Proc Natl Acad Sci U S A*, 101, 17132-7.

- MICHAEL, K. E., DUMBAULD, D. W., BURNS, K. L., HANKS, S. K. & GARCIA, A. J. 2009. Focal adhesion kinase modulates cell adhesion strengthening via integrin activation. *Molecular biology of the cell*, 20, 2508-19.
- MILES, A. A. & MILES, E. M. 1952a. Vascular reactions to histamine, histamine-liberator and leukotaxine in the skin of guinea-pigs. *The Journal of Physiology*, 118, 228-57.
- MILES, A. A. & MILES, E. M. 1952b. Vascular reactions to histamine, histamine-liberator and leukotaxine in the skin of guinea-pigs. *J Physiol*, 118, 228-57.
- MINAMI, T., KUWAHARA, K., NAKAGAWA, Y., TAKAOKA, M., KINOSHITA, H., NAKAO, K., KUWABARA, Y., YAMADA, Y., YAMADA, C., SHIBATA, J., USAMI, S., YASUNO, S., NISHIKIMI, T., UESHIMA, K., SATA, M., NAKANO, H., SENO, T., KAWAHITO, Y., SOBUE, K., KIMURA, A., NAGAI, R. & NAKAO, K. 2012. Reciprocal expression of MRTF-A and myocardin is crucial for pathological vascular remodelling in mice. *EMBO J*, 31, 4428-40.
- MIRALLES, F., POSERN, G., ZAROMYTIDOU, A. I. & TREISMAN, R. 2003. Actin dynamics control SRF activity by regulation of its coactivator MAL. *Cell*, 113, 329-42.
- MITRA, S. K., HANSON, D. A. & SCHLAEPFER, D. D. 2005. Focal adhesion kinase: in command and control of cell motility. *Nat Rev Mol Cell Biol*, 6, 56-68.
- MIWA, T. & KEDES, L. 1987. Duplicated CArG box domains have positive and mutually dependent regulatory roles in expression of the human alpha-cardiac actin gene. *Molecular and cellular biology*, 7, 2803-13.
- MOLLER, B., RASMUSSEN, C., LINDBLOM, B. & OLOVSSON, M. 2001. Expression of the angiogenic growth factors VEGF, FGF-2, EGF and their receptors in normal human endometrium during the menstrual cycle. *Mol Hum Reprod*, 7, 65-72.
- MONTANEZ, E., USSAR, S., SCHIFFERER, M., BOSL, M., ZENT, R., MOSER, M. & FASSLER, R. 2008. Kindlin-2 controls bidirectional signaling of integrins. *Genes Dev*, 22, 1325-30.
- MORITA, T., MAYANAGI, T. & SOBUE, K. 2007. Dual roles of myocardin-related transcription factors in epithelial mesenchymal transition via slug induction and actin remodeling. *J Cell Biol*, 179, 1027-42.
- MUEHLICH, S., WANG, R., LEE, S. M., LEWIS, T. C., DAI, C. & PRYWES, R. 2008. Serum-induced phosphorylation of the serum response factor coactivator MKL1 by the extracellular signal-regulated kinase 1/2 pathway inhibits its nuclear localization. *Mol Cell Biol*, 28, 6302-13.
- MURGA, M., FERNANDEZ-CAPETILLO, O. & TOSATO, G. 2005. Neuropilin-1 regulates attachment in human endothelial cells independently of vascular endothelial growth factor receptor-2. *Blood*, 105, 1992-9.
- MUROHARA, T., HOROWITZ, J. R., SILVER, M., TSURUMI, Y., CHEN, D., SULLIVAN, A. & ISNER, J. M. 1998. Vascular endothelial growth factor/vascular permeability factor enhances vascular permeability via nitric oxide and prostacyclin. *Circulation*, 97, 99-107.
- NAGY, A. 2000. Cre recombinase: the universal reagent for genome tailoring. *Genesis*, 26, 99-109.

- NAGY, J. A., BENJAMIN, L., ZENG, H., DVORAK, A. M. & DVORAK, H. F. 2008. Vascular permeability, vascular hyperpermeability and angiogenesis. *Angiogenesis*, 11, 109-19.
- NAGY, J. A., MASSE, E. M., HERZBERG, K. T., MEYERS, M. S., YEO, K. T., YEO, T. K., SIOUSSAT, T. M. & DVORAK, H. F. 1995. Pathogenesis of ascites tumor growth: vascular permeability factor, vascular hyperpermeability, and ascites fluid accumulation. *Cancer Res*, 55, 360-8.
- NAKAMURA, S., HAYASHI, K., IWASAKI, K., FUJIOKA, T., EGUSA, H., YATANI, H. & SOBUE, K. 2010. Nuclear import mechanism for myocardin family members and their correlation with vascular smooth muscle cell phenotype. *The Journal of biological chemistry*, 285, 37314-23.
- NAWROTH, R., POELL, G., RANFT, A., KLOEP, S., SAMULOWITZ, U., FACHINGER, G., GOLDING, M., SHIMA, D. T., DEUTSCH, U. & VESTWEBER, D. 2002. VE-PTP and VE-cadherin ectodomains interact to facilitate regulation of phosphorylation and cell contacts. *EMBO J*, 21, 4885-95.
- NAYAK, G. & COOPER, G. M. 2012. p53 is a major component of the transcriptional and apoptotic program regulated by PI 3-kinase/Akt/GSK3 signaling. *Cell Death & Disease*, 3, e400.
- NISHIJIMA, K., NG, Y. S., ZHONG, L., BRADLEY, J., SCHUBERT, W., JO, N., AKITA, J., SAMUELSSON, S. J., ROBINSON, G. S., ADAMIS, A. P. & SHIMA, D. T. 2007. Vascular endothelial growth factor-A is a survival factor for retinal neurons and a critical neuroprotectant during the adaptive response to ischemic injury. *Am J Pathol*, 171, 53-67.
- NORMAN, C., RUNSWICK, M., POLLOCK, R. & TREISMAN, R. 1988. Isolation and properties of cDNA clones encoding SRF, a transcription factor that binds to the c-fos serum response element. *Cell*, 55, 989-1003.
- OKAZAKI, T., EBIHARA, S., TAKAHASHI, H., ASADA, M., KANDA, A. & SASAKI, H. 2005. Macrophage colony-stimulating factor induces vascular endothelial growth factor production in skeletal muscle and promotes tumor angiogenesis. *J Immunol*, 174, 7531-8.
- OLIVETTI, G., MELISSARI, M., CAPASSO, J. M. & ANVERSA, P. 1991. Cardiomyopathy of the aging human heart. Myocyte loss and reactive cellular hypertrophy. *Circ Res*, 68, 1560-8.
- OLSON, E. N. & NORDHEIM, A. 2010a. Linking actin dynamics and gene transcription to drive cellular motile functions. *Nature reviews. Molecular cell biology*, 11, 353-65.
- OLSON, E. N. & NORDHEIM, A. 2010b. Linking actin dynamics and gene transcription to drive cellular motile functions. *Nat Rev Mol Cell Biol*, 11, 353-65.
- PAN, Q., CHANTHERY, Y., LIANG, W. C., STAWICKI, S., MAK, J., RATHORE, N., TONG, R. K., KOWALSKI, J., YEE, S. F., PACHECO, G., ROSS, S., CHENG, Z., LE COUTER, J., PLOWMAN, G., PEALE, F., KOCH, A. W., WU, Y., BAGRI, A., TESSIER-LAVIGNE, M. & WATTS, R. J. 2007a. Blocking neuropilin-1 function has an additive effect with anti-VEGF to inhibit tumor growth. *Cancer cell*, 11, 53-67.
- PAN, Q., CHANTHERY, Y., WU, Y., RATHORE, N., TONG, R. K., PEALE, F., BAGRI, A., TESSIER-LAVIGNE, M., KOCH, A. W. & WATTS, R. J. 2007b. Neuropilin-1 binds to VEGF121 and regulates endothelial cell migration and sprouting. *The Journal of biological chemistry*, 282, 24049-56.

- PANAYIOTOU, R., MIRALLES, F., PAWLOWSKI, R., DIRING, J., FLYNN, H. R., SKEHEL, M. & TREISMAN, R. 2016. Phosphorylation acts positively and negatively to regulate MRTF-A subcellular localisation and activity. *Elife*, 5.
- PAOLINELLI, R., CORADA, M., ORSENIGO, F. & DEJANA, E. 2011. The molecular basis of the blood brain barrier differentiation and maintenance. Is it still a mystery? *Pharmacol Res*, 63, 165-71.
- PARKER, M. W., XU, P., LI, X. & VANDER KOOI, C. W. 2012. Structural basis for selective vascular endothelial growth factor-A (VEGF-A) binding to neuropilin-1. *The Journal of biological chemistry*, 287, 11082-9.
- PARLAKIAN, A., CHARVET, C., ESCOUBET, B., MERICKSKAY, M., MOLKENTIN, J. D., GARY-BOBO, G., DE WINDT, L. J., LUDOSKY, M. A., PAULIN, D., DAEGELEN, D., TUIL, D. & LI, Z. 2005. Temporally controlled onset of dilated cardiomyopathy through disruption of the SRF gene in adult heart. *Circulation*, 112, 2930-9.
- PARLAKIAN, A., TUIL, D., HAMARD, G., TAVERNIER, G., HENTZEN, D., CONCORDET, J. P., PAULIN, D., LI, Z. & DAEGELEN, D. 2004. Targeted inactivation of serum response factor in the developing heart results in myocardial defects and embryonic lethality. *Mol Cell Biol*, 24, 5281-9.
- PARMACEK, M. S. 2007. Myocardin-related transcription factors: critical coactivators regulating cardiovascular development and adaptation. *Circulation research*, 100, 633-44.
- PARSONS, J. T. 2003. Focal adhesion kinase: the first ten years. *J Cell Sci*, 116, 1409-16.
- PARSONS, S. J. & PARSONS, J. T. 2004. Src family kinases, key regulators of signal transduction. *Oncogene*, 23, 7906-9.
- PASAPERA, A. M., SCHNEIDER, I. C., RERICHA, E., SCHLAEPFER, D. D. & WATERMAN, C. M. 2010. Myosin II activity regulates vinculin recruitment to focal adhesions through FAK-mediated paxillin phosphorylation. *The Journal of Cell Biology*, 188, 877-90.
- PEIRSON, S. N., BUTLER, J. N. & FOSTER, R. G. 2003. Experimental validation of novel and conventional approaches to quantitative real-time PCR data analysis. *Nucleic Acids Res*, 31, e73.
- PICARD, D. 1994. Regulation of protein function through expression of chimaeric proteins. *Curr Opin Biotechnol*, 5, 511-5.
- PIPES, G. C., CREEMERS, E. E. & OLSON, E. N. 2006a. The myocardin family of transcriptional coactivators: versatile regulators of cell growth, migration, and myogenesis. *Genes Dev*, 20, 1545-56.
- PIPES, G. C., CREEMERS, E. E. & OLSON, E. N. 2006b. The myocardin family of transcriptional coactivators: versatile regulators of cell growth, migration, and myogenesis. *Genes & development*, 20, 1545-56.
- PITULESCU, M. E., SCHMIDT, I., BENEDITO, R. & ADAMS, R. H. 2010. Inducible gene targeting in the neonatal vasculature and analysis of retinal angiogenesis in mice. *Nat Protoc*, 5, 1518-34.
- PLATTNER, R., KADLEC, L., DEMALI, K. A., KAZLAUSKAS, A. & PENDERGAST, A. M. 1999. c-Abl is activated by growth factors and Src family kinases and has a role in the cellular response to PDGF. *Genes Dev*, 13, 2400-11.
- PLOW, E. F., MELLER, J. & BYZOVA, T. V. 2014. Integrin function in vascular biology: a view from 2013. *Curr Opin Hematol*, 21, 241-7.

- POLLARD, T. D. 2007. Regulation of actin filament assembly by Arp2/3 complex and formins. *Annu Rev Biophys Biomol Struct*, 36, 451-77.
- POSERN, G., MIRALLES, F., GUETTLER, S. & TREISMAN, R. 2004. Mutant actins that stabilise F-actin use distinct mechanisms to activate the SRF coactivator MAL. *The EMBO journal*, 23, 3973-83.
- POSERN, G., SOTIROPOULOS, A. & TREISMAN, R. 2002. Mutant actins demonstrate a role for unpolymerized actin in control of transcription by serum response factor. *Molecular biology of the cell*, 13, 4167-78.
- PRAHST, C., HEROULT, M., LANAHAN, A. A., UZIEL, N., KESSLER, O., SHRAGA-HELED, N., SIMONS, M., NEUFELD, G. & AUGUSTIN, H. G. 2008. Neuropilin-1-VEGFR-2 complexing requires the PDZ-binding domain of neuropilin-1. *J Biol Chem*, 283, 25110-4.
- PREDESCU, S. A., PREDESCU, D. N. & MALIK, A. B. 2007. Molecular determinants of endothelial transcytosis and their role in endothelial permeability. *Am J Physiol Lung Cell Mol Physiol*, 293, L823-42.
- QI, Y., LIU, J., WU, X., BRAKEBUSCH, C., LEITGES, M., HAN, Y., CORBETT, S. A., LOWRY, S. F., GRAHAM, A. M. & LI, S. 2011. Cdc42 controls vascular network assembly through protein kinase Ciota during embryonic vasculogenesis. *Arterioscler Thromb Vasc Biol*, 31, 1861-70.
- RAIMONDI, C., BRASH, J. T., FANTIN, A. & RUHRBERG, C. 2016. NRP1 function and targeting in neurovascular development and eye disease. *Prog Retin Eye Res*, 52, 64-83.
- RAIMONDI, C., FANTIN, A., LAMPROPOULOU, A., DENTI, L., CHIKH, A. & RUHRBERG, C. 2014. Imatinib inhibits VEGF-independent angiogenesis by targeting neuropilin 1-dependent ABL1 activation in endothelial cells. *The Journal of experimental medicine*, 211, 1167-83.
- RAIMONDI, C. & RUHRBERG, C. 2013. Neuropilin signalling in vessels, neurons and tumours. *Seminars in cell & developmental biology*, 24, 172-8.
- REYMOND, N., IM, J. H., GARG, R., VEGA, F. M., BORDA D'AGUA, B., RIOU, P., COX, S., VALDERRAMA, F., MUSCHEL, R. J. & RIDLEY, A. J. 2012a. Cdc42 promotes transendothelial migration of cancer cells through beta1 integrin. *The Journal of Cell Biology*, 199, 653-68.
- REYMOND, N., IM, J. H., GARG, R., VEGA, F. M., BORDA D'AGUA, B., RIOU, P., COX, S., VALDERRAMA, F., MUSCHEL, R. J. & RIDLEY, A. J. 2012b. Cdc42 promotes transendothelial migration of cancer cells through beta1 integrin. *J Cell Biol*, 199, 653-68.
- RICO, B., BEGGS, H. E., SCHAHIN-REED, D., KIMES, N., SCHMIDT, A. & REICHARDT, L. F. 2004. Control of axonal branching and synapse formation by focal adhesion kinase. *Nat Neurosci*, 7, 1059-69.
- RIVARD, A., PRINCIPE, N. & ANDRES, V. 2000. Age-dependent increase in c-fos activity and cyclin A expression in vascular smooth muscle cells. A potential link between aging, smooth muscle cell proliferation and atherosclerosis. *Cardiovasc Res*, 45, 1026-34.
- ROBINSON, M. J. & COBB, M. H. 1997. Mitogen-activated protein kinase pathways. *Curr Opin Cell Biol*, 9, 180-6.
- ROBINSON, S. D., REYNOLDS, L. E., KOSTOUROU, V., REYNOLDS, A. R., DA SILVA, R. G., TAVORA, B., BAKER, M., MARSHALL, J. F. & HODIVALA-DILKE, K. M. 2009. Alpha v beta3 integrin limits the contribution of neuropilin-1 to vascular endothelial growth factor-induced angiogenesis. *J Biol Chem*, 284, 33966-81.

- ROBINSON, S. D., REYNOLDS, L. E., WYDER, L., HICKLIN, D. J. & HODIVALA-DILKE, K. M. 2004. Beta3-integrin regulates vascular endothelial growth factor-A-dependent permeability. *Arterioscler Thromb Vasc Biol*, 24, 2108-14.
- ROTH, L., PRAHST, C., RUCKDESCHEL, T., SAVANT, S., WESTROM, S., FANTIN, A., RIEDEL, M., HEROULT, M., RUHRBERG, C. & AUGUSTIN, H. G. 2016. Neuropilin-1 mediates vascular permeability independently of vascular endothelial growth factor receptor-2 activation. *Sci Signal*, 9, ra42.
- RUDINI, N. & DEJANA, E. 2008. Adherens junctions. *Current biology : CB*, 18, R1080-2.
- RUHRBERG, C. 2003. Growing and shaping the vascular tree: multiple roles for VEGF. *Bioessays*, 25, 1052-60.
- RUHRBERG, C., GERHARDT, H., GOLDING, M., WATSON, R., IOANNIDOU, S., FUJISAWA, H., BETSHOLTZ, C. & SHIMA, D. T. 2002. Spatially restricted patterning cues provided by heparin-binding VEGF-A control blood vessel branching morphogenesis. *Genes & Development*, 16, 2684-98.
- SADOK, A. & MARSHALL, C. J. 2014. Rho GTPases: masters of cell migration. *Small GTPases*, 5, e29710.
- SAINT-GENIEZ, M., MAHARAJ, A. S., WALSH, T. E., TUCKER, B. A., SEKIYAMA, E., KURIHARA, T., DARLAND, D. C., YOUNG, M. J. & D'AMORE, P. A. 2008. Endogenous VEGF is required for visual function: evidence for a survival role on muller cells and photoreceptors. *PLoS One*, 3, e3554.
- SAKURAI, Y., OHGIMOTO, K., KATAOKA, Y., YOSHIDA, N. & SHIBUYA, M. 2005. Essential role of Flk-1 (VEGF receptor 2) tyrosine residue 1173 in vasculogenesis in mice. *Proc Natl Acad Sci U S A*, 102, 1076-81.
- SALIKHOVA, A., WANG, L., LANAHAN, A. A., LIU, M., SIMONS, M., LEENDERS, W. P., MUKHOPADHYAY, D. & HOROWITZ, A. 2008. Vascular endothelial growth factor and semaphorin induce neuropilin-1 endocytosis via separate pathways. *Circ Res*, 103, e71-9.
- SARGIACOMO, M., SCHERER, P. E., TANG, Z., KUBLER, E., SONG, K. S., SANDERS, M. C. & LISANTI, M. P. 1995. Oligomeric structure of caveolin: implications for caveolae membrane organization. *Proc Natl Acad Sci U S A*, 92, 9407-11.
- SATO, M., MARUOKA, M. & TAKEYA, T. 2012. Functional mechanisms and roles of adaptor proteins in abl-regulated cytoskeletal actin dynamics. *J Signal Transduct*, 2012, 414913.
- SATTLER, M. & SALGIA, R. 1998. Role of the adapter protein CRKL in signal transduction of normal hematopoietic and BCR/ABL-transformed cells. *Leukemia*, 12, 637-44.
- SAWADA, Y., TAMADA, M., DUBIN-THALER, B. J., CHERNIAVSKAYA, O., SAKAI, R., TANAKA, S. & SHEETZ, M. P. 2006. Force sensing by mechanical extension of the Src family kinase substrate p130Cas. *Cell*, 127, 1015-26.
- SCHALLER, M. D. 2001. Biochemical signals and biological responses elicited by the focal adhesion kinase. *Biochim Biophys Acta*, 1540, 1-21.
- SCHALLER, M. D., OTEY, C. A., HILDEBRAND, J. D. & PARSONS, J. T. 1995. Focal adhesion kinase and paxillin bind to peptides mimicking beta integrin cytoplasmic domains. *J Cell Biol*, 130, 1181-7.

- SCHALLER, M. D. & PARSONS, J. T. 1995. pp125FAK-dependent tyrosine phosphorylation of paxillin creates a high-affinity binding site for Crk. *Mol Cell Biol*, 15, 2635-45.
- SCHALLER, M. D. & SCHAEFER, E. M. 2001. Multiple stimuli induce tyrosine phosphorylation of the Crk-binding sites of paxillin. *The Biochemical Journal*, 360, 57-66.
- SCHEPPKE, L., AGUILAR, E., GARIANO, R. F., JACOBSON, R., HOOD, J., DOUKAS, J., CAO, J., NORONHA, G., YEE, S., WEIS, S., MARTIN, M. B., SOLL, R., CHERESH, D. A. & FRIEDLANDER, M. 2008. Retinal vascular permeability suppression by topical application of a novel VEGFR2/Src kinase inhibitor in mice and rabbits. *J Clin Invest*, 118, 2337-46.
- SCHLAEPFER, D. D., MITRA, S. K. & ILIC, D. 2004. Control of motile and invasive cell phenotypes by focal adhesion kinase. *Biochim Biophys Acta*, 1692, 77-102.
- SCHUBERT, W., FRANK, P. G., WOODMAN, S. E., HYOGO, H., COHEN, D. E., CHOW, C. W. & LISANTI, M. P. 2002. Microvascular hyperpermeability in caveolin-1 (-/-) knock-out mice. Treatment with a specific nitric-oxide synthase inhibitor, L-NAME, restores normal microvascular permeability in Cav-1 null mice. *J Biol Chem*, 277, 40091-8.
- SCHWARTZ, M. A. & SHATTIL, S. J. 2000. Signaling networks linking integrins and rho family GTPases. *Trends in biochemical sciences*, 25, 388-91.
- SCHWARZ, Q. & RUHRBERG, C. 2010. Neuropilin, you gotta let me know: should I stay or should I go? *Cell Adhesion & Migration*, 4, 61-6.
- SEGHEZZI, G., PATEL, S., REN, C. J., GUALANDRIS, A., PINTUCCI, G., ROBBINS, E. S., SHAPIRO, R. L., GALLOWAY, A. C., RIFKIN, D. B. & MIGNATTI, P. 1998. Fibroblast growth factor-2 (FGF-2) induces vascular endothelial growth factor (VEGF) expression in the endothelial cells of forming capillaries: an autocrine mechanism contributing to angiogenesis. *J Cell Biol*, 141, 1659-73.
- SELVARAJ, A. & PRYWES, R. 2004a. Expression profiling of serum inducible genes identifies a subset of SRF target genes that are MKL dependent. *BMC Mol Biol*, 5, 13.
- SELVARAJ, A. & PRYWES, R. 2004b. Expression profiling of serum inducible genes identifies a subset of SRF target genes that are MKL dependent. *BMC molecular biology*, 5, 13.
- SENGER, D. R., GALLI, S. J., DVORAK, A. M., PERRUZZI, C. A., HARVEY, V. S. & DVORAK, H. F. 1983. Tumor cells secrete a vascular permeability factor that promotes accumulation of ascites fluid. *Science*, 219, 983-5.
- SHAW, P. E. & SAXTON, J. 2003. Ternary complex factors: prime nuclear targets for mitogen-activated protein kinases. *Int J Biochem Cell Biol*, 35, 1210-26.
- SHAY-SALIT, A., SHUSHY, M., WOLFOVITZ, E., YAHAV, H., BREVIARIO, F., DEJANA, E. & RESNICK, N. 2002. VEGF receptor 2 and the adherens junction as a mechanical transducer in vascular endothelial cells. *Proc Natl Acad Sci U S A*, 99, 9462-7.
- SHIMIZU, M., MURAKAMI, Y., SUTO, F. & FUJISAWA, H. 2000. Determination of cell adhesion sites of neuropilin-1. *J Cell Biol*, 148, 1283-93.
- SHOJI, W., ISOGAI, S., SATO-MAEDA, M., OBINATA, M. & KUWADA, J. Y. 2003. Semaphorin3a1 regulates angioblast migration and vascular development in zebrafish embryos. *Development*, 130, 3227-36.

- SHORE, P., WHITMARSH, A. J., BHASKARAN, R., DAVIS, R. J., WALTHO, J. P. & SHARROCKS, A. D. 1996. Determinants of DNA-binding specificity of ETS-domain transcription factors. *Molecular and cellular biology*, 16, 3338-49.
- SINGH, N. N. & RAMJI, D. P. 2006. The role of transforming growth factor-beta in atherosclerosis. *Cytokine Growth Factor Rev*, 17, 487-99.
- SINI, P., CANNAS, A., KOLESKE, A. J., DI FIORE, P. P. & SCITA, G. 2004. Abl-dependent tyrosine phosphorylation of Sos-1 mediates growth-factor-induced Rac activation. *Nat Cell Biol*, 6, 268-74.
- SIX, I., KUREISHI, Y., LUO, Z. & WALSH, K. 2002. Akt signaling mediates VEGF/VPF vascular permeability in vivo. *FEBS Lett*, 532, 67-9.
- SODROSKI, J., PATARCA, R., PERKINS, D., BRIGGS, D., LEE, T. H., ESSEX, M., COLIGAN, J., WONG-STAAAL, F., GALLO, R. C. & HASELTINE, W. A. 1984. Sequence of the envelope glycoprotein gene of type II human T lymphotropic virus. *Science*, 225, 421-4.
- SOKER, S., MIAO, H. Q., NOMI, M., TAKASHIMA, S. & KLAGSBRUN, M. 2002a. VEGF165 mediates formation of complexes containing VEGFR-2 and neuropilin-1 that enhance VEGF165-receptor binding. *Journal of cellular biochemistry*, 85, 357-68.
- SOKER, S., MIAO, H. Q., NOMI, M., TAKASHIMA, S. & KLAGSBRUN, M. 2002b. VEGF165 mediates formation of complexes containing VEGFR-2 and neuropilin-1 that enhance VEGF165-receptor binding. *J Cell Biochem*, 85, 357-68.
- SOKER, S., TAKASHIMA, S., MIAO, H. Q., NEUFELD, G. & KLAGSBRUN, M. 1998. Neuropilin-1 is expressed by endothelial and tumor cells as an isoform-specific receptor for vascular endothelial growth factor. *Cell*, 92, 735-45.
- SOTIROPOULOS, A., GINEITIS, D., COPELAND, J. & TREISMAN, R. 1999. Signal-regulated activation of serum response factor is mediated by changes in actin dynamics. *Cell*, 98, 159-69.
- STAN, R. V., TSE, D., DEHARVENGT, S. J., SMITS, N. C., XU, Y., LUCIANO, M. R., MCGARRY, C. L., BUITENDIJK, M., NEMANI, K. V., ELGUETA, R., KOBAYASHI, T., SHIPMAN, S. L., MOODIE, K. L., DAGHLIAN, C. P., ERNST, P. A., LEE, H. K., SURIAWINATA, A. A., SCHNED, A. R., LONGNECKER, D. S., FIERING, S. N., NOELLE, R. J., GIMI, B., SHWORAK, N. W. & CARRIERE, C. 2012. The diaphragms of fenestrated endothelia: gatekeepers of vascular permeability and blood composition. *Dev Cell*, 23, 1203-18.
- STENZEL, D., FRANCO, C. A., ESTRACH, S., METTOUCHI, A., SAUVAGET, D., ROSEWELL, I., SCHERTEL, A., ARMER, H., DOMOGATSKAYA, A., RODIN, S., TRYGGVASON, K., COLLINSON, L., SOROKIN, L. & GERHARDT, H. 2011a. Endothelial basement membrane limits tip cell formation by inducing Dll4/Notch signalling in vivo. *EMBO Rep*, 12, 1135-43.
- STENZEL, D., FRANCO, C. A., ESTRACH, S., METTOUCHI, A., SAUVAGET, D., ROSEWELL, I., SCHERTEL, A., ARMER, H., DOMOGATSKAYA, A., RODIN, S., TRYGGVASON, K., COLLINSON, L., SOROKIN, L. & GERHARDT, H. 2011b. Endothelial basement membrane limits tip cell formation by inducing Dll4/Notch signalling in vivo. *EMBO reports*, 12, 1135-43.

- STENZEL, D., LUNDKVIST, A., SAUVAGET, D., BUSSE, M., GRAUPERA, M., VAN DER FLIER, A., WIJELATH, E. S., MURRAY, J., SOBEL, M., COSTELL, M., TAKAHASHI, S., FASSLER, R., YAMAGUCHI, Y., GUTMANN, D. H., HYNES, R. O. & GERHARDT, H. 2011c. Integrin-dependent and -independent functions of astrocytic fibronectin in retinal angiogenesis. *Development*, 138, 4451-63.
- STEWART, M. W. 2012. The expanding role of vascular endothelial growth factor inhibitors in ophthalmology. *Mayo Clin Proc*, 87, 77-88.
- SULPICE, E., DING, S., MUSCATELLI-GROUX, B., BERGE, M., HAN, Z. C., PLOUET, J., TOBELEM, G. & MERKULOVA-RAINON, T. 2009. Cross-talk between the VEGF-A and HGF signalling pathways in endothelial cells. *Biol Cell*, 101, 525-39.
- SUN, Q., CHEN, G., STREB, J. W., LONG, X., YANG, Y., STOECKERT, C. J., JR. & MIANO, J. M. 2006a. Defining the mammalian CArGome. *Genome research*, 16, 197-207.
- SUN, Y., BOYD, K., XU, W., MA, J., JACKSON, C. W., FU, A., SHILLINGFORD, J. M., ROBINSON, G. W., HENNIGHAUSEN, L., HITZLER, J. K., MA, Z. & MORRIS, S. W. 2006b. Acute myeloid leukemia-associated Mkl1 (Mrtf-a) is a key regulator of mammary gland function. *Molecular and cellular biology*, 26, 5809-26.
- SUN, Z., LI, X., MASSENA, S., KUTSCHERA, S., PADHAN, N., GUALANDI, L., SUNDVOLD-GJERSTAD, V., GUSTAFSSON, K., CHOY, W. W., ZANG, G., QUACH, M., JANSSON, L., PHILLIPSON, M., ABID, M. R., SPURKLAND, A. & CLAESSION-WELSH, L. 2012. VEGFR2 induces c-Src signaling and vascular permeability in vivo via the adaptor protein TSA. *The Journal of experimental medicine*, 209, 1363-77.
- TAKAGI, S., KASUYA, Y., SHIMIZU, M., MATSUURA, T., TSUBOI, M., KAWAKAMI, A. & FUJISAWA, H. 1995. Expression of a cell adhesion molecule, neuropilin, in the developing chick nervous system. *Dev Biol*, 170, 207-22.
- TAKAHASHI, T., YAMAGUCHI, S., CHIDA, K. & SHIBUYA, M. 2001. A single autophosphorylation site on KDR/Flk-1 is essential for VEGF-A-dependent activation of PLC-gamma and DNA synthesis in vascular endothelial cells. *EMBO J*, 20, 2768-78.
- TANJORE, H., ZEISBERG, E. M., GERAMI-NAINI, B. & KALLURI, R. 2008. Beta1 integrin expression on endothelial cells is required for angiogenesis but not for vasculogenesis. *Developmental dynamics : an official publication of the American Association of Anatomists*, 237, 75-82.
- TATTON, L., MORLEY, G. M., CHOPRA, R. & KHWAJA, A. 2003. The Src-selective kinase inhibitor PP1 also inhibits Kit and Bcr-Abl tyrosine kinases. *J Biol Chem*, 278, 4847-53.
- TAYLOR, W. R. & ALEXANDER, R. W. 1993. Autocrine control of wound repair by insulin-like growth factor I in cultured endothelial cells. *Am J Physiol*, 265, C801-5.
- TEESALU, T., SUGAHARA, K. N., KOTAMRAJU, V. R. & RUOSLAHTI, E. 2009. C-end rule peptides mediate neuropilin-1-dependent cell, vascular, and tissue penetration. *Proceedings of the National Academy of Sciences of the United States of America*, 106, 16157-62.
- THIBEAULT, S., RAUTUREAU, Y., OUBAHA, M., FAUBERT, D., WILKES, B. C., DELISLE, C. & GRATTON, J. P. 2010. S-nitrosylation of beta-catenin

- by eNOS-derived NO promotes VEGF-induced endothelial cell permeability. *Mol Cell*, 39, 468-76.
- TIBBS, C. J. 1987. Hepatitis B, tropical ulcers, and immunisation strategy in Kiribati. *Br Med J (Clin Res Ed)*, 294, 537-40.
- TING, A. Y., KAIN, K. H., KLEMKE, R. L. & TSIEN, R. Y. 2001. Genetically encoded fluorescent reporters of protein tyrosine kinase activities in living cells. *Proc Natl Acad Sci U S A*, 98, 15003-8.
- TORRES-VAZQUEZ, J., GITLER, A. D., FRASER, S. D., BERK, J. D., VAN, N. P., FISHMAN, M. C., CHILDS, S., EPSTEIN, J. A. & WEINSTEIN, B. M. 2004. Semaphorin-plexin signaling guides patterning of the developing vasculature. *Dev Cell*, 7, 117-23.
- TOUTANT, M., COSTA, A., STUDLER, J. M., KADARE, G., CARNAUD, M. & GIRAULT, J. A. 2002. Alternative splicing controls the mechanisms of FAK autophosphorylation. *Mol Cell Biol*, 22, 7731-43.
- TREISMAN, R. 1995. DNA-binding proteins. Inside the MADS box. *Nature*, 376, 468-9.
- TSE, D. & STAN, R. V. 2010. Morphological heterogeneity of endothelium. *Semin Thromb Hemost*, 36, 236-45.
- TULLAI, J. W., SCHAFFER, M. E., MULLENBROCK, S., KASIF, S. & COOPER, G. M. 2004. Identification of transcription factor binding sites upstream of human genes regulated by the phosphatidylinositol 3-kinase and MEK/ERK signaling pathways. *The Journal of biological chemistry*, 279, 20167-77.
- TURNER, C. E. 2000. Paxillin and focal adhesion signalling. *Nat Cell Biol*, 2, E231-6.
- UEMURA, A., KUSUHARA, S., WIEGAND, S. J., YU, R. T. & NISHIKAWA, S. 2006. Tlx acts as a proangiogenic switch by regulating extracellular assembly of fibronectin matrices in retinal astrocytes. *The Journal of Clinical Investigation*, 116, 369-77.
- VALDEMBRI, D., CASWELL, P. T., ANDERSON, K. I., SCHWARZ, J. P., KONIG, I., ASTANINA, E., CACCAVARI, F., NORMAN, J. C., HUMPHRIES, M. J., BUSSOLINO, F. & SERINI, G. 2009. Neuropilin-1/GIPC1 signaling regulates alpha5beta1 integrin traffic and function in endothelial cells. *PLoS Biol*, 7, e25.
- VAN AELST, L. & D'SOUZA-SCHOREY, C. 1997. Rho GTPases and signaling networks. *Genes Dev*, 11, 2295-322.
- VARTIAINEN, M. K., GUETTLER, S., LARIJANI, B. & TREISMAN, R. 2007. Nuclear actin regulates dynamic subcellular localization and activity of the SRF cofactor MAL. *Science*, 316, 1749-52.
- VIEIRA, J. M., SCHWARZ, Q. & RUHRBERG, C. 2007. Selective requirements for NR1 ligands during neurovascular patterning. *Development*, 134, 1833-43.
- WALLEZ, Y., CAND, F., CRUZALEGUI, F., WERNSTEDT, C., SOUCHELNYTSKYI, S., VILGRAIN, I. & HUBER, P. 2007. Src kinase phosphorylates vascular endothelial-cadherin in response to vascular endothelial growth factor: identification of tyrosine 685 as the unique target site. *Oncogene*, 26, 1067-77.
- WANG, D. Z., LI, S., HOCKEMEYER, D., SUTHERLAND, L., WANG, Z., SCHRATT, G., RICHARDSON, J. A., NORDHEIM, A. & OLSON, E. N. 2002a. Potentiation of serum response factor activity by a family of myocardin-related transcription factors. *Proc Natl Acad Sci U S A*, 99, 14855-60.

- WANG, D. Z., LI, S., HOCKEMEYER, D., SUTHERLAND, L., WANG, Z., SCHRATT, G., RICHARDSON, J. A., NORDHEIM, A. & OLSON, E. N. 2002b. Potentiation of serum response factor activity by a family of myocardin-related transcription factors. *Proceedings of the National Academy of Sciences of the United States of America*, 99, 14855-60.
- WANG, J., WANG, S., LI, M., WU, D., LIU, F., YANG, R., JI, S., JI, A. & LI, Y. 2015a. The Neuropilin-1 Inhibitor, ATWLPPR Peptide, Prevents Experimental Diabetes-Induced Retinal Injury by Preserving Vascular Integrity and Decreasing Oxidative Stress. *PLoS One*, 10, e0142571.
- WANG, J. Y. 2014. The capable ABL: what is its biological function? *Mol Cell Biol*, 34, 1188-97.
- WANG, L., MUKHOPADHYAY, D. & XU, X. 2006a. C terminus of RGS-GAIP-interacting protein conveys neuropilin-1-mediated signaling during angiogenesis. *FASEB J*, 20, 1513-5.
- WANG, L., ZENG, H., WANG, P., SOKER, S. & MUKHOPADHYAY, D. 2003. Neuropilin-1-mediated vascular permeability factor/vascular endothelial growth factor-dependent endothelial cell migration. *J Biol Chem*, 278, 48848-60.
- WANG, M., ZHAO, D., SPINETTI, G., ZHANG, J., JIANG, L. Q., PINTUS, G., MONTICONE, R. & LAKATTA, E. G. 2006b. Matrix metalloproteinase 2 activation of transforming growth factor-beta1 (TGF-beta1) and TGF-beta1-type II receptor signaling within the aged arterial wall. *Arterioscler Thromb Vasc Biol*, 26, 1503-9.
- WANG, Y., CAO, Y., YAMADA, S., THIRUNAVUKKARASU, M., NIN, V., JOSHI, M., RISHI, M. T., BHATTACHARYA, S., CAMACHO-PEREIRA, J., SHARMA, A. K., SHAMEER, K., KOCHER, J. P., SANCHEZ, J. A., WANG, E., HOEPPNER, L. H., DUTTA, S. K., LEOF, E. B., SHAH, V., CLAFFEY, K. P., CHINI, E. N., SIMONS, M., TERZIC, A., MAULIK, N. & MUKHOPADHYAY, D. 2015b. Cardiomyopathy and Worsened Ischemic Heart Failure in SM22-alpha Cre-Mediated Neuropilin-1 Null Mice: Dysregulation of PGC1alpha and Mitochondrial Homeostasis. *Arterioscler Thromb Vasc Biol*, 35, 1401-12.
- WANG, Z., WANG, D. Z., HOCKEMEYER, D., MCANALLY, J., NORDHEIM, A. & OLSON, E. N. 2004. Myocardin and ternary complex factors compete for SRF to control smooth muscle gene expression. *Nature*, 428, 185-9.
- WATANABE, N., MADAULE, P., REID, T., ISHIZAKI, T., WATANABE, G., KAKIZUKA, A., SAITO, Y., NAKAO, K., JOCKUSCH, B. M. & NARUMIYA, S. 1997. p140mDia, a mammalian homolog of Drosophila diaphanous, is a target protein for Rho small GTPase and is a ligand for profilin. *EMBO J*, 16, 3044-56.
- WEGENER, K. L. & CAMPBELL, I. D. 2008. Transmembrane and cytoplasmic domains in integrin activation and protein-protein interactions (review). *Mol Membr Biol*, 25, 376-87.
- WEINL, C., RIEHLE, H., PARK, D., STRITT, C., BECK, S., HUBER, G., WOLBURG, H., OLSON, E. N., SEELIGER, M. W., ADAMS, R. H. & NORDHEIM, A. 2013. Endothelial SRF/MRTF ablation causes vascular disease phenotypes in murine retinæ. *J Clin Invest*, 123, 2193-206.
- WEINLANDER, K., NASCHBERGER, E., LEHMANN, M. H., TRIPAL, P., PASTER, W., STOCKINGER, H., HOHENADL, C. & STURZL, M. 2008.

- Guanylate binding protein-1 inhibits spreading and migration of endothelial cells through induction of integrin alpha4 expression. *FASEB J*, 22, 4168-78.
- WEIS, S., SHINTANI, S., WEBER, A., KIRCHMAIR, R., WOOD, M., CRAVENS, A., MCSHARRY, H., IWAKURA, A., YOON, Y. S., HIMES, N., BURSTEIN, D., DOUKAS, J., SOLL, R., LOSORDO, D. & CHERESH, D. 2004a. Src blockade stabilizes a Flk/cadherin complex, reducing edema and tissue injury following myocardial infarction. *The Journal of Clinical Investigation*, 113, 885-94.
- WEIS, S., SHINTANI, S., WEBER, A., KIRCHMAIR, R., WOOD, M., CRAVENS, A., MCSHARRY, H., IWAKURA, A., YOON, Y. S., HIMES, N., BURSTEIN, D., DOUKAS, J., SOLL, R., LOSORDO, D. & CHERESH, D. 2004b. Src blockade stabilizes a Flk/cadherin complex, reducing edema and tissue injury following myocardial infarction. *J Clin Invest*, 113, 885-94.
- WEIS, S. M. & CHERESH, D. A. 2005. Pathophysiological consequences of VEGF-induced vascular permeability. *Nature*, 437, 497-504.
- WELTI, J., LOGES, S., DIMMELER, S. & CARMELIET, P. 2013. Recent molecular discoveries in angiogenesis and antiangiogenic therapies in cancer. *The Journal of Clinical Investigation*, 123, 3190-200.
- WEST, H., RICHARDSON, W. D. & FRUTTIGER, M. 2005. Stabilization of the retinal vascular network by reciprocal feedback between blood vessels and astrocytes. *Development*, 132, 1855-62.
- WHITAKER, G. B., LIMBERG, B. J. & ROSENBAUM, J. S. 2001. Vascular endothelial growth factor receptor-2 and neuropilin-1 form a receptor complex that is responsible for the differential signaling potency of VEGF(165) and VEGF(121). *J Biol Chem*, 276, 25520-31.
- WODICKA, L. M., CICERI, P., DAVIS, M. I., HUNT, J. P., FLOYD, M., SALERNO, S., HUA, X. H., FORD, J. M., ARMSTRONG, R. C., ZARRINKAR, P. P. & TREIBER, D. K. 2010. Activation state-dependent binding of small molecule kinase inhibitors: structural insights from biochemistry. *Chem Biol*, 17, 1241-9.
- WOOD, J. M., BOLD, G., BUCHDUNGER, E., COZENS, R., FERRARI, S., FREI, J., HOFMANN, F., MESTAN, J., METT, H., O'REILLY, T., PERSOHN, E., ROSEL, J., SCHNELL, C., STOVER, D., THEUER, A., TOWBIN, H., WENGER, F., WOODS-COOK, K., MENRAD, A., SIEMEISTER, G., SCHIRNER, M., THIERAUCH, K. H., SCHNEIDER, M. R., DREVS, J., MARTINY-BARON, G. & TOTZKE, F. 2000. PTK787/ZK 222584, a novel and potent inhibitor of vascular endothelial growth factor receptor tyrosine kinases, impairs vascular endothelial growth factor-induced responses and tumor growth after oral administration. *Cancer research*, 60, 2178-89.
- WOODRING, P. J., HUNTER, T. & WANG, J. Y. 2001. Inhibition of c-Abl tyrosine kinase activity by filamentous actin. *J Biol Chem*, 276, 27104-10.
- WOODRING, P. J., HUNTER, T. & WANG, J. Y. 2003. Regulation of F-actin-dependent processes by the Abl family of tyrosine kinases. *J Cell Sci*, 116, 2613-26.
- WU, X., SUETSUGU, S., COOPER, L. A., TAKENAWA, T. & GUAN, J. L. 2004. Focal adhesion kinase regulation of N-WASP subcellular localization and function. *J Biol Chem*, 279, 9565-76.
- YAMAMOTO, H., EHLING, M., KATO, K., KANAI, K., VAN LESSEN, M., FRYE, M., ZEUSCHNER, D., NAKAYAMA, M., VESTWEBER, D. &

- ADAMS, R. H. 2015. Integrin beta1 controls VE-cadherin localization and blood vessel stability. *Nat Commun*, 6, 6429.
- YANNUZZI, L. A., NEGRAO, S., IIDA, T., CARVALHO, C., RODRIGUEZ-COLEMAN, H., SLAKTER, J., FREUND, K. B., SORENSON, J., ORLOCK, D. & BORODOKER, N. 2012. Retinal angiomatous proliferation in age-related macular degeneration. 2001. *Retina*, 32 Suppl 1, 416-34.
- YAQOUB, U., CAO, S., SHERGILL, U., JAGAVELU, K., GENG, Z., YIN, M., DE ASSUNCAO, T. M., CAO, Y., SZABOLCS, A., THORGEIRSSON, S., SCHWARTZ, M., YANG, J. D., EHMAN, R., ROBERTS, L., MUKHOPADHYAY, D. & SHAH, V. H. 2012. Neuropilin-1 stimulates tumor growth by increasing fibronectin fibril assembly in the tumor microenvironment. *Cancer Research*, 72, 4047-59.
- ZACCHIGNA, S., PATTARINI, L., ZENTILIN, L., MOIMAS, S., CARRER, A., SINIGAGLIA, M., ARSIC, N., TAFURO, S., SINAGRA, G. & GIACCA, M. 2008. Bone marrow cells recruited through the neuropilin-1 receptor promote arterial formation at the sites of adult neoangiogenesis in mice. *J Clin Invest*, 118, 2062-75.
- ZAIDEL-BAR, R., MILO, R., KAM, Z. & GEIGER, B. 2007. A paxillin tyrosine phosphorylation switch regulates the assembly and form of cell-matrix adhesions. *Journal of Cell Science*, 120, 137-48.
- ZAROMYTIDOU, A. I., MIRALLES, F. & TREISMAN, R. 2006. MAL and ternary complex factor use different mechanisms to contact a common surface on the serum response factor DNA-binding domain. *Molecular and cellular biology*, 26, 4134-48.
- ZHANG, H., VUTSKITS, L., PEPPER, M. S. & KISS, J. Z. 2003a. VEGF is a chemoattractant for FGF-2-stimulated neural progenitors. *J Cell Biol*, 163, 1375-84.
- ZHANG, R., WANG, N., ZHANG, M., ZHANG, L. N., GUO, Z. X., LUO, X. G., ZHOU, H., HE, H. P. & ZHANG, T. C. 2015. Rho/MRTF-A-Induced Integrin Expression Regulates Angiogenesis in Differentiated Multipotent Mesenchymal Stem Cells. *Stem Cells Int*, 2015, 534758.
- ZHANG, X., AZHAR, G., CHAI, J., SHERIDAN, P., NAGANO, K., BROWN, T., YANG, J., KHRAPKO, K., BORRAS, A. M., LAWITTS, J., MISRA, R. P. & WEI, J. Y. 2001. Cardiomyopathy in transgenic mice with cardiac-specific overexpression of serum response factor. *Am J Physiol Heart Circ Physiol*, 280, H1782-92.
- ZHANG, X., AZHAR, G., FURR, M. C., ZHONG, Y. & WEI, J. Y. 2003b. Model of functional cardiac aging: young adult mice with mild overexpression of serum response factor. *Am J Physiol Regul Integr Comp Physiol*, 285, R552-60.
- ZHANG, X., AZHAR, G., HELMS, S., BURTON, B., HUANG, C., ZHONG, Y., GU, X., FANG, H., TONG, W. & WEI, J. Y. 2011. Identification of New SRF Binding Sites in Genes Modulated by SRF Over-Expression in Mouse Hearts. *Gene Regul Syst Bio*, 5, 41-59.
- ZHANG, Y. E. 2009. Non-Smad pathways in TGF-beta signaling. *Cell Res*, 19, 128-39.
- ZHANG, Z., DONG, Z., LAUXEN, I. S., FILHO, M. S. & NOR, J. E. 2014. Endothelial cell-secreted EGF induces epithelial to mesenchymal transition and endows head and neck cancer cells with stem-like phenotype. *Cancer Res*, 74, 2869-81.

APPENDIX

Data from the qPCR array (see Chapter 4)

Position	Symbol	Fold Change	Comments
A01	Myl12a	1.0519	OKAY
A02	Actn1	0.7013	OKAY
A03	Actn3	1.583	C
A04	Actn4	1.3095	OKAY
A05	Actr2	1.1773	OKAY
A06	Actr3	1.1076	OKAY
A07	Akt1	0.9462	OKAY
A08	Arf6	0.6251	B
A09	Arhgdia	0.8747	OKAY
A10	Arhgef7	1.2933	OKAY
A11	Baiap2	1.2029	A
A12	Bcar1	2.1172	B
B01	Capn1	0.7571	B
B02	Capn2	1.231	OKAY
B03	Cav1	1.4154	OKAY
B04	Cdc42	0.8581	OKAY
B05	Cfl1	0.9138	OKAY
B06	Crk	1.031	OKAY
B07	Csf1	0.6637	B
B08	Ctnn	1.1166	B
B09	Diap1	0.5774	B
B10	Dpp4	0.7739	B
B11	Egf	0.2688	B
B12	Egfr	11.7184	B
C01	Enah	1.6058	B
C02	Ezr	1.4965	B
C03	Fap	1.583	C
C04	Fgf2	0.1954	B
C05	Hgf	0.3052	B
C06	Igf1	2.7873	B
C07	Igf1r	1.0737	OKAY
C08	Ilk	1.0396	OKAY

C09	Itga4	1.5544	B
C10	Itgb1	1.0734	OKAY
C11	Itgb2	1.1073	B
C12	Itgb3	0.2494	B
D01	Limk1	1.5174	B
D02	Mapk1	1.0121	OKAY
D03	Met	1.583	C
D04	Mmp14	0.8042	B
D05	Mmp2	6.8223	B
D06	Mmp9	1.1394	B
D07	Msn	1.0788	OKAY
D08	Myh10	1.0009	OKAY
D09	Myh9	0.975	OKAY
D10	Mylk	2.0966	B
D11	Pak1	0.7361	B
D12	Pak4	1.4968	B
E01	Pfn1	1.1229	OKAY
E02	Pik3ca	1.3146	B
E03	Plaur	1.0447	B
E04	Plcg1	0.9675	OKAY
E05	Pld1	1.0384	B
E06	Prkca	1.0729	B
E07	Pten	0.8205	OKAY
E08	Ptk2	1.6675	OKAY
E09	Ptk2b	0.4819	B
E10	Ptpn1	0.6248	B
E11	Pxn	0.4373	A
E12	Rac1	1.0348	OKAY
F01	Rac2	1.1531	B
F02	Rasa1	0.8551	A
F03	Rdx	1.1774	OKAY
F04	Rho	1.583	C
F05	Rhoa	0.9075	OKAY
F06	Rhob	1.0658	OKAY
F07	Rhoc	1.0874	OKAY
F08	Rnd3	1.1532	B
F09	Rock1	3.9617	A
F10	Sh3pxd2a	1.8503	B

F11	Src	0.7834	B
F12	Stat3	1.227	B
G01	Svil	1.1619	B
G02	Tgfb1	0.9624	OKAY
G03	Timp2	1.2328	B
G04	Tln1	1.2744	OKAY
G05	Vasp	1.1386	A
G06	Vcl	0.8838	OKAY
G07	Vegfa	0.0845	B
G08	Vim	1.1868	OKAY
G09	Wasf1	1.583	C
G10	Wasf2	1.0053	OKAY
G11	Wasl	1.0659	B
G12	Wipf1	0.6821	B
H01	Actb	1	OKAY
H02	B2m	1.0435	OKAY
H03	Gapdh	1.1637	OKAY
H04	Gusb	1.7468	OKAY
H05	Hsp90ab1	1.0494	OKAY
H06	MGDC	1.583	C
H07	RTC	1.9751	OKAY
H08	RTC	1.9521	OKAY
H09	RTC	2.1049	OKAY
H10	PPC	1.657	OKAY
H11	PPC	1.631	OKAY
H12	PPC	1.8718	OKAY

List of publications

- RAIMONDI, C., FANTIN, A., **LAMPROPOULOU, A.**, DENTI, L., CHIKH, A. & RUHRBERG, C. 2014. Imatinib inhibits VEGF-independent angiogenesis by targeting neuropilin 1-dependent ABL1 activation in endothelial cells. *The Journal of experimental medicine*, 211, 1167-83.
- LAMPROPOULOU, A.** & RUHRBERG, C. 2014. Neuropilin regulation of angiogenesis. *Biochem Soc Trans*, 42, 1623-8.
- FANTIN, A., **LAMPROPOULOU, A.**, GESTRI, G., RAIMONDI, C., SENATORE, V., ZACHARY, I. & RUHRBERG, C. 2015. NRP1 Regulates CDC42 Activation to Promote Filopodia Formation in Endothelial Tip Cells. *Cell Rep*, 11, 1577-90.
- FANTIN, A., **LAMPROPOULOU, A.**, SENATORE, V., BRASH, J. T., PRAHST, C., LANGE, C. A., LIYANAGE, S. E., RAIMONDI, C., BAINBRIDGE, J. W., AUGUSTIN, H. G. & RUHRBERG, C. 2017. VEGF165-induced vascular permeability requires NRP1 for ABL-mediated SRC family kinase activation. *J Exp Med*, 214, 1049-1064.
- BRASH J.T., A., **LAMPROPOULOU, A.**, & RUHRBERG, C. 2017. The role of the Neuropilins in developmental biology. In: *The Neuropilins: Role and Function in Health and Disease*, Springer International Publishing, DOI 10.1007/978-3-319-48824-0_6